

Hydrate Phase Equilibria Study of CO2 Containing Gases in Thermodynamic Promoter Aqueous Mixtures

Veronica Belandria

▶ **To cite this version:**

Veronica Belandria. Hydrate Phase Equilibria Study of CO2 Containing Gases in Thermodynamic Promoter Aqueous Mixtures. Other. Ecole Nationale Supérieure des Mines de Paris, 2012. English. NNT : 2012ENMP0018 . pastel-00718604

HAL Id: pastel-00718604

https://pastel.hal.science/pastel-00718604

Submitted on 17 Jul 2012

HAL is a multi-disciplinary open access archive for the deposit and dissemination of scientific research documents, whether they are published or not. The documents may come from teaching and research institutions in France or abroad, or from public or private research centers.

L'archive ouverte pluridisciplinaire **HAL**, est destinée au dépôt et à la diffusion de documents scientifiques de niveau recherche, publiés ou non, émanant des établissements d'enseignement et de recherche français ou étrangers, des laboratoires publics ou privés.

ParisTech
INSTITUT DES SCIENCES ET TECHNOLOGIES
PARIS INSTITUTE OF TECHNOLOGY

MINES ParisTech

Ecole doctorale n°432 : Sciences des Métiers de l' Ingénieur

Doctorat ParisTech

T H È S E

pour obtenir le grade de docteur délivré par

l'École Nationale Supérieure des Mines de Paris

Spécialité " Génie des Procédés "

présentée et soutenue publiquement par

Veronica BELANDRIA

le 18 juin 2012

Etude Expérimentale des Equilibres d'hydrates de Mélanges de Gaz Contenant du CO_2 en Solutions Aqueuses de Promoteur Thermodynamique

Hydrate Phase Equilibria Study of CO_2 Containing Gases in Thermodynamic Promoter Aqueous Mixtures

Directeur de thèse : **Dominique RICHON**
Co-directeur de thèse : **Amir H. MOHAMMADI**

Jury

M. Arne GRAUE, Professor, Physics and Technology, University of Bergen	Rapporteur
Mme Maaike C. KROON, Professor, Chemical Engineering and Chemistry, Eindhoven TU	Rapporteur
M. Cornelis J. PETERS, Professor, Chemical Engineering, The Petroleum Institute, Abu Dhabi	Président
M. Luis A. GALICIA-LUNA, Professor, ESIQIE, Instituto Politecnico Nacional	Examinateur
M. Rafael LUGO, Dr, Chimie et Physico-chimie Appliquées, IFP Energies Nouvelles	Examinateur
M. Amir H. MOHAMMADI, Dr (HDR), CEP/TEP Fontainebleau, MINES ParisTech	Examinateur
M. Dominique RICHON, Professor, CEP/TEP Fontainebleau, MINES ParisTech	Examinateur

MINES ParisTech
Centre Énergétique et Procédés
35, rue Saint Honoré, 77305 Fontainebleau Cedex, France

T H E S E

Contents

List of Figures 4
List of Tables 7
Nomenclature 8

Chapter 1: Introduction 12

1.1 The Growing Need for CO_2 Capture 12
1.1.1 Carbon dioxide: Properties, formation, and phase behavior of the CO_2 + water system 14
1.1.2 Solutions for Capturing CO_2 17

1.2 Gas Hydrates: An Introductory Overview 20
1.2.1 Historical Background 20
1.2.2 Definition and Crystalline Structures 23
1.2.3 Phase Diagrams 25
1.2.4 Gibbs' Phase Rule Consideration 29
1.2.5 Gas Hydrates Potential in Industry and Process Engineering 29
1.2.6 CO_2 Capture by Gas Hydrate Crystallization 30
1.2.7 Use of Thermodynamic Promoters 35
1.2.8 TBAB Semi-Clathrates 37

1.3 Objective and Scope of the work 42

Chapter 2: Experimental Methods and Analysis Techniques for Gas Hydrates Phase Equilibrium Measurement 47

2.1 Overview 47

2.2 Visual versus Non-visual Techniques 49

2.3 The Isochoric Method 51

2.4 Apparatuses for the Determination of Hydrate Phase Equilibria 52

2.5 Static-Analytic-Synthetic Measurements 56

2.6 Gas Chromatography 58

2.7 Calibrating Measuring Devices and Experimental Accuracies 61
2.7.1 Pressure Sensors Calibration 62
2.7.2 Temperature Probe Calibration 63
2.7.3 Volumetric Calibrations 64
2.7.4 GC Detector Calibration for Gas Mixtures 65
2.7.5 Refractometer Calibration 66

2.8 Criteria for Equilibrium 67

Chapter 3: Phase Equilibria of Clathrate Hydrates of Methane + Carbon dioxide: New Experimental Data and Predictions 69

3.1 Introduction 71

3.2 Experimental setup and method 72
3.2.1 General hydrate formation and dissociation procedure 75

3.3 Results and discussion 76

Chapter 4: Development of a New Apparatus for Simultaneous Measurements of Gas Hydrates Dissociation Conditions and Compositional Analysis 89

4.1 Introduction 89

4.2 Apparatus 92

4.2.1 Equilibirum cell 94

4.2.2 Sample supplying system 97

4.2.3 Composition analyzing system 97

4.2.4 Measurement, control and acquisition of temperature and pressure 100

4.3 Experimental Procedure 101

4.3.1 Preparation of the feed 101

4.3.2 Fluids supply to the equilibrium cell 102

4.3.3 Isochoric Pressure Search Method 102

4.4 Results and discussion 106

Chapter 5: Thermodynamic Stability of Hydrates from Gas Mixtures Containing CO_2 114

5.1 Introduction 114

5.2 Gas Hydrate Formation in Carbon Dioxide + Nitrogen + Water Systems 116

5.2.1 Equilibrium Dissociation Conditions 117

5.2.2 Compositional Analysis of Equilibrium Phases 121

5.3 Study of Gas Hydrate Formation in (Carbon Dioxide + Hydrogen + Water) Systems 127

5.3.1 Equilibrium Dissociation Conditions 127

5.3.2 Compositional Analysis of Equilibrium Phases 129

Chapter 6: Thermodynamic Stability of Semi-Clathrate Hydrates 136

6.1 Phase Equilibria of Semi-Clathrate Hydrates of Carbon Dioxide, Methane and Nitrogen in Non-Stoichiometric TBAB Aqueous Solutions 139

6.2 Thermodynamic Properties of Semi-Clathrate Hydrates of (Carbon Dioxide + Nitrogen) Gas Mixtures in TBAB Aqueous Mixtures 145

6.2.1 Phase Equilibrium Measurements for Semi-Clathrate Hydrates of the CO_2 + N_2 + Tetra-n-Butylammonium Bromide Aqueous Solution Systems 146

6.2.2 Compositional Properties for Semi-Clathrate Hydrates of the CO_2 + N_2 + Tetra-n-Butylammonium Bromide Aqueous Solution Systems 154

Chapter 7: Conclusions and Outlook 163

7.1 Conclusions 164

7.2 Outlook 175

References 178

Acknowledgements 193

Curriculum Vitae 195

Publications 196

Appendix A: Measured Hydrate Phase Equilibrium Data for CO_2 Containing Gases 199

Appendix B: Tetra-n-Butyl Ammonium Bromide + Water Systems: Density Measurements and Correlation 215

List of Figures

1.1 Worldwide CO_2 industrial emissions and economic recessions in the past 50 years. 13
1.2 Carbon dioxide hydrates phase equilibrium in CO_2 + water system. 15
1.3 Hydrate crystal unit structures: sI, sII and sH 23
1.4 Typical phase diagram for pure water 26
1.5 Pressure-temperature diagram for methane + water system in the hydrate region 27
1.6 Pressure-temperature phase diagram for hydrocarbon + water systems. 28
1.7 Pressure-temperature phase diagram for multicomponent natural gas systems. 28
1.8 Carbon dioxide hydrate phase boundary compared to nitrogen, hydrogen and methane 31
1.9 Flow diagram of a hydrate-based CO_2 recovery process 33
1.10 Flow diagram of an integrated cryogenic and hydrate CO_2 capture process 33
1.11 Conceptual separation stages required for recovering CO_2 from (CO_2 + N_2) hydrates 34
1.12 Promotion effect of various quaternary ammonium salts on the phase equilibrium conditions of CO_2 clathrate hydrates. 38
1.13 TBAB semi-clathrate structure 39
1.14 Temperature-composition phase diagram of (TBAB + H_2O) semi-clathrates under atmospheric pressure, as reported by Arjmandi and coworkers (2007). Symbols represent experimental data and figures along the composition lines stand for hydration numbers. 40
1.15 Carbon dioxide + TBAB semi-clathrates phase boundary. 40
2.1 Process design strategy. 47
2.2 Detail of Deaton and Frost's hydrate formation equilibrium cell 53
2.3 (a) Schematic diagram of the QCM, and (b) the QCM mounted within a high pressure cell. 54
2.4 High-pressure micro DSC VII measurement device. 55
2.5 Hydrate dissociation conditions (HDC) determination following the isochoric pressure-search method. 58
2.6 Front view of the gas chromatograph used in this work and main components 59
2.7 Gas chromatogram exhibiting an effective separation of a (CO_2 + N_2) gas mixture. 60
2.8 Calibration devices used in this work. 61
2.9 Relative uncertainty on pressure transducers calibration 62
2.10 Pt-100 Platinum resistance thermometer probe calibration. 64
2.11 Thermal conductivity detector calibration 66
2.12 Refractive index calibration for TBAB aqueous solutions 67
2.13 Chromatogram profile for a (CO_2 + N_2) gas mixture in the presence of TBAB aqueous solution 68
3.1 Flow diagram of the experimental setup 73
3.2 Partial pictures of the apparatus 74
3.3 Representative isochoric curve, and pressure and temperature plots obtained during a hydrate formation/dissociation experiment. 76
3.4 Experimental dissociation pressures for methane simple hydrates 77
3.5 Experimental dissociation pressures for carbon dioxide simple hydrates. 77
3.6 Experimental dissociation pressures for various (methane + carbon dioxide) gas hydrates at different CO_2 load mole fractions 78
3.7 Relative deviation of experimental dissociation pressures for (CO_2 + CH_4) clathrate hydrates and predictions of HWHYD thermodynamic model 80
3.8 Experimental, calculated (using eq. 3.2) and predicted (HWHYD model) dissociation pressures for (CO_2 + CH_4) clathrate hydrates 81
3.9 Relative deviation of the experimental and predicted (HWHYD model) dissociation pressures for various (CO_2 + CH_4) clathrate hydrates 82
3.10 Relative deviation of experimental and calculated pressures (using eq. 3.2) dissociation pressures for (CO_2 + CH_4) clathrate hydrates. 83
3.11 Experimental dissociation conditions for various (CO_2 + CH_4) clathrate hydrates and predictions of the thermodynamic model (HWHYD, 2000), at different CO_2 mole fractions loaded 84

3.12 Comparison of experimental dissociation pressures for various (CO_2 + CH_4) clathrate hydrates with the calculated values using eq. (3.2) 85
4.1 Schematic flow diagram of the new apparatus. 93
4.2 Partial pictures of the main components of the new apparatus 93
4.3 Cross section of the equilibrium cell and photograph of equilibrium cell on its aluminum support. 94
4.4 (a) Lateral section of the equilibrium cell (b) Detail of the protection grid for the capillary sampler. 95
4.5 (a) Lateral and (b) cross sections of the grid support. 96
4.6 Chromatogram profile for nitrogen gas samples under gas-hydrate-liquid water equilibrium 97
4.7 Flow diagram of the electromagnetic rapid on-line sampler-injector 98
4.8 Layout for chromatograms acquisition using Winilab III software. 99
4.9 Layout for temperature and pressure data acquisition software 100
4.10 Hydrate formation/dissociation process, cooling and heating isochors and determination of hydrate phase boundaries and composition of the equilibrium phases 103
4.11 Hydrate dissociation conditions measured in this work for (methane + carbon dioxide) clathrate hydrates at various CO_2 load mole fractions. 106
4.12 Hydrate dissociation conditions (literature and this work) for (methane + carbon dioxide) clathrate hydrates at selected CO_2 load mole fractions 107
4.13 **(**a) *p-y* phase diagram of (methane + carbon dioxide) clathrate hydrates at different equilibrium temperatures (b) *p-z* phase diagram of (methane + carbon dioxide) clathrate hydrates at 280.2 K 109
4.14 Pressure-composition phase diagram of the (methane + carbon dioxide) clathrate hydrates : This work and CSMGem model predictions 111
5.1 Experimental dissociation conditions for (nitrogen + carbon dioxide) clathrate hydrates at different CO_2 load mole fractions. This work and HWHYD model predictions 118
5.2 Experimental dissociation conditions for (nitrogen + carbon dioxide) clathrate hydrates at different CO_2 load mole fractions: Literature, this work and HWHYD model predictions 119
5.3 ARD between experimental and predicted dissociation pressures for (nitrogen + carbon dioxide) clathrate hydrates at different CO_2 mole fractions loaded. 121
5.4 Pressure - composition phase diagram for (nitrogen + carbon dioxide + water) systems under (L_w-H-G) equilibrium at different temperatures 122
5.5 Pressure - composition phase diagram for (nitrogen + carbon dioxide + water) systems under (L_w-H-G) equilibrium at selected temperatures. 124
5.6 Pressure - composition phase diagram for the (nitrogen + carbon dioxide + water) systems under (L_w-H-G) equilibrium: Experimental and literature 125
5.7 Pressure-composition phase diagram for the (nitrogen + carbon dioxide + water) systems under (L_w-H-G) equilibrium at selected temperatures. This work and CSMGem model predictions 126
5.8 Experimental (literature and this work) dissociation conditions for gas hydrates of (CO_2 + H_2) formed in the presence water at various feed gas compositions. 128
5.9 Pressure - gas phase composition phase diagram for (hydrogen + carbon dioxide + water) systems under (L_w-H-G) equilibrium at different temperatures 131
5.10 Pressure - gas phase composition phase diagram for (hydrogen + carbon dioxide + water) systems under (L_w-H-G) equilibrium at different temperatures. This work and literature 133
6.1 Experimental dissociation conditions (literature and this work) for (methane + TBAB) semi-clathrates. 142
6.2 Experimental dissociation conditions (literature and this work) for (carbon dioxide + TBAB) semi-clathrates 143
6.3 Experimental hydrate dissociation conditions (literature and this work) for (nitrogen + TBAB) semi-clathrates. 144
6.4 Dissociation conditions (Literature and this work) for semi-clathrates of (CO_2 + N_2) formed at various CO_2 feed gas compositions in the presence of TBAB aqueous solutions 148
6.5 Experimental dissociation conditions for semi-clathrates of (0.749 mole fraction CO_2 + 0.251 mole fraction N_2) formed in the presence of TBAB aqueous solutions and predictions of CSMGem and HWHYD thermodynamic models in the absence of thermodynamic promoter 151

6.6 Experimental dissociation conditions for semi-clathrates of (0.399 mole fraction CO_2 + 0.601 mole fraction N_2) formed in the presence of TBAB aqueous solutions and predictions of CSMGem and HWHYD thermodynamic models in the absence of thermodynamic promoter 152
6.7 Experimental dissociation conditions for semi-clathrates of (0.151 mole fraction CO_2 + 0.849 mole fraction N_2) formed in the presence of TBAB aqueous solutions and predictions of CSMGem and HWHYD thermodynamic models in the absence of thermodynamic promoter 153
6.8 Pressure-composition (gas phase) diagram for semi-clathrates of the (CO_2 + N_2 + TBAB + H_2O) systems at various temperatures and 0.05 mass fractions TBAB 159
6.9 Pressure-composition (gas phase) diagram for semi-clathrates of the (CO_2 + N_2 + TBAB + H_2O) systems at various temperatures and 0.30 mass fractions TBAB 160
6.10 Pressure-composition (gas phase) diagram for semi-clathrates of the (CO_2 + N_2 + TBAB + H_2O) systems at selected temperatures and different initial TBAB concentrations. 161
6.11 Pressure-composition (TBAB in the liquid phase) diagram for semi-clathrates of (CO_2 + N_2 + TBAB + H_2O) systems at various temperatures and 0.05 mass fractions TBAB 162

List of Tables

1.1 Summary of major economic crises leading to important growth of global CO_2 industrial emissions since the 1960s 13
1.2 Main features of post-combustion, pre-combustion and oxy-fuel combustion capture approaches 19
1.3 Significant research contributions relevant to clathrate hydrate formation of CO_2 and tetra alkyl ammonium salts from 1778 to 2007 22
1.4 Molecular diameter to cavity diameter ratio for cavity type for the gases of interest within this research. 24
1.5 Literature experimental studies for hydrate phase equilibria of gas mixtures containing CO_2 + CH_4, N_2 and H_2. 36
2.1 Commonly used experimental procedures for measuring hydrate dissociation conditions 50
2.2 Pressure transducers calibration coefficients 63
3.1 Purities and suppliers of chemicals 72
3.2 Operating conditions of the gas chromatograph. 74
4.1 Experimental data reported in the literature for the dissociation conditions of the binary gas hydrates of (carbon dioxide + methane). 90
4.2 Experimental data reported in the literature for the *p*, *T*, and composition of the gas and hydrate phases at (L_w-H-G) equilibrium conditions for the binary clathrate hydrates of (carbon dioxide + methane) 90
4.3 Main characteristics of previous and new experimental setups. 91
5.1 Literature phase equilibrium data of the (carbon dioxide + nitrogen + water) ternary hydrate system. 115
5.2 Review of the compositions of the gas and hydrate phases at hydrate equilibrium conditions reported in the literature for (carbon dioxide + nitrogen + water) ternary system. 115
5.3 Literature review of the experimental data on compositions of the gas and hydrate phases for the (carbon dioxide + hydrogen + water) systems. 116
5.4 Summary of the hydrate phase equilibrium data measured in this work for (CO_2 + N_2 + H_2O) systems. 124
5.5 Experimental studies on molar compositions of gas hydrates formed in the (CO_2 + H_2 + H_2O) ternary systems. 132
5.6 Summary of the hydrate phase equilibrium data measured in this work for the (CO_2 + H_2 + H_2O) systems 133
6.1 Experimental data available in the literature for (CH_4 + TBAB) semi-clathrates 137
6.2 Experimental data available in the literature for (CO_2 + TBAB) semi-clathrates. 137
6.3 Experimental data available in the literature for (N_2 + TBAB) semi-clathrates 137
6.4 Experimental data available in the literature for (CO_2 + N_2 + TBAB) semi-clathrates. 138
6.5 Purities and suppliers of materials 140
6.6 Semi-clathrate hydrate phase equilibrium data for the (CO_2 + N_2 + TBAB + H_2O) systems 149
6.7 Operating conditions of a conceptual CO_2 hydrate-based separation process from (CO_2 + N_2) gas mixtures at two concentrations of TBAB in aqueous solutions. 158

Nomenclature

List of symbols

AARD absolute average relative deviation [%]

ARD absolute relative deviation [%]

B coefficient of density correlation

DE differential evolution

e parameter of coefficient equation for density correlation

f fugacity or parameter of coefficient equation for density correlation

F number of independent variables or degrees of freedom

g parameter of coefficient equation for density correlation

G gas

H hydrate

H Henry's constant [MPa]

HDC hydrate dissociation condition

L liquid

n number of moles

N number of components

p pressure [MPa]

q hydration number

RD relative deviation [%]

t time (min, s)

T temperature [K]

V volume [m^3]

v molar volume [m^3/mol]

x mole fraction in liquid/aqueous phase

y mole fraction in gas phase

w mass fraction

z water-free mole fraction of CO_2 in hydrate phase

Greek Letters

η refractive index

π number of phases

ρ density

θ fractional cage occupancy of hydrate guests

Subscripts

i i^{th} unknown variables

D refers to refractive index in n_D

m refers to gas mixture

L = large cage

S = small cage

R retention tine in gas chromatography

W water

1 refers to carbon dioxide

2 refers to methane, nitrogen or hydrogen

3 refers to water

Superscripts

exp experimental

G gas phase

H hydrate phase

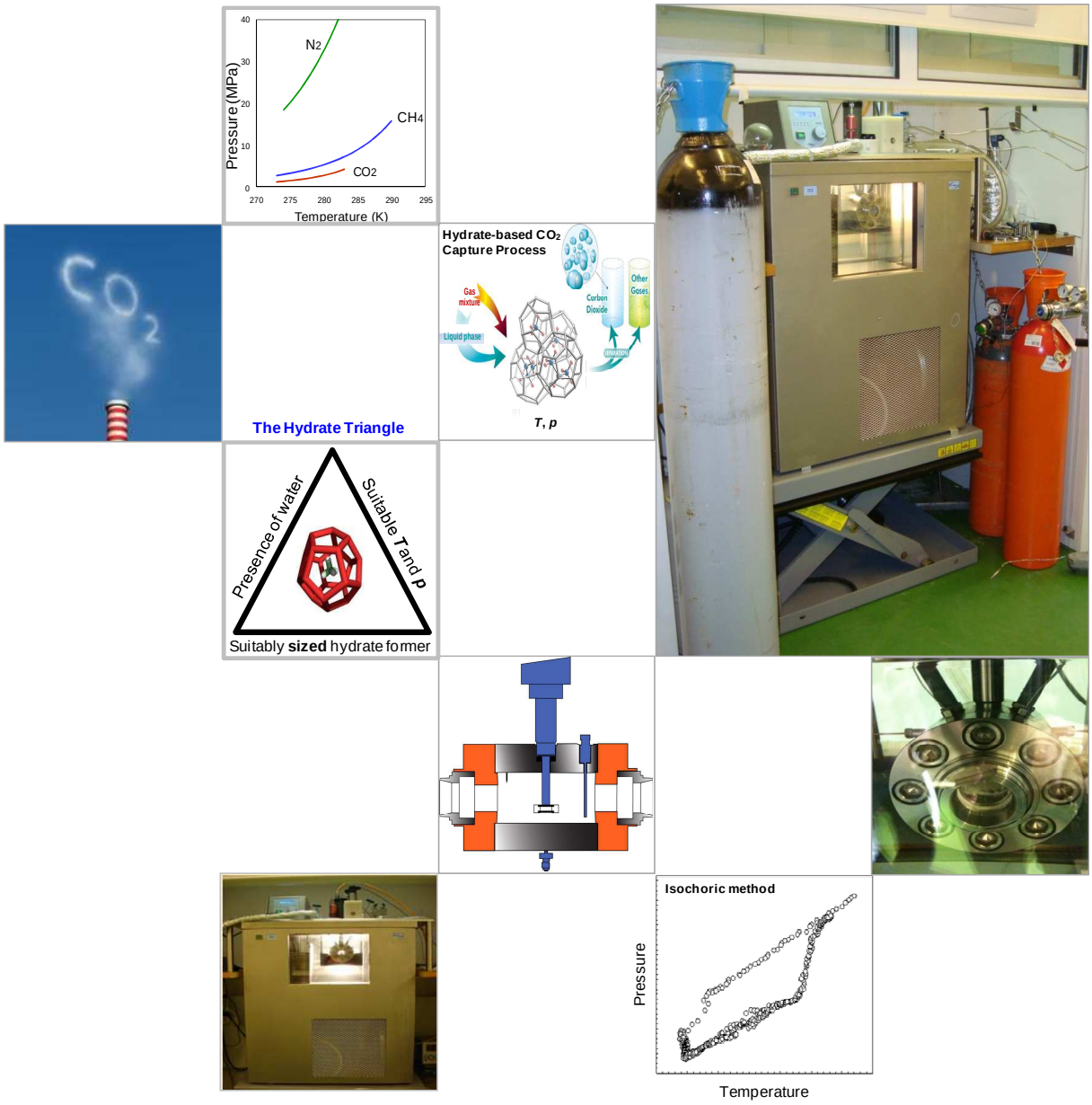
L liquid phase

pred predicted

t total

1

Introduction



1

Résumé

Ce chapitre introductif présente le contexte industriel et les motivations liés à la recherche sur les hydrates de dioxyde de carbone. Cette thèse est consacrée à l´étude expérimentale des équilibres de phases de systèmes conduisant à la formation d´hydrates de dioxyde de carbone. En conséquence, nous donnons tout d´abord un aperçu général sur les hydrates et les clathrates, ainsi que sur leurs applications potentielles dans l'industrie et en génie des procédés, y compris dans le domaine du captage de CO_2. Les principes fondamentaux des équilibres de phases en présence d´hydrates et l'utilisation de promoteurs thermodynamiques permettant d´améliorer les conditions de formation d'hydrates sont mis en évidence. Enfin, nous décrivons les objectifs et les grandes lignes de la thèse.

Abstract

This introductive chapter provides the industrial context and motivations behind carbon dioxide hydrate research. As this thesis is concerned with the phase equilibria of carbon dioxide hydrate-forming systems from experimental point of view, a general overview to clathrate hydrate compounds and their potential application in industry and process engineering, including CO_2 capture is given. The fundamentals of hydrate phase equilibria and the use of thermodynamic promoters to enhance the hydrate formation conditions are highlighted and finally, the aims and the outline of the thesis are presented.

1 Introduction

1.1 The Growing Need for CO_2 Capture

One of today's major challenges within process engineering is the implementation of safer, economical and sustainable technologies to meet human ever-increasing needs. Accurate thermodynamic data form the basis in determining the feasibility of applying new processes in industry. This thesis deals with experimental thermodynamics aspects in the context of an alternative carbon dioxide (CO_2) separation approach, through gas hydrate formation.

It is believed that global atmospheric concentrations of CO_2, methane (CH_4) and nitrous oxide (N_2O) have significantly increased as a result of continued economic development and industrialization. Preliminary estimates show a global increase in CO_2 emissions of more than 5 % in 2010 alone, which is the highest growth rate registered over the past two decades (Olivier *et al*., 2011), as evidenced in Figure 1.1. The major recent economic crises leading to important growth of global CO_2 industrial emissions are listed in Table 1.1. In addition to the increasing levels of CO_2 and other greenhouse gases in the atmosphere, global mean surface temperatures have also increased (IPCC, 2007).

As a result, two major issues arise from today's global energy discussion. The first is centered on the role of CO_2 in climate change and the second is the long-term sustainability of energy supply. Doubling or even tripling of the global energy demand is expected by 2050 (World Energy Council, 2012), while the latest IPCC (2007) assessment calls for 50 to 85% reduction in global emissions during the same period, in order to avoid dangerous changes in the atmosphere.

In light of these issues, worldwide efforts for a coordinated cooperation in scientific and public policy matters around environmental and energy goals, have resulted in the creation of international conventions and treaties, such as the Kyoto Protocol, promoted by the United Nations Framework Convention on Climate Change (UNFCCC). Within this context, sustainable development, energy supply security and mitigating climate change are the main drivers for energy research beginning the twenty first Century (European Commission, 2007).

Carbon dioxide Capture and Storage (CCS) have thus become a priority within energy research. CCS refers to capturing CO_2 directly from the emission sources by technological means, transport it and store it permanently (Tzimas & Peteves, 2003). As this thesis is

primarily concerned with CO_2 capture applications, no further discussion is given to carbon dioxide transportation or sequestration technologies.

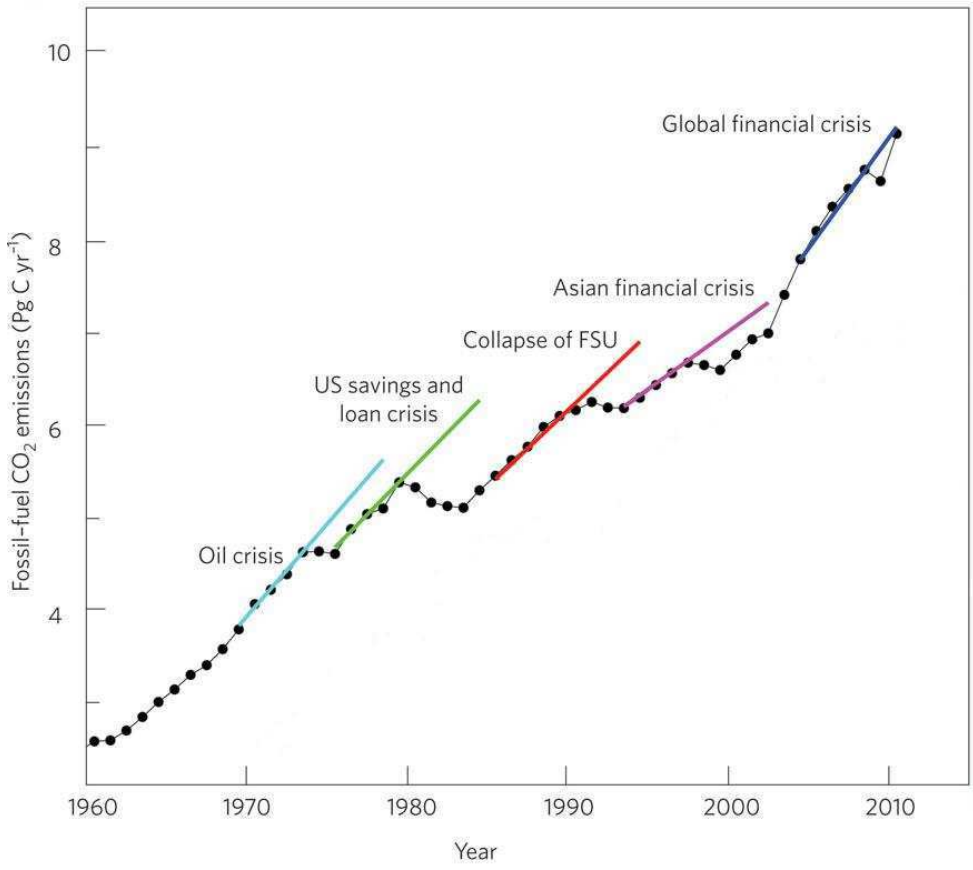


Figure 1.1. Worldwide CO_2 industrial emissions and economic recessions in the past 50 years (modified from Peters *et al*., 2012). CO_2 emissions are given in Petagrams (Pg) of carbon per year. A Petagram is equal to a trillion (1,000,000,000,000) kilograms or a billion (1,000,000,000) tones. Linear trends are fitted to the five years preceding the beginning of each crisis.

Table 1.1. Summary of major economic crises leading to important growth of global CO_2 industrial emissions since the 1960s, as shown in Figure 1.1 (Peters *et al*., 2012).

Year	Event
1973	Oil crisis
1979	The US savings and loans crisis
1989	The collapse of the Former Soviet Union (FSU)
1997	The Asian financial crisis
2009	The recent global credit crisis

As stated in the European Commission (2007) report, current priorities within CO_2 capture include: CO_2 separation from flue gas (CO_2 + nitrogen), CO_2 separation from synthetic fuels (CO_2 + hydrogen) and CO_2 separation from biogas (CO_2 + CH_4). Consistent with these imperatives, this thesis contributes to the three preceding CO_2 capture objectives.

In 2007, the SECOHYA CO_2-Hydrate Separation project was established in France, jointly with the *Agence Nationale de la Recherche* (ANR) and five academic partners. The goal of this project is to develop a separation process to capture CO_2 based on a principle of gas hydrate crystallization (SECOHYA, 2007). The Thermodynamics and Phase Equilibria Laboratory (CEP-TEP) from MINES ParisTech, as member of this partnership, was requested to perform accurate hydrate phase equilibrium measurements of (carbon dioxide and methane, nitrogen or hydrogen) gas mixtures in the presence of tetra-n-butyl ammonium bromide (abbreviated TBAB) aqueous solutions. The scope of the task was specifically targeted to enhancing the fundamental knowledge of hydrate formation and dissociation and elucidating the promotion effect of the latter additive, from thermodynamic point of view (SECOHYA, 2007).

Although the phase behavior of gas hydrates has been extensively studied for decades, better understanding of thermodynamics of CO_2 hydrate-forming systems and reliable phase equilibrium data in the presence of thermodynamic additives are fundamental for developing thermodynamically well-founded models and to establish the feasibility of industrial processes involving carbon dioxide hydrates.

1.1.1 Carbon dioxide: Properties, formation, and phase behavior of the CO_2 + water system

Before studying the stability of mixed hydrate systems containing carbon dioxide, it is useful to consider some properties of CO_2 as a pure compound, as well as the phase behavior of CO_2 + water (H_2O) mixtures.

Carbon dioxide is a colorless, non-polar compound. It is considered non-harmful (below 1%, by volume), naturally abundant, inert and relatively cheap. Carbon dioxide has a triple point at a temperature of 216.6 K and pressure of 0.519 MPa (NIST WebBook, 2001), and a critical point located at 304.2 K and 7.380 MPa (NIST WebBook, 2001). Along with methane, ethane and propane, carbon dioxide is one of hydrate formers typically found in natural gas (Sloan & Koh, 2008).

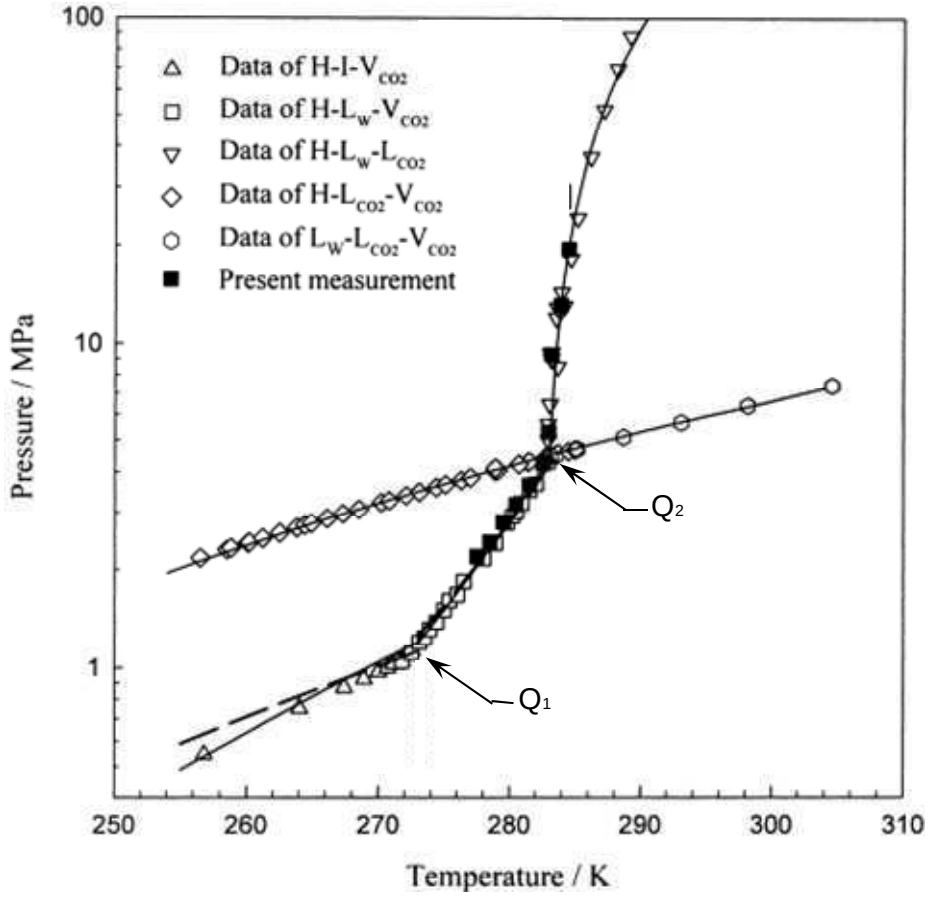


Figure 1.2. Carbon dioxide hydrates phase equilibrium in CO_2 + water system. Symbols represent experimental data and lines are calculated three-phase equilibrium pressures using a lattice fluid equation of state (Yang *et al*., 2000).

Most relevant properties of carbon dioxide hydrate include: a density of 1120 kg · m³ at 276 K, measured via X-ray diffraction by Udachin *et al*. (2001); and molecular weight and molar volume values of 0.1556 kg · kmol and $1.389 \cdot 10^{4}$ $m^3 \cdot mol^{-1}$, respectively, reported by Anderson (2003).

Figure 1.2 illustrates the phase behavior of CO_2 + water (H_2O) system, involving the formation of hydrate (H), water-rich liquid (L_W), CO_2-rich vapor (V_{CO2}), CO_2-rich liquid (L_{CO2}), and ice (I) phases. From this pressure-temperature phase diagram it can be seen that the stability region of CO_2 hydrates lies in the middle of the hydrate + ice + vapor (H–I–V_{CO2}), hydrate + liquid water + vapor (H–L_W–V_{CO2}) and hydrate + liquid water + liquid CO_2 (H–L_W–L_{CO2}) equilibrium curves. Any pressure-temperature condition within this region will lead to the coexistence of CO_2 hydrates together with gaseous CO_2 and liquid water. The lowest measured dissociation condition along the (H–L_W–V_{CO2}) line for hydrates formed in

the (CO_2 + H_2O) system is 1048 KPa at 271.8 K (Larson, 1955). Two quadruple points are distinguished, namely Q_1 and Q_2, located at (T = 273.1 K; p = 1.256 MPa) and (T = 283.0 K; p = 4.499 MPa), respectively (Sloan, 1998). Q_1 is the quadruple point, where ice + water + hydrate + gas (I-L_W-H- V_{CO2}) coexist, while Q_2 is a (L_W-H-V_{CO2}-L_{CO2}) equilibrium point.

The idealized dissociation of CO_2 hydrate to gaseous CO_2 and liquid water at the (H–L_W–V_{CO2}) equilibrium can be represented through the following equation:

$$CO_2 \cdot qH_2O(s) \leftrightarrow CO_2\,(g) + qH_2O\,(l) \qquad (1.1)$$

where q represents the number of hydrate water molecules per guest molecule, namely hydration number. The concept of hydration number is used later in Chapters 4 and 5 for determining the composition of mixed hydrate systems.

Based on reaction (1.1), the amount of energy required for dissociating CO_2 hydrates (per mole of CO_2 in the hydrate) has been reported to vary from (57.7 to 65.22) kJ · mol^{-1} (Anderson, 2003). This advantageous exothermic nature of CO_2 hydrate's formation compared to the heat of CH_4 hydrate dissociation (54.49 kJ· mol^{-1}) can be fully exploited for sequestering CO_2 with simultaneous production of natural gas from methane hydrates (Goel, 2006).

Gaseous carbon dioxide is mainly formed as a by-product from combustion of fossil fuels (*e.g.* natural gas, coal and oil). The combustion of all carbon-based fuels follows a very similar chemical reaction. As an example, the well-known reaction of carbon with oxygen is given below, where CO_2 enthalpy of formation is -393.5 kJ · mol^{-1}, as reported in the NIST WebBook (2001).

$$C + O_2 \rightarrow CO_2 \qquad (1.2)$$

The major industrial sectors releasing CO_2 to the atmosphere include: thermal power generation, cement production, natural gas and oil refining, gas flaring, iron and steel production, gas leakages and waste (OECD/IEA, 2008). Since fossil fuels are usually combusted with excess air, other compounds are also formed together with CO_2, *i.e.* nitrogen (N_2), carbon monoxide (CO), water vapor, oxygen (O_2), *etc.* The ratio of these products in the exhaust gases and the exact temperature and pressure conditions depend on the plant type, operating conditions and the parameters of the combustion process (Tzimas & Peteves, 2003).

Indeed, the majority of CO_2 emission sources have a molar CO_2 concentration that has been reported to vary from roughly 15 mole % in flue gases, to about 4 mole % in natural gas combustion in combined cycle (IEA, 2001). Whereas in other processes involving hydrogen (H_2) production from fossil fuels, *e.g*. steam-natural gas reforming and/or integrated coal gasification power plants, a stream of almost pure CO_2 is produced (~ > 95 mole %.) In such processes, it has been estimated that one ton of H_2 produced may also produce about 9 tons of carbon dioxide (Collodi & Wheeler, 2010).

As result of its increased concentration (0.039 %, by volume) in the atmosphere (NOAA, 2012), carbon dioxide is currently considered a primary greenhouse gas contributing to the so-called global warming effect. Regardless remaining controversies and debates on this issue, research efforts are currently undergoing worldwide for continuing the development of technological solutions to enable CO_2 capture.

1.1.2 Solutions for Capturing CO_2

According to the Intergovernmental Panel on Climate Change (IPCC) special report on CCS, the power plants activity constitutes more than 60 % of CO_2 emissions, where N_2 and CO_2 are the most significant components (IPCC, 2007). On the other hand, the IEA (2008) assessment states that CCS technology alone has the potential to reduce greenhouse gas emission by 20 % by 2050. CCS is thus recommended as "*…one of the most promising solutions to stabilize atmospheric levels of CO_2…"* (IPCC, 2007).

Based on process conditions, such as: CO_2 concentration, temperature, pressure, fuel type and degree of required CO_2 removal from the feed; most common CO_2 capture technologies fall under three general categories, namely: post-combustion, pre-combustion and oxy-fuel combustion. The first two approaches are considered economically feasible under specific conditions, while the third one is at demonstration phase (IPCC, 2007). The Lacq oxyfuel combustion CCS project, briefly described below, is an example of this. A variety of processes have been thus developed for separating and capturing CO_2, and many of them are commercially available, as indicated in Table 1.2.

These processes are generally based on gas phase separation, absorption into a liquid, *i.e*. amines absorption (Rubin & Rao, 2002), adsorption on a solid, and more recently, hybrid techniques such as adsorption/membrane systems, *etc*.

Table 1.2. Main features of post-combustion, pre-combustion and oxy-fuel combustion capture approaches

Capture approach	Separation task / feed	*p T* and feed composition	Method	Current application	Advantages	Drawbacks
Post-combustion	Flue gas (CO_2 / N_2)	Near atmospheric pressure < 373 K 4 – 15 mole % CO_2	Absorption (Chemical solvents)	Separation of CO_2 from natural gas and flue gases	Well established process Solvent can be recycled Degree of CO_2 purity > 95% Non dependence on human operators, minimizing labor costs Likely to be incorporated in existing power plants without significant modifications Commercially available Sorbent can be reused	High regeneration costs Degradation of solvents due to the presence of impurities and by-products Low CO_2 loading capacity Solvent can form corrosive solutions with flue gases. Lost solvent precipitates. Large equipment size Sorbent susceptible to degradation
			Adsorption (Solid sorbents)		Low concentrations of CO_2 yield an optimum performance	Cannot handle easily large concentrations of CO_2 Adsorption time is not practical Low degree of CO_2 separation Poor selectivity of sorbents to CO_2 Operation costs higher than absorption processes
Pre-combustion	Syngas (CO_2 / H_2)	> 0.5 MPa > 373 K ~35 mole % CO_2	Physical absorption *e.g*. Pressure Swing Adsorption (PSA) and Temperature Swing Adsorption (TSA).	Production of hydrogen (mainly for fertilizer manufacture)	Requires less energy for regeneration than chemical absorption processes Less expensive than post-combustion capture	Requires a high partial pressure of CO_2 in the feed Capacity proportional to CO_2 partial pressure and temperature Low selectivity of solvent causes H_2 losses
			Membrane separation		Commercially available Low maintenance required Needs less energy than PSA	Low degree of selectivity to CO_2
Oxy-fuel combustion	Oxyfuel exhaust gas (O_2 / N_2)	> 5 MPa < 323 K ~90 mole % CO_2	Cryogenic separation	Refinery of liquefied CO_2	Flue gas is mostly CO_2 and H_2O Water can be removed by condensation Separation of CO_2 is relatively inexpensive No need of control equipment for impurities Smaller size of equipment since only O_2 is supplied for combustion	Corrosion might be caused by SO_2 High cost of O_2 production Operation and capital costs similar to post-combustion processes

Some other innovative concepts have been reviewed by Granite and O'Brien (2005). They include: electrochemical pumps, metal organic frameworks, ionic liquids, and enzyme-based, cryogenic and bio-mimetic approaches. The progress of CO_2 capture technologies is an extensive topic itself and it has been well covered, with different levels of detail, in several reviews available in the literature (Tzimas & Peteves, 2003; Aaron & Tsouris, 2005; Zachary & Titus, 2008; Yang *et al*. 2008; Figueroa *et al*. 2008; Pennline *et al*. 2008 and Herzog, 2009). Essentially, the major benefits and drawbacks of the three CO_2 capture approaches; as well as approximate process conditions are summarized in Table 1.2.

It is worthwhile to note that the conditions of the feed differ somewhat for the three approaches. As stated by Tzimas and Peteves (2003) "*syngas has a higher CO_2 concentration than flue gas and it is generally available at a higher pressure and temperature*". Besides, it has been estimated that the exhaust gas from oxyfuel combustion is produced at even higher pressures at ambient temperature.

As can be seen in Table 1.2, many of these technologies have proved their technical feasibility for capturing CO_2 from industrial emissions. However, to address the current lack of demonstrated capabilities for large-scale CO_2 capture (Figueroa *et al*., 2008; Folger, 2010), a number of demonstration projects are planned or undergoing worldwide. Examples are the Mountaineer power plant in West Virginia (USA) and the Lacq project in France. The first started capturing a portion of a 20 MW coal-based plant CO_2 emissions in 2009 using chilled ammonia. About 100,000 tons of CO_2 per year are stored in a deep saline aquifer injection well. The cost of the project is US$70 million, and it could be expanded to 235 MW in 2014-2015, as reported by the National Mining Association (NMA, 2012). The Lacq project is Europe's first integrated CO_2 capture and storage facility using oxyfuel combustion technology, including CO_2 injection in a depleted on-shore hydrocarbon reservoir (TOTAL, 2007). The test started in 2010 and it plans to capture 120,000 tons of CO_2 over two years, at a cost of US$85.6 million (TOTAL, 2007).

In continuation to the above efforts, critical issues regarding large energy consumption, corrosion, foaminess, low capacities, safety and environmental concerns are the focus of most current CO_2 capture research projects. As a result, the development of alternative energy efficient and less costly processes for CO_2 capture is necessary. In this regard, gas hydrates

crystallization approach has been proposed as an emerging concept to capture CO_2 (Spencer, 1997; Kang & Lee, 2000; Duc *et al*., 2007).

As gas hydrates (also denoted clathrate hydrates) have the capacity to store/separate gases, there is a large field of potentially interesting applications, such as CO_2 sequestration and CH_4 recovery from natural gas hydrates in deep sea sediments (Ohgaki *et al*., 1994), natural gas processing, storage and transportation (Koh, 2002), H_2 separation from steam reforming processes (Sugahara *et al*., 2005), H_2 storage (Strobel *et al*., 2006), sea water desalination (Seo & Lee, 2001), *etc*.

1.2 Gas Hydrates: An Introductory Overview

The purpose of this section is to provide a concise overview of clathrate hydrates fundamentals in order to set the theoretical formalisms for studying the phase equilibria of gas hydrate forming systems.

1.2.1 Historical Background

Prominent scientists of the 18^{th} and 19^{th} centuries including Joseph Priestley (1778), Sir Humphrey Davy (1810) and Michel Faraday (1823) are associated with the early discovery of gas hydrates (Makogon, 1997; Sloan & Koh, 2008). An approximation to hydrates' composition was first reported for Cl_2 hydrates (Faraday, 1823). Afterwards gas hydrate research remained mainly a scientific curiosity for more than a century. A considerable number of hydrate formers together with the pressure and temperature conditions at which they are formed and their chemical compositions were identified over this period, including CO_2 hydrate systems investigated by Polish physicist and chemist Zygmunt Florenty Wróblewski in 1882 (Wróblewski, 1882).

Traditionally, the progress of clathrate hydrates research and development has been divided into three historical periods. Hammerschmidt's discovery of hydrate plugs in natural gas pipelines in 1934 marked the beginning of an industry-oriented second research period (Sloan & Koh, 2008),

under the auspices of oil and gas companies. Most relevant research contributions related to CO_2 hydrates within this second period include the determination of the hydrate phase boundary between (273 and 283) K in the mid-1900s (Deaton & Frost, 1946), and the classification of CO_2 hydrate crystal as a structure I for the first time via X-ray diffraction technique (von Stackelberg & Müller, 1954).

More recently, the existence of natural gas hydrates as an energy resource (Makogon, 1965) intensified worldwide hydrate research interest within the scientific community and energy industry. This event established the beginning of the third historical research period.

Today gas hydrates are known to exist in the universe. The most common research interests on Earth focus in three large fields: 1) its avoidance in the oil and gas industry (Sloan & Koh, 2008), 2) as an alternative energy resource (Makogon, 2010), and 3) their beneficial application to novel technologies, such as: transport of natural gas as frozen hydrate (Gudmundsson & Hveding, 1995), high pressure SIMTECHE CO_2 hydrate separation process (Tam *et al.*, 2001), air conditioning system using clathrate hydrate slurry (Obata *et al*., 2003), CO_2 gas hydrate engine systems (Obara *et al*., 2011), *etc.*

The major scientific research achievements over the past two centuries are thoroughly reviewed by Davidson (1973), Makogon (1997), Sloan and Koh (2008), Giavarini and Hester (2011), *etc*. The contributions listed in Table 1.3 are meant to provide a chronological background to carbon dioxide hydrate research, from about 1778 until just before starting the present research (2007).

Table 1.3. Significant research contributions relevant to clathrate hydrate formation of CO_2 and tetra alkyl ammonium salts from 1778 to 2007 (Makogon, 1997; Sloan & Koh, 2008).

1st research period	1778	Priestley	Formed SO_2 hydrates
	1810	Davy	Identified Cl_2 hydrate
	1823	Faraday	Deduced Cl_2 hydrate's composition as $(C1_2 \cdot 10H_20)$
	1882	Cailletet and Bordet	Measured mixed gas hydrate systems: $CO_2 + PH_3$ and $H_2S + PH_3$
		Wróblewski	Studied CO_2 hydrate formation in $CO_2 + H_2O$ system
	1894 and 1897	Villard	Determined CO_2 hydrate composition as $CO_2 \cdot 6H_2O$ and CO_2 hydrate dissociation curve in the range of (267 to 283) K
	1902	de Forcrand	Extensively used Clausius-Claypeyron equation to determine enthalpies of dissociation and compositions of gas hydrates
	1934	Hammerschmidt	Realized that formation of natural gas hydrates was responsible for plugging natural gas pipelines and discovered thermodynamic inhibitors
2nd research period	1940	Fowler	Identified hydrates of tetra alkylammonium salts (TBAX)
	1946	Deaton and Frost	Measured dissociation pressures of CO_2 hydrates between (273 and 283) K
	1949	Unruh and Katz	Reported (L_W–H–V) data for $CO_2 + CH_4$ mixed hydrates
	1954	von Stackelberg and Müller	Determined hydrate crystal structures I and II through X-ray diffraction and classified CO_2 hydrate as a type I
	1959	van der Waals and Platteeuw (vdWP)	Proposed a statistical thermodynamic model for calculating hydrate formation conditions
		McMullan and Jeffrey	Examined hydrates formed by quaternary alkylammonium salts using X-ray diffraction
3rd research period	1972	Parrish and Prausnitz	Applied vdWP model to natural gases and mixed hydrates
	1984	Dyadin and Udachin	Further investigated TBAX hydrates
	1987	Ripmeester and coworkers	Reported the existence hydrate structure H hydrates
	1997	Spencer	Patented a method of selectively separating CO_2 from multicomponent gaseous streams through CO_2 clathrate formation
	2000	Kang and Lee	Proposed a new hydrate-based gas separation process for recovering > 99 mole % of CO_2 from flue gas using THF as hydrate promoter
	2003	Shimada and coworkers	Found that TBAB hydrate crystals could be used to separate small gas molecules
	2007	Duc and coworkers	Investigated ($CO_2 + N_2$) hydrates using TBAB as a thermodynamic promoter

1.2.2 Definition and Crystalline Structures

Gas hydrates or clathrate hydrates are ice-like crystalline compounds, which are formed through a combination of water and guest molecules under suitable conditions of low temperature and high pressures (Sloan & Koh, 2008). In a gas hydrate, hydrogen-bonded 'host' water molecules form special cavities and 'guest' gas molecules are trapped inside the cavities. The hydrate structure is stabilized by the repulsive interactions between guests and hosts molecules (Sloan & Koh, 2008). The majority of gas hydrates are known three common crystal structures: structure I (sI), structure II (sII) and structure H (sH), where each structure is composed of a certain number of cavities formed by water molecules (Mohammadi & Richon, 2009*a*). Figure 1.3 provides a hydrate structure summary for sI, sII and sH.

As shown in Figure 1.3, all hydrate structures have repetitive crystal units. However, they differ in the number and sizes of the cages and in their unit cells.

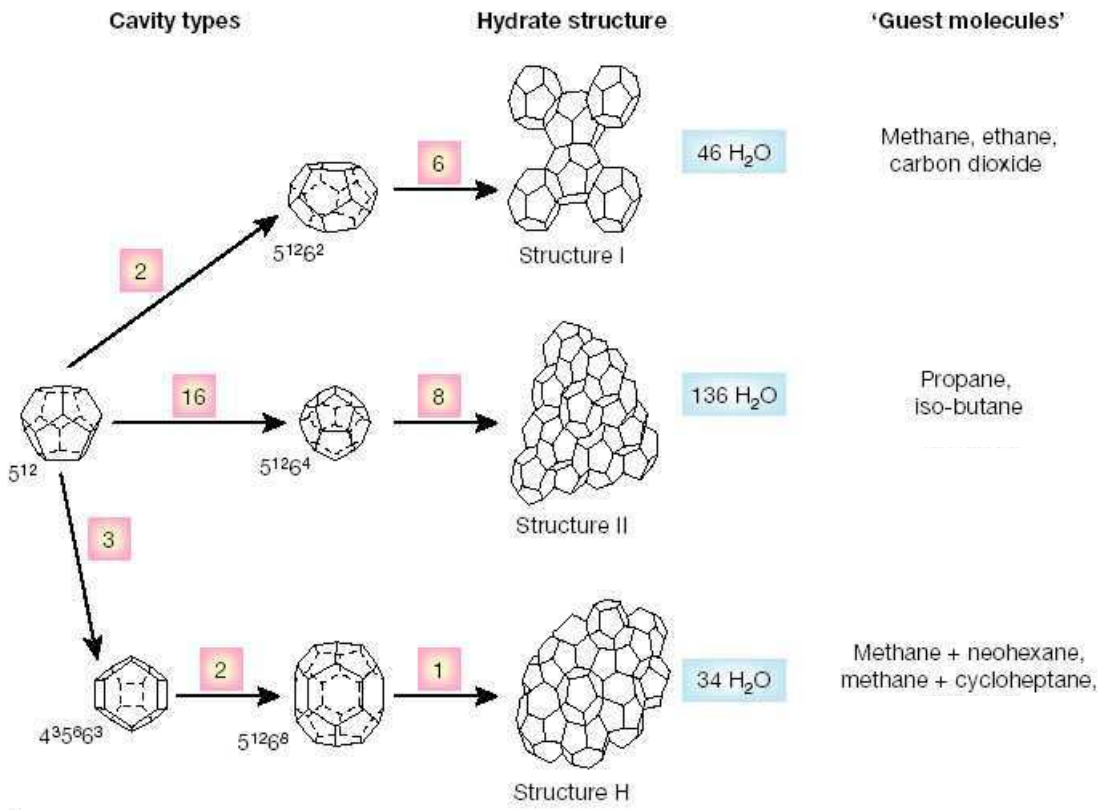


Figure 1.4. Hydrate crystal unit structures: sI, sII and sH (Sloan, 2003). Shaded squares represent the number of cavity types, superscripts indicate the number of faces per cavity type and the shaded rectangles give the number of water molecules per hydrate structure.

Hydrate crystal structures I and II were first determined through x-ray diffraction methods by von Stackelberg and Müller (1954). They found that each structure is composed of a certain number of large and small cavities formed by water molecules. For example, structure I clathrate hydrates are composed of two 12-pentagonal (5^{12}) cavities and two $5^{12}6^2$ (2-hexagonal face) cavities. The existence of a new hydrate structure, known as sH, was reported by Ripmeester and coworkers (1987). This third structure requires both large (~ 6-7 Å) and small (~ 4-5 Å) molecules, such as light oil fractions and CH_4, respectively. Many other structures beyond the scope of this work have been reported afterwards. Extensive reviews on clathrate hydrates crystalline structures are given by Sloan and Koh (2008) and Carroll (2009).

For a guest molecule to enter a cavity, it must meet dimensional, physicochemical and morphological criteria. Typical examples of hydrate forming substances include CH_4, ethane (C_2H_6), propane (C_3H_8), CO_2, N_2, H_2 and H_2S. Of the gases of interest within this work, CO_2 and CH_4 are known to form sI as simple hydrates, while N_2 and H_2 have been classified as sII hydrate formers (Sloan & Koh, 2008). This could be explained by the ratios of molecular diameter to cavity diameter listed in Table 1.4. In simple hydrate formers, stable structures occur, as a rule, within the upper and lower limits in diameter ratios of about 1.0 and 0.76, respectively (Sloan & Koh, 2008). For instance, CO_2 with a ratio of 1.0 is capable of occupying both the small (5^{12}) and large ($5^{12}6^2$) cages of sI. Although the diameter ratio of CH_4 to the small cavity of sII is 0.87, it has been determined that CH_4 stabilizes the small and large cavities of sI with a diameter ratio of 0.86.

Table 1.4. Molecular diameter to cavity diameter ratio for cavity type for the gases of interest within this research (Sloan & Koh, 2008).

Guest hydrate former		Structure I		Structure II	
Molecule	Diameter (Å)	5^{12}	$5^{12}6^2$	5^{12}	$5^{12}6^4$
H_2	2.72	0.533	0.464	0.542	0.408
N_2	4.1	0.804	0.700	0.817	0.616
CH_4	4.36	0.855	0.744	0.868	0.655
CO_2	5.12	1.00	0.834	1.02	0.769

In nitrogen hydrates, N_2 stabilizes the small cavities of sII (size ratio of 0.82) and it also occupies in less degree the large ($5^{12}6^4$) sII cavities. At moderate pressures, in all three-hydrate structures, each cavity can contain at most one guest molecule (Englezos, 1993). However, it is interesting to note that since nitrogen is so small (~ 4 Å), more than one molecule can easily fit the large cavities of sII. Hence, multiple cage occupancy can occur at pressures higher than 30 MPa (Sloan & Koh, 2008).

When two different guests molecules combine in a binary or mixed clathrate hydrate, the situation is quite different. Complex guest size–structural relations and/or transitions may occur and affect the thermodynamic equilibrium between coexisting phases. For example, the addition of 1 mole % C_3H_8 to pure CH_4 hydrates has been reported to cause a decrease in the hydrate formation pressure of up to 42 % due to a structure change (Sloan & Koh, 2008). Crystalline structures thus play a significant role on the equilibrium state (three-phase temperature, pressure and gas hydrate composition) required for hydrate stability. The microscopic aspects discussed in the preceding paragraphs are meant to provide the basis for better understanding gas hydrates phase equilibria discussed in the following sections.

1.2.3 Phase Diagrams

The phase behavior of gas hydrates considerably changes depending on the size and chemical nature of guest molecules. The relationship between microscopic structure, just described, and macroscopic hydrate phase properties can be better understood through the study of phase diagrams. A brief description of phase diagrams for single-component, two-component, three-component and multicomponent systems is thus provided to gain a fundamental insight into the phase equilibria of hydrate forming systems.

A typical phase diagram for pure water exhibiting gas, liquid, and solid phases is shown in Figure 1.4. In the triple point, found at 273.16 K and $6.117 \cdot 10^{-4}$ MPa (Lide, 2004), all three phases are in equilibrium. The phases are separated by phase boundaries, where phase transitions occur. The phase boundary between liquid and gas ends at the critical point, located at 647.1 K and 22.064 MPa (Wagner *et al.*, 2000). Above this point a single fluid phase referred to as a supercritical fluid is formed.

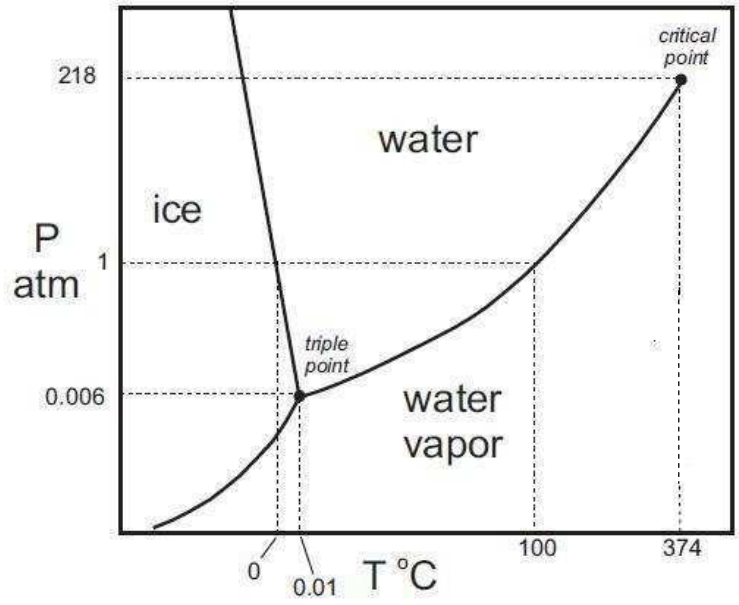


Figure 1.3. Typical phase diagram for pure water (Perkins & Brady, 2007).

As an example of the phase behavior for two-component systems, the phase diagram of (CH_4 + H_2O) binary mixtures is considered. Depending on the pressure and temperature conditions, four stability regions are defined in Figure 1.5, namely: liquid water + methane gas (L_w + V_{CH4}) located at high temperatures and moderate pressures; at high pressures crystallization occurs and the liquid water + methane hydrate (L_w + H_{CH4}) zone appears; if temperature decreases, water ice + methane hydrate (I + H_{CH4}) is formed; finally, a subsequent pressure decrease establishes the water ice + methane gas (I + V_{CH4}) zone.

The phase diagram shown in Figure 1.6 is the equivalent of Figure 1.5 for systems containing hydrocarbon (*e.g.*, C_2H_6, C_3H_8 or i-C_4H_{10}) + H_2O, CO_2 + H_2O (Figure 1.1) or hydrogen sulfide (H_2S) + H_2O. In this diagram a three-phase (L_W-V-L_{HC}) equilibrium curve at high temperature and high-pressure conditions is depicted. Also, a second quadruple point, Q_2, in which L_W, H, V and L_{HC} coexist, is formed at the intersection of the L_W-V-L_{HC} with the L_W-H-V equilibrium curves. Similar to Figure 1.2, for systems with two quadruple points, the hydrate region falls in between the I-H-V curve (at conditions below Q_1), the L_W-H-V line (between Q_1 and Q_2), and the L_W-H-L_{HC} line at temperatures and pressures above Q_2 (Sloan & Koh, 2008).

In Figure 1.7, the lower zone of the pressure-temperature phase diagram for natural gases without liquid hydrocarbon is similar to that shown in Figure 1.6. However, the main differences are that the L_W-H-V curve occurs at a fixed composition of hydrocarbon mixture, and that the quadruple point (Q_1) appears at a lower pressure. In the case in which natural gases contain heavier components, the (L_W-H-V) phase boundary represents the hydrate formation region equivalent to the region between the quadruple point (Q_1) and the upper quadruple point (Q_2) of Figure 1.6 (Sloan & Koh, 2008).

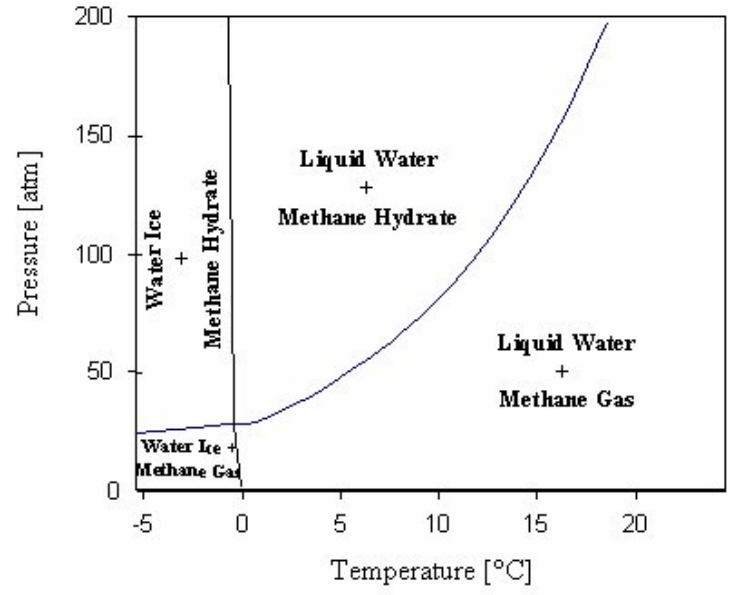


Figure 1.4. Pressure-temperature diagram for methane + water system in the hydrate region (GasHyDyn Center, ENSMSE).

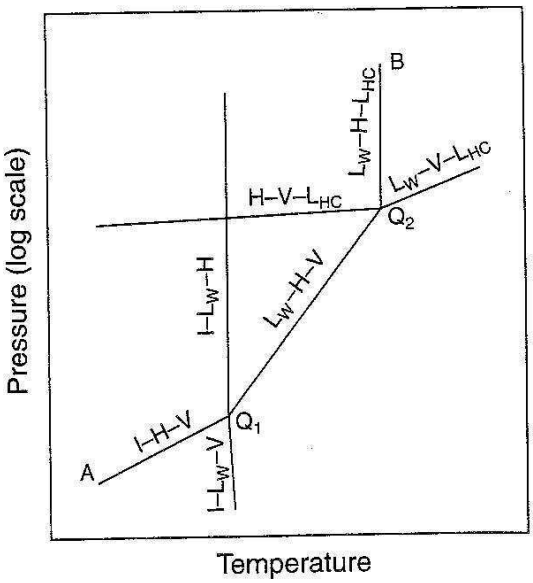


Figure 1.5. Pressure-temperature phase diagram for hydrocarbon + water systems (Sloan & Koh, 2008).

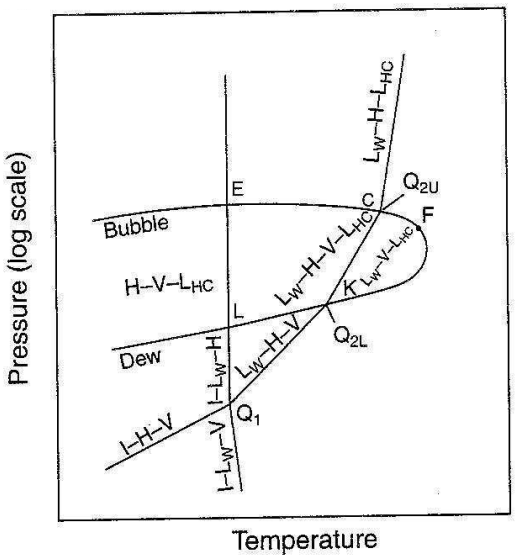


Figure 1.6. Pressure-temperature phase diagram for multicomponent natural gas systems (Sloan & Koh, 2008).

In addition, the dew and bubble-point curves can be distinguished in the phase envelope region in Figure 1.7. At low pressures and moderate temperatures, the (L_W-H-V) line intersects the phase envelope and a second liquid begins to form (L_W-H-V-L_{HC}). As pressure continues to raise, more of the second liquid forms as expected, until a point where the amount of the second liquid reaches a maximum. Beyond the critical point, the amount of the second liquid decreases until it totally disappears (Carroll, 2009).

1.2.4 Gibbs' Phase Rule Consideration

In the above phase diagrams, the equilibrium relationships are established by the equality in all potentials likely to modify the system. Upon equilibrium, no further changes occur in the macroscopic properties of the system with time. Thus, the equilibrium state of a PVT system containing *N* chemical species and π phases is function of a certain number of intensive properties, namely: *T*, *p*, and composition of each phase (Smith *et al*., 2001). These measured quantities are independent of the amount of phase present.

In clathrate hydrates, the number of independent variables needed to specify the system (*F*), also called degrees of freedom, is given by the Gibbs' Phase Rule for non-reacting systems, presented without derivation as (Smith *et al*., 2001):

$$F = 2 - \pi + N \qquad (1.3)$$

The application of the Gibbs' Phase Rule, in the thermodynamic analysis of systems under (hydrate + liquid + vapor) equilibrium, is addressed later in experimental Chapters 4 and 5.

1.2.5 Gas Hydrates Potential in Industry and Process Engineering

Although for many years gas hydrates have been considered an industrial concern, especially in oil and gas production and in processing and transportation facilities (Sloan & Koh, 2008), positive applications of gas hydrates are currently considered a subject of increasing research

interest, based on the number of studies recently published in the literature (Eslamimanesh *et al*., 2012).

Suitable conditions for clathrate hydrate formation may commonly occur in broad areas including energy and climate subject matters. During hydrocarbon production, gas hydrate formation may affect flow assurance and safety from wells to processing facilities (Sloan, 2003). In the natural environment, hydrates may be found in the sediments of the deep-sea continental margins, the subsurface of Arctic permafrost regions, and in deep glacial ice (Englezos, 1993). Other applications include hydrates as means of gas separation, storage material for H_2, cool energy storage and recovery, seawater desalination, water removal from industrial effluents, edible products, and bioengineering (Sloan & Koh, 2008).

Domains of gas hydrates application also include power plants, oil and gas refining, hydrogen and ammonia processing, iron and steel manufacturing, cement production, natural gas production with high concentrations of acid gases (H_2S and CO_2), coal gasification, shift conversion, *etc.*

The role of gas hydrates in disasters such as the Macondo well blowout in the Gulf of Mexico in 2010 has been reported in the literature (Koh *et al*., 2011) and it is not addressed in this work.

1.2.6 CO_2 Capture by Gas Hydrate Crystallization

Gas hydrates crystallization is a reversible process that has been proposed as an emerging concept for CO_2 capture (Seo *et al*., 2000; Linga *et al*., 2007*a*). It has been estimated that hydrate-based processes are less energy intensive and thereby are considered a promising alternative for separating CO_2 from industrial gases (Kang & Lee, 2000; Duc *et al*., 2007).

The approach of gas hydrates as means of separation, especially in CO_2 capture, uses the van der Waals interactions between water molecules to encage gas molecules in the hydrate structure (SECOHYA, 2007). The concept consists in mixing water and a gas mixture containing CO_2 under hydrate-forming conditions, typically (and unless some appropriate additives are used) at low temperatures (< 300 K) and moderate pressures (> 0.6 MPa).

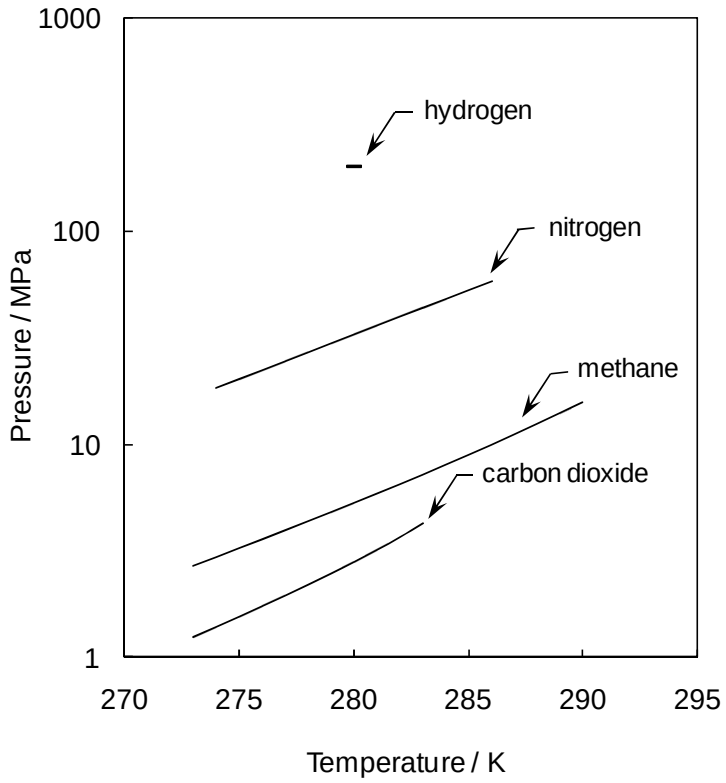


Figure 1.7. Carbon dioxide hydrate phase boundary compared to nitrogen, hydrogen and methane. CO_2, CH_4 and N_2 hydrate phase boundaries were predicted using HWHYD model and the point for H_2 hydrates is the data point reported by Mao and Mao (2004).

Based on the difference in the pressure and temperature conditions required for CO_2 hydrate formation compared to other industrial/flue gases (Figure 1.8), it is expected that CO_2 will preferentially enter the hydrate phase and thereby be separated.

Figure 1.9 shows a schematic flow diagram of the hydrate-based gas separation (HBGS) process suggested by Kang *et al.* (2000), especially for recovering CO_2 from flue gas. The flue gas from a power plant is first passed through the commercial desulfurization facility for SO_X removal. The pretreated flue gas goes to the first hydrator charged with an aqueous solution containing thermodynamic additive. However, the next two hydrators contain only water. More than 99

mole % of CO_2 is expected to be removed from the flue gas through this process (Kang *et al.*, 2000).

When gas hydrate crystals are formed the concentration of CO_2 in the hydrate phase is different than that in the original gas mixture. The CO_2-rich phase is then dissociated by depressurization and/or heating at ambient temperature to recover the enriched CO_2 gas. This results in a fractionation similar to that between a gas phase and a liquid phase in a distillation column. The main difference is that the fractionation is between a gas phase and a solid phase (SECOHYA, 2007).

A noticeable progress in processes involving CO_2 gas hydrates can be evidenced through the studies reported in the literature. Among the most recent proposals, Surovtseva *et al.* (2011) have suggested a CO_2 capture technology incorporating two low-temperature processes, namely cryogenic condensation and hydrate formation. This separation approach, as shown Figure 1.10, can be applied to industrial gasification facilities, where more than 80 mole % of CO_2 is expected to be captured at temperatures around 275 K and pressures above 5 MPa.

In CO_2 recovering from flue gas, pressure, temperature and compositional data are useful for engineering purposes. The isothermal *p-x* diagram given in Figure 1.11 conceptually illustrates the two-stage separation required to achieve the recovery of more than 95 mole % CO_2 from a (CO_2 + N_2 + H_2O) mixture by hydrate crystallization (Kang & Lee, 2000). Because of the importance of such data, simultaneous compositional analysis and hydrate phase equilibria measurements have been considered within the scope of this work.

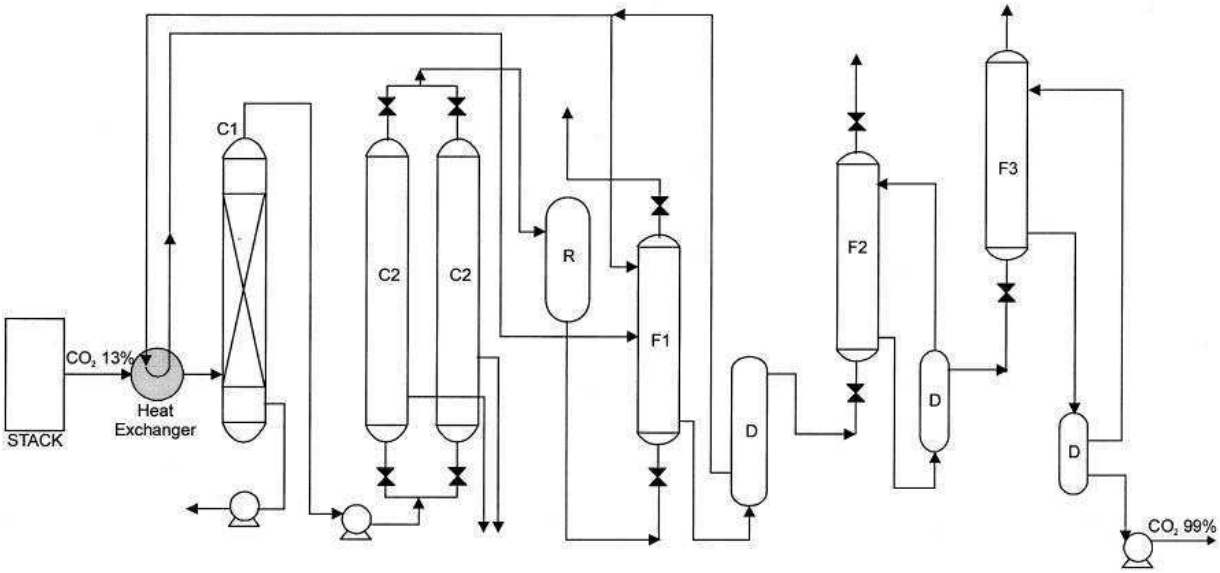


Figure 1.8. Flow diagram of a hydrate-based CO_2 recovery process, as proposed by Kang and Lee (2000). C_1: precipitator, C_2: condenser, D: dissociation unit, R: reservoir, F_1: first hydrator containing thermodynamic additive aqueous solution, F_2 and F_3: second and third hydrators.

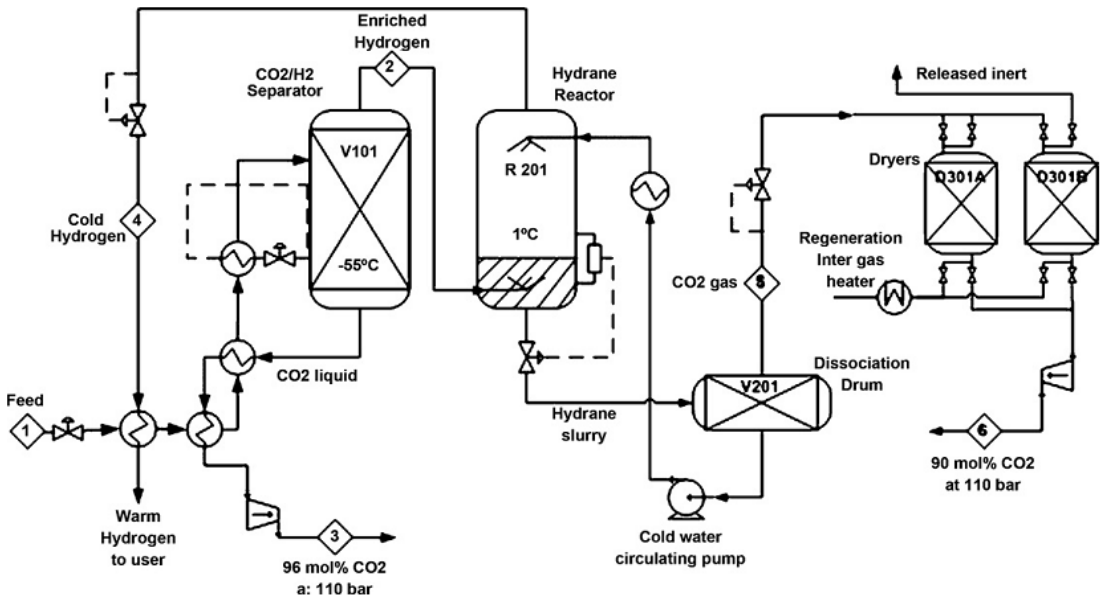


Figure 1.9. Flow diagram of an integrated cryogenic and hydrate CO_2 capture process, as suggested by Surovtseva *et al.* (2011).

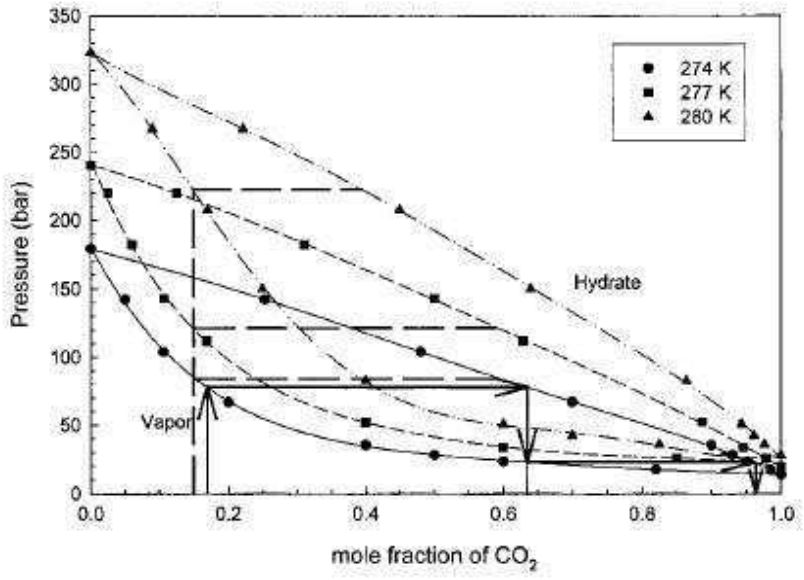


Figure 1.10. Conceptual separation stages required for recovering CO_2 from (CO_2 + N_2) hydrates at three different temperatures, as proposed by Kang and Lee (2000).

As shown in Figure 1.8, high pressure conditions are in theory required to form hydrates from gas mixtures containing N_2 or H_2. However, flue gas emissions are in general close to atmospheric pressure (Table 1.2). Operative costs would significantly increase if compression of these gases is considered in order to satisfy hydrate formation conditions. This is a major drawback of hydrate-based separation processes that reduces its energy efficiency. The impact of such phenomenon could be, however, minimized by using thermodynamic promoters. Consequently, there has been recently an increased interest in some large guest molecules that promote hydrate formation, known as thermodynamic additives. Such chemicals shift the hydrate phase boundary, reducing the pressure and amount of cooling required for gas hydrate formation.

As mentioned earlier, potential domains of application of hydrate crystallization approach include: seawater desalination, wastewater treatment, oil and gas separation, storage and transportation of natural gas, and CO_2 capture. Thus, the study of thermodynamic additives capable of reducing the hydrate formation pressure and increasing the gas hydrate equilibrium temperature and/or formation rate along with possible modification of the selectivity of hydrate

cages for encaging various gas molecules in the water cages (Mohammadi *et al*., 2011*a*) has become an emerging subject of industrial and scientific interest.

1.2.7 Use of Thermodynamic Promoters

Gas hydrate based-separation processes could be improved by looking for appropriate thermodynamic additives to decrease the operative pressure when necessary. Since the presence of thermodynamic additives alters the state of the liquid phase, the pressure-temperature conditions at which hydrates form are consequently shifted to milder conditions. In recent years, considerable efforts have been made to investigate gas hydrate crystallization approach for separating a specific gas constituent from a multi-component gaseous mixture under favorable temperature and pressure conditions.

Table 1.5 provides an overview of the state-of-the-art on hydrate phase equilibrium studies reported in the literature by the time this research began (in 2008). Emphasis is given to gas mixtures containing CO_2, CH_4, N_2 or H_2. Up to date studies are referred in later sections. Furthermore, an exhaustive compilation of hydrate phase equilibrium data is provided by Sloan and Koh (2008). Also, other studies can be found in a comprehensive review by Eslamimanesh and coworkers (2012).

The selection of appropriate thermodynamic additives is subjected to the potential field of application. Various intermediate sized hydrocarbons have been identified as thermodynamic promoters, namely the sII hydrate-formers: cyclopentane, neopentane, benzene, and cyclohexane, and the sH hydrate-formers: methylcyclopentane, methylcyclohexane, neohexane, and 2,2,3 trimethylbutane. Such intermediate sized hydrocarbons are known as heavy hydrate formers (HHF). Common for the HHFs is their relatively low solubility in water. This characteristic may be attractive when considering, *e.g.*, desalination or wastewater treatment where the main purpose of hydrate formation is to produce a cleaner water phase (SECOHYA, 2007).

Table 1.5. Literature experimental studies for hydrate phase equilibria of gas mixtures containing $CO_2 + CH_4$, N_2 and H_2.

1949	Unruh and Katz	$CO_2 + CH_4 + H_2O$	Reported phase equilibrium data and determined vapor phase concentration indirectly
1971	Robinson and Mehta	$CO_2 + H_2O$	Measured CO_2 hydrate phase equilibrium at T = 274 – 283 K and p = 1.3 – 4.5 MPa
1983	Berecz and Balla-Achs	$CO_2 + CH_4 + H_2O$	Hydrates exhibited instability at CO_2 mole fraction > 50%
1991	Adisasmito and coworkers	$CO_2 + CH_4 + H_2O$	Confirmed and extended Unruh and Katz data. Demonstrated feasibility of using gas hydrates as separation method of CO_2 from CH_4-rich gases.
1996	Ohgaki and coworkers	$CO_2 + CH_4 + H_2O$	Measured P and compositional (L_W–H–V) equilibrium data at 283 K
1997	Spencer	$CO_2 + H_2 + H_2S + H_2O$	Patented the principle of CO_2 capture by gas hydrate crystallization
1999	Fan and Guo	$CO_2 + CH_4 + H_2O$ $CO_2 + N_2 + H_2O$	Concluded that a 3.48 mole % CH_4/CO_2 slightly increases the hydrate formation pressure and N_2 significantly increases hydrate formation pressure compared to pure CO_2 hydrates
2000	Seo and coworkers	$CO_2 + CH_4 + H_2O$ $CO_2 + N_2 + H_2O$	Measured (H-Lw-V) equilibrium dissociation conditions and hydrate and vapor phase compositions
2001	Kang and coworkers	$CO_2 + N_2 + H_2O$	Studied p-T ranges of hydrate stability with and without hydrate promoter. Demonstrated high pressure requirements in the case without additive
2002	Hachikubo and coworkers	$CO_2 + CH_4 + H_2O$	Reported (L_W-H-V) equilibrium data
2004	Tajima and coworkers	$CO_2 + N_2 + O_2 + H_2O$	Compared various CO_2 separation processes and showed that gas hydrate technology consumes the largest amount of energy due to the higher pressure conditions required to form hydrates
2005	Uchida and coworkers	$CO_2 + CH_4 + H_2O$	Measured the change of vapor-phase composition using gas chromatography and Raman spectroscopy
2005	Sugahara and coworkers	$CO_2 + H_2 + H_2O$	Investigated isothermal phase equilibrium (pressure–composition in the gas phase) in the presence of gas hydrate phase
2006	Kumar and coworkers	$CO_2 + H_2 + H_2O$	Determined incipient equilibrium hydrate formation conditions
2007	Duc and coworkers	$CO_2 + H_2O$ $N_2 + H_2O$ $CO_2 + N_2 + TBAB + H_2O$	Compared equilibrium pressure of CO_2 and N_2 pure hydrates with and without TBAB. Concluded hydrate crystallization pressure decreases by a factor from 10 to 50 for both CO_2 and N_2 hydrates when adding TBAB
2007	Linga and coworkers	$CO_2 + N_2 + H_2O$ $CO_2 + H_2 + H_2O$	Provided basic thermodynamic and kinetic data for conceptual process design
2008	Beltran and Servio	$CO_2 + CH_4 + H_2O$	Measured (L_W–H–V) equilibrium conditions and gas phase compositions
2008	Bruusgaard and coworkers	$CO_2 + N_2 + H_2O$	Measured (L_W–H–V) equilibrium conditions including gas phase compositions

In oil and gas separation, and storage and transportation applications, where the purpose of the additives is to boost the conversion of gas into hydrates, it may be, however, desirable to be able to separate the hydrate promoters from the remaining hydrate formers under atmospheric pressure. This makes the use of water-soluble hydrate formers as promoters an attractive option. Various organic compounds belong to the group of water-soluble hydrate formers.

Examples are acetone, ethylene oxide, trimethylene oxide, tetrahydrofuran (THF), 1,3-dioxalane, 1,3-dioxane, and 1,4-dioxane (Kang *et al*., 2001; Seo *et al*., 2001; Mandal & Laik, 2008). In fact**,** the hydrate promotion effects of THF have been extensively studied (Kang *et al*., 2001; Seo *et al*., 2001; Lee *et al*., 2005; Delahaye *et al*., 2006; Sabil, 2010). Especially, since it forms, at atmospheric pressure, the same crystal structure (sII hydrate) as those formed (generally at elevated pressures) by several natural gas hydrate-formers. Nevertheless, most of the above mentioned substances are not suitable for practical purposes because of their high costs, toxicity or volatility**.**

Among the variety of thermodynamic additives that have been proved to reduce the operative conditions of gas hydrates formation, tetraalkyl ammonium salts, such as Tetra n-Butyl Ammonium Bromide (hereafter, TBAB), have the advantage of being stable at atmospheric pressure (Kamata *et al*., 2004), more environmentally friendly and easy to handle. Other features of using ammonium salts additives as hydrate promoters include an overall increase in the CO_2 capture rate of up to 90 % (Figueroa *et al.*, 2004).

1.2.8 TBAB Semi-Clathrates

A different type of clathrate compound with large organic functional groups, known as ‘semi-clathrates’ (sc), is formed in the presence of tetra-alkylammonium or quaternary ammonium salts (Jeffrey, 1984). The formation of hydrates from such ionic compounds was, perhaps, first studied by Fowler and coworkers in 1940 and further investigated by McMullan and Jeffrey in 1959, Davidson (1973) and later by Dyadin and Udachin in 1984.

A large number of quaternary ammonium salts, generally denoted TBAX (with X being bromide, chloride, fluoride, nitrate *etc*), are known to form semi-clathrates. For instance, as shown in Figure 1.12, Tetra-n-Butyl Ammonium Fluoride (TBAF) has shown to drastically increase the temperature required for forming CO_2 semi-clathrates compared to TBAB and Tetra-n-Butyl Ammonium Chloride (TBAC) hydrate promoters (Li *et al*., 2010). On the other hand, TBAB is considered a non-volatile, non-flammable and non-toxic compound (Tanasawa & Takao, 2002; Obata *et al*., 2003; Chatti *et al*., 2005). Furthermore, TBAB has been suggested in potential alternatives to industrial/flue gas separation (Shimada *et al*., 2003; Kamata *et al*., 2004; Duc *et al*., 2007), H_2 storage (Chapoy *et al*., 2007), transport processes (Fukushima *et al*., 1999; Hashimoto *et al*., 2006), *etc*., with promising results. Therefore, the present investigation focuses on TBAB as thermodynamic hydrate promoter.

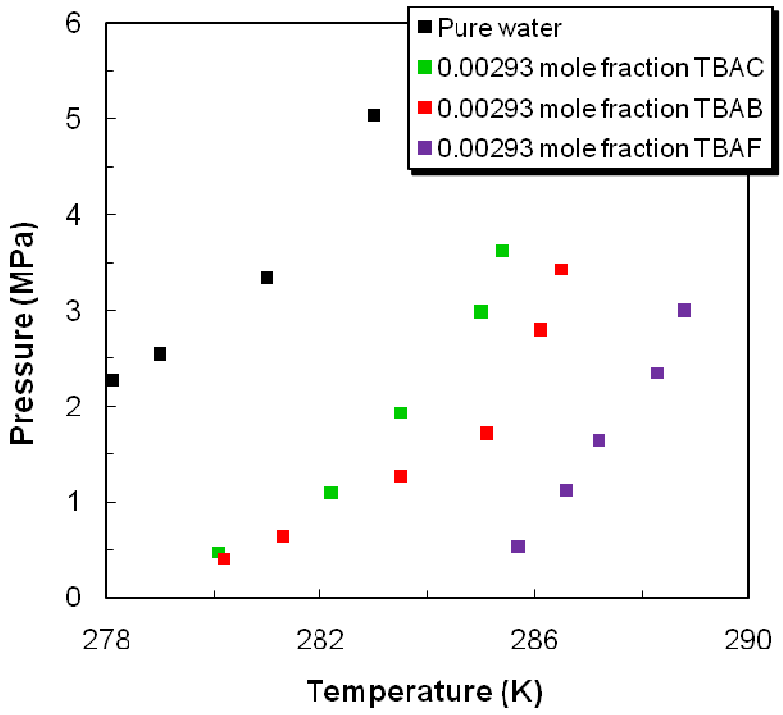


Figure 1.11. Promotion effect of various quaternary ammonium salts on the phase equilibrium conditions of CO_2 clathrate hydrates, as reported by Li *et al*. (2010). Symbols represent phase boundaries for (CO_2 + TBAC), (CO_2 + TBAB), and (CO_2 + TBAF) semi-clathrates in $2.93 \cdot 10^{-3}$ mole fraction of thermodynamic additive in aqueous solutions. Solid line represents the phase boundary of CO_2 clathrate hydrates without additive (predicted by CSMGem hydrate model).

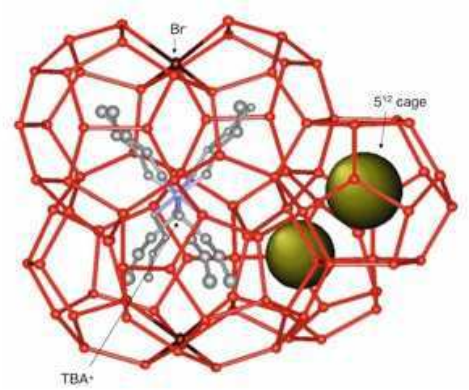


Figure 1.12. TBAB semi-clathrate structure, as reported by Shimada *et al*. (2005).

In TBAB semi-clathrates ($(C_4H_9)_4N^+Br^-\cdot qH_2O$), the bromide anions ($Br^-$) are hydrogen-bonded and selectively incorporated into the water lattices, while the tetra-n-butyl ammonium cations (TBA^+) behave as guest species (Jeffrey, 1984). As shown in Figure 1.13, in pure TBAB hydrate crystal with water molecules, the Br^- anion takes part of the crystal framework, while TBA^+ is located in the middle of a tetragonal cage arrangement. The shaded circles illustrate the empty dodecahedral (5^{12}) cages available for separating small gas molecules, such as CH_4 (Shimada *et al*., 2005).

As TBAB forms different hydrate crystal structures depending on the initial concentration of TBAB in aqueous solution and on temperature (Lipkowski *et al*., 2002), their structural behavior is quite complex and it has not been fully established. The temperature-composition phase diagram given in Figure 1.14, shows the two types of TBAB crystalline structures typically formed at atmospheric pressure, namely type A and type B. Morphologically, type A has been described to have a columnar (tetragonal) shape, while type B has an undefined (orthorhombic) form composed of thin crystals (Dyadin & Udachin, 1984; Oyama *et al*., 2005). From structural point of view, type B has been reported to have two TBAB cations and 76 H_2O molecules (Shimada *et al*., 2005). Furthermore, Oyama *et al*. (2005) reported a concentration of 18 wt.% as the intersection between the equilibrium curves of these two crystals. A maximum stability is observed at about 40 wt.% for type A (Shimada *et al*., 2003) and near 32 wt.% (Oyama *et al*., 2005) for type B. Additionally, the hydration number in TBAB semi-clathrate has been reported to vary from 2.03 to 36.0 (Lipkowski *et al*., 2002). Other hydration numbers of 26.0 and 38.0

have also been reported for type A and type B, respectively (Oyama *et al.*, 2005), accounting for the number of unique crystal structures formed.

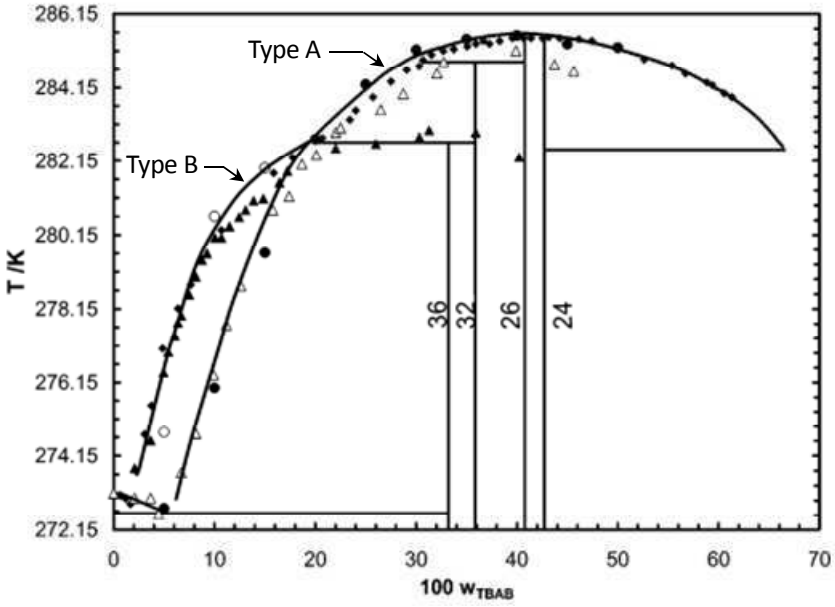


Figure 1.13. Temperature-composition phase diagram of (TBAB + H_2O) semi-clathrates under atmospheric pressure (Jeffrey & McMullan, 1967; Arjmandi and coworkers, 2007). Symbols represent experimental data and figures along the composition lines stand for hydration numbers.

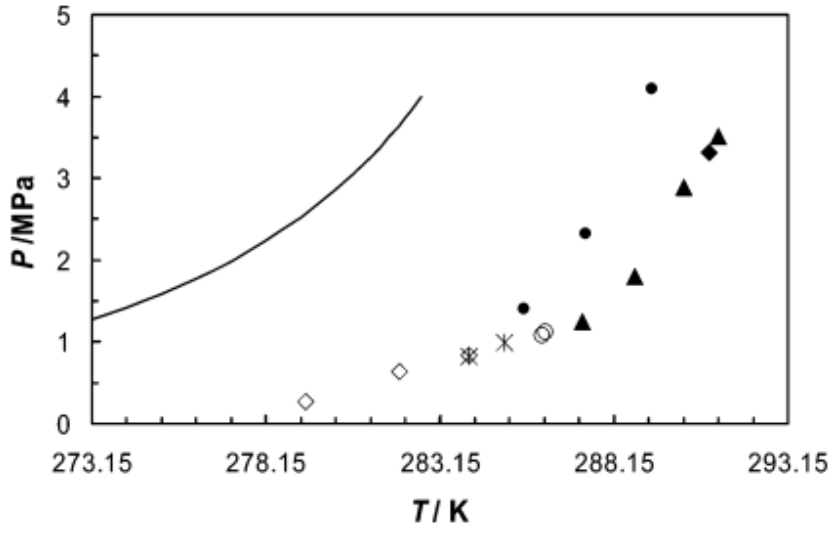


Figure 1.14. Carbon dioxide + TBAB semi-clathrates phase boundary. Symbols represent experimental data at different concentrations of TBAB in aqueous solutions. Solid line is the carbon dioxide hydrate phase boundary predicted by HWHYD model (Arjmandi *et al*. 2007).

Various gas molecules such as CO_2, CH_4, N_2, H_2 and H_2S, are likely of being selectively encaged in TBAB sc hydrates (Oyama *et al.*, 2005). Thus, the phase equilibria of TBAB semi-clathrates in the presence of the above gases have been a subject of numerous investigations in the last decade. For instance, Chapoy *et al.* (2007) measured dissociation conditions for (H_2 + TBAB) and (H_2 + TBAF) semi-clathrates. They compared the dissociation pressures to those of H_2 and (H_2 + THF) clathrate hydrates and suggested that H_2 is most likely enclathrated in (H_2 + TBAB) and (H_2 + TBAF) semi-clathrates. In addition, they reported an increased storage capacity in semi-clathrates of one order of magnitude (at 1 MPa), compared to that of (H_2 + THF) clathrates.

Duc *et al.* (2007) demonstrated that the presence of TBAB considerably decreases the formation pressure of simple hydrates (CO_2 or N_2) and mixed hydrates (CO_2 + N_2). Their experimental results suggest that CO_2 selectivity in the hydrate phase can be increased at least by four times compared to that of the gas phase. Also, a gas storage capacity of 30-35 (volume of gas per volume of hydrate) can be obtained for mixed hydrates (CO_2 + N_2 + TBAB). A representative phase diagram obtained by Arjmandi *et al.* (2007) for (CO_2 + TBAB) sc at different concentrations of TBAB in aqueous solutions is given in Figure 1.15. In their work, Arjmandi and coworkers concluded that hydrates formed from (CO_2 + TBAB) are more stable than (CO_2 + H_2O) hydrates.

The effect of 0.293 mole % TBAB on CO_2 separation efficiency from CO_2 (16.60 mole %) + N_2 binary mixtures by formation of semi-clathrate hydrates at 277.7 K and feed pressures ranging from 3.36 to 7.31 MPa was studied by Fan *et al.* (2009). Their results demonstrated that CO_2 could be remarkably enriched in the hydrate phase in the presence of TBAB even under lower feed pressure. In the same year, equilibrium formation pressures of CO_2 (0.159 mole fraction) + N_2 + TBAB were reported by Lu *et al.* (2009) at (0.05; 0.153; 0.348; 0.407 and 0.457) TBAB mass fraction in the temperature range of (278.05 to 287.85) K.

Deschamps and Dalmazzone (2009) measured hydrate dissociation temperature and pressure conditions for the formation of semi-clathrates from a CO_2 (0.249 mole fraction) + N_2 gas mixture in the presence of 0.4 mass fraction TBAB in aqueous solution using differential scanning calorimetry (DSC) technique. The effect of TBAB concentration on the dissociation

conditions of sc formed from flue gas mixtures has been recently investigated by Meysel *et al.* (2011). They reported three-phase (solid + liquid + vapor) equilibrium conditions for semi-clathrate formation from three binary mixtures of (CO_2 + N_2), with cylinder compositions of (0.20, 0.50 and 0.75 mole fraction of CO_2) in solutions of (0.05, 0.10 and 0.20) mass fraction TBAB.

In spite of the increasing number of investigations related to TBAB semi-clathrate, the role of this additive in the selective removal of CO_2 from multi-component gas streams is not fully understood. Thermodynamic data available in the literature are rather scarce. In addition, only two thermodynamic predictive approaches (Mohammadi *et al.*, 2010; Paricaud, 2011) have been proposed so far for semi-clathrates of (H_2 + TBAB) and (CO_2 + TBAB). Thus, there is a significant opportunity for investigating the phase equilibria of CO_2 containing gas mixtures in TBAB aqueous mixtures. Especially, as these data are required not only for practical purposes, but also for developing thermodynamic models capable of predicting the phase behavior of semi-clathrates.

1.3 Objective and Scope of the work

This work addresses the previous discussed limiting aspects of hydrate phase equilibria of CO_2 containing gas mixtures in the presence of TBAB aqueous solutions.

Provided that gas hydrates offer the possibility for developing a novel technology for CO_2 separation from flue and industrial gases, the conceptual design of a separation process based on gas hydrate crystallization requires reliable phase equilibrium data of CO_2 gas mixtures under hydrate forming conditions. As indicated earlier, compositional measurements need to be carried out to characterize the involved phases. With this intention, the following gas mixtures: **(**CO_2 + CH_4**)**, **(**CO_2 + N_2**)** and **(**CO_2 + H_2**)**, relevant to CCS technologies based on gas hydrates are studied. In addition, the phase equilibria of some of these gases are investigated in the presence of TBAB aqueous mixtures. The aim of this thesis is:

To provide reliable experimental data on the hydrate phase equilibria of gas mixtures containing CO_2 in the presence of pure water and TBAB aqueous solutions, as a function of the

concentration of TBAB and temperature, to enhance the fundamental knowledge of hydrate formation and dissociation from thermodynamics point of view.

The specific objectives and expected contributions of this thesis are as follows:

- To develop a new experimental set-up for gas hydrates phase equilibria studies. A significant outcome is expected in terms of the accuracy of the data measured, the apparatus suitability for (gas-liquid-hydrate) equilibrium measurements at high pressures, and the incorporation of a capillary sampling device coupled with gas chromatography for compositional analysis.

- Determination of the hydrate dissociation conditions and compositional data for: (a) (CO_2 + CH_4), (CO_2 + N_2) and (CO_2 + H_2) hydrates; and (b) CO_2, CH_4, N_2 and (CO_2 + N_2) semi-clathrates in the presence of TBAB aqueous solutions. Better understanding of the thermodynamic stability of the above systems, along with the most favorable process operating conditions (temperatures and pressures) and separation efficiencies (compositions) are expected to be obtained from these measurements.

- Elucidation of the effect of TBAB on the equilibrium conditions of CO_2, CH_4, N_2 and (CO_2 + N_2) semi-clathrates, for establishing the role of TBAB as thermodynamic promoter.

- Investigation of the reliability of thermodynamic models predictions for CO_2 hydrate-forming systems.

This thesis consists of seven chapters. Having examined the industrial context, along with current state-of-the-art of phase equilibrium studies for CO_2 hydrate-forming systems in this introductive chapter and with the objectives of the thesis established; the following chapter covers the theoretical basis for the experimental determination of thermodynamic properties of gas hydrates. The principles and preferred experimental procedures, along with the criteria for establishing equilibrium are also discussed in the 2nd chapter. Besides, other experimental issues, such as the calibration of measuring devices, uncertainties, and the determination of the phase compositions in equilibrium with gas hydrates are addressed as well in the 2nd chapter.

The core of the comprehensive experimental work carried out throughout this thesis is presented in Chapters 3 to 6. Phase equilibrium measurements of gas hydrates of (methane + carbon dioxide), which were performed using an existent apparatus, are the subject of the 3rd chapter. The generated hydrate dissociation data along with literature data are compared with the predictions of a thermodynamic model and a literature empirical equation, discussions are made on the deviations between experimental and predicted data. Comparisons are also presented with literature data. The identification of pertinent experimental difficulties encountered and the need of measuring reliable compositional data for mixed hydrate systems at high pressures and in the presence of corrosive gases provided the justification for developing a new and more versatile experimental set-up.

A combination of new and adopted features from the literature was thus considered in the design of the new apparatus. The development of the new equipment, based on the 'static-analytic' technique with capillary gas phase sampling, is detailed in Chapter 4. The apparatus incorporates precise and accurate measuring devices and the visual observation of the presence of gas hydrates and phase behavior, with promising results. As an example, new hydrate dissociation and compositional data measured for (CO_2 + CH_4 + H_2O) systems are presented in the 4th chapter.

In the 5th chapter, the phase equilibria for gas hydrates of (CO_2 + N_2 + H_2O) and (CO_2 + H_2 + H_2O) are investigated. The conditions at which CO_2 separation is thermodynamically favored and the effect of the composition of the feed on the equilibrium dissociation pressures are discussed. Moreover, comparisons with literature data are presented and analyses are provided on the deviations obtained between experimental and predicted data using two thermodynamic literature models for the (CO_2 + N_2 + H_2O) systems.

The 6th chapter is devoted to experimental measurements of gases in TBAB aqueous mixtures. The promotion effect of TBAB is thoroughly discussed in this chapter. In addition, optimum operating conditions for separating CO_2 from flue gases are proposed based on the experimental data.

In the 7th and final chapter of this thesis, the general concluding remarks are presented together with some directions for further investigating the thermodynamics of semi-clathrates.

2

Experimental Methods and Analysis Techniques for Gas Hydrates Phase Equilibrium Measurement



† Extracted from the forthcoming book by Deiters and Kraska (2012).

2

Résumé

Dans ce chapitre, nous fournissons les formalismes théoriques pertinents en relation avec la détermination expérimentale des propriétés thermodynamiques de systèmes contenant des hydrates de gaz. L'accent est mis principalement sur les techniques expérimentales concernant les pressions modérées et relativement élevées. Les appareils les plus courants et les procédures expérimentales utilisées y sont décrites. Les principes, le choix des techniques utilisées et les critères en vue d'établir un équilibre sont expliqués. De plus, nous discutons l'étalonnage des différents capteurs et du détecteur du chromatographe en phase gazeuse, les incertitudes expérimentales correspondantes, l'échantillonnage difficile des fluides et la détermination des compositions des phases à l'équilibre pour les mélanges de gaz.

Abstract

In this chapter the theoretical formalisms relevant to the experimental determination of thermodynamic properties of systems containing gas hydrates are provided. Emphasis is given to experimental techniques at pressures ranging from moderate to relatively high pressures. The most common devices and experimental procedures employed are described. The principles, the choice of the techniques used and the criteria for establishing equilibrium are explained. Likewise, the calibration of measuring sensors and gas chromatograph detector, the corresponding experimental uncertainties, and the challenging fluid sampling and determination of the equilibrium phase compositions for gas mixtures are discussed.

2 Experimental Methods and Analysis Techniques for Gas Hydrates Phase Equilibrium Measurement

2.1 Overview

Design, development and operation of chemical processes require a cyclical and interactive strategy involving conceptual, experimental, modeling and simulation stages (Richon, 2009). A proper design process should follow the sequence from conception of ideas through literature review, selection, design and construction of equipment, methods, tests and set up, measurements, data reliability and consistency tests to the final implementation, as depicted in Figure 2.1.

The development of new technologies based on gas hydrates crystallization approach requires specific temperature and pressure conditions and the utilization of complex systems with many components that are beyond usual operations and existing databases. Moreover, industrial design relies on accurate modeling and modeling relies on reliable experimental data (Richon, 2009). Thus, experimental thermodynamics are of industrial significance.

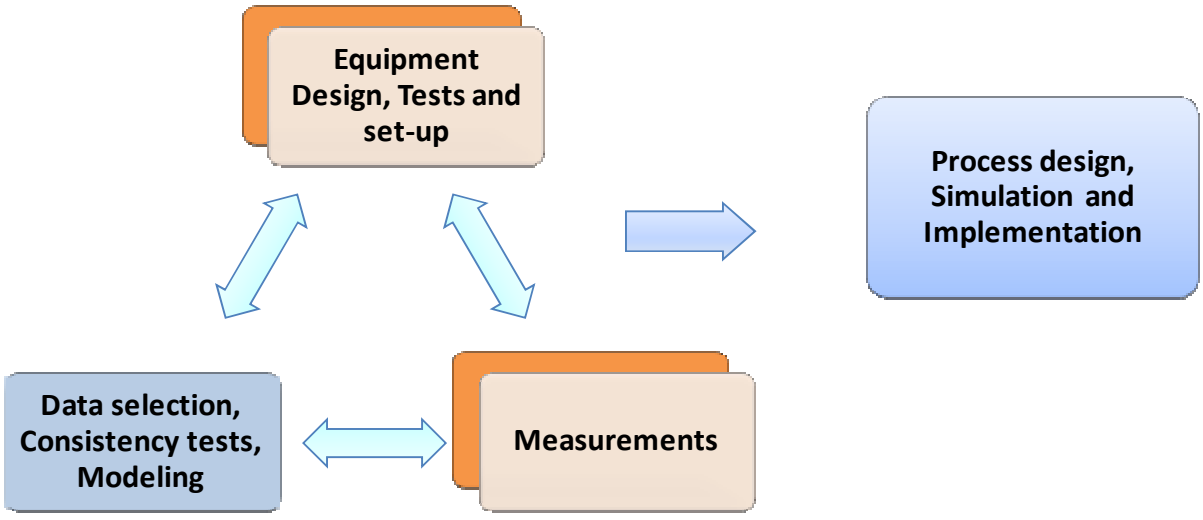


Figure 2.1. Process design strategy (adapted from Richon, 2009 and Soo, 2011). The highlighted blocks indicate the stages addressed in this research.

Suitable combination of temperature and pressures above the gas-hydrate-liquid phase boundary is normally required for hydrate formation. Therefore, phase behavior studies for systems containing gas hydrates are mainly concerned with experimental techniques suited for pressures ranging from moderate to relatively high pressures, so only these types of techniques are concisely discussed.

A variety of methods have been developed for high-pressure fluid phase equilibria measurement. Nonetheless, their suitability will depend on the application, the system under investigation, the properties to be measured and the required accuracy. Several review articles on this subject are available in the literature. For instance, some of the most meaningful contributions possibly are: The Volume VII of The International Union of Pure and Applied Chemistry (IUPAC) monograph series on 'Experimental Thermodynamics' (Weir & de Loos, 2005), which contains a valuable state-of-the-art covering thermodynamic measurement techniques for multicomponent mixtures. Also, the series of reviews published by Dohrn and coworkers (1995, 2002, 2010, 2011) that not only provide a compilation of systems for which high-pressure phase-equilibrium data have been investigated over the past three decades, but a classification scheme of experimental methods as well. Moreover, the advancements on accurate and effective experimental equipment for phase equilibrium measurements are examined by Richon (1996) and Richon and de Loos (2005); and the broad range of static and dynamic equipment are reviewed by Raal and Mühlbauer (1998).

Richon (1996) and Dohrn *et al*. (2010) propose different classifications of experimental methods for the determination of high-pressure phase equilibria. Both classifications share several similarities, however, the one proposed by Richon (1996) is based on the method of equilibration between phases in equilibrium, whereas Dohrn *et al*. (2010) classify the different experimental methods according to the way compositions of the equilibrium phases are measured and whether the mixture to be investigated is prepared with precisely known composition or not, namely 'analytical methods and synthetic methods' (Deiters & Schneider, 1986).

Even if classification of the methods for measuring phase equilibria is not straightforward, returning to the classification proposed by Richon (1996) and Richon and de Loos (2005),

essentially two main categories are distinguished: dynamic (open circuit) methods involve forced circulation of one or more phases, whereas in static methods (closed circuits) equilibrium can be achieved with or without recirculation of fluid phases, generally using an internal stirring mechanism to reduce the time required for reaching equilibrium (Raal & Mühlbauer, 1998). Refined schemes based on this classification can be found in the book of Raal and Mühlbauer (1998) and in the doctoral dissertation of Afzal (2009).

Based on the above classification, this work takes advantage of a combination of features from static, analytical and synthetic methods and the use of modern measuring devices and materials to bring about a new perspective for performing hydrate phase equilibrium measurement. In particular, special attention is given to the precision and accuracy of the results obtained. The principles, the choice of the techniques used and the criteria for equilibrium are presented in this chapter. In addition, the calibration of measuring sensors and gas chromatograph detector, experimental uncertainties and the determination of the equilibrium phase compositions for gas mixtures are discussed.

2.2 Visual versus Non-visual Techniques

A further distinction among the most frequently used experimental methods for determining hydrate equilibrium conditions can be made between those based on visual and non-visual means of hydrate detection. Particularly at low pressures, visual observation of the formation and dissociation of hydrate crystals was successfully implemented in a Pyrex tube flow apparatus by Hammerschmidt in 1934 and in a windowed cell by Deaton and Frost in 1937 (Sloan & Koh, 2008).

As the above method requires the visual observation of hydrate crystals (at constant temperature or pressure) it may only be used at temperatures above the freezing point of water to avoid any confusion with ice crystals (Schroeter *et al*., 1983). Also time for equilibration might take several hours, thus it may become somewhat time consuming. As an alternative, hydrate phase equilibrium measurement at high and low pressures can be performed in a constant volume

(isochoric) cell without need of visual observation and the intersection point of the cooling and heating isochors is considered the dissociation condition.

Three modes have been thus established for operating a hydrate formation apparatus: isobaric, isothermal and isochoric (Sloan & Koh, 2008). Table 2.1 summarizes the fundamentals of each method. The feasibility of using isothermal method for measuring hydrate dissociation pressures has been recently investigated for (CO_2 + H_2O) system in a titanium variable volume cell (Fontalba *et al.*, 1984), with promising results (D. Richon, Personal Communication, March 9, 2012). As equilibrium is reached within 5 minutes, a significant amount of time could be potentially saved using this technique for measuring hydrate dissociation data. The hydrate dissociation pressure is identified by the presence of a plateau in a pressure versus piston-displacement plot. The composition of the hydrate phase can be determined from the PVT data and the amount of gas released during hydrate dissociation (known from the with of the plateau). For multicomponent systems additional calculations are required, possibly compromising the accuracy of the obtained equilibrium data.

The hydrate dissociation point is a repeatable thermodynamic equilibrium point (Tohidi *et al.*, 2000) and is defined as the temperature and pressure condition where the last hydrate crystal melts (Gjertsen & Fadnes, 2006).

Table 2.1. Commonly used experimental procedures for measuring hydrate dissociation conditions (Sloan & Koh, 2008).

Method	**Principle**	**Hydrate formation**	**Hydrate dissociation**
Isothermal	Constant temperature	Temperature increase	Visual observation of hydrate crystal disappearance
Isobaric	Constant pressure	Exchange of gas or liquid from an external reservoir	
Isochoric	Constant volume	Pressure decrease	Intersection point of cooling and heating isochors (nonvisual technique)

Therefore, in all three procedures hydrate dissociation is used to determine the hydrate dissociation (*p, T*) condition. In the isothermal and isobaric methods, the equilibrium condition is determined (at constant pressure or temperature, respectively) by visual observation of a phase change, *e.g*. hydrate crystals disappearance. Whereas a corresponding change in pressure as a function of temperature (due to density changes) in a constant volume cell indicates hydrate formation and/or dissociation in the isochoric method described below.

2.3 The Isochoric Method

Hydrate dissociation data can be accurately determined using an isochoric apparatus. The technique is based on the classical isochoric procedure developed in Professor Kobayashi's laboratory (Marshall *et al*., 1964) and further improved by Tohidi and coworkers (2000), who outlined the impact of measuring techniques, mixing efficiency, heating method and heating rate on the accuracy of hydrate dissociation point measurements.

In a typical isochoric experiment, hydrates are formed by decreasing the system temperature. The differential pressure change ∂p is measured with respect to the accompanying differential temperature change ∂T in a constant volume cell. For each load of known composition, pressure is monitored as a function of temperature making possible the determination of a *p-T* isochor (Richon & de Loos, 2005). The quantity $(\partial p/\partial T)_V$ represents the slope of an isochoric path in a *p-T* phase diagram. Hydrates are then dissociated through stepwise heating. The intersection of the cooling and heating curves represents a phase transition, thereby indicating the hydrate dissociation (*p, T*) point (Ohmura *et al*., 2004). By plotting several experimental isochors obtained at different pressures for a given load, the complete hydrate phase boundary of a system is obtained.

In the isochoric method, the equilibrium condition is established through temperature and pressure measurement. No visual observation or complicated calculations are required, allowing a reliable determination of hydrate equilibrium data. Additionally, the technique is suitable over the entire range of hydrate formation temperatures and pressures, and fewer amounts of fluids

are used, as no volume changes are required. Furthermore, it is suited to automated control of experiments (Rivollet, 2005; Khalil, 2006). Thus, isochoric methods are considered rather advantageous to investigate the phase behavior of multicomponent mixtures, compared to isobaric and isothermal approaches with visual observation requirement. For the above reasons, the isochoric method combined with stepwise heating and efficient mixing (Tohidi *et al.*, 2000) is applied in the present investigation.

2.4 Apparatuses for the Determination of Hydrate Phase Equilibria

It is beyond the scope of this work to provide an exhaustive review of the experimental equipment that have been employed for measuring hydrate phase equilibria. The features of the most commonly used apparatus and experimental techniques considered in this section have been mainly derived from the excellent review of Sloan and Koh (2008), with the addition of representative examples from the literature in order to illustrate their main advantages, but also some of the experimental difficulties typically encountered. Three proven experimental approaches representative of current developments are mentioned in the following paragraphs.

The static technique is one of the classical procedures for measuring hydrate phase equilibrium data, especially at high pressures. The starting point of contemporary experimental studies carried out in static apparatuses is that of Deaton and Frost (1937). In their apparatus, a glass windowed equilibrium cell, shown in Figure 2.2, was placed in a thermo-regulated bath. The cell was equipped with a valve system to allow for inlet and outlet gas flow regulation. The use of thermocouples and pressure transducers enabled measurement of temperatures and pressures. The protocol in obtaining phase equilibrium data involved visual confirmation of hydrate formation and disappearance. The above basic principles have not significantly changed over the past decades. Indeed, recent advances in the design of hydrate phase equilibria static equipment incorporate modern measuring instruments that improve experimental uncertainties; designs and materials that extend the operating ranges, careful construction and operation to investigate unusual conditions and systems; improvements in the data acquisition and minimization of monotony.

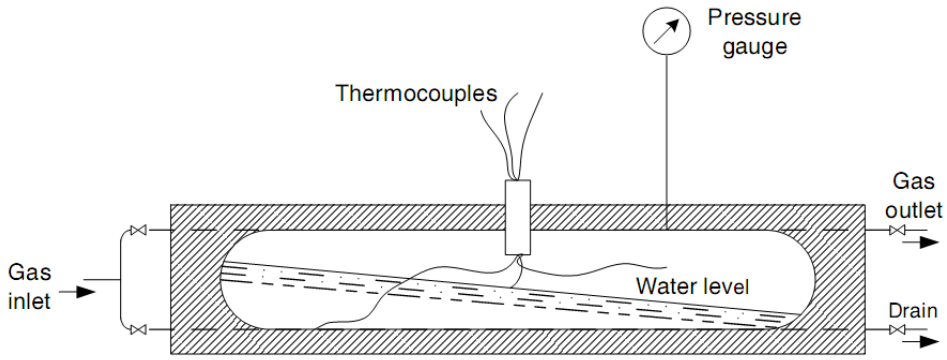


Figure 2.2. Detail of Deaton and Frost's hydrate formation equilibrium cell (as cited by Sloan & Koh, 2008).

Although accurate and thermodynamically consistent data can be obtained through static and dynamic approaches, static methods are generally preferred for the determination of phase equilibrium data (Oellrich, 2004). Some of the main advantages of static devices include:

- The simplicity of the technique and experimental set-up
- It can be applied at any temperature and over a wide pressure range
- Suitable for single and multiple component systems, allowing reliable evaluation of industrial systems
- Easy modification of total compositions and quantities of fluid samples
- Small amount of material needed
- Possibility of observing the phase behavior at high pressures

Time required to ensure that the system has achieved thermodynamic equilibrium remains still a major drawback for the determination of hydrate phase equilibria under static conditions, making it a quite time consuming method, especially when long metastable periods occur.

The Quartz Crystal Microbalance (QCM) exploited by Tohidi and coworkers (Burgass *et al*., 2002; Mohammadi *et al*., 2003) is an example of an alternative experimental approach suitable for measuring equilibrium data of gas hydrates (Figure 2.3). The QCM consists of a thin disk of quartz placed between two electrodes. Crystal oscillation at a particular resonant frequency is activated when an electric current passes across the electrodes. Hydrate formation is then detected by a change in the resonance frequency once hydrates have adhered to the surface of the

quartz crystal. Pressure and temperature of the system are measured using a pressure transducer and a thermocouple in a high pressure cell (Sloan & Koh, 2008).

The main advantage of QCM method is that it uses small amounts of samples (~ one droplet of water), resulting in a significant reduction in the time required for each experiment (Mohammadi *et al*., 2003). Although the QCM method has been considered unfeasible (Sloan & Koh, 2008) due to good contact requirement between the surface of the quartz crystal and hydrates, Lee *et al*., (2012) have recently demonstrated that by modifying the droplet size, this method yields acceptable results, especially, for rapid and practical gas hydrate application purposes, *i.e*. selecting a hydrate promoter from among various candidates.

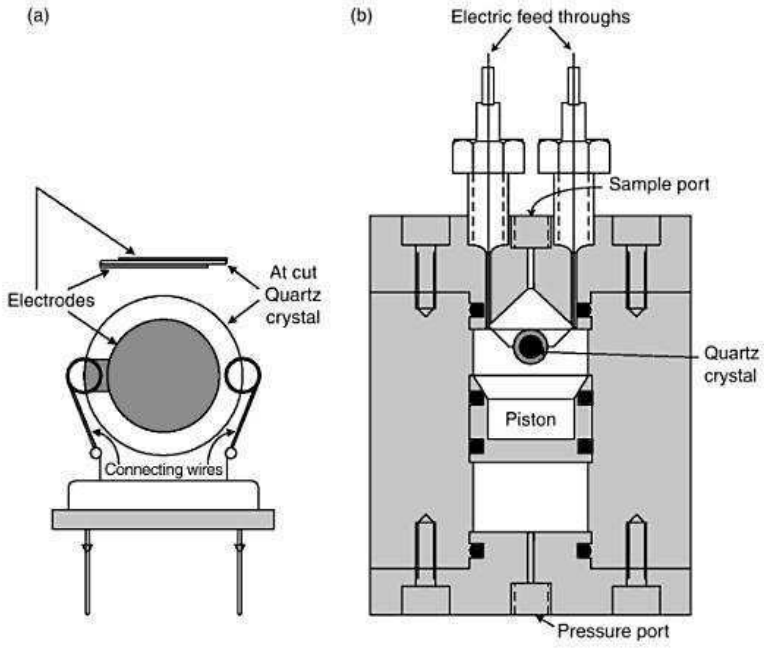


Figure 2.3. (a) Schematic diagram of the QCM, and (b) the QCM mounted within a high pressure cell (Burgass *et al*., 2002 and Mohammadi *et al*., 2003, as cited by Sloan & Koh, 2008).

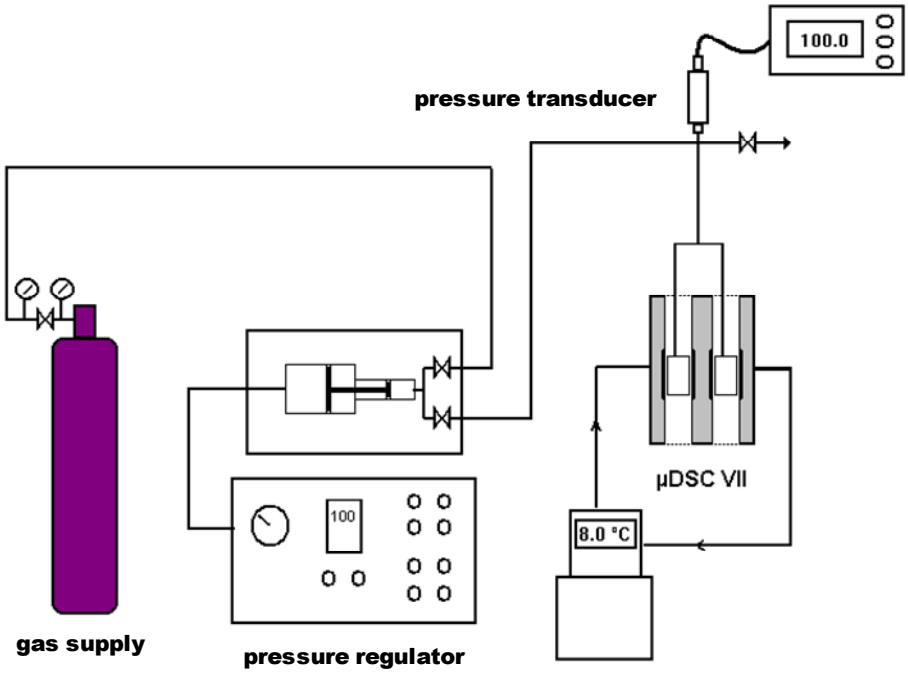


Figure 2.4. High-pressure micro DSC VII measurement device (Deschamps & Dalmazzone, 2009).

Most recently the use of calorimetric methods such as DSC has been extended to the determination of hydrate phase equilibria data and thermal property data for gas hydrates. A micro-DSC analyzer coupled with special high-pressure vessels, namely High Pressure Differential Scanning Calorimetry (HP-DSC) technique was introduced by Dalmazzone *et al.* (2002) to characterize the thermodynamic stability boundaries of methane and natural gas hydrates in solutions of inhibitors. The same technique has been applied to investigate dissociation enthalpies and the phase equilibria of TBAB semi-clathrates with gases (Deschamps & Dalmazzone, 2009). The device, as shown in Figure 2.4, consists of a microDSC VII, which measures the difference in heat flow between the sample and reference material. It can operate at temperatures between (228.15 and 393.15) K and up to 40 MPa coupled to a pressure multiplicator.

The main advantage of the micro-DSC technique is that it provides thermodynamic and thermal data simultaneously. Compared to PVT techniques, microcalorimetry has been reported (Le Parlouër *et al*., 2004) to be relatively faster and to require smaller sample amounts (~ 5 mg). However, differences in thermodynamic properties measured through similar calorimetric

techniques can be significantly larger than stated experimental uncertainties. For instance, considerable scatter has been recently reported for the equilibrium temperatures of tetrabutylphosphonium bromide semi-clathrates, measured through DSC by different laboratories (Suginaka *et al*., 2012).

The above descriptions of selected devices and experimental procedures are meant to provide the underlying principles for investigating the phase behavior of gas hydrates. Each method has its own advantages and limitations. However, the one based on the static apparatus, potentially one of the simplest and most accurate approaches, is selected for this work. The apparatus is operated following a combination of static, analytic and synthetic procedures. Such approach allows simultaneous determination of the (*p*-*T*) hydrate dissociation conditions and compositional: liquid (*x*), gas (*y*) and hydrate (*z*), phase equilibrium data for the gas hydrate systems of interest in this investigation.

2.5 Static-Analytic-Synthetic Measurements

There is no universal experimental technique capable of fully characterizing the phase behavior of multicomponent systems over the whole range of temperature and pressures. For mixtures with more than two components the information obtainable by non-analytical methods is limited (Raal & Mühlbauer, 1998). Thus, a combined “static-analytic” and synthetic approach is applied for obtaining reliable hydrate phase equilibrium data of CO_2 containing gas mixtures.

The hydrate dissociation conditions and the composition of the gas phase in equilibrium with the hydrate and liquid phases are determined via the so-called “static-analytic” technique, whereas a synthetic method is used to estimate the liquid and hydrate phase compositions (for systems containing pure water). Because sampling and analyzing liquid and hydrate phases is much more challenging, the combination of the above two methods in one set-up leads to the possibility of obtaining thermodynamic data of multiple phases simultaneously. An experimental set-up combining the above mentioned techniques has been developed within this research and it is fully described in Chapter 4.

The experimental procedure is as follows: a mixture of known composition is prepared in the equilibrium cell by introducing one component after the other. By accurately knowing the volume of the cell and the pressure and temperature of the mixture, the total number of moles and the composition of the feed can be precisely determined. Furthermore, the amount of liquid supplied to the cell is also precisely known. During the experiment temperature is varied following the isochoric pressure search method with stepwise heating and efficient mixing (Tohidi *et al*., 2000; Rovetto *et al*., 2006). After equilibrium has been obtained, small representative gas phase samples are withdrawn *in situ* without disturbing the equilibrium condition at each temperature step via an electromagnetic rapid online sampler-injector (ROLSI™) presented in detail in Chapter 4.

Compositional analysis is carried out through gas chromatography for the gas phase, whereas the liquid phase is analyzed at the reference temperature 293 K using a calibrated refractometer only for semi-clathrates formed from (CO_2 + N_2 + TBAB + H_2O). For systems investigated in the absence of TBAB, the compositions of the hydrate and aqueous phases are precisely calculated applying a material balance approach adopted from Ohgaki *et al*. (1996) in combination with the experimental data and volumetric properties, outlined in Chapter 4.

A pressure-temperature plot, as shown in Figure 2.5, is obtained from each experimental run. The intersection between the cooling and heating curves indicates the equilibrium transition from (hydrate + liquid + gas) to (liquid + gas) and hence is reported as the hydrate dissociation point. The procedure is repeated at different pressures in order to determine the hydrate phase boundaries over a wide temperature range.

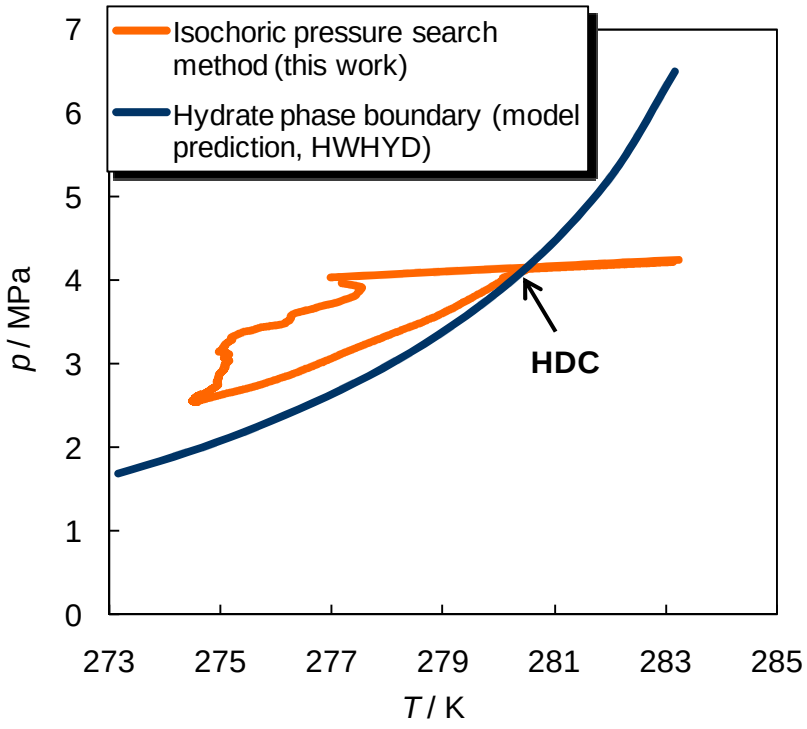


Figure 2.5. Hydrate dissociation conditions (HDC) determination following the isochoric pressure-search method and hydrate phase boundary (model predictions, HWHYD 2000) for the (0.748 mole fraction CO_2 + 0.252 mole fraction N_2 + water) system.

2.6 Gas Chromatography

Since the invention of the first gas chromatograph detector by British chemists James and Martin (1952) more than half a century ago, this instrumental technique also referred to as 'gas-liquid partition chromatography', has become widespread adopted for analyzing complex multi-component gas mixtures by industry and researchers. Up to 30 % of global gas chromatograph (GC) systems are currently implemented in Europe alone. The share is followed by United States and Japan.

Gas chromatography is a practical method of separation for analytical purposes. The type of GC used in this work involves separating the compounds of a gas mixture carried by the flow of an inert gaseous mobile phase (carrier gas), which are adsorbed onto the surface of an inert solid stationary phase. Figure 2.6 is a picture of the (Varian, CP3800) gas chromatograph used in this

work, with its main components: the injection system, the oven, the column (placed inside the oven) and the detector.

The gas sample is introduced, through the injector port, into the chromatographic column where separation takes place. The column is placed in the thermostated oven. The compounds of the mixture are separated throughout the column based on their affinity and interaction with the stationary phase, which translates into a characteristic gas chromatographic retention time. The thermal conductivity detector used in this work measures the heat conductivity of each separated compound that flows through the column, resulting in a peak area signal. The area of a peak in the chromatogram is proportional to the amount of each compound in the gas mixture. It must be noted that retention times in GC are extremely sensible to the column temperature and the carrier gas flow rate, which must be kept constant. The theoretical and practical aspects of this technique are treated in detail by Tranchant (1995).

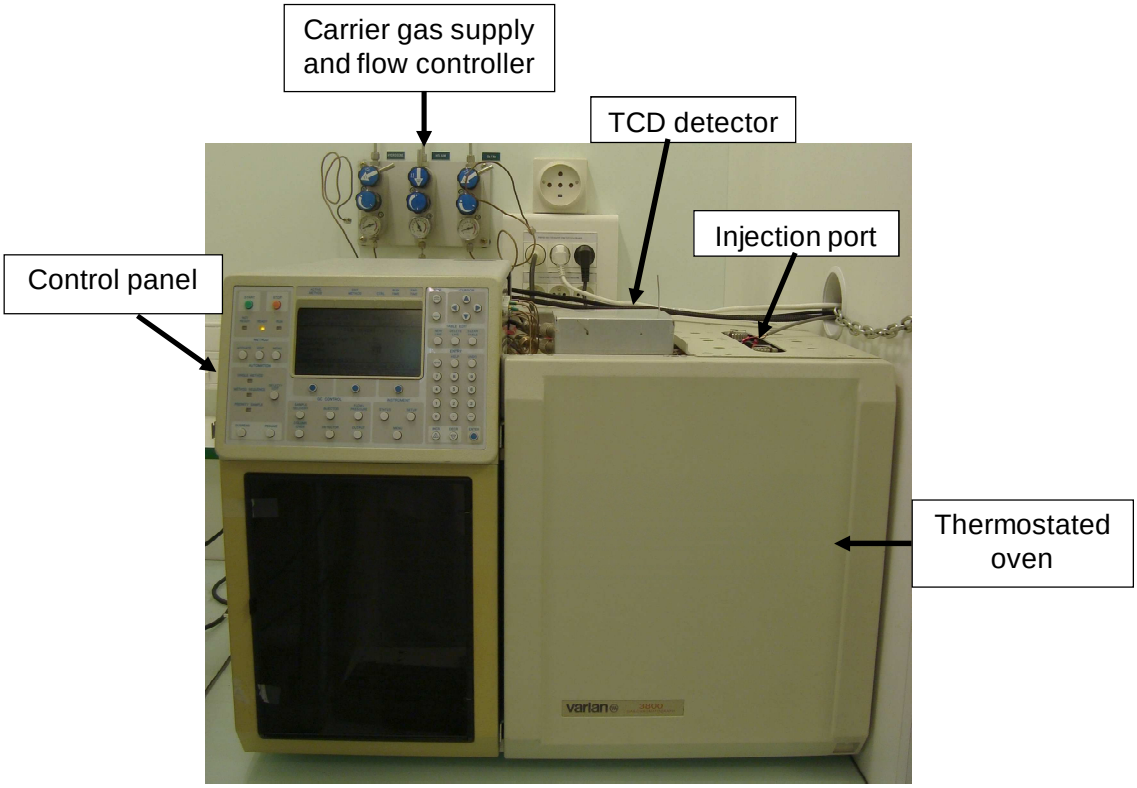


Figure 2.6. Front view of the gas chromatograph used in this work and main components.

2.6.1 Chromatographic Conditions

Several tests were performed to find the best chromatographic conditions to achieve favorable response times and peak resolution (difference in the retention times) in the separation of (CO_2 and CH_4), (CO_2 and N_2) and (CO_2 and H_2) gas mixtures. Four main factors contribute to achieve this separation: column packing type, column temperature, carrier gas flow rate and physical properties of components (Raal & Mühlbauer, 1998). Thus, different columns with different lengths and different temperature programming conditions were tested. A good separation of components is found via a 4 m long column packed with 80-100 mesh Porapak Q. It was noticed that increasing the oven temperature, with the aim of reducing the retention times for these components, leads to difficulties in CO_2 and CH_4 separations.

The oven temperature was thus set to 323 K and the carrier gas used was helium (He) with a 25 ml/min flow rate, except for the compositional analysis of (CO_2 + H_2) gas mixtures, where N_2 was used as a carrier gas because of the proximity in the thermal conductivities of He and H_2. Proper GC operating conditions used in this work are given in Chapter 3. A typical chromatogram showing two peaks each with a different retention time (t_{R1} and t_{R2}) for CO_2 and N_2 is presented in Figure 2.7.

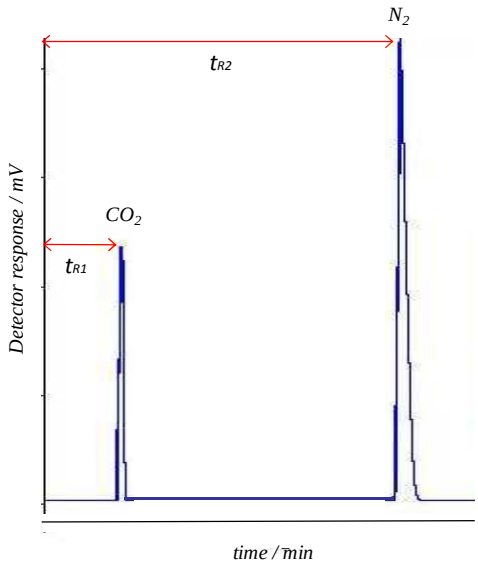


Figure 2.7. Gas chromatogram exhibiting an effective separation of a (0.748 mole fraction CO_2 + 0.252 mole fraction N_2) gas mixture.

2.7 Calibrating Measuring Devices and Experimental Accuracies

As hydrate phase equilibrium data with the highest possible accuracy are needed for developing reliable thermodynamic predictive tools and hydrate-based industrial processes, calibration of measuring instruments is a key concern in this work. The accuracy of the results depends to a large extent on the accuracy of measuring instruments. Thus, careful calibration of all measuring devices, *i.e*., temperature probes, pressure transducers, gas chromatograph detectors and *etc*. was performed against reference instruments (Figure 2.8) prior to performing the experimental work and periodically checked to determine the accuracy with which data are measured.



Figure 2.8. Calibration equipment used in this work: Dead weight balance device, temperature bath with reference platinum resistance thermometer probe, variable volume cell with displacement transducer for volumetric calibrations and gas chromatograph with a gas tight calibration syringe (clockwise).

2.7.1 Pressure Sensors Calibration

Pressure inside the equilibrium cell is directly measured by calibrated capacitance pressure transducers. Druck™ (type PTX611) pressure transducers are maintained at a constant temperature higher than the highest temperature of the study to avoid any possible condensation on the pressure measuring system. Calibration is carried out against a dead weight balance (Desgranges & Huot 5202S CP, Aubervilliers, France) for ranges from (0.3 to 40) MPa.

Pressure calibration is performed by connecting the reference instrument to a source of pressure (often nitrogen) and to the inlet of the equilibrium cell. The calibration procedure consists on counter-balancing the total downward forces (*i.e.* gravitational force of a central piston with added weights, as well as the atmospheric pressure measured via a Druck (model DPI 141) digital barometer with that of the pressure exercised by nitrogen gas loaded into the cell. Once this is achieved, pressure readings from the cell pressure transducers are allowed to stabilize and are recorded against the real pressure, which is calculated from the weights added to the piston.

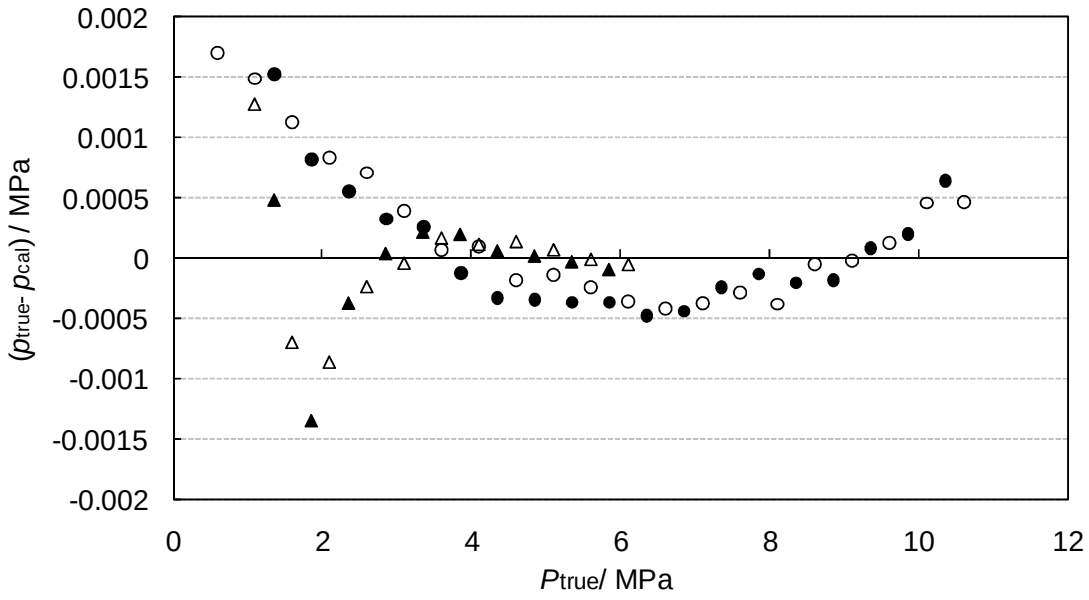


Figure 2.9. Relative uncertainty on pressure transducers calibration from (0.6 to 10.6) MPa. LPT: ▲, increasing pressure; Δ, decreasing pressure. HPT: ●, increasing pressure; ○, decreasing pressure; calibration uncertainty is the deviation between measured and calculated pressure.

Table 2.2. Pressure transducers calibration coefficients.

Pressure Transducer	Calibration range / MPa	$p_{cal} = a\ p_{read}^2 + b\ p_{read} + c$
LPT	0.3 - 6.1	$a = -2.064\ 10^{-6}$ MPa^{-1} $b = 0.1002$ $c = -4.340\ 10^{-3}$ MPa
HPT	0.3 - 10.6	$a = -6.218\ 10^{-7}$ MPa^{-1} $b = 0.1006$ $c = 2.667\ 10^{-4}$ MPa

Pressures read through the instrument and from the reference are fitted to a second order polynomial correlation, allowing true pressure values to be found. Table 2.2 gives the obtained calibration coefficients for low and high-pressure transducers (LPT and HPT, respectively). As an example, typical deviations observed through pressure transducer calibration are presented in Figure 2.9. Pressure measurement uncertainty is estimated to be within ± 0.002 MPa from the relative deviations shown in the latter experimental curve.

2.7.2 Temperature Probe Calibration

Temperature is measured via Pt-100 Platinum Resistance Thermometer (PRT) probes, which are calibrated against a 25 Ω PRT reference probe (TINSLEY type 5187 SA) with a certified calibration from the *Laboratoire National d'Essais* (LNE, Paris). Pt-100 sensors and the reference probe are submerged in a temperature bath (Lauda Ultra-Kryomat, Ruk 50) with ethanol and water (for low and higher temperature ranges, respectively).

The temperature of the bath is increased and decreased at uniform intervals from (210 to 360) K in order to detect any hysteresis within the sensors. Temperature signals are allowed to stabilize at each temperature step and are read out, within 0.01 K, on a micro-ohmmeter data Acquisition/Switch Unit (Hewlett-Packard, model 34420A). Similar to the procedure described above for the determination of equilibrium pressures, a plot of T_{true} against T_{read}, results in a second order polynomial relation (Figure 2.10). The equation of this line is subsequently used to determine true temperature values. The maximum uncertainty on temperature measurement resulting from this calibration is within ± 0.02 K.

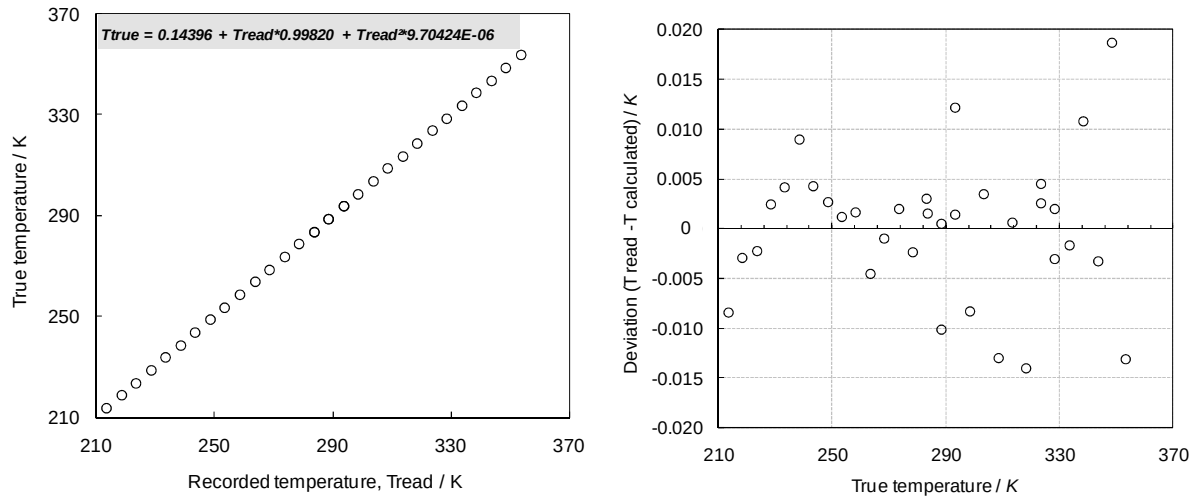


Figure 2.10. Pt-100 Platinum resistance thermometer probe calibration.

2.7.3 Volumetric Calibrations

As it is discussed later in Chapter 4, precise knowledge of the total volume of the equilibrium cell is crucial for the accurate determination of the compositions of the liquid and hydrate phases by mass balance approach. The internal volume of the cell is thus determined by using a variable volume cell (VVC) assembly, as shown in Figure 2.8. The VVC consists of a void cylinder of known internal diameter, a piston with appropriate O-ring and a displacement transducer fitted to the piston to record the variation on the linear displacement inside the cylinder. The VVC is connected to the equilibrium cell. All transfer lines; the equilibrium cell and the VVC assembly are evacuated. The VVC is filled with a pure liquid; ethanol is used for this purpose and the assembly is connected to a pressurizing fluid (*i.e.* nitrogen) to move the piston. The equilibrium cell and transfer lines are filled with ethanol. Pressure is monitored until an abrupt pressure increase is detected inside the cell. At this point, the length travelled by the piston is registered. The volume of the equilibrium cell is equivalent to the volume of liquid loaded into the cell, which is geometrically determined from the displacement of the piston and the cylinder internal diameter. The procedure is repeated at least three times to ensure reproducibility of the results and an average value is reported. The maximum uncertainty on the internal volumes obtained through this procedure are expected to be within $\pm$ 0.5 cm^3.

2.7.4 GC Detector Calibration for Gas Mixtures

In order to determine a quantitative relationship between the response of the detector and the composition of gas mixtures separated by gas chromatography, a calibration of the Thermal Conductivity Detector (TCD) for each compound is performed. A direct injection calibration method (Raal & Mühlbauer, 1998) is used to achieve the accuracy of results required within the project. In this method, known volumes of pure components are directly injected into the GC via the injector port by using precision chromatography syringes (SGE Analytical Science; 50µL, 100µL, 250µL and 500µL Gas Tight Syringes) for preparing calibration standards and GC injections. TCD calibration is conducted once all analytical conditions (see section 2.6.1) of the chromatograph have been optimized to achieve satisfactory separation of (CO_2 and CH_4), (CO_2 and N_2) and (CO_2 and H_2) gas mixtures.

The TCD was calibrated for carbon dioxide, methane, nitrogen and hydrogen. The calibration curves were fitted to second-order polynomial equations relating the number of moles and area under the peaks from the chromatogram. The composition of the gas phase at a given (p,T) condition is thus determined from the peak area ratio of the unknown sample and the coefficients of the corresponding polynomial equation for each compound. A typical calibration curve and the corresponding deviation results for CO_2 are shown in Figure 2.11. Similar deviations are obtained for CH_4, N_2 and H_2. Therefore, the uncertainty in measuring compositions of the gas phase through gas chromatography is estimated to be within $\pm$ 1 - 2%.

Using the experimental procedure described earlier to measure hydrate equilibrium data for gas mixtures with and without TBAB, and assuming the corresponding standard uncertainties have a normal distribution, it is estimated that maximum overall uncertainty for pressure and temperature measurements, derived from isochoric plots, is within $\pm$ 0.05 MPa and $\pm$ 0.2 K, respectively. The maximum uncertainty in all measurements is attributed to the deviations in measuring compositions of the gas phase by gas chromatography. Such deviations are estimated to be within $\pm$ 1 – 2 % as explained above. Other uncertainties for the liquid and hydrate phases are expected to be better than 1 %. Therefore the overall uncertainty for compositional measurements is expected to be less than 2 %.

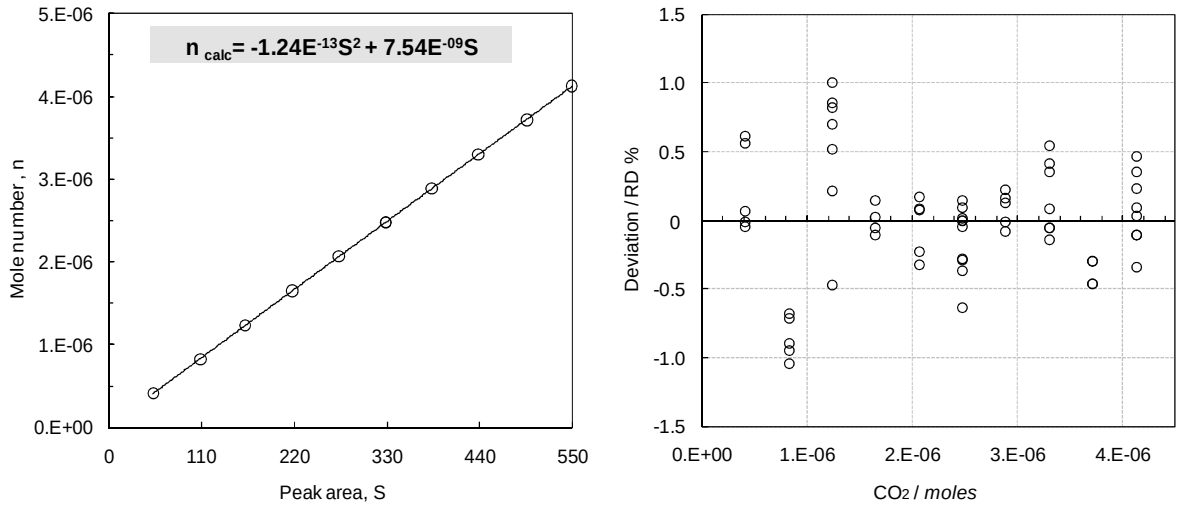


Figure 2.11. Thermal conductivity detector calibration for CO_2 using a 100 µl gas calibration syringe: second order calibration curve (left), calibration deviation (right).

2.7.5 Refractometer Calibration

A refractometer calibration was performed in order to determine the composition of the liquid phase at equilibrium with semi-clathrates formed from CO_2 + N_2 + TBAB aqueous solutions. Samples of (TBAB + water) mixtures were prepared in the concentration range from (0 to 0.50) mass fractions TBAB following the gravimetric method detailed in Chapter 6. Refractive index measurements were carried out at 293.15 K using an ABBE refractive index instrument, previously calibrated with deionized water and ethanol with accuracy greater than $2 \cdot 10^{-4}$.

Refractive indices (n_D) for the (TBAB + water) binary mixtures as function of compositions are plotted in Figure 2.12. It can be observed from the experimental results that n_D exhibit a linear behavior over the investigated concentration range. The maximum accuracy on refractive index measurement are thus expected to be better than 0.1%.

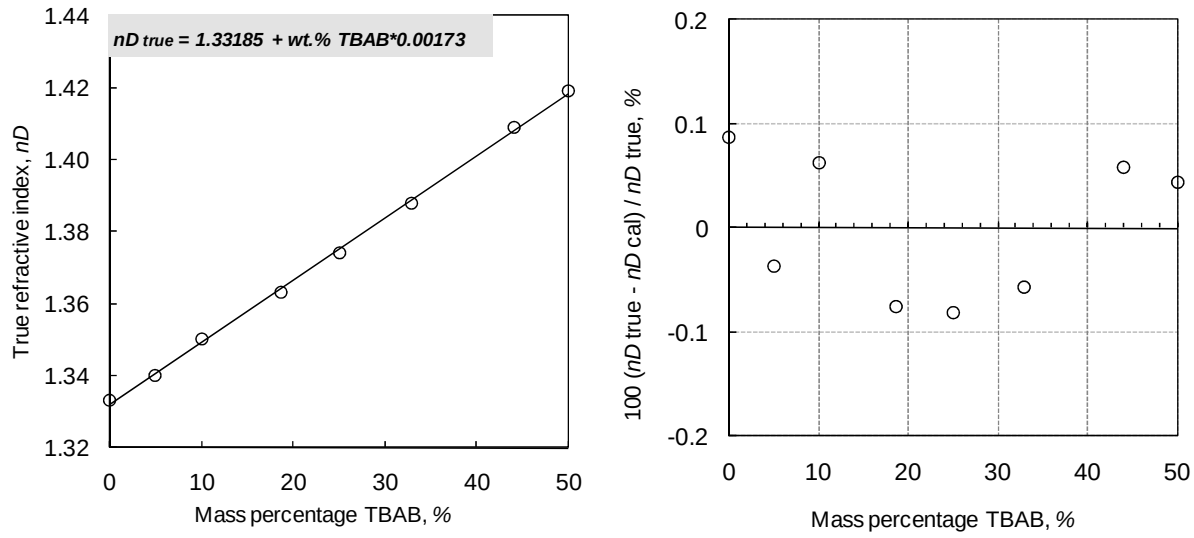


Figure 2.12. Refractive index calibration for TBAB aqueous solutions: second order calibration curve (*left*), calibration deviation (right).

2.8 Criteria for Equilibrium

The state for equilibrium, as previously discussed, implies a condition in which thermodynamic properties do not change over time. Since hydrates are slow to form near the dissociation point, relatively long periods are required for the pressure to come to equilibrium after a temperature change (Marshall *et al.*, 1964). In order to ensure a true thermal equilibrium state while decreasing the time required to achieving this condition, especially in static methods, thorough mixing of the cell contents is essential. It has been demonstrated that step heating combined with adequate time at each temperature interval results in generating reliable experimental data (Tohidi *et al.*, 2000). Moreover, as the heating rate has a strong impact on the accuracy of hydrate dissociation measurements (Tohidi *et al.* 2000; Rovetto *et al.* 2006), the dissociation part of the isochoric loop must be performed at a sufficiently slow heating rate of about 0.12 K/h to allow the system to reach equilibrium (Sloan & Koh, 2008).

Once the above conditions have been satisfied, stability in pressure, temperature, gas phase composition and refractive index are monitored to establish the attainment of equilibrium. Several gas phase samples are taken through ROLSI^{TM} sampler and are analyzed by gas

chromatography at each temperature interval during hydrate dissociation. It is considered that equilibrium has been reached when the composition of the gas phase of at least five samples agree to within 0.001 molar fractions. At this point, average concentrations are registered as the gas phase composition at the corresponding temperature and pressure condition. An actual example of compositional analysis carried out to establish the attainment of equilibrium is given in Figure 2.13. A consistent detector response is exhibited throughout the entire temperature interval.

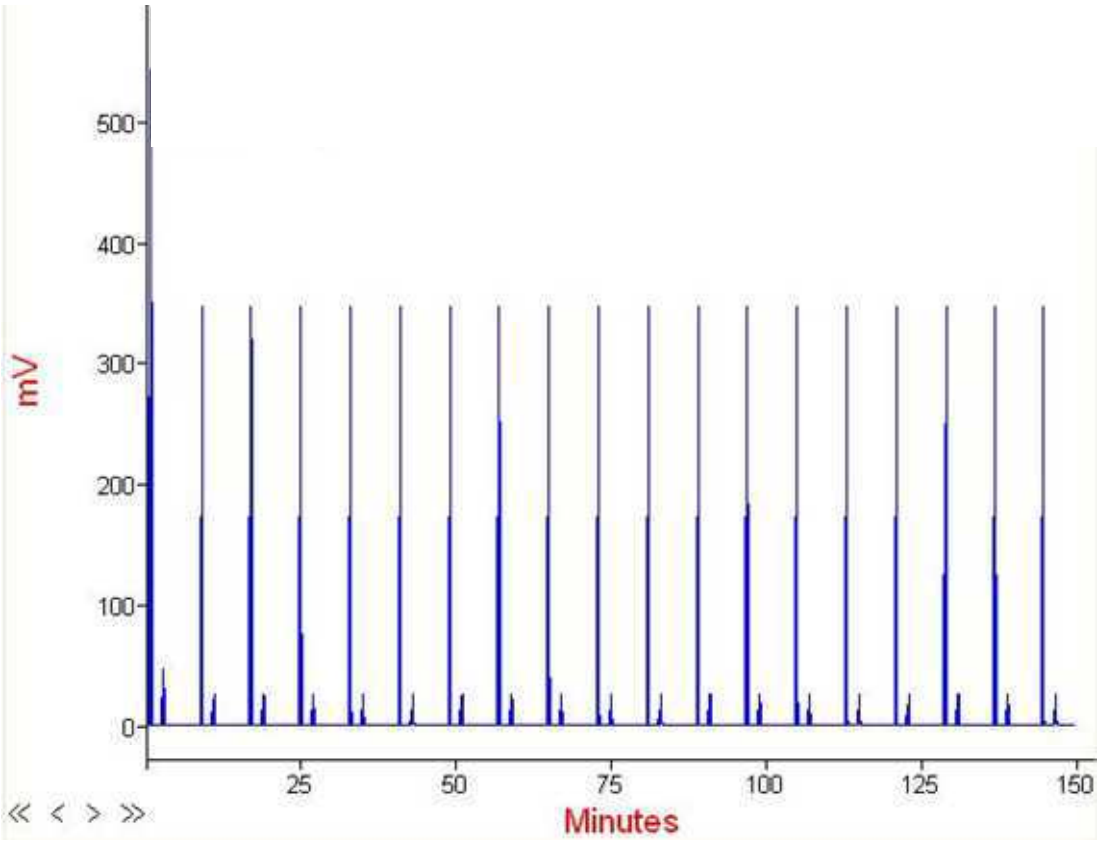
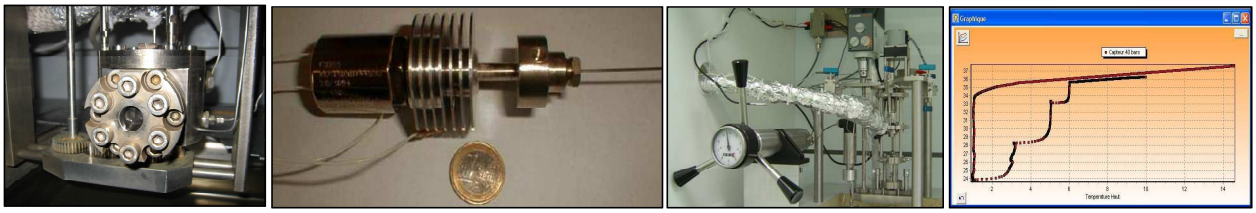


Figure 2.13. Chromatogram profile for a (0.151 mole fraction CO_2 + 0.849 mole fraction N_2) gas mixture in the presence of TBAB aqueous solution (mass fraction, w = 0.05) at T = 287.0 K and p = 14.525 MPa.

3

Phase Equilibria of Clathrate Hydrates of Methane + Carbon dioxide: New Experimental Data and Predictions†



† Content published in *Fluid Phase Equilib. 2010, 296, 60-65.*

3

Résumé

Ce chapitre fournit des conditions de dissociation d'hydrates de gaz de (méthane + dioxyde de carbone) à des concentrations faibles, moyennes et élevées en dioxyde de carbone. Les mesures d'équilibres de phases ont été réalisées entre 279 et 290 K à pressions jusqu'à 13 MPa. Une méthode isochore dite "isochoric pressure-search method" a été utilisée pour effectuer les mesures. Les données de dissociation générées par cette étude ainsi que celles disponibles dans la littérature sont comparées aux prédictions via un modèle thermodynamique et via l'équation empirique décrite dans le chapitre précédent. Une discussion est faite au sujet des écarts entre données expérimentales et données prédites.

Abstract

This chapter provides dissociation conditions of gas hydrates of (methane + carbon dioxide) at low, medium and high concentrations of carbon dioxide. The phase equilibrium measurements were conducted in the temperature ranges from (279 to 290) K and pressures up to 13 MPa. An isochoric pressure-search method was used to perform the measurements. The dissociation data generated in this study along with the experimental data available in the literature are compared with the predictions of a thermodynamic model and a previously reported empirical equation. A discussion is made on the deviations between the experimental and predicted data.

3 Phase Equilibria of Clathrate Hydrates of Methane + Carbon dioxide: New Experimental Data and Predictions

3.1 Introduction

Because gas or clathrate hydrates have the capability to store/separate gases (Englezos, 1993, Sloan & Koh, 2008), the development of alternative technologies based on this concept has gained much attention in exploration and production activities within the oil and gas industry. Examples are carbon dioxide (CO_2) sequestration and methane (CH_4) recovery from natural gas hydrates in deep sea sediments (Oghaki *et al.*, 1994), transport of natural gas as frozen hydrate (Gudmundsson *et al*., 1995), removal of high CO_2 content in natural gas by formation of gas hydrates (Azmi *et al*., 2010), *etc*. As methane is the predominant component of natural gas, reliable experimental data on the phase behavior of (CO_2 + CH_4) gas mixtures under hydrate forming conditions are thus required to enhance the understanding of natural gas hydrates and for process development purposes.

The first experimental study of (CH_4 + CO_2) hydrates was reported by Unruh and Katz (1949). Two decades later, Berecz and Balla-Achs (1983) reported that hydrates of (CO_2 and CH_4) exhibited a maximum and a minimum in the hydrate isotherms and isobars at 0.50 CO_2 mole fractions and higher. Then, Adisasmito *et al*. (1991) confirmed and extended the measurements done by Unruh and Katz (1949). Their data did not show the unusual hydrate instability reported by Berecz and Balla-Achs (1983). Meanwhile, Ohgaki *et al.* (1996) reported phase equilibrium data for the (CH_4 + CO_2) clathrate hydrates at 280 K. Later, Fan and Guo (1999), Seo *et al.* (2000) and Hachikubo *et al.* (2002) reported few hydrate dissociation data for (CH_4 + CO_2) gas mixtures. Among the aforementioned equilibrium data, the experimental data of Unruh and Katz (1949), Berecz and Balla-Achs (1983), Adisasmito *et al*. (1991), Fan and Guo (1999) and Hachikubo *et al.* (2002) apparently represent hydrate dissociation conditions. However, Fan and Guo (1999) reported few hydrate dissociation data for a 0.0348 mole fraction of carbon dioxide containing gas. Hachikubo *et al.* (2002) reported three hydrate dissociation data for 0.25, 0.50 and 0.77 mole fractions of carbon dioxide containing gases.

Moreover, Unruh and Katz (1949) and Adisasmito *et al*. (1991) reported their hydrate dissociation data generally at temperatures near the ice point though some of their data are at higher temperatures. No discussions were made on possible hydrate structure change(s) or comparison with any thermodynamic model. This literature review indicates a need for generating more dissociation data for the (CH_4 + CO_2) clathrate hydrates, studying the stable hydrate structure and also investigating the reliability of the thermodynamic models predictions for the aforementioned clathrate hydrate systems.

In this chapter, the dissociation conditions of the (CO_2 + CH_4) clathrate hydrates at low, medium and high concentrations of CO_2, investigated in the temperature range from (279 to 290) K and up to 13 MPa, are presented. An isochoric pressure-search method (Tohidi *et al*., 2000; Afzal *et al*., 2007; Mohammadi *et al*., 2008) was used to estimate the dissociation conditions. The dissociation data generated along with the literature data are compared with the predictions of a thermodynamic model and a previously reported empirical equation (Adisasmito *et al*., 1991).

3.2 Experimental setup and method

Purities and suppliers of the chemicals used in this work are given in Table 3.1. A detailed description of the apparatus used in this study is provided in the literature (Afzal *et al*., 2007; Mohammadi *et al.*, 2008). A simplified flow diagram of the experimental setup is shown in Figure 3.1 and partial pictures of its main components are shown in Figure 3.2. Briefly, the apparatus is based on the "static–analytic" method (Richon, 1996) with capillary fluid phase sampling (Laugier & Richon, 1986). The heart of this apparatus is an equilibrium cell made of 316 stainless steel and suitable for measurements at pressures up to 40 MPa. The cell has a volume of (57.5 ± 0.5) cm^3 and two sapphire windows. A magnetic stirrer ensures agitation to facilitate reaching equilibrium.

Table 3.1. Purities and suppliers of chemicals.[a]

chemical	supplier	Purity / (volume %)
Methane	Messer Griesheim	99.995
Carbon dioxide	Air Liquide	99.995

[a] Deionized water was used in all experiments.

Two platinum resistance thermometers (Pt100) inserted into the vessel were used to measure temperatures and check for equality of temperatures within temperature measurement uncertainty, which is estimated to be less than 0.1 K. This temperature uncertainty estimation results from calibration against a 25-Ω reference platinum resistance thermometer. The pressure in the cell was measured using the low pressure transducer (Druck, type PTX611 for pressures up to 20 MPa). Pressure measurement accuracies are estimated to be better than 2 kPa.

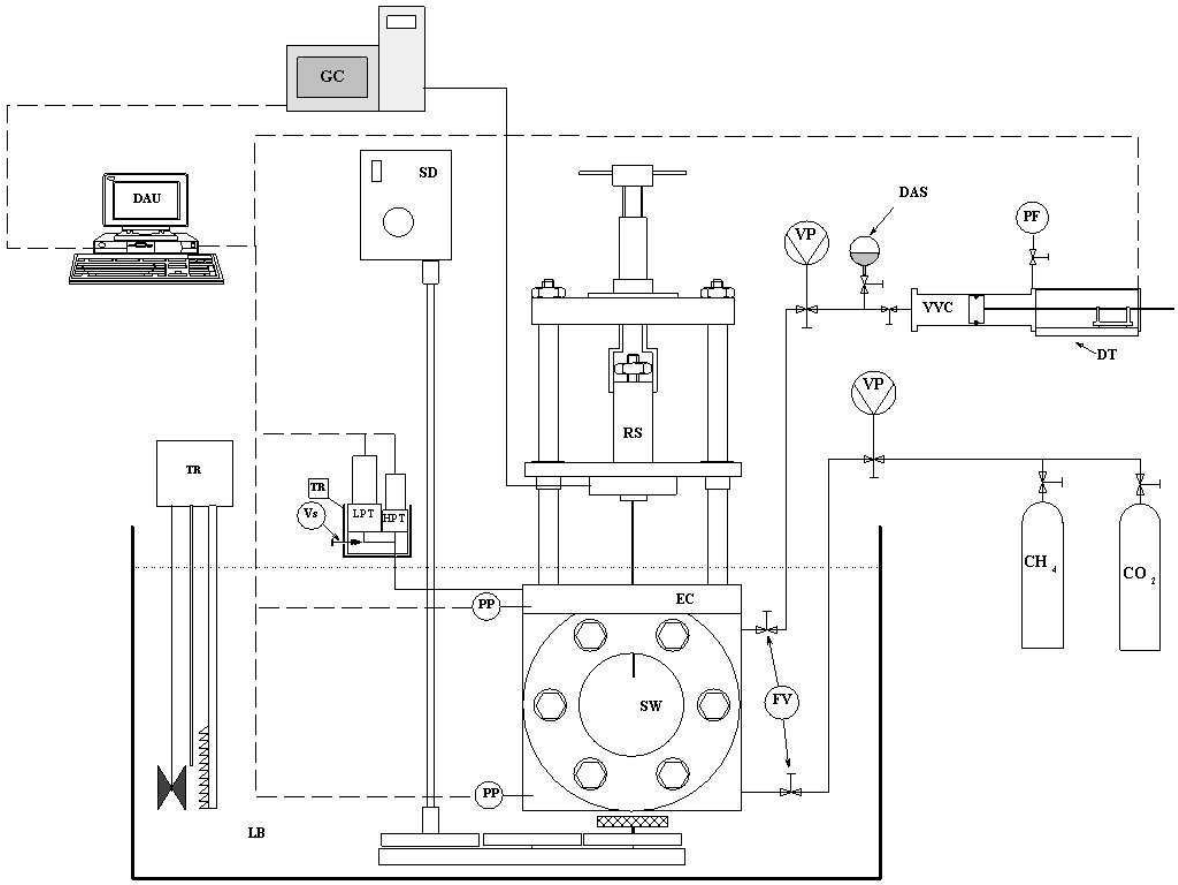


Figure 3.1. Flow diagram of the experimental setup. DAS: degassed aqueous solution; DAU: data acquisition unit; DT: displacement transducer; EC: equilibrium cell; FV: feeding valve; GC: gas chromatograph; HPT: high pressure transducer; LB: liquid bath; LPT: low pressure transducer; PF: pressurizing fluid; PP: platinum probes; RS: ROLSI™ sampler; SD: stirring device; SW: sapphire windows, TR: temperature regulator; VP: vacuum pump; Vs: isolation valve of LPT; VVC: variable volume cell.

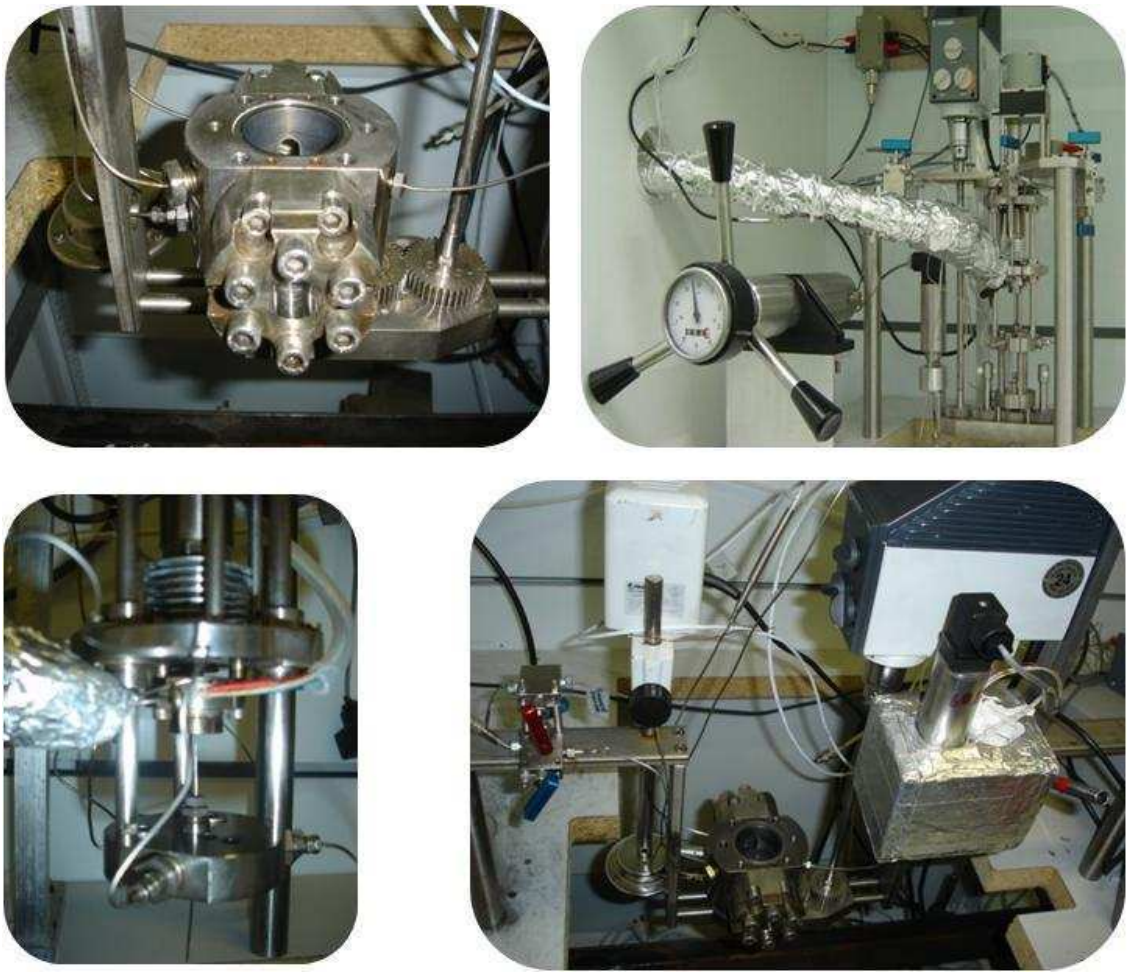


Figure 3.2. Partial pictures of the apparatus used: equilibrium cell (*top left*), volumetric press (*top right*), measurement and stirring assembly (*bottom left*), movable pneumatic ROLSI^{TM} sampler (*bottom right*).

Table 3.2. Operating conditions of the gas chromatograph.

Carrier gas	Helium
Gas flow rate (ml/min)	25
Detector	TCD
Detector temperature (K)	393
TCD wire temperature (K)	448
Oven temperature (K)	323

3.2.1 General hydrate formation and dissociation procedure

The isochoric pressure-search method (Tohidi *et al.*, 2000; Afzal *et al.*, 2007; Mohammadi *et al.*, 2008) was followed to determine the hydrate dissociation pressures and temperatures. The reliability of the experimental method used has been demonstrated in the literature (Afzal *et al.*, 2007; Mohammadi *et al.*, 2008; Mohammadi *et al.*, 2009). Before starting the experiment, the cell was evacuated to eliminate the presence of air. The gas mixture was prepared in the cell by introducing first a certain amount of CO_2, and then CH_4 from the corresponding cylinders through a pressure-regulating valve. After temperature and pressure were stabilized, the valve in the line connecting the vessel and the gas cylinder was closed. The composition of the gas mixture was analyzed and confirmed using a gas chromatograph (Varian, CP3800) coupled with a pneumatic ROLSI^{TM} sampler (Guilbot *et al.*, 2000). The gas chromatograph (GC) equipped with a thermal conductivity detector (TCD) was appropriately programmed with proper flow rates, oven and detector temperatures for the compounds studied, which are given in Table 3.2. A packed analytical column in stainless steel tubing (Agilent J&W, Porapak Q) with 1.83 m length, 2 mm inner diameter and 0.177 mm mesh opening size was used for all the systems measured.

Subsequently, about 10% (by volume) of the cell was filled with water using the volumetric press shown in Figure 3.2. The cell was immersed into the temperature-controlled bath and the temperature was slowly decreased to form the hydrate. Hydrate formation in the cell was detected by a noticeable pressure drop. The temperature was then increased in steps of 0.1 K. At every temperature step, the temperature was kept constant with sufficient time to achieve an equilibrium state in the cell. As implemented by Ohmura and coworkers (2004), a pressure-temperature diagram was obtained for each experimental run from which the hydrate dissociation point was found (Figure 3.3). The point at which the slope ($\partial p/\partial T$) of pressure-temperature data plots changes sharply is considered to be the point at which all hydrate crystals have dissociated and, hence, is reported as the equilibrium condition (Ohmura *et al.*, 2004). As mentioned earlier, the procedure is repeated at different pressures in order to determine the hydrate phase boundaries over the studied temperature range.

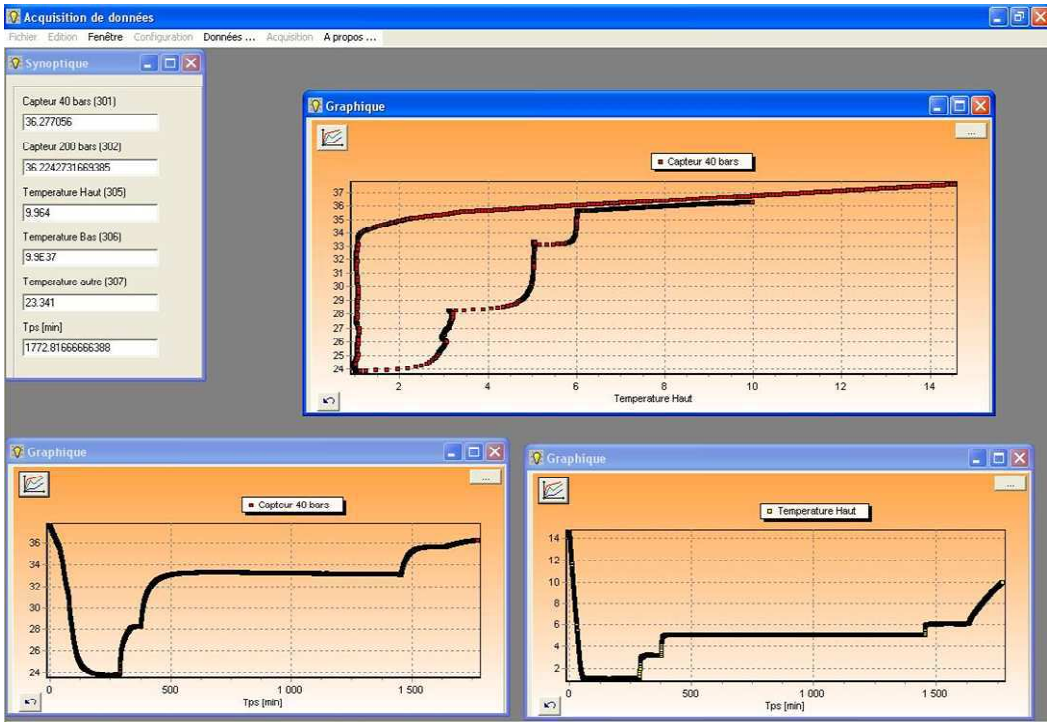


Figure 3.3. Representative isochoric curve and pressure and temperature plots obtained during a hydrate formation/dissociation experiment, showing characteristic times for reaching equilibrium and overall behavior for CO_2 + CH_4 systems: pressure *vs.* temperature (*top*), pressure (*bottom left*) and temperature (*bottom right*) as a function of time. CO_2 molar composition in gas feed was 0.272.

3.3 Results and discussion

The dissociation data for methane and carbon dioxide simple hydrates were first measured. These data along with some selected literature data are illustrated in Figures 3.4 and 3.5. The good agreement demonstrates the reliability of the isochoric pressure-search method (Tohidi *et al.*, 2000; Afzal *et al.*, 2007; Mohammadi *et al.*, 2008) used in this work. Figures 3.4 and 3.5 also show the predictions of a thermodynamic model (HWHYD, 2000). A detailed description of this model is given elsewhere (Tohidi *et al.*, 1993). Briefly, it is based on the equality of fugacity concept, which uses the Valderrama modification of the Patel-Teja equation of state (Valderrama, 1990) and non-density dependent mixing rules (Avlonitis *et al.*, 1994) for modeling the fluid phases while the van der Waals and Platteeuw (1959) theory is used for modeling the hydrate phase.

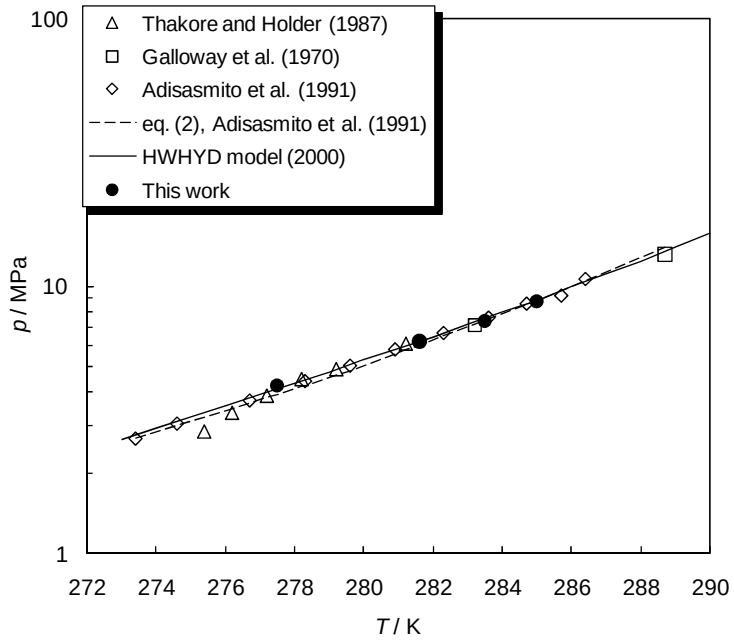


Figure 3.4. Experimental (literature and this work) dissociation pressures for methane simple hydrates, together with thermodynamic model (HWHYD, 2000) predictions assuming sI and calculated values using eq. (3.2).

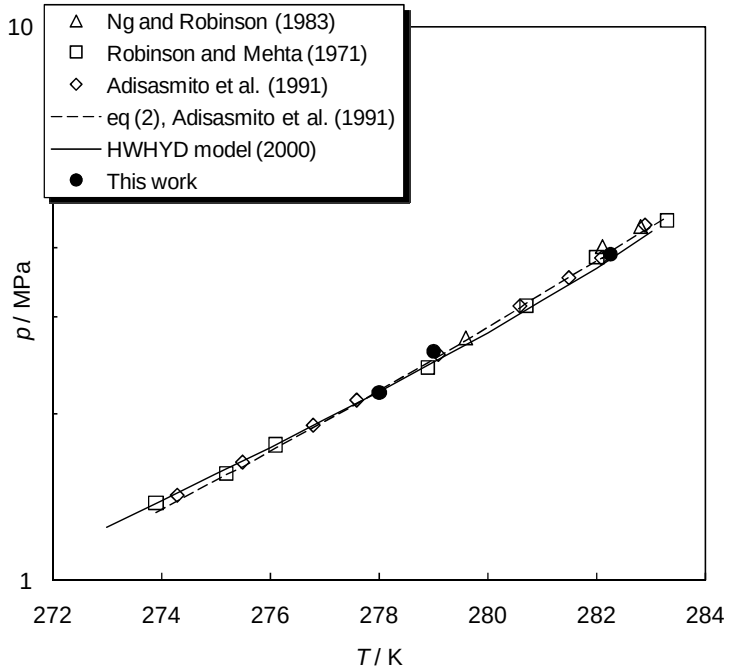


Figure 3.5. Experimental (literature and this work) dissociation pressures for carbon dioxide simple hydrates, together with thermodynamic model (HWHYD, 2000) predictions assuming sI and calculated values using eq. (3.2).

The hydrate dissociation conditions for the (methane + carbon dioxide + water) systems were investigated at different concentrations of carbon dioxide to study the effect of carbon dioxide composition in the mixture. The composition of the (methane + carbon dioxide) gas mixtures along with the experimental hydrate dissociation conditions in the presence of pure water are given in Table A.1 (Appendix A) and are shown in Figure 3.6. Initial gas compositions are expressed in mole fractions in the gas phase. Because the equilibrium pressure of CO_2 hydrates is lower than that of CH_4 hydrates (Figures 3.4 and 3.5), it is noted, as expected, that mixed (CO_2 + CH_4) hydrates are thermodynamically more stable as the concentration of CO_2 in the feed gas decreases. For example, at 289.2 K the dissociation pressures for gas mixtures of 0.730, 0.490 and 0.264 molar concentration of CO_2 are 13.06, 12.41 and 11.62 MPa, respectively.

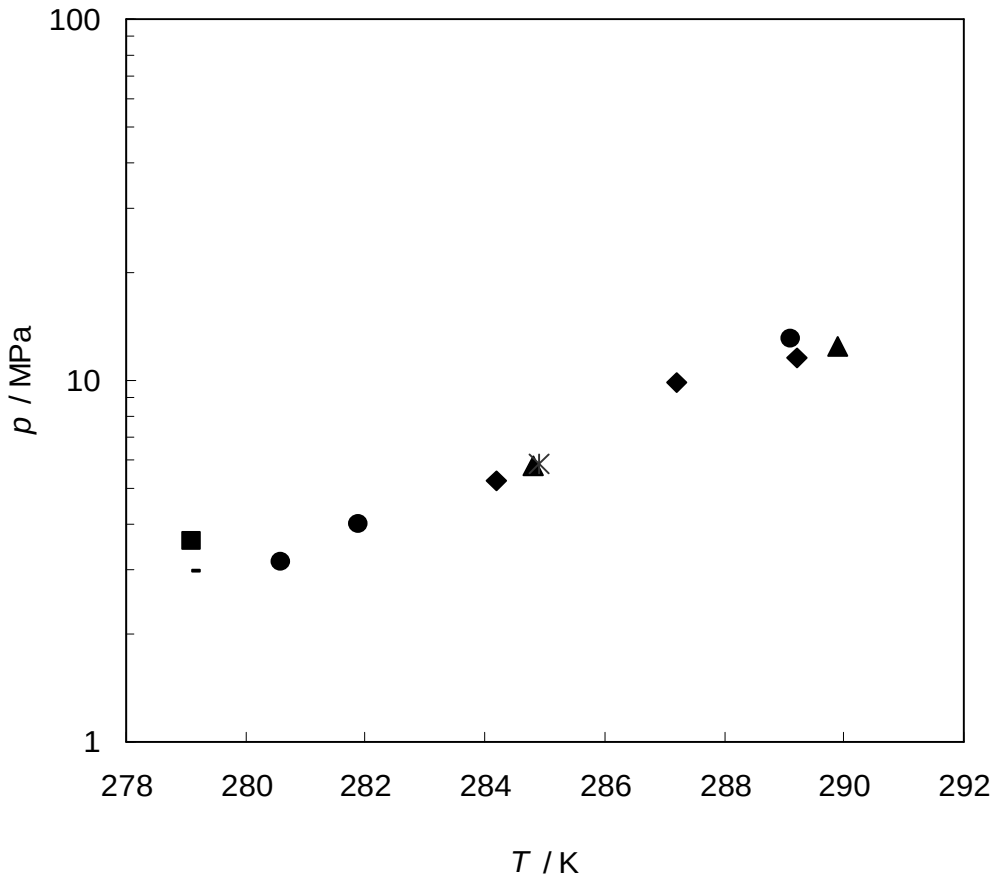


Figure 3.6. Experimental dissociation pressures from this work for various (methane + carbon dioxide) gas hydrates at different CO_2 load mole fractions: 0.264 (♦); 0.272 (■); 0.490 (▲); 0.500 (*); 0.504 (—); 0.730 (•).

The predictions of the thermodynamic model (HWHYD, 2000) are also reported in Table A.1. The experimental and predicted dissociation conditions are shown in Figures 3.7 and 3.8. As can be observed in these figures and also in Table A.1, the thermodynamic model (HWHYD, 2000) generally overestimates the dissociation pressures for the (carbon dioxide + methane) clathrate hydrates studied in this work. Both structures I and II have been assumed for predicting the dissociation conditions. Assuming structure I, however, leads to lower deviations between the predicted and experimental data suggesting the stable structure for the (carbon dioxide + methane) clathrate hydrates studied in this work is likely structure I.

The relative deviation (*RD*) given in Table A.1 was calculated using the following equation:

$$RD(\%) = \frac{p_{\exp} - p_{pred}}{p_{\exp}} \times 100 \qquad (3.1)$$

where p_{exp} and p_{pred} represent experimental and predicted dissociation pressures, respectively.

Table A.1 and Figure 3.7 also include the predictions using the correlation proposed by Adisasmito and coworkers (1991):

$$ln\,(p_{calc}/MPa) = A + B(T/K)^{-1} + Cy + D(T/K)^{-2} + Ey(T/K)^{-1} + Fy^2 \qquad (3.2)$$

where p_{calc} = calculated pressure, T = temperature, y = mole per cent of carbon dioxide in the vapor phase (water-free basis), and the values for the constants are: A= 175.3, B= - 89009, C= 0.07392, D= 1.1307 x 10^7, E= -23.392, and F= 3.9566 x 10^{-5}.

An acceptable agreement is generally observed between the predicted values using eq. (3.2) and the experimental data generated in this work.

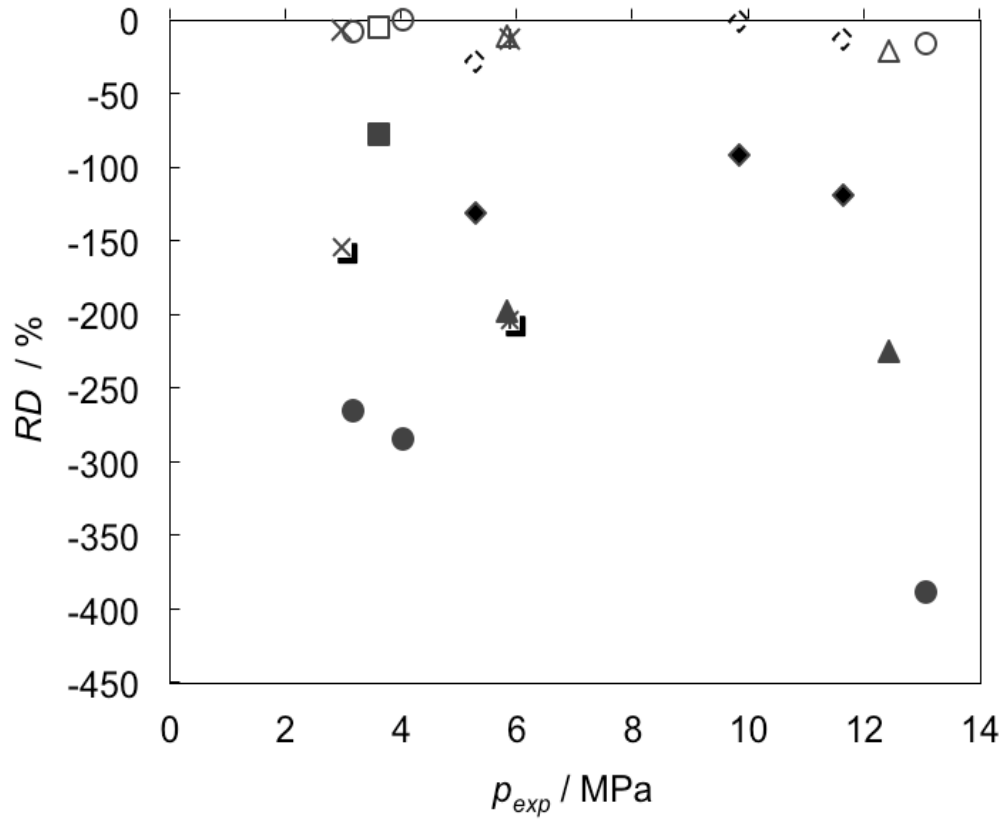


Figure 3.7. Relative deviation (*RD*) of experimental dissociation pressures (p_{exp}) for (CO_2 + CH_4) clathrate hydrates and predictions of the thermodynamic model (HWHYD, 2000). *RD* assuming sI: 0.264 (◊); 0.272 (□); 0.490 (△); 0.500 (*); 0.504 (x); 0.730 (○). *RD* assuming sII: 0.264 (♦); 0.272 (■); 0.490 (▲); 0.500 (* shadow); 0.504 (x shadow); 0.730 (●).

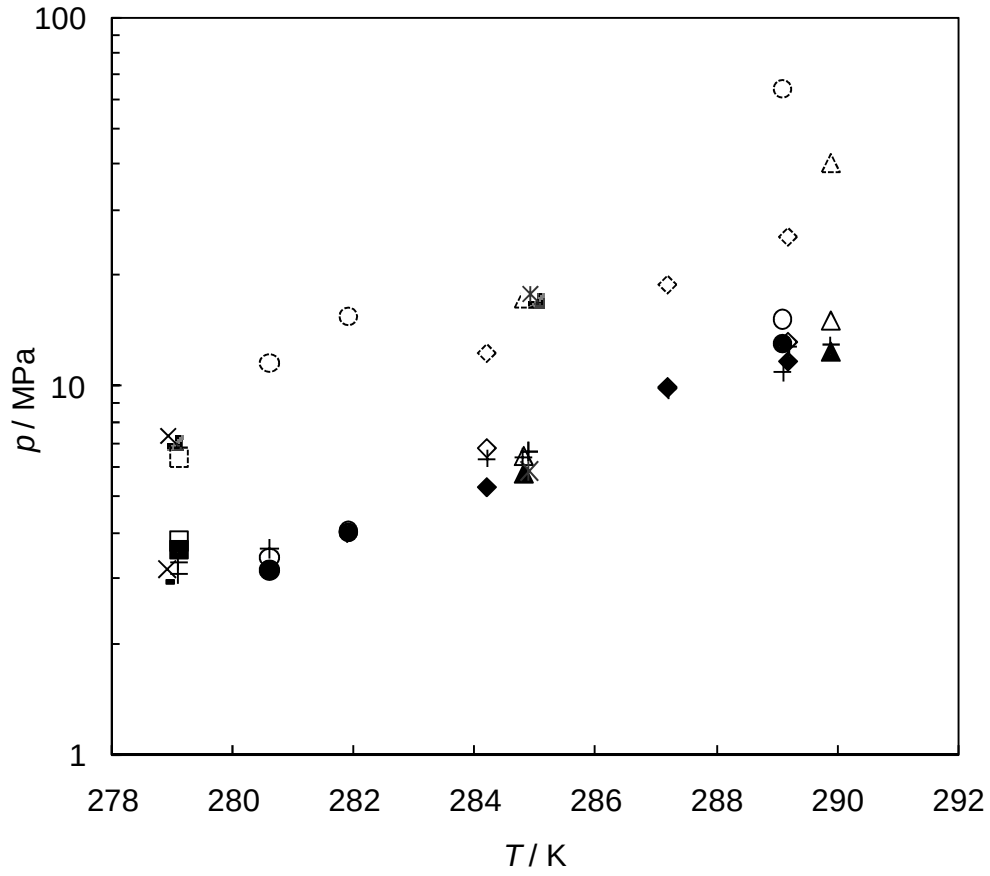


Figure 3.8. Experimental, calculated using (eq. 3.2) and predicted dissociation pressures for (CO_2 + CH_4) clathrate hydrates. This work at different CO_2 mole fractions loaded: 0.264 (♦); 0.272 (■); 0.490 (▲); 0.500 (*); 0.504 (**—**); 0.730 (●). Calculated pressures using eq. (3.2) proposed by Adisasmito and coworkers (1991): **(+)**. Thermodynamic model (HWHYD, 2000) predictions assuming sI at different CO_2 mole fractions loaded: 0.264 (◊); 0.272 (□); 0.490 (∆); 0.500 (+); 0.504 (x); 0.730 (○). Thermodynamic model (HWHYD, 2000) predictions assuming sII at different CO_2 mole fractions loaded: 0.264 (◊ shadow); 0.272 (□ shadow); 0.490 (∆ shadow); 0.500 (* shadow); 0.504 (x shadow); 0.730 (○ shadow).

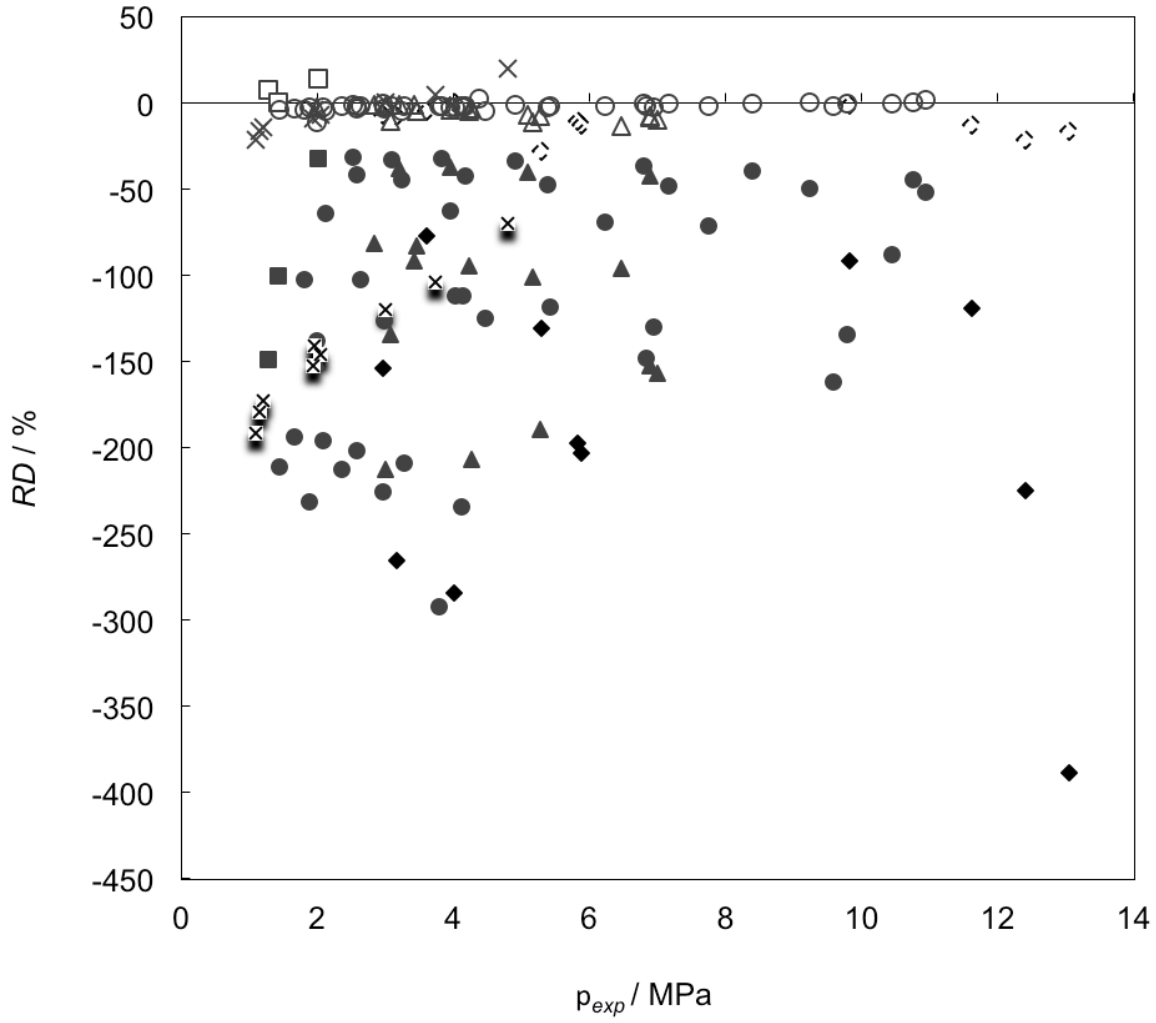


Figure 3.9. Relative deviation (*RD*) of the experimental and predicted (HWHYD model, 2000) dissociation pressures (p_{exp}) for various (CO_2 + CH_4) clathrate hydrates at different CO_2 mole fractions loaded. *RD* (%) assuming sI: This work (◊); Hachikubo *et al*., 2002 (□); Adisasmito *et al*., 1991 (○); Unruh and Katz, 1949 (△); Fan and Guo, 1999 (x). *RD* (%) assuming sII: This work (♦); Hachikubo *et al*., 2002 (■); Adisasmito *et al*., 1991 (●); Unruh and Katz, 1949 (▲); Fan and Guo, 1999 (x shadow).

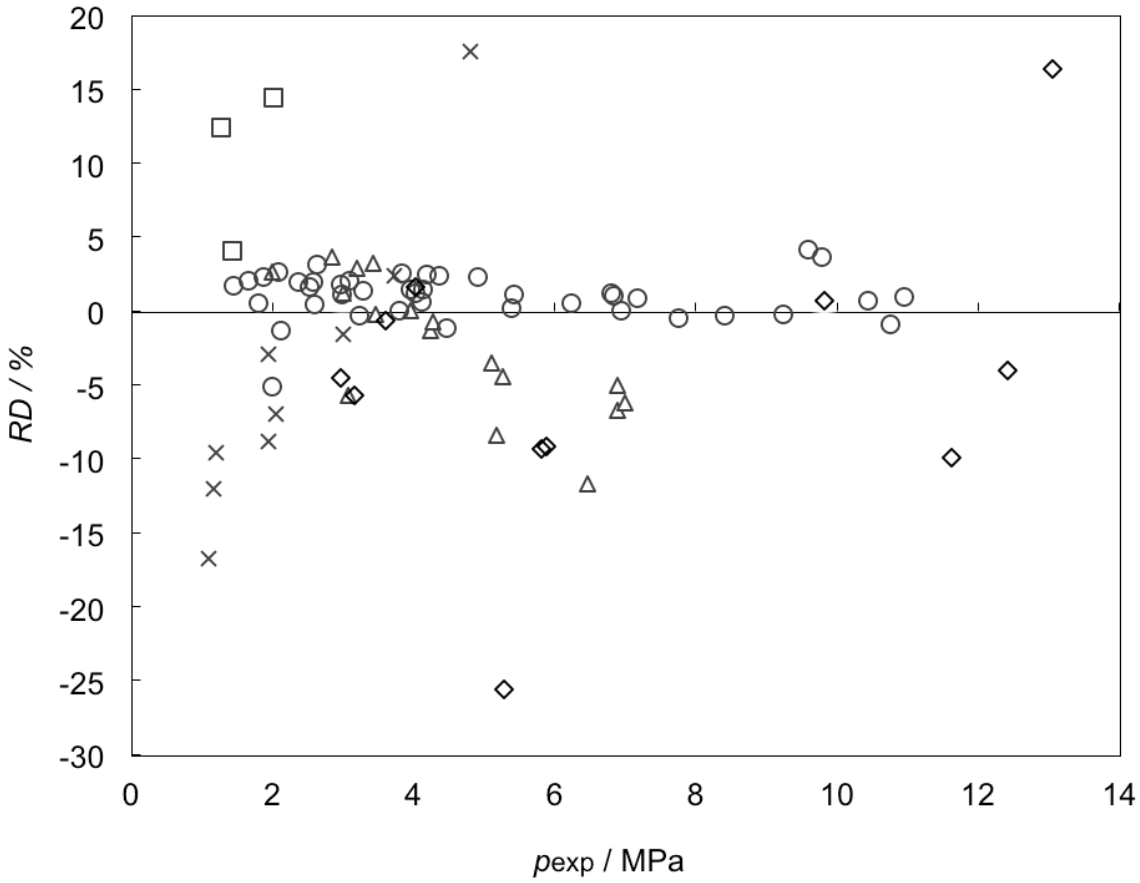


Figure 3.10. Relative deviation (*RD*) of experimental dissociation pressures (p_{exp}) for (CO_2 + CH_4) clathrate hydrates and calculated pressures using eq. (3.2) proposed by Adisasmito and coworkers (1991): This work (◊); Hachikubo *et al*., 2002 (□); Adisasmito *et al*., 1991 (○); Unruh and Katz, 1949 (△); Fan and Guo, 1999 (x).

Figures 3.9 and 3.11 compare the experimental dissociation data reported in the literature for various (methane + carbon dioxide) clathrate hydrates with the predictions of the thermodynamic model (HWHYD, 2000). These figures also show that the model (HWHYD, 2000) over predicts the dissociation conditions of the experimental dissociation data reported in the literature for (methane + carbon dioxide) clathrate hydrates. Again, both structures I and II for the predictions of the dissociation conditions were assumed and lower deviations between the predicted and experimental data by assuming structure I are observed suggesting the stable hydrate structure for the (carbon dioxide + methane) clathrate hydrates reported in the literature is likely structure I. However, the final proof for the stable structure of the (methane + carbon dioxide) clathrate

hydrates requires direct measurements by suitable physical techniques (*e.g.*, NMR, X-ray, or Raman spectroscopy).

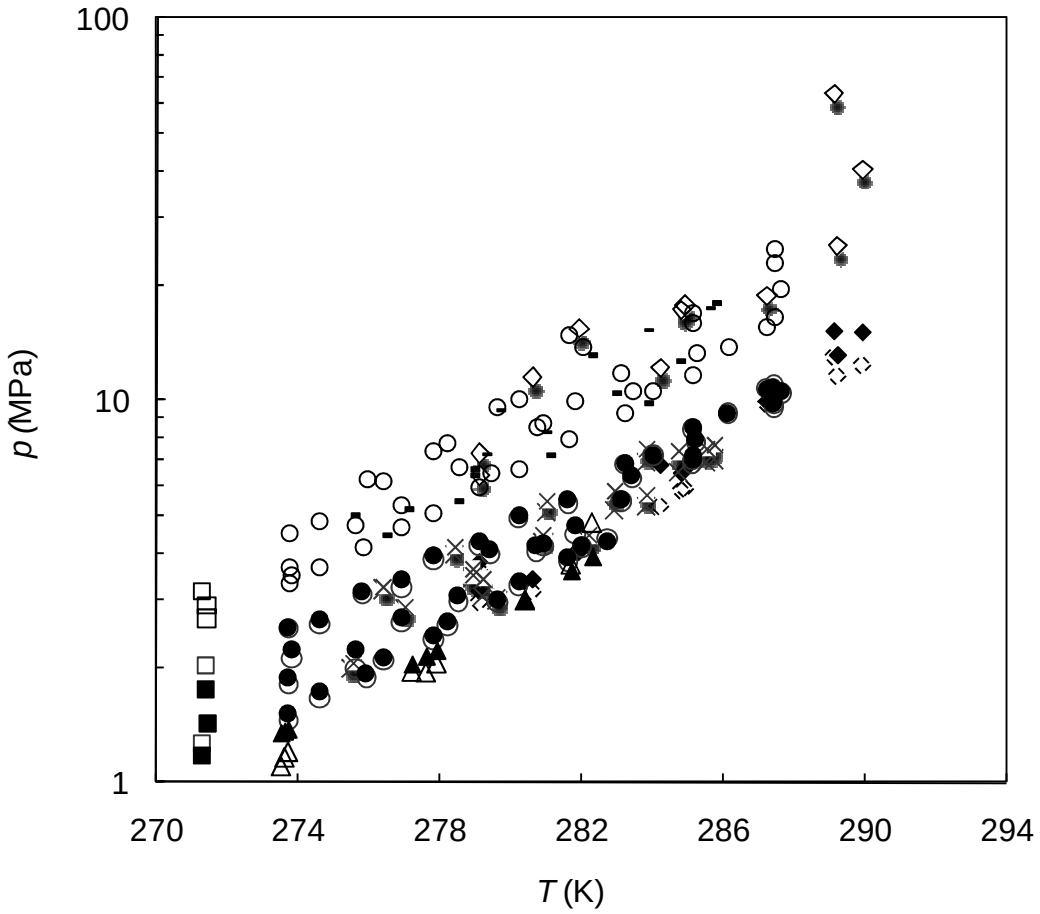


Figure 3.11. Experimental dissociation conditions for various (CO_2 + CH_4) clathrate hydrates and predictions of the thermodynamic model (HWHYD, 2000), at different CO_2 mole fractions loaded: This work (◊). Literature: Hachikubo *et al*., 2002 (□); Adisasmito *et al*., 1991 (○); Unruh and Katz, 1949 (x); Fan and Guo, 1999 (△). Thermodynamic model (HWHYD, 2000) predictions assuming sI: This work (♦). Literature: Hachikubo *et al*., 2002 (■); Adisasmito *et al*., 1991 (●); Unruh and Katz, 1949 (-); Fan and Guo, 1999 (▲). Thermodynamic model (HWHYD, 2000) predictions assuming sII: This work (◊ shadow). Literature: Hachikubo *et al*., 2002 (□ shadow); Adisasmito *et al*., 1991 (○ shadow); Unruh and Katz, 1949 (x shadow); Fan and Guo, 1999 (△ shadow).

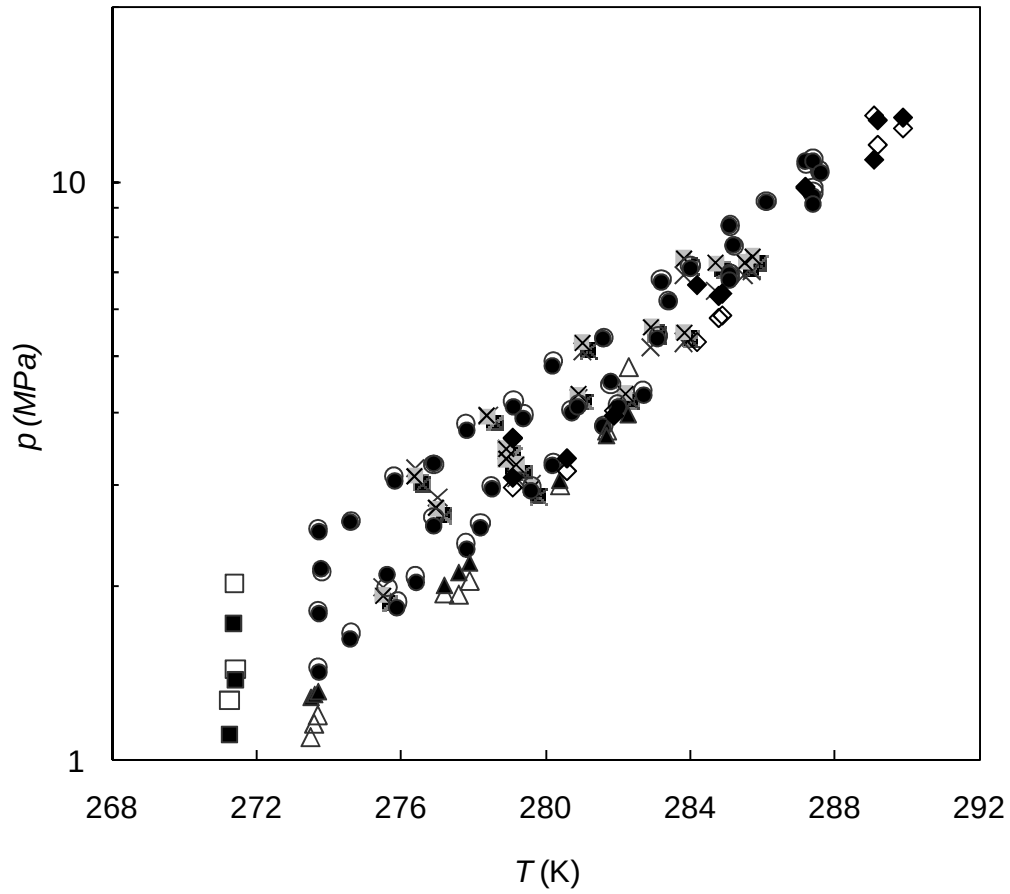


Figure 3.12. Comparison of experimental dissociation pressures for various (CO_2 + CH_4) clathrate hydrates with the calculated values using eq. (3.2). Experimental dissociation pressures at different CO_2 mole fractions loaded: This work (◊); Hachikubo *et al*., 2002 (□); Adisasmito *et al*., 1991 (○); Unruh and Katz, 1949 (x); Fan and Guo, 1999 (△). Calculated dissociation pressures with eq. (3.2): This work (♦); Hachikubo *et al*., 2002 (■); Adisasmito *et al*., 1991 (●); Unruh and Katz, 1949 (x shadow); Fan and Guo, 1999 (▲).

The experimental dissociation data reported in the literature have also been compared with the calculated pressures using the equation proposed by Adisasmito and coworkers (1991) in Figures 3.10 and 3.12. As can be seen, the agreement between the calculated values and experimental data using eq. (3.2) is acceptable. In overall, as shown earlier, the model (HWHYD, 2000) unreliably predicts the dissociation conditions for (methane + carbon dioxide) clathrate hydrates in the presence of pure water. Similar results are expected from other thermodynamic models. This suggests that reconsideration of thermodynamic models for predicting dissociation

conditions of (methane + carbon dioxide) clathrate hydrates is necessary. These models have generally been developed for hydrocarbon systems. For the systems containing carbon dioxide, model parameters likely require readjustments using reliable experimental data.

In addition, a number of technical difficulties (*e.g*. plugging of capillary sampler, long metastable periods, unsuitability for investigating corrosive gases, *etc.*) were encountered for measuring compositional equilibrium data. Because such measurements have been considered within the scope of this research, it was decided to develop a new apparatus suitable for generating accurate hydrate phase equilibria and compositional data simultaneously, which is the subject of the next chapter.

4

Development of a New Apparatus for Simultaneous Measurements of Gas Hydrate Dissociation Conditions and Compositional Analysis[†]



[†] Content published in *Ind. Eng. Chem. Res. 2011, 50, 5783–5794*; *Ind. Eng. Chem. Res.* 2011, 50 (8), 4722-4730 and *Ind. Eng. Chem. Res.* 2011, 50 (10), 6455-6459.

4

Résumé

Ce chapitre est consacré à la description d'un nouvel outil expérimental basé sur la technique «statique-analytique» avec échantillonnage en phase gazeuse au moyen d'un capillaire, spécialement conçu, construit et amélioré pour mesurer avec précision les équilibre de phases : pression, température et compositions en présence d'hydrates de gaz. Cet appareil est adapté à des mesures entre 233 et 373 K, pour des pressions pouvant atteindre 60 MPa et il est compatible avec l'utilisation de gaz corrosifs. La procédure expérimentale developpée pour mesurer les conditions de dissociation des hydrates est similaire à celle décrite dans le chapitre 3. En outre, les compositions de la phase gazeuse en équilibre avec l'hydrate de gaz et de la phase aqueuse sont mesurées par chromatographie en phase gazeuse. Une approche basée sur une étude des bilans de matière est utilisée pour estimer les compositions des phases hydrates et aqueuse. Afin de définir les capacités réelles et la fiabilité de l'appareillage et de la méthode utilisée, de nouveaux équilibres de phases du système (dioxyde de carbone + eau + méthane) ont été mesurés dans des conditions de formation d'hydrates et les résultats comparés aux données de la littérature. Ce chapitre se termine par une discussion basée sur la comparaison entre les prédictions des modèles thermodynamiques et les données obtenues dans ce travail.

Abstract

This chapter is devoted to the description of a new experimental set-up based on the "static-analytic" technique with gas phase capillary sampling, specially designed, built, and improved to accurately measure phase equilibrium pressure, temperature, and compositions under gas hydrate formation conditions. The apparatus is suitable for measurements at temperatures ranging from (233 to 373) K, pressures up to 60 MPa and it is compatible with corrosive gases. The experimental procedure used to measure the hydrate dissociation conditions is similar to the one described in Chapter 3. In addition, the compositions of the gas phase in equilibrium with gas hydrate and aqueous phase are measured through gas chromatography technique. A material balance based approach is used for estimating the compositions of the hydrate and aqueous phases. In order to determine the capabilities and reliability of the apparatus and method used, new phase equilibrium data in the (carbon dioxide + methane + water) system under hydrate formation conditions were measured and compared with literature data. A discussion based on the comparison between the predictions of thermodynamic models and the data measured in this work is also given.

4 Development of a New Apparatus for Simultaneous Measurements of Gas Hydrate Dissociation Conditions and Compositional Analysis

4.1 Introduction

Considerable research has been devoted in the last decades to examine potential industrial applications of gas hydrate technology (Adisasmito *et al.,* 1991; Ohgaki *et al*., 1996; Hachikubo *et al*., 2002; Sloan & Koh, 2008). Thermodynamic models based on accurate experimental equilibrium data are needed to reliably predict hydrate thermodynamic properties for potential industrial applications. As most of the existing models have been developed for hydrocarbon systems, model parameters must be re-considered for hydrates containing carbon dioxide using reliable phase equilibrium data (Adisasmito *et al.,* 1991; Ohgaki *et al*., 1996; Hachikubo *et al*., 2002; Sloan & Koh, 2008, Belandria *et al*., 2010). In addition, any error in the measurement of hydrate phase equilibrium properties will lead to significant errors in model's predictions. Consequently, accurate measurement of the phase behavior of mixed clathrate hydrates containing CO_2 is necessary.

A number of experimental devices and methods for measuring hydrate phase equilibrium of gas mixtures reported in the literature have been reviewed by Sloan and Koh (2008). Experimental determination of the composition of the existing phases in equilibrium with gas hydrate by "static-analytic" method is generally not easy. Some of the most common technical difficulties are: long metastable periods, ineffective agitation, difficulties to sample the phases without disturbing the thermodynamic equilibrium, lack of visibility inside the equilibrium cell, plugging of sampling valves, *etc*.

All of the above are to be considered in the design of an experimental apparatus for hydrate phase equilibrium measurements. Traditionally the experimental methods involve measuring hydrate phase boundaries, compositional data are scarcely measured (Sloan & Koh, 2008).

Table 4.1. Experimental data reported in the literature for the dissociation conditions of the binary gas hydrates of (carbon dioxide + methane).

Authors	**Dissociation conditions ranges (*T* and *p*)**	**Range of CO_2 mole fraction in gaseous mixture**	**Number of experimental data**
Adisasmito *et al.* (1991)	273.7 - 287.6 K 2.52 - 10.95 MPa	0.08 - 0.85	41
Hachikubo *et al.* (2002)	271.0 K 1.27 - 2.02 MPa	0.25 - 0.77	3
Belandria *et al.* (2010)	279.1 - 289.9 K 2.96 - 13.06 MPa	0.264 - 0.730	11
Unruh and Katz (1949)	275.5 - 285.7 K 1.99 - 7.0 MPa	0.055 - 0.71	17
Fan and Guo (1999)	273.5 - 282.3 K 1.10 - 4.80 MPa	0.9652	9
Seo *et al.* (2000)	272.66 - 283.56 K 1.5 - 5.0 MPa	0 - 1.0	17
This work	277.9 - 285.5 K 2.72 - 8.27 MPa	0.206 - 0.744	9

Table 4.2. Experimental data reported in the literature for the *p*, *T*, and composition of the gas and hydrate phases at (L_w-H-G) equilibrium conditions for the binary clathrate hydrates of (carbon dioxide + methane).

Authors	***T* and *p* ranges**	**Mole fraction of CO_2 in the gas (*y*), hydrate (*z*) and/or aqueous phases**	**Number of experimental data**
Ohgaki *et al.* (1996)	280.3 K 3.04 - 5.46 MPa	*y*, *z*	31
Seo *et al.* (2000)	274.36 - 283.56 K 1.5 - 5.0 MPa	*y*, *z*	26
Uchida *et al.* (2005)	258-274.1 K and 190 K 0.5-3 MPa and 0.1 MPa	*y*, *z*	-
Beltran and Servio (2008)	275.14 - 285.34 K 2.36 - 7.47 MPa	*y*	22
Bruusgaard *et al.* (2010)	274.02 - 280.05 K 1.66 - 4.03 MPa	*y*	12
This work	273.6 - 284.2 K 1.510 - 7.190 MPa	*y*, *x*, *z*	41

Although a significant amount of research has been carried out for mixed hydrates of carbon dioxide and methane (Unruh & Katz, 1949; Ohgaki *et al*., 1996; Fan & Guo, 1999; Seo *et al*., 2000; Hachikubo *et al*., 2002; Beltran & Servio, 2008; Belandria *et al*., 2010; Bruusgaard *et al.*, 2010), the compositions of the gas, hydrate, and liquid phases reported in the literature are still limited. A summary of the experimental conditions at which literature data (including this work) have been reported is given in Tables 4.1 and 4.2.

In the previous chapter a small (~57.5 cm^3) equilibrium cell was used for measuring the hydrate dissociation conditions of (CO_2 + CH_4) gas mixtures in the presence of pure water. Based on the limitations of the latter apparatus and the current needs for gas hydrate investigations, an alternative and possibly more efficient way to simultaneously measure the boundary of gas hydrate formation and the compositions of the existing phases in equilibrium with mixed hydrates is presented in this chapter. The main features of both apparatuses are quickly reviewed in Table 4.3.

Table 4.3. Main characteristics of previous and new experimental setups.

Feature	**Previous**	**New**
Volume of the cell	~ 60 cm^3	~ 200 cm^3
Agitation system	Magnetic rod	Magnetically driven Rushton turbine
Liquid bath / visibility	Huber (CC40) T range ~ (233 to 473) K No visual observation during the course of an experiment	Tamson Instruments (TV4000LT) T range ~ (233 to 373) K Sight windows
Equilibrium cell	316 stainless steel p ~ 40 MPa	Alloy A286 (High temperature stainless steel, XN26TW) p ~ 60 MPa
Gas mixture preparation	In the equilibrium cell	
ROLSI^{TM} sampler	Pneumatic (movable)	Electromagnetic
Temperature measurement	Indirectly (in the body of the cell)	*In situ* (in the cell interior)

The new approach is based on the "static-analytical" method (Richon, 1996) and capillary sampling technique (Laugier & Richon, 1986). For this purpose, an experimental set-up suitable for measurements in the temperature range of (233 to 373) K and compatible with corrosive fluids was designed, constructed and validated. The core of the apparatus is an equilibrium cell entirely designed, built, and improved "in house", which can withstand pressures up to 60 MPa. A major advantage of this apparatus is the combination of precise and accurate measuring devices and the visual observation of the presence of gas hydrates and phase behavior. The isochoric technique (Tohidi *et al*., 2000; Afzal *et al*., 2007; Mohammadi *et al*., 2008) earlier described is used to determine the hydrate temperature and pressure dissociation conditions. For composition measurement of the gas phase under hydrate formation conditions, an electromagnetic ROLSI^{TM} sampler (Guilbot *et al*., 2000) was installed and connected online to a gas chromatograph.

The compositions of the liquid and hydrate phases are calculated using the material balance approach proposed by Ohgaki *et al.* (1996) in combination with the experimental data and the volumetric properties evaluated from equations of state for gas mixtures. A suitable mathematical approach is used to solve the non-linear material balance equations. This chapter describes the characteristics of the aforementioned unique measurement system and demonstrates its effectiveness and capabilities.

4.2 Apparatus

With the aim of developing a flexible apparatus suitable for gas hydrate phase equilibrium measurements, a combination of new and adopted features from the literature were considered. The main characteristics of this set-up are: suitability for corrosive fluids (high pressures), strong agitation, precise and accurate measuring devices, gas phase compositional analysis and visual observation inside the equilibrium cell during the course of the experiment. A schematic diagram of this apparatus is shown in Figure 4.1. The experimental setup consists of four major sections: an equilibrium cell, a sample supplying system, a composition analyzing system, and a pressure-temperature measurement system. Partial pictures of the main components are shown in Figure 4.2.

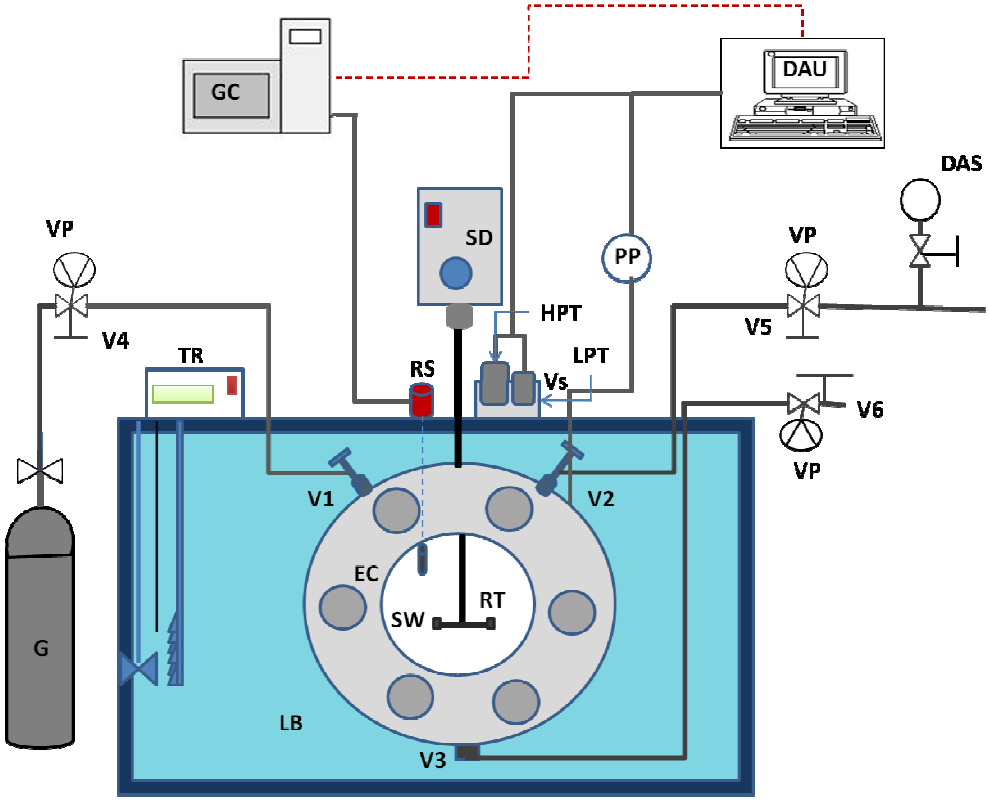


Figure 4.1. Schematic flow diagram of the new apparatus. DAS: degassed aqueous solution; DAU: data acquisition unit; EC: equilibrium cell; G: Gas cylinder; GC: gas chromatograph; HPT: high pressure transducer; LB: liquid bath; LPT: low pressure transducer; PP: platinum probe; RS: ROLSI™ sampler; RT: Rushton turbine; SD: stirring device; SW: sapphire windows, TR: temperature regulator; V_1, V_2, V_4, V_5: feeding valves; V_3, V_6: purge valves; VP: vacuum pump; Vs: isolation valve for LPT; WP: high pressure pump.



Figure 4.2. Partial pictures of the main components of the new apparatus (From left to right: Equilibrium cell, ROLSI™ sampler, pressure transducers, valve arrangement and agitation device, windowed bath).

4.2.1 Equilibirum cell

The core of the apparatus, the equilibrium cell, was entirely designed, built and improved by the workshop of CEP-TEP (MINES ParisTech, France). It was made of a high temperature stainless steel material (Type X6NiCrTiMoVB25-15-2 / Alloy 286) to withstand hydrogen embrittlement and pressures up to 60 MPa. The internal volume of the cell of (201.0 $\pm$ 0.5 cm^3, including transfer lines) is known from careful calibration using a variable volume cell coupled to a displacement transducer. The cell is suitable for measurements within temperatures ranging from (233 to 373) K.

The cell is cylindrical in shape and it consists of two major parts: (1) a main body and (2) two sapphire windows. The 166 mm long, 83 mm diameter main body is horizontally placed on an aluminum support (Figure 4.3). Two sapphire windows are located in the front and the back of the cell enabling the visual observation of the presence of gas hydrates and phase behavior occurring inside the equilibrium cell. All pieces of the cell are tightened by sixteen bolts and the seal between the main body and the sapphire windows is achieved with polytetrafluoroethylene (PTFE) O-rings which sit in circular channels on both sides. Three inlet/outlet ports suitable for pressure and temperature sensors have been drilled in the main body of the cell (Figure 4.3).

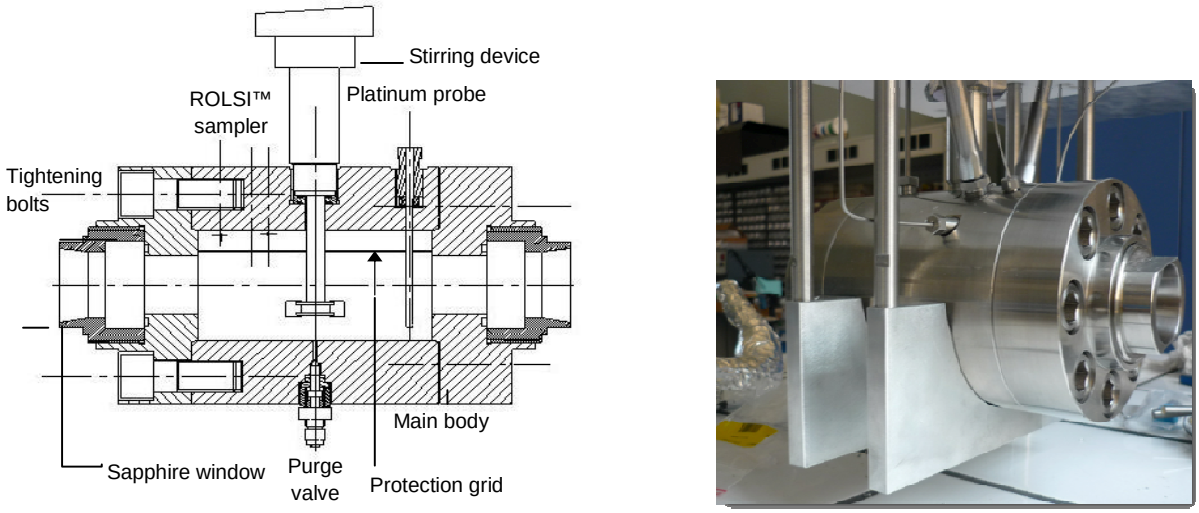


Figure 4.3. Cross section of the equilibrium cell with stirring and measurement arrangement (*left*). Photograph of equilibrium cell on its aluminum support (*right*).

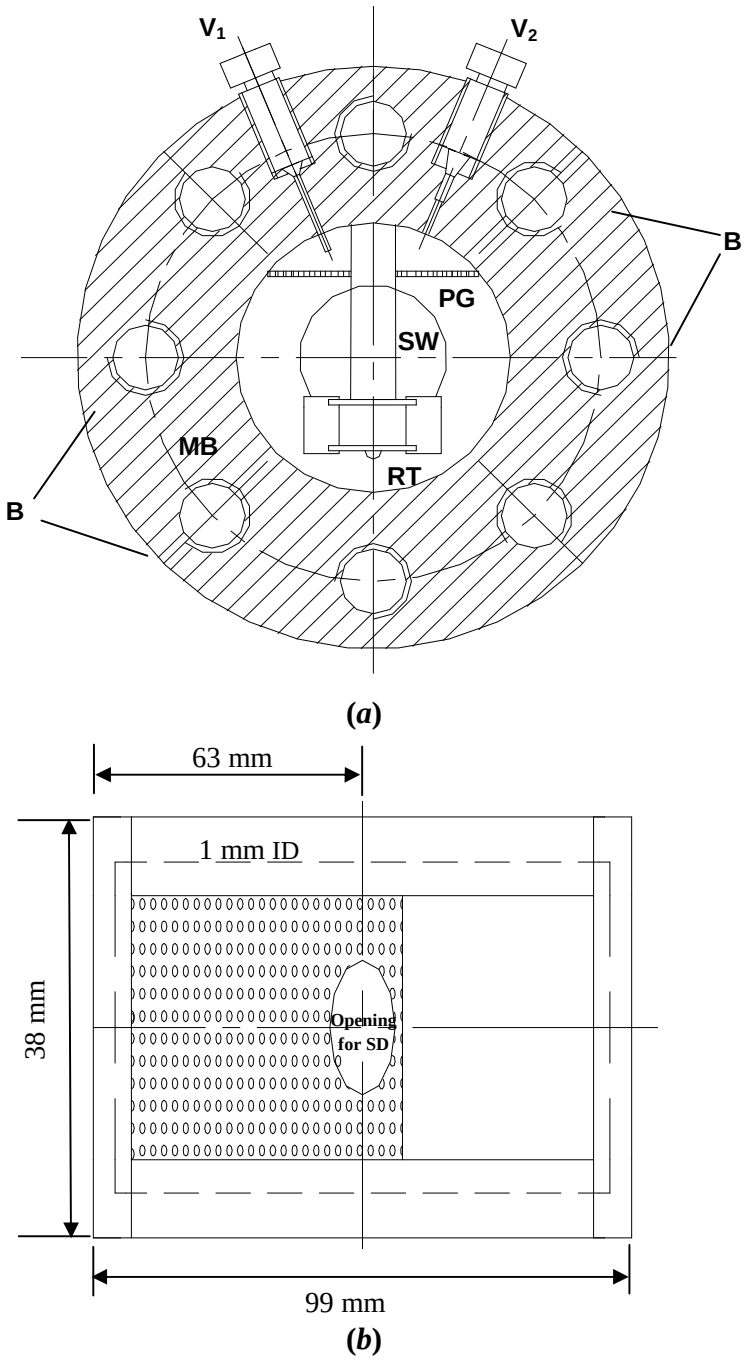


Figure 4.4. **(*a*)** Lateral section of the equilibrium cell showing the position of the protection grid. B: tightening bolts; MB: main body; PG: protection grid; RT: Rushton turbine; SW: sapphire windows; V_1 and V_2 : feeding valves. **(*b*)** Detail of the protection grid for the capillary sampler. SD: stirring device.

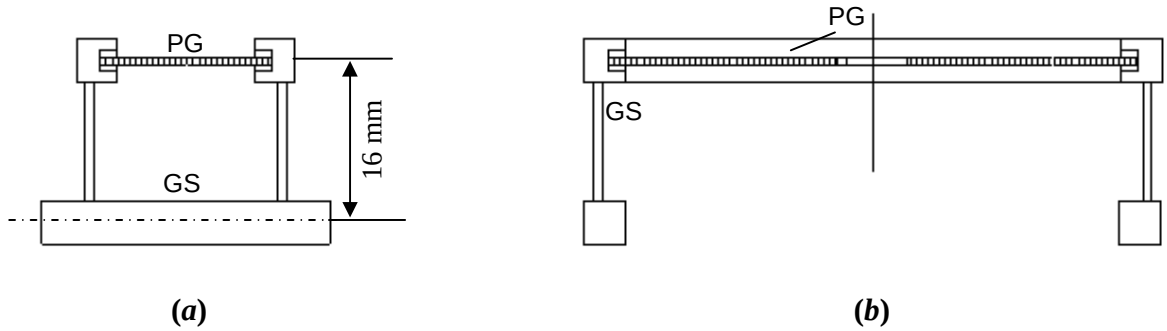


Figure 4.5. (*a*) Lateral and (*b*) cross sections of the grid support. GS: PTFE grid support; PG: protection grid.

A stainless steel (316) grid support horizontally placed inside the cell was installed to protect the capillary sampler from plugging by hydrate particles. The protecting framework was fixed by a PTFE support at approximately 20 mm from the top. Such arrangement as shown in Figures 4.4 and 4.5, allows sampling and analyzing the gas phase in equilibrium with the hydrate and liquid phases, in a way that hydrate particles do not enter or plug the capillary. Plugging of capillary sampler by hydrate crystals can seriously compromise the reliability of vapor phase composition measurements during hydrate formation (Ruffine *et al.*, 2010). The arrangement just described can be used to overcome this experimental difficulty. As shown in Fig. 4.6, a remarkable sampling repeatability is obtained for nitrogen gas samples taken under gas-hydrate-liquid equilibrium, demonstrating the value of the latter capillary protection arrangement.

A motor-driven turbine agitation system (Top Industrie, France) enables to stir the cell contents at a speed up to 2000 rpm to increase the fluids contact and enhance water conversion into hydrate.

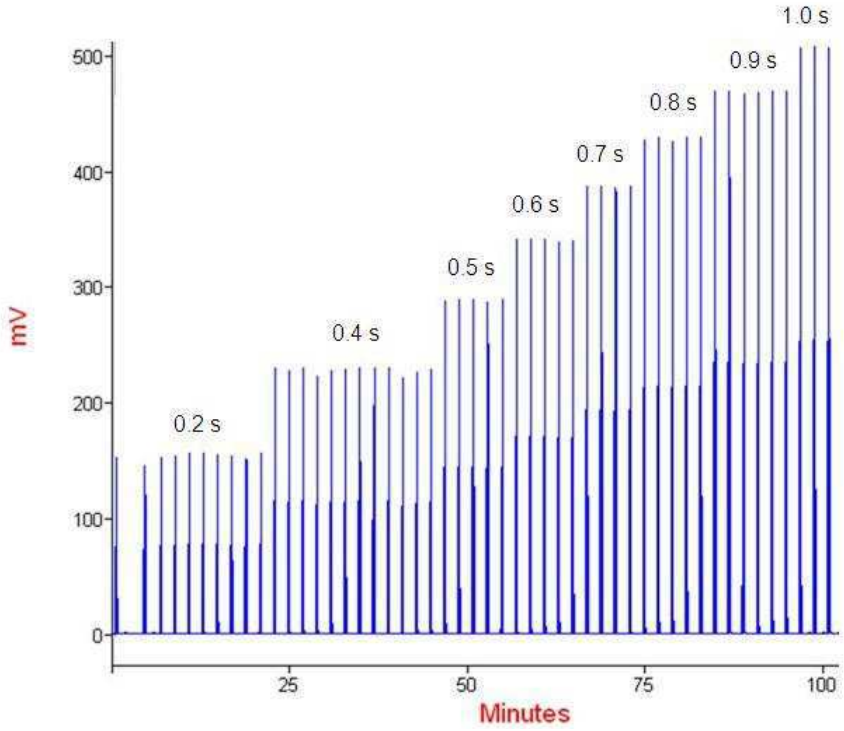


Figure 4.6. Chromatogram profile for nitrogen gas samples under gas-hydrate-liquid water equilibrium (15 MPa and 272 K) at different capillary opening time (seconds) using ROLSI^{TM}.

4.2.2 Sample supplying system

The sample supplying system consists of gas cylinders, a vacuum pump with an electronic manostat (Leybold, model Trivac D) and a high-pressure syringe pump (Teledyne Isco, model 260D), which allows measuring the amount of liquid supplied to the system.

4.2.3 Composition analyzing system

The composition analyzing system consists of an electromagnetic online micro sampler (rapid on-line sampler-injector: ROLSI^{TM}) developed at the Ecole des Mines de Paris (Laugier & Richon, 1986; Guilbot *et al.*, 2000). The small size of the samples (1-5 µL) compared to the volume of the cell (~ 201 cm^3), ensures thermodynamic equilibrium is not disturbed during sampling.

Over the years, many modifications have been carried out to the original ROLSI™. The electromagnetic version used in this apparatus (ROLSI™ evolution IV) shown in Figure 4.2, is smaller than the one described by Guilbot *et al.* (2000) and entirely automatable, it is actuated by an electromagnet allowing significant new features, more robustness and increased operational life (Afzal *et al.* 2008*a*). Figure 4.7 gives a flow diagram of the latest version of this sampler-injector. The micro sampler is a compact device with no dead volumes and it consists of a Monel 400 capillary tube with internal diameter of less than 0.15 mm. Reliable and representative samples may be obtained by adjusting the sample size through the valve's opening time (between 10 milliseconds and approximately one second) and frequency, with an outstanding repeatability. It allows samplings from (0.3 to 80 MPa) and temperatures from cryogenic up to 523 K.

Samples are swept along the carrier gas (outlet) heated transfer line, ensuring direct injection into the GC column. Sampling can be carried out only through electric power, thus the capillary is normally closed for highest safety. The materials of construction (Monel 400 or Inox 316L) enable to extend its applicability to corrosive and viscous systems (ROLSI™).

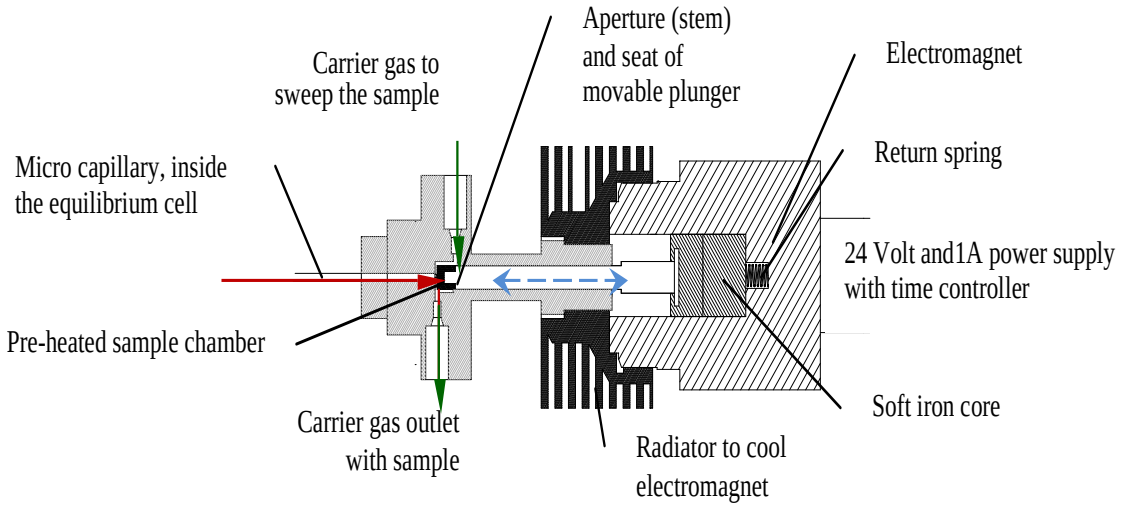


Figure 4.7. Flow diagram of the electromagnetic rapid on-line sampler-injector: ROLSI™ (Afzal *et al.*, 2008*b*).

The ROLSI^{TM} was vertically installed in the equilibrium cell and connected to a gas chromatograph (GC) on-line. The micro sampler and the lines connecting to the GC are independently heated to a temperature well above that of the equilibrium cell to avoid any condensation or adsorption of the components. The temperature of the sampling valve and transfer lines are set through the ROLSI^{TM} control unit. To make sampling possible, the pressure inside the cell must be higher than the pressure of the carrier gas stream from the GC. The ROLSI^{TM} is actuated using the control unit, which allows setting the valve's opening time with a resolution of 0.01 s. Thus, for a given pressure in the cell, the frequency and the amount of sample withdrawn can be adjusted.

The analysis work was carried out using a gas chromatograph (Varian, CP3800) equipped with a thermal conductivity detector (TCD). The GC was connected to a computer fitted with the Perichrom Winilab III software (Figure 4.8). The characteristics of the chromatographic column are described in section 2.6.1 and the chromatographic conditions were similar to those given in Chapter 3. The composition of the gas phase is determined by gas chromatography, as explained in Chapter 2, while the composition of water in the gas phase is considered negligible in the experimental conditions investigated in this study (Mohammadi & Richon, 2009*b*). However, other methods as "dilutor technique" may be used if necessary to measure the water content of the gas phase (Mohammadi *et al.*, 2004).

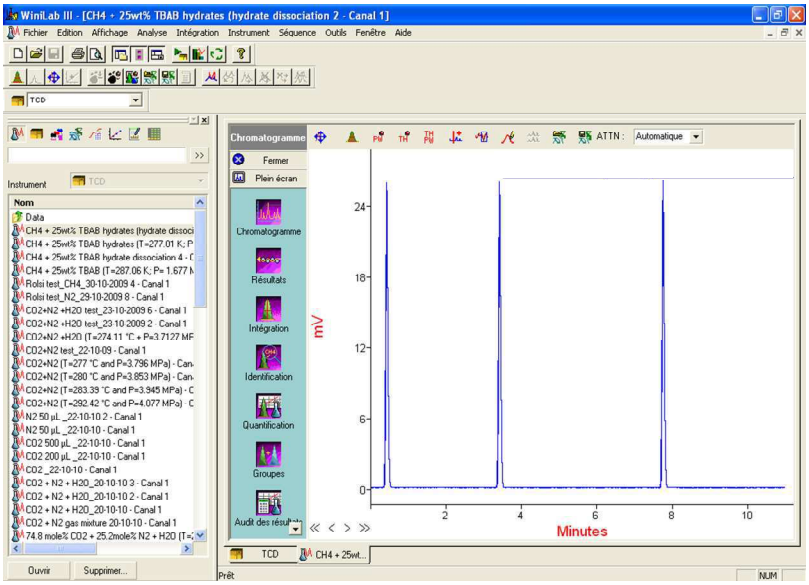


Figure 4.8. Layout for chromatograms acquisition using Winilab III software.

4.2.4 Measurement, control and acquisition of temperature and pressure

Temperature is controlled using a thermostatic ethanol bath (Tamson Instruments, TV4000LT). The thermostatic bath is equipped with a glass window, which allows the visual observation of the cell content throughout the experiments. One platinum temperature probe (Pt100) inserted in the cell interior was used to measure the temperature inside the cell within measurement uncertainties, which are estimated to be less than 0.02 K with a second order polynomial calibration equation, as mentioned in Chapter 2. The temperature probe was carefully calibrated against a reference platinum resistance thermometer, as indicated also in Chapter 2.

The equilibrium pressure was measured using two calibrated pressure transducers (Druck^{TM}, type PTX611). Pressure ratings for low (LPT) and high (HPT) pressure transducers are 8 and 40 MPa, respectively. Both pressure transducers are maintained at constant temperature (temperature higher than the highest temperature of the study) using an air-thermostat thermally regulated by a proportional–integral–derivative controller (WEST instrument, model 6100).

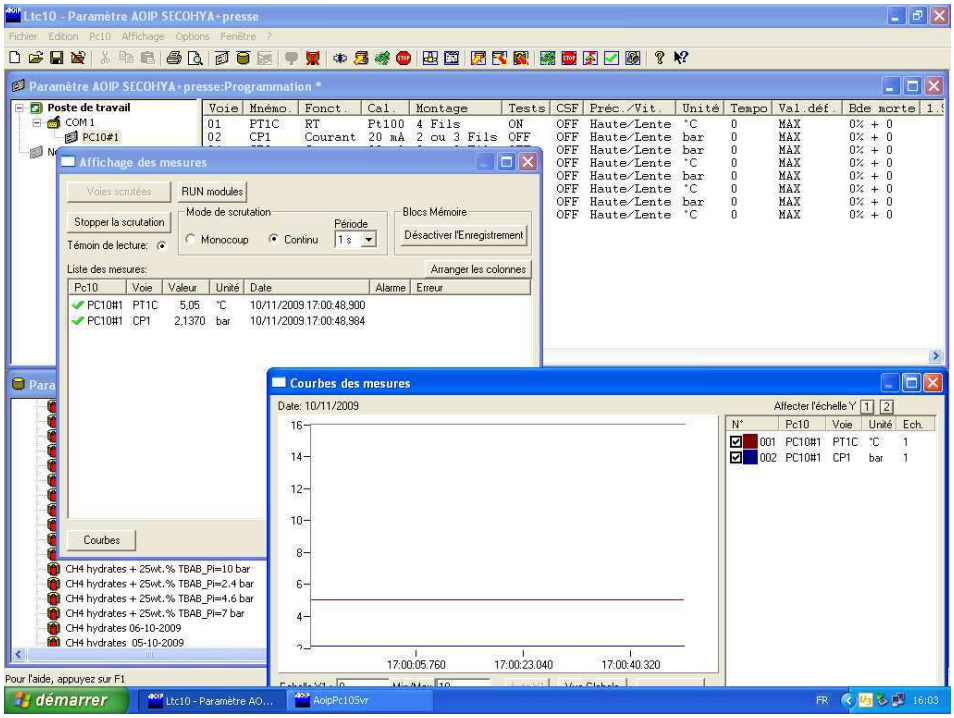


Figure 4.9. Layout for temperature and pressure data acquisition through AOIP Ltc10 software.

After calibrating the pressure transducers against a dead weight balance (Desgranges & Huot 5202S CP, Aubervilliers, France), pressure accuracy was estimated to be better than 0.002 MPa using a second order polynomial calibration equation, as described in Chapter 2. A major advantage of this apparatus is the combination of precise and accurate measuring devices and the visual observation of the presence of gas hydrates and phase behavior. The apparatus is also equipped with a safety pressure relief valve.

The data acquisition unit (AOIP, PC10) was coupled with a personal computer to measure and automatically register pressure, temperature and time data. The data acquisition software (AOIP, Ltc10) also allows adjusting the rate of data acquisition. Continuous recording of pressures and temperatures allows detecting any subtle changes in the system and true equilibrium conditions. A representative view of the temperature and pressure data acquisition software is shown in Figure 4.9.

4.3 Experimental Procedure

Phase equilibrium measurements (*p*, *T*, *y*) under hydrate formation conditions were carried out using the apparatus described in the previous section and the experimental procedure as follows.

4.3.1 Preparation of the feed

Research grade carbon dioxide (99.995 mole% purity) supplied by Air Liquide and CH_4 (99.995 mole % purity) supplied by Messer Griesheim, were used without further purification. Gas mixtures composed of CO_2 and CH_4 were prepared in the equilibrium cell. After the equilibrium cell was well cleaned and evacuated with vacuum pump, a specified amount of each gas (through pressure measurement) was introduced at ambient temperature into the volume-calibrated cell from the corresponding gas cylinders through a pressure-regulating valve. Once temperature and pressure were stabilized, the on-line valve connecting the vessel and the gas cylinder was closed. As pressure, temperature and the total volume of the equilibrium cell are known, the total number of moles loaded to the cell is easily calculated by applying an appropriate *p-V-T* relation, such as the ideal gas law. The initial composition of the gas mixture is determined by gas chromatography (GC). Several samples are taken through ROLSI^{TM} sampler and analyzed by

GC. Agreement between the overall compositions obtained by PVT and chromatographic methods assures this approach as a highly reliable one. Molar concentrations of CH_4 and CO_2 are measured within an experimental uncertainty of $\pm$ 1-2 %.

4.3.2 Fluids supply to the equilibrium cell

An amount of typically 10 % (by volume) of the equilibrium cell was subsequently filled with distilled and deionized water using a high-pressure syringe pump. All amounts of substances supplied to the cell were quantified.

4.3.3 Isochoric Pressure Search Method

Hydrate dissociation conditions were measured according to the isochoric pressure search method (Tohidi *et al*., 2000; Afzal *et al*., 2007; Mohammadi *et al.*, 2008), as described in Chapter 3. Briefly, the cell was immersed into the temperature-controlled bath and the temperature was decreased to form hydrate, while agitating at a constant speed of 1500 rpm. The temperature of the system was kept constant for at least 24 hours to overcome the metastable period and allow complete hydrate formation. Hydrate formation in the cell was detected by a noticeable pressure drop. Once hydrate formation was completed and equilibrium conditions were reached, at least seven samples of the gas phase were taken through the ROLSI^{TM} sampler at a given temperature and pressure for repeatability checks. The composition of the gas phase at equilibrium with the hydrate and liquid phases was determined through GC analysis.

Temperature was then increased in steps at sufficiently slow rate of about 0.1 *K*/h (Tohidi *et al*., 2000; Rovetto *et al*., 2006). At every temperature step, temperature was kept constant and the composition of the gas phase was successively analyzed, until meeting the criteria for equilibrium described in Chapter 2. At this point (typically reached within four hours), it was assumed that equilibrium had been reached and average concentrations were registered as the composition of the gas phase at the corresponding temperature and pressure condition.

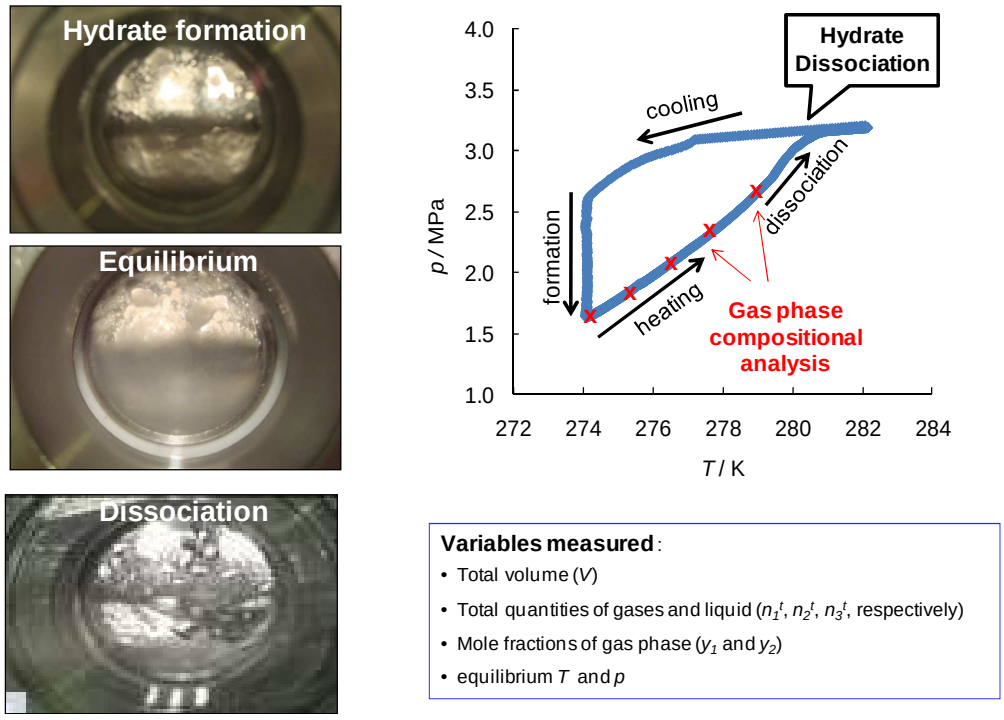


Figure 4.10. Hydrate formation/dissociation process inside the high-pressure visual cell (*left*), cooling and heating isochors and determination of hydrate phase boundaries and composition of the equilibrium phases (*right*).

Temperature and pressure data were collected twice per minute throughout the experiment. As implemented by Ohmura and coworkers (2004), a pressure-temperature diagram was obtained for each experimental run, from which the hydrate dissociation condition (HDC) was determined. The point at which the slope of pressure-temperature data plots changes sharply was considered to be the point at which all hydrate crystals have dissociated and, hence, it is reported as the hydrate dissociation point (Ohmura *et al*., 2004). Figure 4.10 illustrates the typical course of a gas hydrate formation-dissociation experiment.

There is a fundamental difference between hydrate formation and dissociation conditions, since the gas and aqueous phases are initially disordered on a molecular level, the initial hydrate formation is affected by a metastability period, while hydrate crystals are ordered structures in nature and they are quickly dissociated when taken out of their *p*-*T* stability region (Sloan & Koh, 2008).

For measuring an equilibrium condition at a higher pressure, the pressure of the system was increased by successively supplying water to the equilibrium cell until achieving the desired pressure. In this way, several *p*, *T* and gas phase composition equilibrium data were obtained in parallel to the hydrate dissociation conditions from each experimental run. Maximum uncertainties in the pressure and temperature measurements are expected to be within ± 0.05 MPa and ± 0.2 K, respectively. The maximum overall uncertainty is attributed to the uncertainty in measuring compositions of the gas phase by gas chromatography, which is estimated to be less than 1% as explained in Chapter 2.

The experimental quantities measured in every hydrate formation and dissociation experiment are as follows: total volume (*V*), each total quantity of CO_2, methane and water (n_1^t, n_2^t, n_3^t, respectively), mole fractions of gas phase (y_1 and y_2) and the equilibrium temperature (*T*) and pressure (*p*). Starting from the (*p*, *T*, *y*) data for the three-phase equilibrium, the compositions of the hydrate and aqueous phases are calculated using a material balance approach proposed by Ohgaki and coworkers (1996) in combination with the Peng-Robinson (1976) equation of state for gas mixtures. Assuming the perfect gas law is valid throughout the studied pressure range and considering that all types of molecules have the same gaseous molar volume, v^G_i may be replaced by v^G_m and the volume-balance in the equilibrium cell is given as:

$$V = \sum n_i^G v_m^G + \sum n_i^L v_i^L + n^H v^H \tag{4.1}$$

where the subscript *m* denotes the gas mixture and the superscripts *H*, *L*, and *G* represent the hydrate, liquid, and gas phases, respectively. The volumetric properties for the gas mixture (v^G_m), liquid (v^L_i) and the molar volume of ideal hydrate (v^H) were calculated using the CSMGem thermodynamic model (CSMGem, 2008).

In addition, equations (4.2) to (4.4) are derived according to the material balances for the three present components in the system as follows:

$$n_1^t = n_1^G + n_1^L + z\,n^H \tag{4.2}$$
$$n_2^t = n_2^G + n_2^L + (1-z)n^H \tag{4.3}$$
$$n_3^t = n_3^L + q\,n^H \tag{4.4}$$

where the total amount of each component once measured, can be partitioned into gas, liquid (aqueous phase), and hydrate (*z*) phases for CO_2 and CH_4 (n_1^t, n_2^t, respectively), and liquid and hydrate phases for water (n_3^t).

The expressions for mole fractions of CO_2 in the gas phase (y_1) and CO_2 (x_1) and CH_4 (x_2) in the liquid phase are given by equations (4.5) to (4.7):

$$y_1 = n_1^G / \sum n_i^G \tag{4.5}$$

$$x_1 = n_1^L / \sum n_i^L \tag{4.6}$$

$$x_2 = n_2^L / \sum n_i^L \tag{4.7}$$

The values of x_1 and x_2 can be estimated from a suitable thermodynamic model. For this purpose, the CSMGem thermodynamic model, which is based on the Gibbs energy minimization (CSMGem, 2008) was used. In the cases where the model did not converge, these values were evaluated applying the apparent Henry's constants of each pure gas system:

$$x_i = f_i(T,P) / H_i(T,P) \tag{4.8}$$

where $f(T, p)$ is the fugacity coefficient, $H(T, p)$ is the apparent Henry's constant, and subscript i refers to the i^{th} component in the mixture. A mathematical approach based on the Newton's numerical method (Constantinides & Moustofi, 1999) coupled with the Differential Evolution optimization strategy (Price & Storn, 1997) was used to solve Equations (4.1) to (4.7) for the seven unknown variables (n_1^G, n_2^G, n_1^L, n_2^L, n_3^L, n^H, and z,). As hydrate composition is variable with temperature, pressure, and the composition of associated fluid phases (Sloan & Koh, 2008), an approximate value of q, based on the (p, T, y) conditions under which hydrates are formed and assuming clathrate hydrate structure I, is first anticipated. A more accurate value is then obtained by iteration. The solving procedure is described in detail elsewhere (Belandria *et al.*, 2011).

4.4 Results and discussion

Hydrate dissociation conditions (*T* and *p*) for the (CO_2 + CH_4 + H_2O) systems were measured at different compositions of CO_2 in the gas feed. The compositions of the (methane + carbon dioxide) gas mixtures along with the experimental hydrate dissociation conditions in the presence of pure water are presented in Table A.2 (Appendix A) and Figure 4.11. In addition, the hydrate dissociation pressures were predicted at the corresponding equilibrium temperature, CO_2 mole fraction in the gas feed, and water mole fraction introduced to the system using two hydrate thermodynamic models: CSMGem and HWHYD, which is based on fugacity equalities of each component throughout all present phases (HWHYD, 2000).

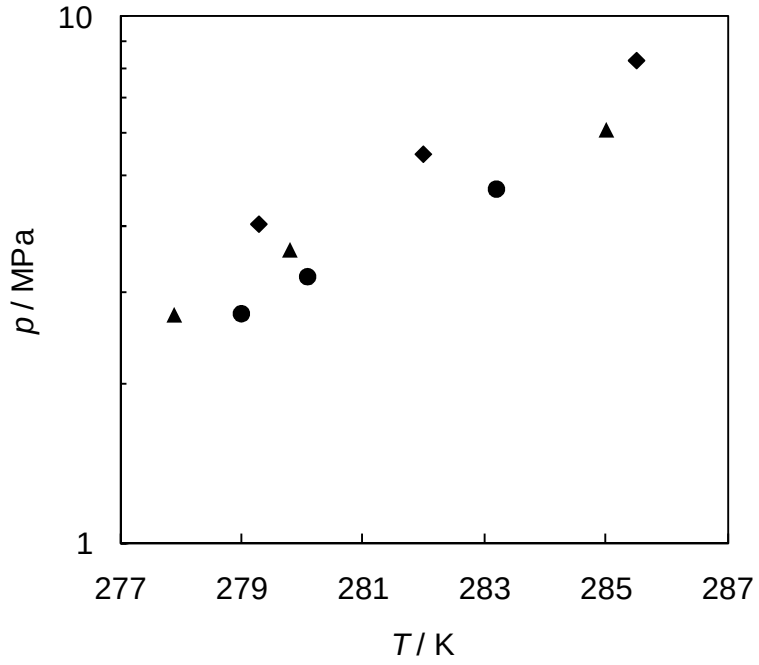


Figure 4.11. Hydrate dissociation conditions measured in this work for (methane + carbon dioxide) clathrate hydrates at various CO_2 load mole fractions: 0.206 (♦); 0.476 (▲) and 0.744 (●).

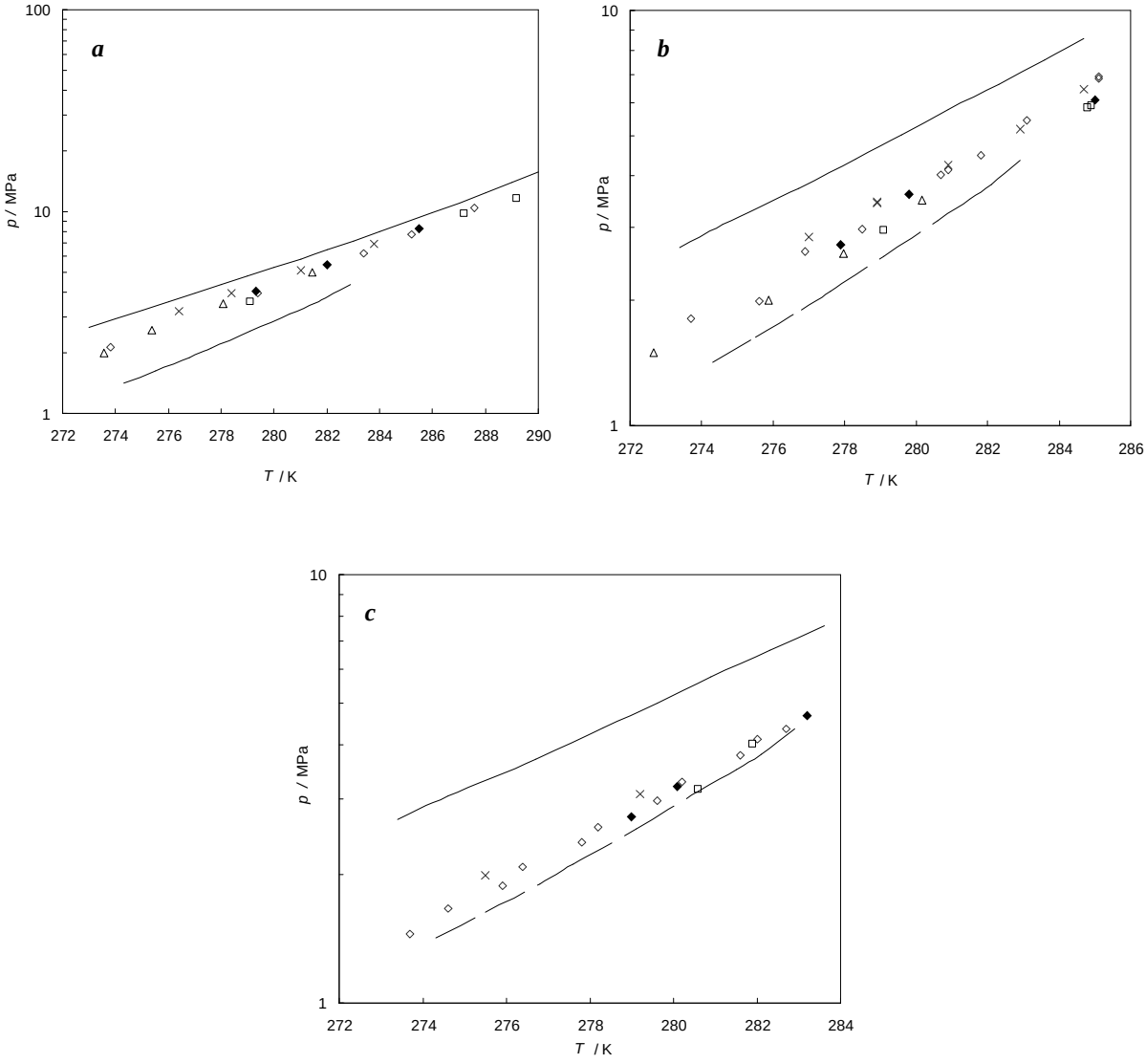


Figure 4.12. Hydrate dissociation conditions (literature and this work) for (methane + carbon dioxide) clathrate hydrates at selected CO_2 load mole fractions. *(a)*: ♦, 0.206 (This work); ◊,0.210-0.250 (Adisasmito *et al*., 1991); □, 0.264 (Belandria *et al*., 2010); x, 0.274 (Unruh & Katz, 1949); ∆, 0.200 (Seo *et al*., 2000); *(b)* : ♦, 0.476 (This work); ◊,0.390-0.500 (Adisasmito *et al*., 1991); □, 0.490-0.504 (Belandria *et al*., 2010); x, 0.539-0.545 (Unruh & Katz, 1949); ∆, 0.600 (Seo *et al*., 2000); *(c)* : ♦, 0.744 (This work); ◊,0.670-0.850 (Adisasmito *et al*., 1991); □, 0.730 (Belandria *et al*., 2010); x, 0.777 (Unruh & Katz, 1949). Dashed line, pure CO_2 hydrates and solid line, pure CH_4 hydrates (Adisasmito *et al*., 1991).

The predicted hydrate dissociation pressures are also listed in Table A.2 along with the absolute relative deviation (*ARD*) from the obtained experimental values. As can be seen, the *ARD* of the predicted hydrate dissociation conditions by HWHYD and CSMGem models are in average 9.7 % and 5.1 %, respectively, which are considered to be in acceptable agreement with the data measured in this work.

For comparison purposes, Figures 4.12*a*, 4.12*b*, and 4.12*c* show the hydrate dissociation conditions measured in this work along with some selected experimental data from the literature (Unruh & Katz, 1949; Adisasmito *et al*., 1991; Seo *et al*., 2000; Hachikubo *et al*., 2002; Belandria *et al*., 2010). The obtained results generally indicate that the hydrate dissociation pressures of the CO_2 containing gas mixtures are greater than those of pure CO_2 hydrates. It is also observed that as the relative amount of CH_4 to CO_2 increases in the feed gas at a given temperature, the equilibrium pressure conditions shift to higher pressures. As can be seen, the agreement between these data and the experimental data reported in the literature is generally acceptable, demonstrating the reliability of the new apparatus and method used in this work.

To the best knowledge of the author, no hydrate structural transition has been reported in the literature for (CO_2 + CH_4) hydrates Therefore, considering that the (CO_2 + CH_4 + H_2O) system likely forms structure I hydrates (Takeya *et al*, 2005; Uchida *et al*, 2005; Sloan & Koh, 2008; Belandria *et al*., 2010) similar to pure CH_4 or CO_2 hydrates, and applying Gibbs phase rule, there are two degrees of freedom at liquid water-hydrate-gas (Lw-H-G) equilibrium conditions for this system (Bruusgaard *et al*., 2010). Therefore, two intensive variables can be changed independently without disturbing the thermodynamic equilibrium.

In this work, temperature and pressure were controlled while the compositions of CH_4 and CO_2 in the gas phase under (L_w-H-G) equilibrium were measured and compared with available literature data (Ohgaki *et al*., 1996; Beltran & Servio, 2008; Bruusgaard *et al*., 2010). As shown in Figures 4.13*a* and 4.13*b*, the molar fractions of CO_2 in the gas and hydrate phases are found to agree with the experimental data reported in the literature within experimental uncertainties. Furthermore, it is observed that the mole fractions of CO_2 in the gas and hydrate phases generally decrease as pressure increases.

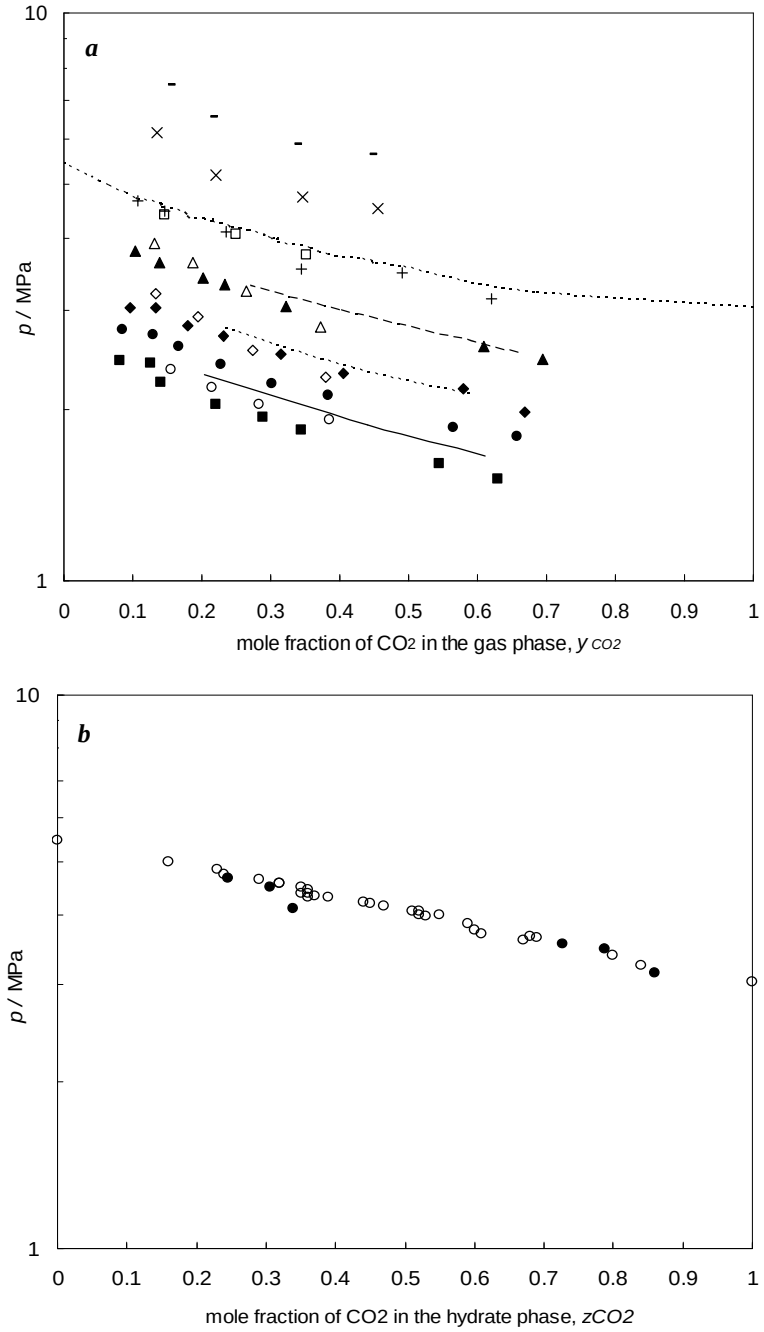


Figure 4.13. *a) p-y* phase diagram of (methane + carbon dioxide) clathrate hydrates at different equilibrium temperatures: This work: ■, 273.6 K; ●, 275.2 K; ♦, 276.1 K; ▲, 278.1 K and +, 280.2 K. Literature : ○, 275.2 K; □,277.2 K; △, 279.2 K; □, 281.2 K; x, 283.2 K; ▬, 285.2 K (Beltran & Servio, 2008); solid line, 274.2 K; ---, 276.2 K; ▬, 278.2 K; (Bruusgaard *et al.*, 2010); ▪▪▪, 280.3 K (Ohgaki *et al.*, 1996). *b)* : *p-z* phase diagram of methane + carbon dioxide clathrate hydrates at □280.2 K : This work: ●, 280.2 K. Literature : ○, 280.3 K (Ohgaki *et al.*, 1996).

This suggests that considerable enrichment of CO_2 in the hydrate phase takes place in the studied systems. It is also observed that the composition of CO_2 in the gas phase increases as temperature increases, which translate in less amount of CO_2 trapped in the hydrate phase at high temperatures. Compositional analysis of the hydrate and liquid phases for the ternary (CO_2 + CH_4 + H_2O) system was determined using the material balance approach described in the experimental section. The non-linear mass balance equations were solved using a suitable mathematical approach, as mentioned earlier. The measured data, results of solving the material balance equations, and the predictions of CSMGem thermodynamic model are summarized in Table A.2 (Appendix A) and illustrated in Figures 4.14*a* through 4.14*e* at selected isothermal conditions.

It should be noted that such pressure-gas phase composition (*p-y*) phase diagrams are essential for designing a (multi-stage operation) CO_2 capture process based on gas hydrates concept. As can be seen in these figures, the predictions of the CSMGem model for the mole fraction of CO_2 in the gas phase are in consistent agreement with the experimental data. However, the thermodynamic model (CSMGem, 2008) shows considerable deviations when predicting the molar compositions of CO_2 in the hydrate phase. This suggests that the parameters of the thermodynamic model may require readjustment using fully compositional analysis + hydrate dissociation experimental data, as such models have generally been developed for hydrates of hydrocarbons using mainly experimental hydrate dissociation data.

As for the unspecified points shown in Table A.2 related to the predictions of the CSMGem model, the model is not able to predict the three-phase equilibrium (Lw-H-G) behavior at the studied conditions. The HWHYD model did not converge at all at the studied experimental conditions.

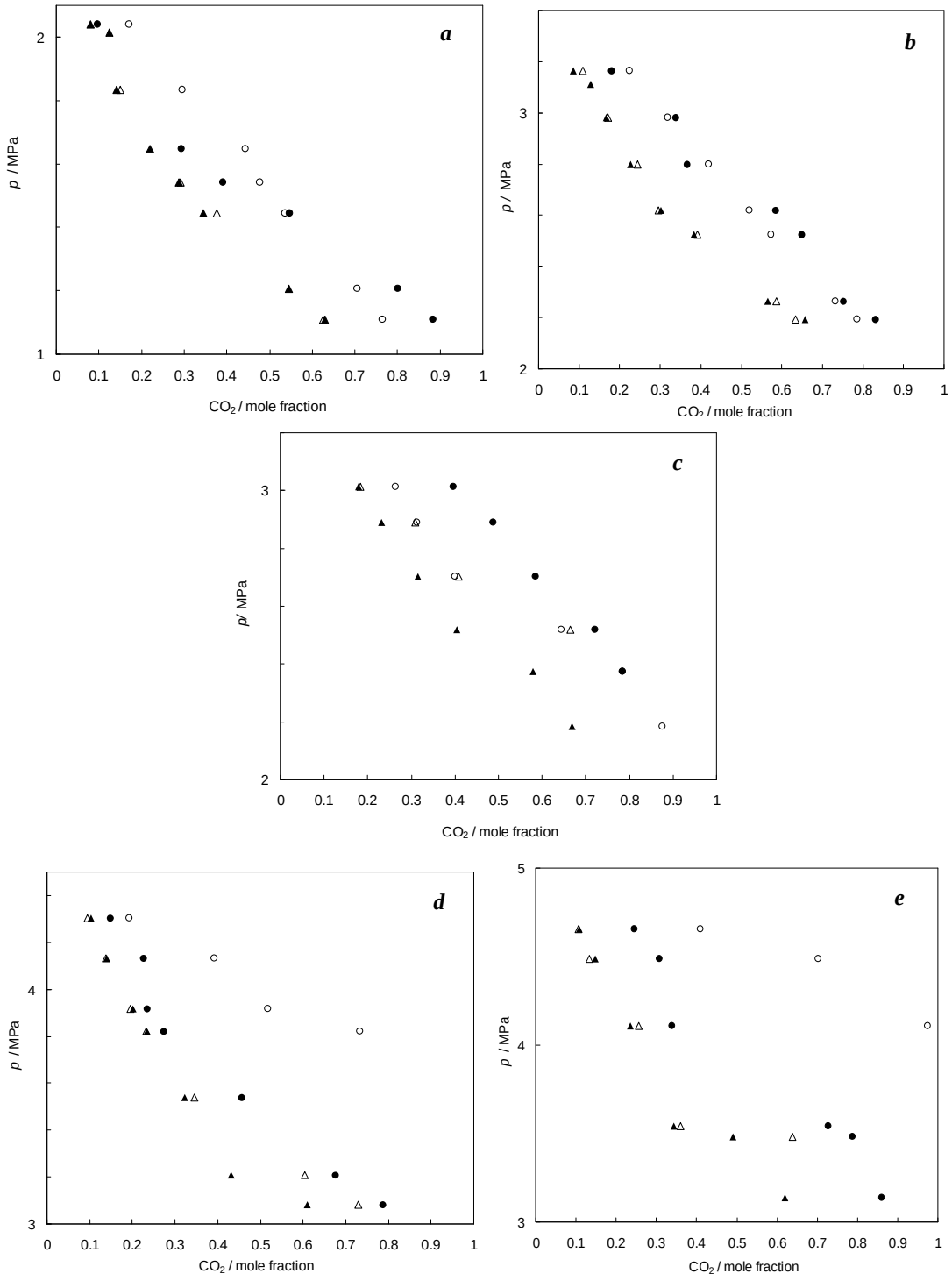
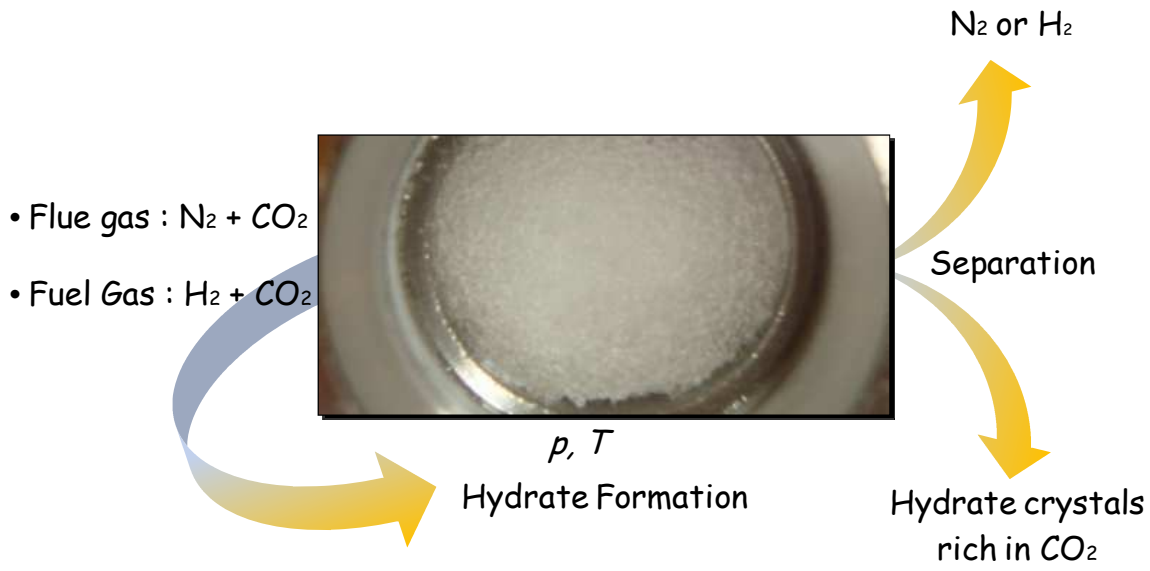


Figure 4.14. Pressure-composition phase diagram of the (methane + carbon dioxide) clathrate hydrates : This work: y_{CO2} (▲); z_{CO2} (●). CSMGem model predictions: y_{CO2} (Δ); z_{CO2} (○). *a)* : 273.6 K ; *b)* 275.2 K ; *c)* 276.1 K ; *d)* 278.1 K ; *e*) 280.2 K.

5

Thermodynamic Stability of Hydrates from Gas Mixtures Containing CO_2[†]



[†] Content published in *Ind. Eng. Chem. Res*. 2011, 50 (8), 4722-4730; *Ind. Eng. Chem. Res.* 2011, 50 (10), 6455-6459 and submitted (Phase Equilibria of CO_2 + N_2 and CO_2 + CH_4 Clathrate Hydrates: Experimental Measurements and Thermodynamic Modelling, 2011).

5

Résumé

Ce chapitre présente des équilibres de phases des systèmes: ”dioxyde de carbone + azote + eau” et ”dioxyde de carbone + hydrogène + eau” en présence d’hydrates de gaz. Les équilibres à trois phases (Lw-H-G) sont mesurés en suivant les procédures expérimentales décrites dans le chapitre précédent. Des teneurs moyennes à hautes de CO_2 en mélanges de gaz sont étudiées sur une large plage de températures. Des résultats on déduit que les pressions d'équilibre de dissociation sont dépendantes de la composition de la charge et sont décalées vers des valeurs d’autant plus faibles que la fraction molaire en CO_2 de la charge est élevée. Les données de dissociation générées ici, ainsi que les données expérimentales disponibles dans la littérature pour le mélange : "dioxyde de carbone + azote" sont comparées avec les prédictions de deux modèles thermodynamiques. Les écarts observés entre valeurs expérimentales et valeurs prédites sont discutés. Les compositions mesurées sont comparées à celles de la littérature et l'accord est généralement acceptable prenant en compte les incertitudes expérimentales. Les analyses thermodynamiques présentées fournissent la base pour une conception de procédés de séparation impliquant des hydrates en vue de la capture du CO_2 dans le cadre de la pré-combustion ou de la post-combustion.

Abstract

This chapter presents the phase equilibria of (carbon dioxide + nitrogen + water) and (carbon dioxide + hydrogen + water) systems containing gas hydrates. The three-phase (L_w-H-G) equilibrium data are measured following the experimental procedures described in the previous Chapter. Medium to high content CO_2 gas mixtures are investigated over a wide temperature range. The equilibrium dissociation pressures are found to be dependent on the composition of the feed and are shifted to lower values as the mole fraction of CO_2 increases in the feed gas. The dissociation data generated along with the experimental data reported in the literature for (carbon dioxide + nitrogen) are compared with the predictions of two thermodynamic literature models. A discussion is made about the deviations observed between experimental and predicted data. The measured compositional data are compared with the literature data and the agreement is found generally acceptable within experimental uncertainties. The thermodynamic analyses presented provide the basis for a conceptual design of hydrate-based schemes for pre-combustion or post-combustion CO_2 capture.

5 Thermodynamic Stability of Hydrates from Gas Mixtures Containing CO_2

5.1 Introduction

Over 60 % of carbon dioxide (CO_2) emission sources come from power plants activity, in which the main constituents are nitrogen (N_2) and CO_2 (IPCC, 2005). Conventional strategies established to capture CO_2 from industrial/flue gases, essentially involve nitrogen-carbon dioxide, hydrogen-carbon dioxide and oxygen-nitrogen separation tasks. Since such separation is the most expensive step of CCS, the challenge is to evaluate and develop energy efficient and environmental friendly technologies to capture the CO_2 produced in large-scale power plants.

Extremely high pressures [100-360 MPa] are required to stabilize structure-II N_2 (Marshall *et al*. 1964) or H_2 gas hydrates (Mao & Mao, 2004) at ambient temperatures. However, CO_2 is enclathrated in hydrate cages at moderate pressure conditions (Sloan & Koh, 2008). Such preferential formation of CO_2 hydrates over N_2 or H_2 hydrates determine the potential of application of the gas hydrate approach for separating CO_2 from treated flue gas, considered a (CO_2 + N_2) gas mixture, or fuel / synthesis gas, mainly composed of (CO_2 + H_2).

Despite the potential use of gas hydrate approach to capture CO_2 from combustion flue gases, the hydrate phase equilibria of the ternary systems including (carbon dioxide + nitrogen or hydrogen + water) have been scarcely studied. To analyze the complex thermodynamic phenomena involved in hydrate-based crystallization processes, above all, the phase behavior of gas hydrates containing CO_2 as a guest molecule should be investigated. In this respect, several related studies have been performed. The experimental phase equilibrium data on the dissociation conditions and compositions of the gas and hydrate phases reported in the literature for the (carbon dioxide + nitrogen + water) and (carbon dioxide + hydrogen + water) ternary systems are summarized in Tables 5.1 and 5.3, respectively.

Literature studies are mainly focused on the determination of equilibrium conditions. Until now, few experimental works report compositional data of the equilibrium phases (Tables 5.2 and 5.5), although they are fundamental for designing separation processes.

Table 5.1. Literature phase equilibrium data of the (carbon dioxide + nitrogen + water) ternary hydrate system.

Authors	CO_2 molar composition in the gas feed	*T* and *p* ranges	Type of data	Number of experimental data
Fan and Guo (1999)	0.9099 and 0.9652	273.1 - 280.2 K 1.22 - 3.09 MPa	HDC (*p*,*T*)	9
Seo *et al.* (2000) Kang *et al.* (2001)	0 - 1	274, 277, 280 K 1.39 - 32.31 MPa	GHE *(p,T,y, z)*	26
Kang *et al.* (2001)	0.0663 - 0.9659	272.9 - 284.3 K 1.57 - 24.12 MPa	HDC (*p*,*T*)	28
Seo and Lee (2004)	0.10 and 0.20	272.1 K 3.20 - 14.50 MPa	GHE *(p,T, y, z)*	8
Linga *et al.* (2007*b*)	0.169, 0.570, 0.830	273.7 K 1.60 - 7.70 MPa	HDC (*p*,*T*)	3
Bruusgaard *et al.* (2008)	0 - 1	275.3 - 283.0 K 1.60 - 22.40 MPa	HDC (*p*,*T*,*y*)	26
Herri *et al.* (2011)	0.16 - 0.59	274.4 - 282.1 K 5.30 - 6.60 MPa	GHLE (*p*,*T*,*y*,*z*)	16

Table 5.2. Review of the compositions of the gas and hydrate phases at hydrate equilibrium conditions reported in the literature for (carbon dioxide + nitrogen + water) ternary system.

Authors	*T* / K and *p* / MPa ranges	Measurement of mole fraction of CO_2 in the gas (*y*) and hydrate (*z*) phases	Number of experimental data
Seo *et al.* (2000)	271.75-284.25 1.2-23.5	*y*, *z*	26
Kang *et al.* (2001)	272-282 1.5-30		26
Seo and Lee (2004)	272.1 3.2 - 14.05	*y*, *z*	8
Bruusgaard *et al.* (2008)	275.3 - 283.0 1.6 - 22.4	*y*	26

Table 5.3. Literature review of the experimental data on compositions of the gas and hydrate phases for the (carbon dioxide + hydrogen + water) systems.

Authors	CO_2 molar composition in the gas feed	*T* and *p* ranges	Type of data	Number of experimental data
Sugahara *et al.* (2005)	*Not reported*	274.3 - 281.9 K 1.42 – 9.13 MPa	GHLE (*p*,*T*,*y*)	43
Kumar *et al.* (2006)	0.392, 0.579, 0.833	273.9 - 281.6 K 1.58 - 10.74 MPa	HDC (*p*,*T*,*y*)	20
Linga *et al.* (2007*a* and 2007*b*)	0.392 and 0.850	273.7 K 1.40 and 5.10 MPa	HDC (*p*,*T*)	2
Li *et al.* (2010)	0.392	274.1 - 278.8 K 5.75 - 11.01 MPa	HDC (*p*,*T*,)	5
Seo and Kang (2010)	0.41	274.15 K 6.50 - 8.90 MPa	GHLE (*p*,*T*,*y*,*z*)	3

This literature review indicates that generating accurate experimental thermodynamic data, elucidating the phase behavior under three-phase equilibrium conditions, and also investigating the reliability of the thermodynamic models predictions for the aforementioned clathrate hydrate system are still needed.

In this chapter, basic phase equilibrium data are provided for the (carbon dioxide + nitrogen + water) and (carbon dioxide + hydrogen + water) hydrates and a thermodynamic analysis is presented to establish the stability region of both systems under hydrate formation conditions. The experimental data are compared with the corresponding data available in the literature and also with the predictions of CSMGem and HWHYD thermodynamic models (for carbon dioxide + nitrogen + water systems).

5.2 Gas Hydrate Formation in Carbon Dioxide + Nitrogen + Water Systems

In this section, dissociation and compositional equilibrium properties under hydrate formation conditions for the (carbon dioxide + nitrogen + water) systems are studied at various concentrations of CO_2 in the feed gas in the temperature range of (273.6 to 285.3) K and

pressures up to about 30 MPa. The studied gas mixtures composed of high purity grade CO_2 (99.995 mole%, supplied by Air Liquide) and N_2 (over 99.99 mole%, supplied by Air Liquide) were prepared in the equilibrium cell and analyzed by gas chromatography. The resultant compositions are given in Table A.4 (Appendix A).

The experimental procedures described in the previous Chapter were followed to simultaneously measure the dissociation conditions (section 5.2.1) and the molar compositions of CO_2 and N_2 in the gas phase at different equilibrium conditions (section 5.5.2). All experimental data are tabulated in Tables A.4 and A.5 (Appendix A). The phase equilibrium data generated in this work are compared with the literature data. Predictions through CSMGem and HWHYD models are also reported for comparisons purposes. Regarding the uncertainty of measurements discussed in this section, ± 0.2 K and ± 0.05 MPa are the maximum expected uncertainties in the dissociation data (section 5.2.1), derived from the isochoric plots as explained in Chapter 2. For compositional equilibrium data (section 5.2.2), maximum uncertainties in molar concentrations in the gas phase are estimated to be within ±1-2%, from TCD calibrations, while measurement uncertainty in the hydrate equilibrium temperature and pressures is estimated to be within ± 0.02 K and ± 0.002 MPa, respectively, from instrument calibrations (Chapter 2). Uncertainties in the amount of liquid supplied to the system are expected to be within ± 0.5%.

5.2.1 Equilibrium Dissociation Conditions

The hydrate dissociation conditions were investigated at five different composition ratios of CO_2 in the feed gas in the presence of water. The compositions of the (CO_2 + N_2) gas mixtures are given in the first column of Table A.4 (Appendix A). Average value of at least seven analyses is reported as the composition of the feed for each gas mixture. The measured hydrate dissociation data reported in Table A.4 are plotted in Figure 5.1. The hydrate phase boundaries of pure carbon dioxide and nitrogen hydrates are also shown. As can be observed in Figure 5.1, the experimental data show that the hydrate dissociation pressures of (CO_2 + N_2) gas mixtures fall in between those of pure CO_2 and N_2 hydrates. It can also be seen from this plot that the hydrate dissociation conditions shift to higher pressures when increasing the N_2/CO_2 ratio in the feed gas.

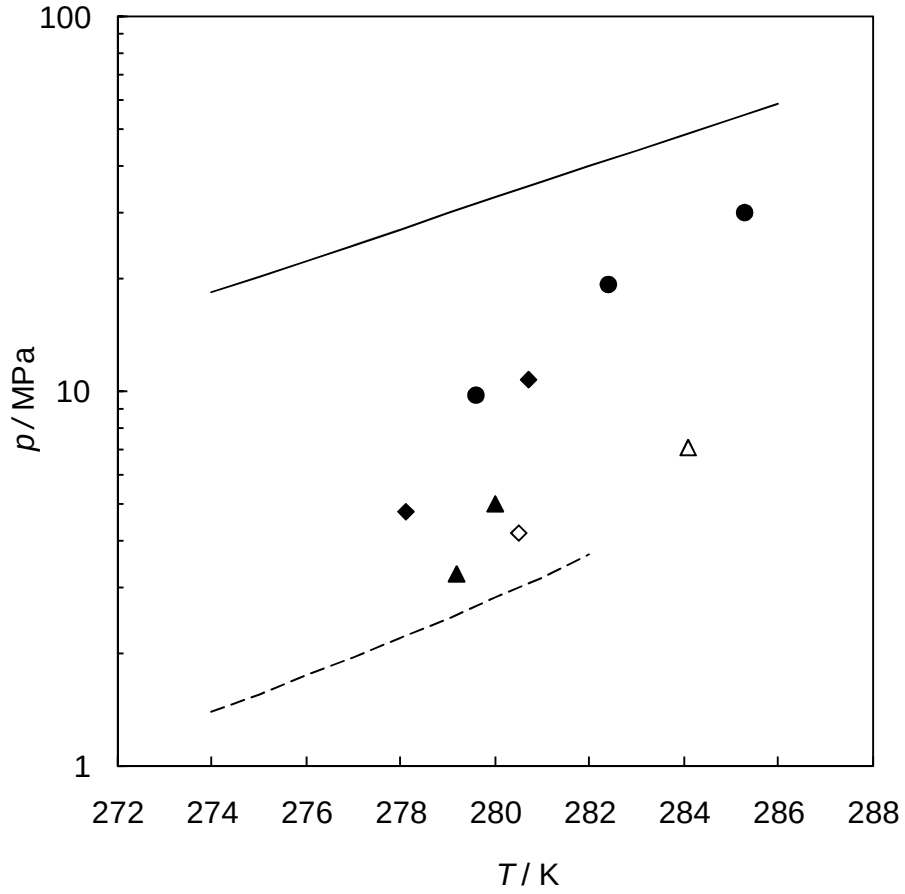


Figure 5.1. Experimental dissociation conditions for (nitrogen + carbon dioxide) clathrate hydrates at different CO_2 load mole fractions. This work: 0.271 (●); 0.476 (♦); 0.748 (◊); 0.773 (▲); 0.812 (Δ). HWHYD model: N_2 hydrates (solid line); CO_2 hydrates (dashed line).

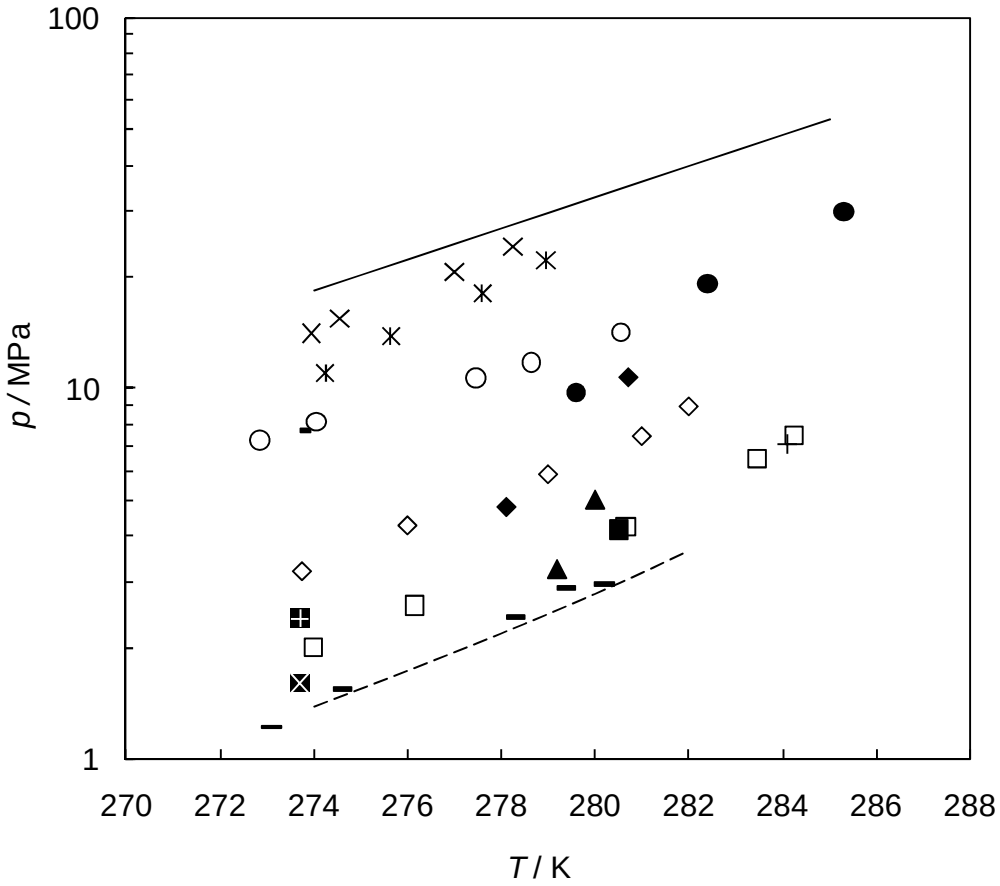


Figure 5.2. Experimental dissociation conditions for (nitrogen + carbon dioxide) clathrate hydrates at different CO_2 load mole fractions. This work: 0.271 (●); 0.476 (♦); 0.748 (■); 0.773 (▲); 0.812 (+). Literature: ▬, 0.9652 (Fan & Guo, 1999); x shadow, 0.830 (Linga *et al.*, 2007*b*); □, 0.778 (Kang *et al.*, 2001); + shadow, 0.570 (Linga *et al.*, 2007*b*); ◊, 0.4815 (Kang *et al.*, 2001); ○, 0.1761 (Kang *et al.*, 2001); -, 0.169 (Linga *et al.*, 2007*b*); *, 0.1159 (Kang *et al.*, 2001); x, 0.0063 (Kang *et al.*, 2001). HWHYD model: N_2 hydrates (solid line); CO_2 hydrates (dashed line).

The hydrate dissociation conditions measured in this work and the corresponding literature data are compared in Figure 5.2. The equilibrium data obtained generally agree with the experimental data reported in the literature within stated experimental uncertainties. However, considerable deviation was observed for the dissociation pressures measured at 0.476 and 0.773 mole fraction of CO_2 and 280.7 and 280 K, respectively.

As indicated in section 1.2.2, carbon dioxide and nitrogen are known to form sI and sII hydrates, respectively (Kang & Lee, 2000; Linga *et al*. 2007*a*). Literature data reveal that depending on the relative amount of CO_2 and N_2 gas molecules occupied in the small and large cavities, the structure of mixed (CO_2 + N_2) hydrates can be considered to be either sI or sII (Kang & Lee, 2000). For instance, Kang *et al*. (2001) have reported a sII transition on hydrates formed at concentrations of 6.63 and 11.59 mole % CO_2 (feed gas) based on the slopes of the equilibrium lines of various (CO_2 + N_2) hydrates. Motivated by this controversy, possible structural transitions of mixed (CO_2 + N_2) hydrates were investigated. Nevertheless, based on the slopes of the equilibrium lines no hydrate structural transitions were observed in the concentration range of 0.271 to 0.812 mole fractions CO_2 (in the feed gas). This fact was expected as structural transitions are reported to occur when the CO_2 molar concentration of the feed gas is near 15 mole %. Furthermore, the obtained equilibrium data suggest that the stable hydrate structure for the (CO_2 + N_2) composition ratio studied in this work is likely structure I. *In situ* Raman spectroscopy measurements carried out by Chazallon (2010) confirm these expectations. Moreover, the results of the latter study indicate that structure II clathrate hydrates of (CO_2 + N_2 + H_2O) are only formed at low (< 0.019) CO_2 mole fractions (in the gaseous feed).

The reliability of two hydrate thermodynamic models: CSMGem (based on the Gibbs energy minimization) and HWHYD (based on the equality of fugacity of each component throughout all phases) was studied by predicting the hydrate dissociation pressures for the studied (CO_2 + N_2) gas mixtures. The predictions were obtained at the corresponding equilibrium temperature, CO_2 mole fraction in the feed gas, and water mole fraction introduced to the system. The obtained values are given in Table A.4 (Appendix A). As can be seen, the absolute relative deviation (*ARD*) of the predicted hydrate dissociation conditions by HWHYD and CSMGem thermodynamic models are in average 3.4 % and 10.3 %, respectively.

Figure 5.3 shows the *ARD* from the obtained experimental values. The scattering in the predicted values suggest that the parameters of both thermodynamic models may require readjustment using reliable hydrate dissociation experimental data; as such models have generally been developed for hydrates of hydrocarbons.

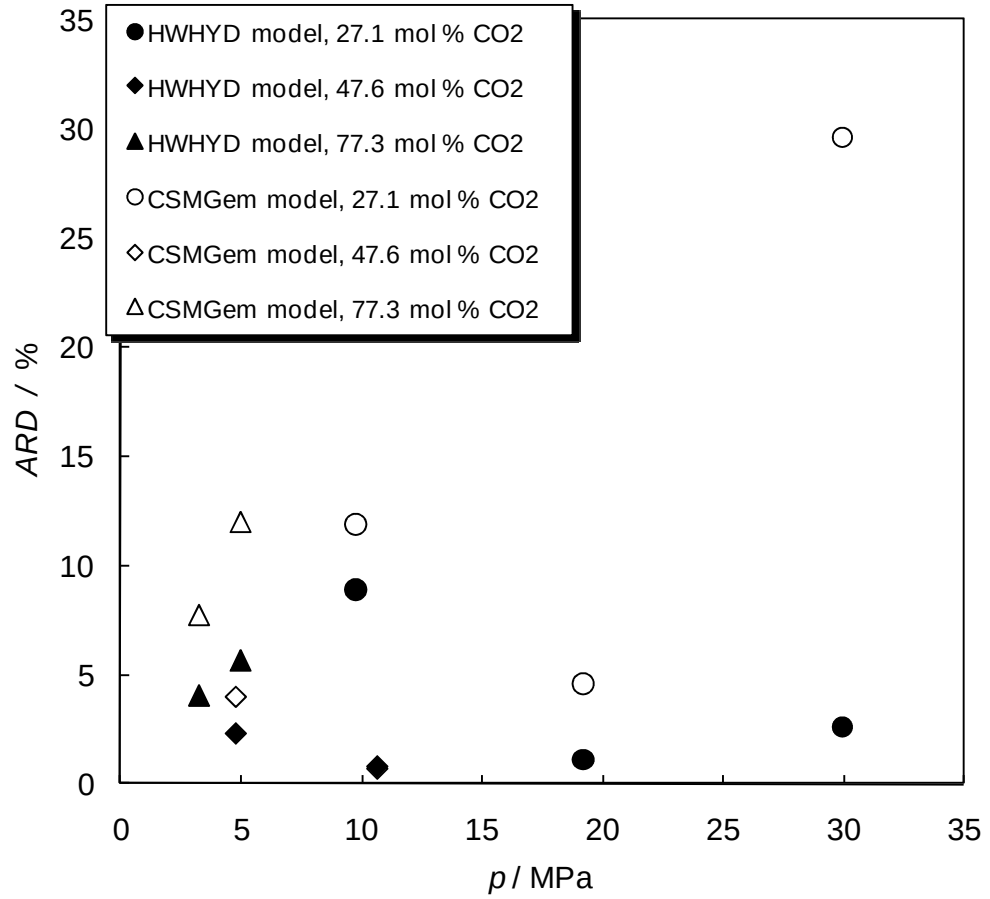


Figure 5.3. *ARD* between experimental dissociation pressures (p_{exp}) measured in this work for (nitrogen + carbon dioxide) clathrate hydrates and predictions of two thermodynamic models (p_{pred}) at different CO_2 mole fractions loaded.

5.2.2 Compositional Analysis of Equilibrium Phases

All experimental data measured in this study are reported in Table A.5 (Appendix A) and are plotted in Figures 5.4 to 5.7. The compositions of N_2 and CO_2 in the gas phase, under liquid water-hydrate-gas (L_w-H-G) equilibrium, at different temperatures were experimentally determined for various (CO_2 + N_2) gas mixtures in the presence of water. It is evident from these measurements that the amount of CO_2 in the gas phase generally decreases, as expected, when pressure increases at a given temperature. This suggests that considerable enrichment of CO_2 in the hydrate phase takes place for the mixed (carbon dioxide + nitrogen) gas hydrates at the temperatures and pressures studied in this work.

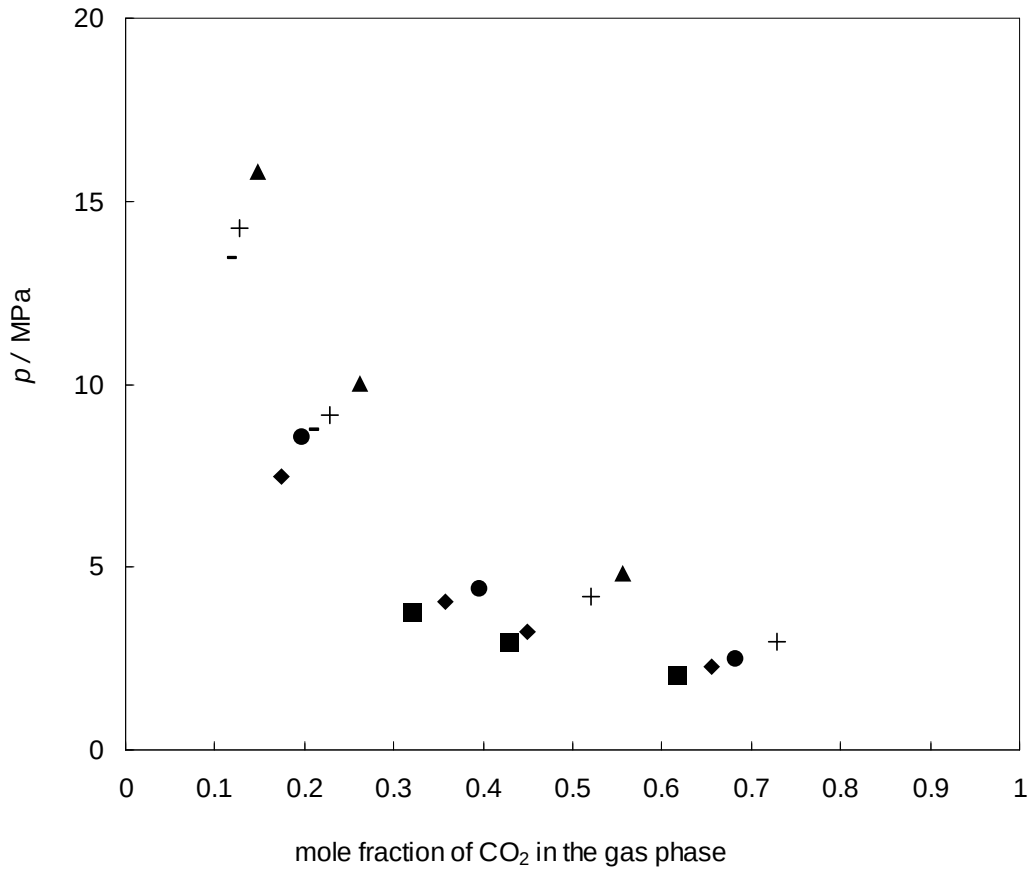


Figure 5.4. Pressure - composition phase diagram for (nitrogen + carbon dioxide + water) systems under (L_w-H-G) equilibrium at different temperatures. This work: 273.6 K (■); 275.2 K (♦); 276.1 K (●); 277.2 K (▬); 278.1 K (+); 279.7 K (▲).

It is also observed that the composition of CO_2 in the gas phase increases as temperature increases, which translates in less amount of CO_2 trapped in the hydrate phase at high temperatures. The experimental data measured in this work along with the corresponding literature data at selected temperatures are separately shown in Figures 5.5, 5.6a, 5.6b and 5.6c. As it can be seen, the mole fractions of CO_2 in the gas phase compare well with those reported by Seo *et al*. (2000) and Bruusgaard *et al*. (2008) at temperatures between 274 and 280 K. However, considerable deviation is observed for the mole fraction of CO_2 in the hydrate phase at high temperatures (*e.g*. 277 and 280 K).

The molar compositions of the aqueous and hydrate phases are determined by solving a system of non-linear material balance equations. As mentioned earlier, a mathematical algorithm based on Newton's numerical method (Constantinides & Moustofi, 1999) and coupled with the differential evaluation (*DE*) optimization strategy (Price & Storn, 1997) is applied. The latter mathematical approach is detailed elsewhere (Belandria *et al.,* 2011). The experimentally measured data, results of solving the material balance equations, and comparison with the predictions of CSMGem thermodynamic model are summarized in Table A.5 (Appendix A) and illustrated in Figures 5.7*a-e* at selected temperatures. As can be expected, the molar composition of carbon dioxide in the hydrate phase generally decreases as pressure increases for a given temperature, which is physically correct considering that competition for cage occupancy between N_2 and CO_2 increases at higher pressures. Also, as seen in these figures the predictions of the CSMGem model for the mole fraction of CO_2 in the gas phase generally agree with the experimental data. However, this thermodynamic model shows considerable deviations when predicting the molar compositions of CO_2 in the hydrate phase. Even much larger deviations (~ 43 %) have been recently reported between hydrate phase compositional measurements through Raman spectroscopy and predictions from the same thermodynamic model (Chazallon, 2010). This suggests that parameters of the latter thermodynamic model may require readjustment using three-phase (L_w-H-G) compositional experimental data, as most of these models have been developed for gas hydrates of hydrocarbons using experimental hydrate dissociation data. As for the undetermined values of some of the points shown in Table A.5 related to the predictions of the CSMGem model, the model is not capable of predicting the three-phase equilibrium (L_w-H-G) behavior at the studied conditions. It should be noted that the predictions of HWHYD model are not reported in this work as this model considers that N_2 forms structure I clathrate hydrates.

The number of hydrate phase equilibrium data measured in this work for (CO_2 + N_2 + H_2O) systems, along with the experimental conditions (CO_2/N_2 feed compositions, equilibrium temperature and pressures) is summarized in Table 5.4. The thermodynamic stability and compositions of the gas, liquid, and hydrate phases of mixed (carbon dioxide + nitrogen) hydrates has been examined at a useful range of temperatures and pressures. These data provide valuable guidelines for the design; selection and adjustment of the parameters of CO_2 capture processes based on gas hydrate crystallization concept.

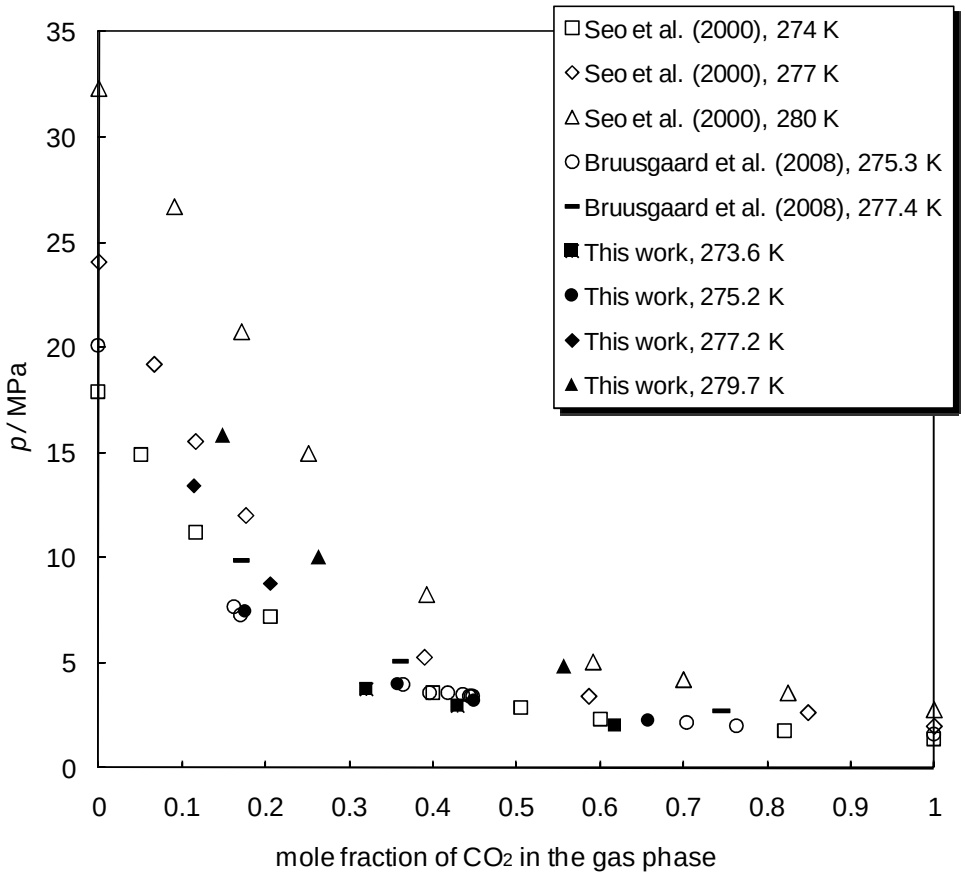


Figure 5.5. Pressure - composition phase diagram for (nitrogen + carbon dioxide + water) systems under (L_w-H-G) equilibrium at selected temperatures.

Table 5.4. Summary of the hydrate phase equilibrium data measured in this work for (CO_2 + N_2 + H_2O) systems.

CO_2 molar composition in the feed	Type of data	*T* Range / K	*p* Range / MPa	Number of experimental data
0.271 - 0.812	HDC (*p*,*T*)	279.2 - 285.3	3.24 - 29.92	9
	GHLE (*p*,*T*,*x*,*y*,*z*)	273.6 - 281.7	2.03 - 17.63	35

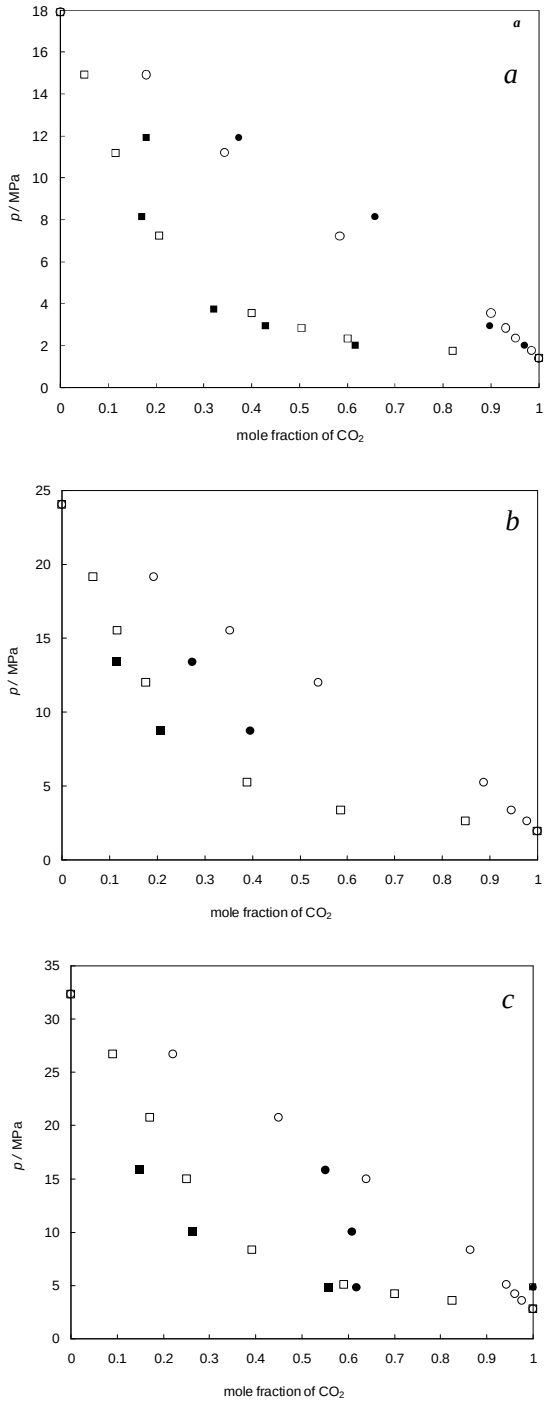


Figure 5.6. Pressure - composition phase diagram for the (nitrogen + carbon dioxide + water) systems under (L_w-H-G) equilibrium: Experimental and literature data. *a)* This work, 273.6 K: y_{CO2} (■); z_{CO2} (●); Seo *et al.* (2000), 274 K: y_{CO2} (□); z_{CO2} (○); *b)* This work, 277.2 K: y_{CO2} (■); z_{CO2} (●); Seo *et al.* (2000), 277 K: y_{CO2}(□); z_{CO2} (○); *c)* This work, 279.7 K: y_{CO2} (■); z_{CO2} (●); Seo *et al.* (2000), 280 K: y_{CO2}(□); z_{CO2} (○).

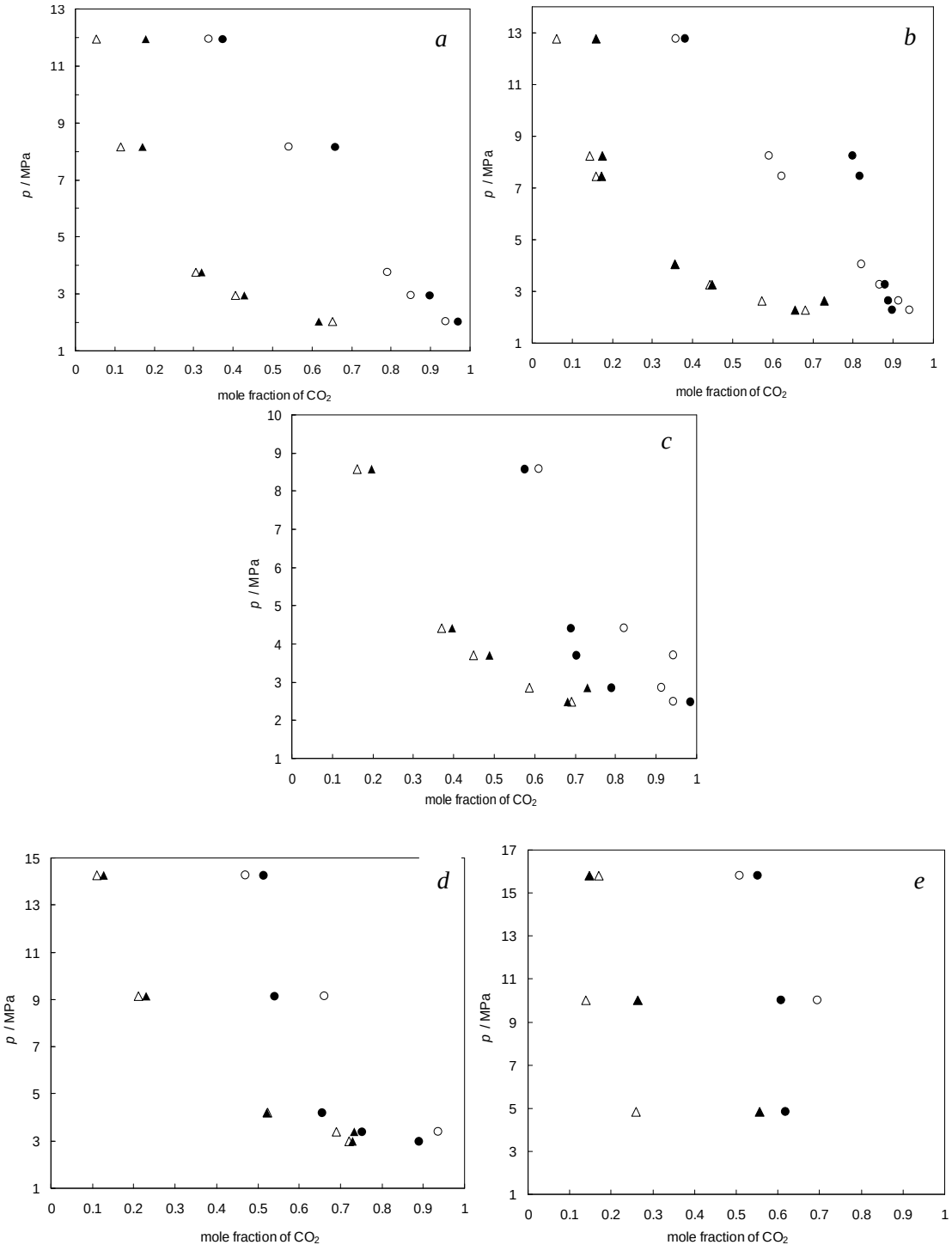


Figure 5.7. Pressure-composition phase diagram for the (nitrogen + carbon dioxide + water) systems under (L_w-H-G) equilibrium at selected temperatures. This work (experimental): y_{CO2} (▲); z_{CO2} (●), CSMGem model predictions: y_{CO2} (Δ); z_{CO2} (○). *a*) 273.6 K, *b)* 275.2 K, *c)* 276.1 K, *d*) 278.1 K, *e)* 279.7 K.

5.3 Study of Gas Hydrate Formation in (Carbon Dioxide + Hydrogen + Water) Systems

In this study, the equilibrium dissociation pressures and compositions of the gas phase for (CO_2 + H_2) hydrates are measured in the CO_2 concentration range from (0.508 to 0.829) mole fraction and in the temperature range of (273.6 to 283.0) K at pressures up to about 25 MPa. The studied gas mixtures composed of high purity grade CO_2 (99.995 mole %, supplied by Air Liquide) and H_2 (over 99.99 mole %, supplied by Air Liquide) were prepared in the equilibrium cell and analyzed by gas chromatography. The resultant compositions are reported in Tables A.6 and A.7 (Appendix A).

The experimental procedures described in the previous chapter were followed to simultaneously measure the dissociation conditions and the molar compositions of CO_2 and H_2 in the gas phase at different equilibrium pressures and temperatures. The typical uncertainty in these measurements is similar to that reported in the preceding section. All experimental data are tabulated in the Appendix A. The phase equilibrium data generated in this work are at last compared with the literature data.

5.3.1 Equilibrium Dissociation Conditions

The effect of the molar concentration of CO_2 was investigated for ternary (CO_2 + H_2 + H_2O) systems at various mole fractions of CO_2 to confirm the thermodynamic validity of CO_2 hydrate-based separation from fuel gas mixtures. The three-phase (L_w-H-G) equilibrium measurements were carried out following the experimental procedure described in Chapter 4. The (CO_2 + H_2) gas mixtures were investigated in the (0.508, 0.709, and 0.829) relative molar fractions of CO_2, with an estimated experimental uncertainty of $\pm$ 1-2 % on molar compositions, derived from gas chromatograph detector calibration.

The experimental dissociation conditions of (CO_2 + H_2) gas hydrates are given in Table A.6 (Appendix A). Figure 5.8 shows the semi-logarithm plot of the dissociation pressure as a function of temperature. Literature data are given in Table 5.3and are also shown in Figure 5.8. A consistent agreement with the dissociation conditions measured in this work is generally found. The dissociation pressures generally shift to higher values as the molar concentration of

CO_2 decreases in the feed in the temperature range of (277.2 to 283.0) K. A drastic increase in the dissociation pressure is particularly observed at high temperatures for hydrates formed from the 0.508 CO_2 mole fraction gas mixtures. As can be noted, the dissociation pressure rapidly increases from 8.53 MPa (at 280.5 K) to 24.76 MPa at the equilibrium temperature of 283.0 K. Such behavior could be attributed to the fact that H_2 begins to compete with CO_2 for hydrate cage occupancy with the increase in the H_2 mole fraction within the (CO_2 + H_2) gas mixture (Kumar *et al.*, 2009 and Li *et al.*, 2010).

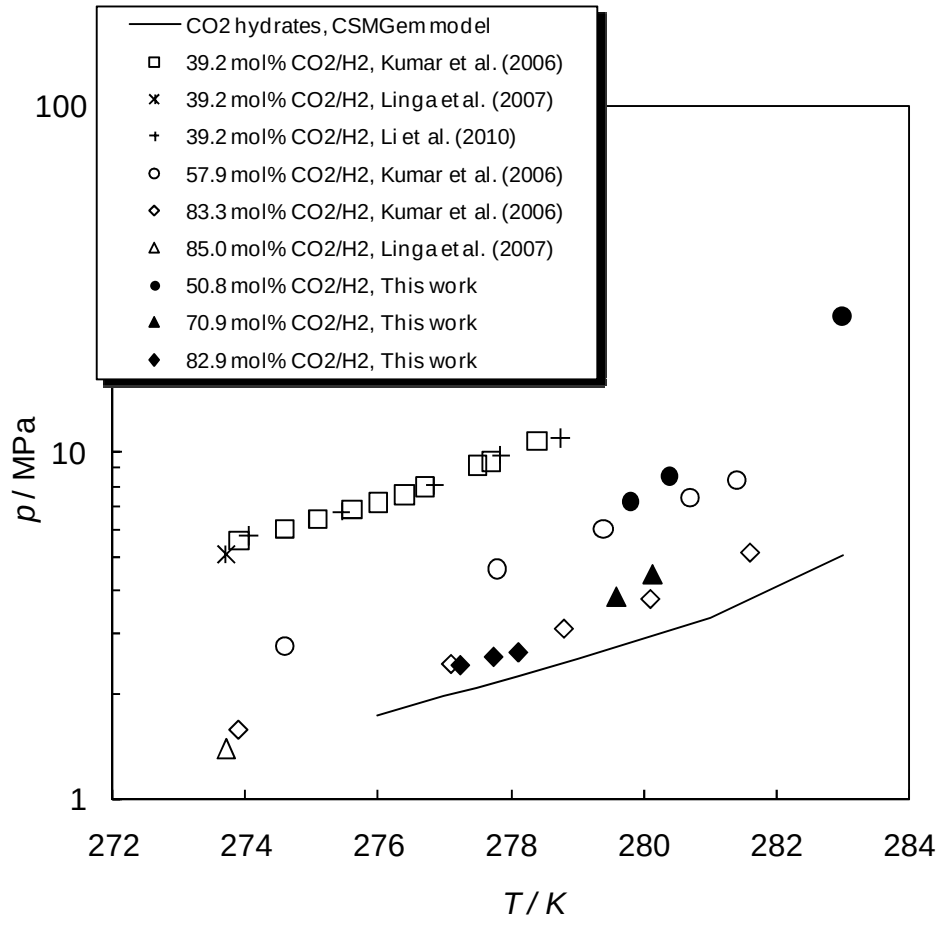


Figure 5.8. Experimental (literature and this work) dissociation conditions for gas hydrates of (CO_2 + H_2) formed in the presence water at various feed gas compositions.

Linga and coworkers (2007*b*) stated that "hydrate formation pressure increases with temperature and in order to minimize compression costs the smallest possible pressure is desired". Thus, based on the obtained results and considering the relative concentration of CO_2 in flue gas or synthesis gas is approximately 40 mole% (Klara & Srivastava, 2002), it is expected that high energy requirements may be necessary for separating CO_2 from H_2 through hydrate formation at relatively high temperatures. However, no hydrate dissociation data are available in the literature at temperatures above the value of 281.4 K reported by Kumar *et al*. (2006) for a CO_2 mole fraction of 0.579. Further phase behavior studies are therefore required at higher temperatures for H_2-rich binary gas mixtures for better assessing the strong dependency of the dissociation pressures on the molar concentration of CO_2 in (CO_2 + H_2 + H_2O) ternary hydrates.

5.3.2 Compositional Analysis of Equilibrium Phases

Compositional data for the gas phase in equilibrium with the hydrate and aqueous phases were measured at different pressures and temperatures for various (CO_2 + H_2) gas mixtures in the presence of water. The molar compositions of CO_2 in the feed gas along with the temperature, pressure and compositions of the gas phase are given in Table A.7 (Appendix A) and shown in Figure 5.9 (water concentration is assumed negligible in the gas phase). The experimental results indicate that as pressure increases, the composition of CO_2 in the gas phase decreases. This may suggest that considerable enrichment of CO_2 in the hydrate phase takes place in the studied systems. However, it should be noted that in (CO_2 + H_2) mixed hydrates, H_2 is assumed to be not enclathrated in the hydrate cages and to behave as a diluent gas towards the formation of CO_2 hydrate (Sugahara *et al.*, 2005).

Table 5.5 summarizes the experimental conditions at which compositional data for the gas and hydrate phases have been reported in the literature for the (carbon dioxide + hydrogen + water) ternary systems. In Figure 5.10, the experimental data measured in this work and literature data are compared. As can be seen, a consistent agreement is generally found with the experimental data reported by Sugahara *et al.* (2005) and Kumar *et al.* (2006) within experimental

uncertainties. However, considerable deviation is observed for the composition of CO_2 in the gas phase reported by Seo and Kang (2010) at 274.15 K.

The molar compositions of the gaseous components in the hydrate phase for the (CO_2 + H_2 + H_2O) systems have been subject of few studies in the literature. Table 5.5 summarizes the main findings reported in those studies. It is clear that the contradictory results are mainly due to three factors: *a*) Temperature and pressure conditions, *b*) Molar compositions of the introduced gaseous feed to the system, and *c*) The experimental techniques. Those who have claimed that H_2 can be trapped into the hydrate cages generally conducted their experiments at very low temperatures. Another factor to consider is that high ratios of H_2 to CO_2 in the gaseous feed were used. As this composition is increased, the possibility of H_2 enclathration into the hydrate cages can be intrinsically increased. Different experimental techniques used for studying the molar compositions of the hydrate phase may also affect the obtained results. Considering the above facts, it is considered that at the experimental conditions investigated in this study only CO_2 is trapped inside gas hydrate cavities. However, as previously mentioned, further experimental works using suitable physical techniques (*e.g.*, NMR, X-ray, or Raman spectroscopy) are recommended for further examining the latter assumption.

The number of hydrate phase equilibrium data measured in this work for (CO_2 + H_2 + H_2O) systems, along with the experimental conditions (CO_2/H_2 feed compositions and equilibrium temperatures and pressures) is summarized in Table 5.56. These experimental data provide valuable information on the thermodynamic stability and gas phase compositions of mixed (carbon dioxide + hydrogen) gas hydrates at useful temperatures and pressures, which can be taken into account in the design of CO_2 pre-combustion processes based on gas hydrate crystallization concept.

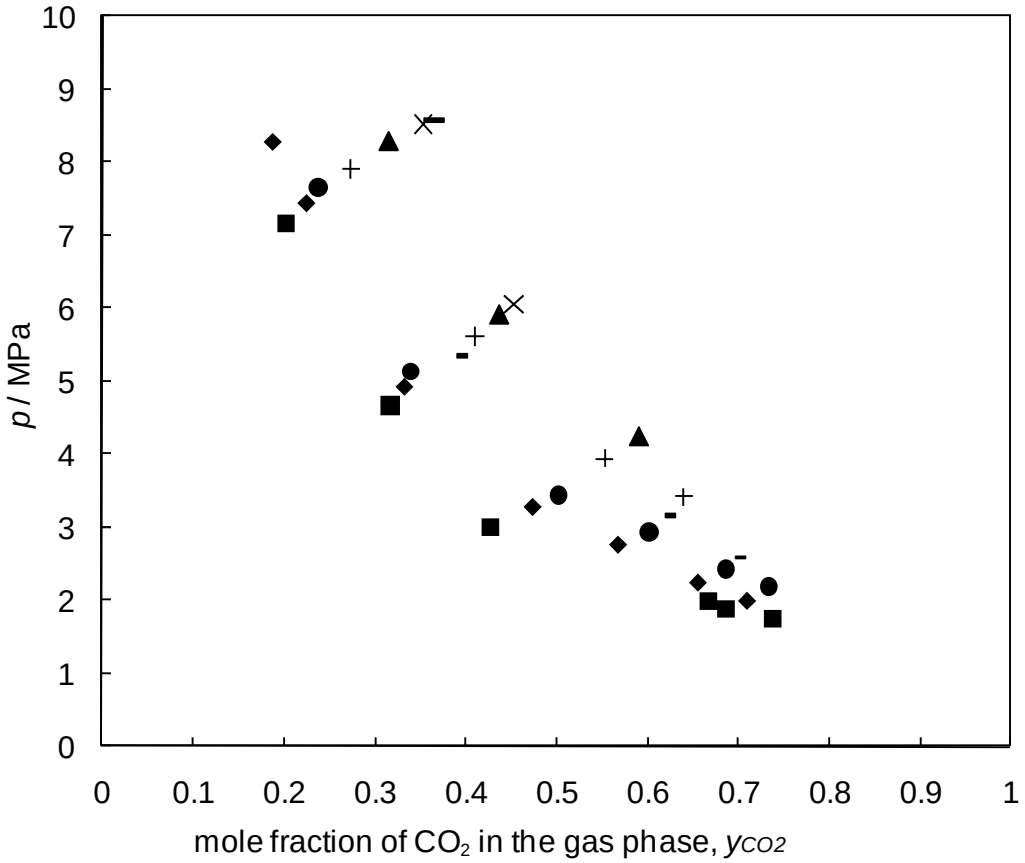


Figure 5.9. Pressure - gas phase composition phase diagram for (hydrogen + carbon dioxide + water) systems under (L_w-H-G) equilibrium at different temperatures. This work: 273.6 K (■); 275.2 K (♦); 276.2 K (●); 277.1 K (-); 278.1 K (+); 279.1 K (▲); 280.1 K (x); 281.2 K (—).

Table 5.5. Experimental studies on molar compositions of gas hydrates formed in the (CO_2 + H_2 + H_2O) ternary systems.

Authors	Gaseous feed compositions introduced to the system / CO_2 mole fraction	*T* / *K*	*p* / *MPa*	Experimental technique	Result
Sugahara *et al.* (2005)	*Not reported*	274.3-281.9	1.42-10	Raman micro-spectroscopy	No H_2 cage occupancy was observed
Sugahara *et al.* (2008)	*Not reported*	274.3-281.9	1.42-10	Raman spectroscopy using quartz windows	No H_2 cage occupancy was observed
	Not reported	243	5.06	Direct gas release method	H_2 molecules adsorb on the hydrate structure (0.007 water-free base mole fraction in the hydrate phase)
Kumar *et al.* (2009)	0.4	163 to 278	8	Powder X-Ray Diffraction	*sI* hydrate formed
				Gas chromatography of released gas from hydrate	92 mole % CO_2 and 8 mole % H_2 were trapped in the hydrate phase
				C NMR	*s*I hydrate formed, 100 % of the large cages were occupied by CO_2
				Raman spectroscopy	*sI* hydrate formed
Seo and Kang (2010)	0.41	274.15	6.5-8.9	C NMR	If silica gel is used to form hydrate, 93 % of small cages and 100 % of large cases are occupied by CO_2
Kim and Lee (2005)	0.2	123.15	0.1	H MAS NMR	Molar composition of CO_2 in the hydrate phase in the range of (96.5 to 98.7) H_2 was entrapped in hydrate
				Gas chromatography of released gas from hydrate	92.5 % CO_2, 7.5 % H_2

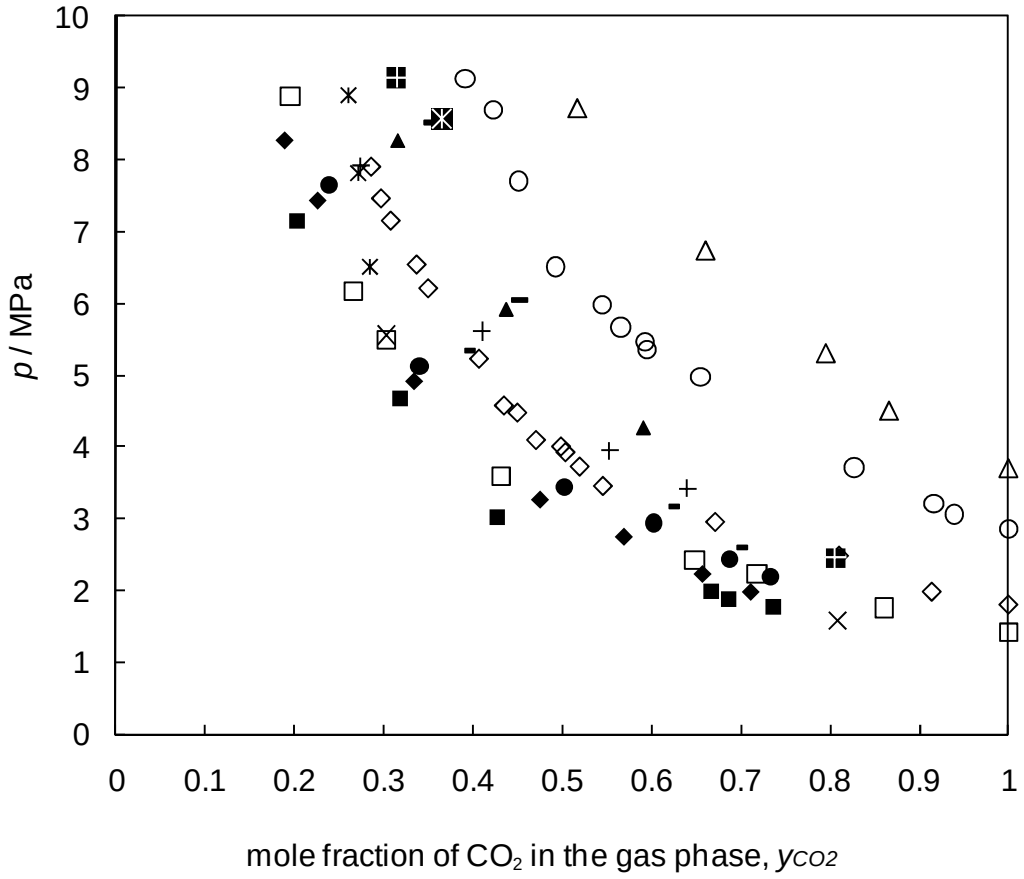


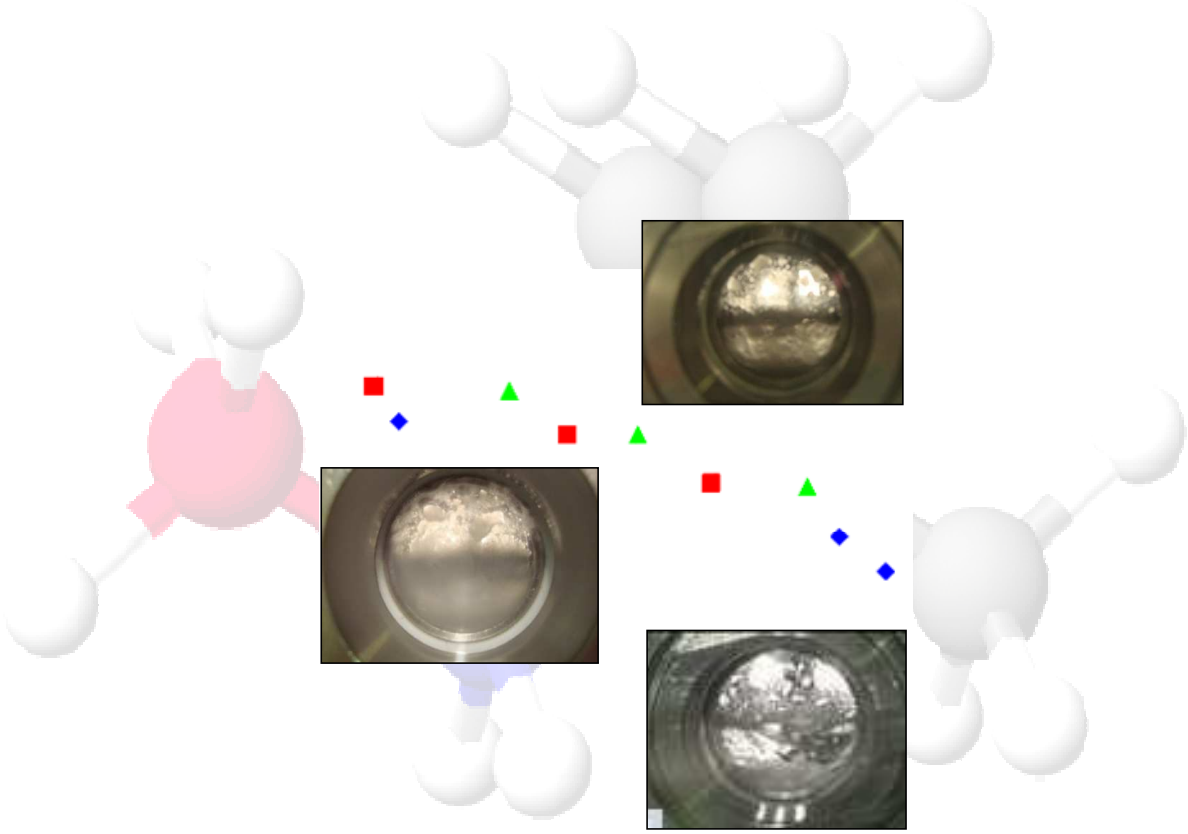
Figure 5.10. Pressure - gas phase composition phase diagram for (hydrogen + carbon dioxide + water) systems under (L_w-H-G) equilibrium at different temperatures. This work: (■) 273.6 K; (♦) 275.2 K; (●) 276.2 K; (-) 277.1 K; (+) 278.1 K; (▲) 279.1 K; 280.1 K (▬); 281.2 K (* shadow). Literature data: Sugahara et *al*. (2005): (□) 274.3 K; (◊) 276.5 K; (○) 280.1 K; (△) 281.9 K; Kumar *et al.* (2006): (x) 273.9 K; (+ shadow) 277 K; Seo and Kang (2010): (*) 274.15 K.

Table 5.6. Summary of the hydrate phase equilibrium data measured in this work for the (CO_2 + H_2 + H_2O) systems.

Feed Composition	Type of data	*T* Range / K	*p* Range / MPa	Number of experimental data
0.508 - 0.829	HDC (*p*,*T*)	277.0 - 283.0	2.44 - 24.76	8
	GHLE (*p*,*T*,*y*)	273.6 - 281.2	1.75 - 8.57	32

6

Thermodynamic Stability of Semi-Clathrate Hydrates[†]



[†] Content published in *J. Chem. Eng. Data*, 2011, 56, 3855-3865; *J. Chem. Thermodyn.*, 2012, 46, 57-61; *Fluid Phase Equilib.*, 2012, 322, 105-112 and submitted in "*Compositional Analysis of the Gas Phase for the CO_2 + N_2 + Tetra-n-Butylammonium Bromide Aqueous Solution Systems under Hydrate Stability Conditions*", 2012.

6

Résumé

Dans ce chapitre, nous étudions la stabilité thermodynamique des semi-clathrates de TBAB avec des gaz purs et des mélanges de gaz. En premier lieu, nous présentons les résultats des mesures d'équilibres de phases réalisées sur les semi-clathrates formés à partir de : (CO_2, CH_4 ou N_2 + TBAB + H_2O). Ensuite, les variables fondamentales du processus telles que conditions de dissociation et composition des phases font l'objet d'une enquête approfondie pour déterminer les régions de stabilité et les conditions de formation des semi-clathrates dans le mélange : (CO_2 + N_2 + TBAB + H_2O). Les conditions de dissociation sont mesurées en utilisant la méthode isochorique avec variation de la pression en fonction de la température décrite au chapitre 4. Les changements, à différentes températures, des compositions des phases gazeuse et liquide pour les équilibres à trois phases sont mesurés par chromatographie en phase gazeuse et réfractométrie, respectivement. L'effet de promotion thermodynamique dû au TBAB en solutions aqueuses est étudié en termes de pressions et de températures de dissociation. Les conditions d'exploitation les plus favorables pour un procédé de séparation du CO_2 basé sur l'utilisation des hydrates sont alors proposées. Les prédictions par des modèles thermodynamiques issus de la littérature sont également utilisées pour examiner l'effet promoteur d'hydrate du TBAB. Les résultats complets de l'étude permettent de montrer que le CO_2 peut être séparé des gaz industriels / de combustion qu'il soit à très faibles ou très haute concentrations, et ce, à des températures douces et des pressions basses pourvu que des solutions aqueuses de TBAB soient utilisées.

Abstract

In this chapter, the thermodynamic stability of TBAB semi-clathrates with pure and mixed gases is studied. First, phase equilibrium measurements carried out for semi-clathrates formed from (CO_2, CH_4 or N_2 + TBAB + H_2O) are presented. Then, fundamental process variables such as dissociation conditions and phase compositional data are thoroughly investigated to determine the stability regions and formation conditions of (CO_2 + N_2 + TBAB + H_2O) semi-clathrates. The dissociation data are measured using the isochoric pressure search method described in Chapter 4. The compositional changes in the gas and liquid phases at different temperatures under three-phase equilibrium are measured by gas chromatography and refractometry technique, respectively. The thermodynamic promotion effect of TBAB in aqueous solutions is studied in terms of dissociation pressures and temperatures and the most favorable operating conditions for a hydrate-based CO_2 separation process are proposed. The predictions of literature thermodynamic models are also used to examine the hydrate promotion effect of TBAB. The measured data suggest that CO_2 can be separated from highly to low concentrated industrial / flue gas mixtures at mild temperatures and low pressures in the presence of TBAB aqueous solutions.

6 Thermodynamic Stability of Semi-Clathrate Hydrates

Introduction

Gas hydrates formation under low temperature and high pressure conditions has been experimentally established in Chapters 3 through 5 for gas mixtures containing CO_2 in the absence of thermodynamic promoter.

As it has been previously discussed, besides pressure, temperature, and composition of the gas mixture, the formation and dissociation of gas hydrates may be also affected by the use of chemical additives with inhibition or promotion effect (Mandal & Laik, 2008). Moreover, the use of hydrate promoters has proven to reduce the pressures required for hydrate stability and increasing the gas hydrate equilibrium temperature. In addition, considerable efforts are currently undergoing to investigate the gas hydrate crystallization approach for separating a specific gas constituent from a multi-component gaseous mixture under favorable temperature and pressure conditions. Therefore, in this chapter the hydrate promotion effect of TBAB aqueous mixtures is investigated.

Relevant experimental literature data (from thermodynamic point of view) in the systems including CH_4, CO_2, N_2 and (CO_2 + N_2) gas mixtures in the presence of TBAB aqueous solutions are provided in Tables 6.1 to 6.4. In spite of the increasing amount of experimental studies reported in the literature in recent years, the role of TBAB in the selective removal of CO_2 from multi-component gas streams is still not clearly understood. Therefore, further experimental phase equilibrium data in the above systems are required for practical purposes and also for tuning predictive thermodynamic models for semi-clathrate systems.

In this study, an attempt has been made to generate in addition to the commonly reported pressure and temperature equilibrium data, reliable compositional equilibrium data for TBAB semi-clathrate hydrates of pure and mixed gases. Such data are normally difficult to measure, time consuming, expensive, and thus rare in the literature. The typical cost of a week effort for obtaining one equilibrium data point is estimated to be about US$2000 (Sloan & Koh, 2008).

Table 6.1. Experimental data available in the literature for (CH_4 + TBAB) semi-clathrates.

Reference	TBAB concentration (mass fraction)	*T* range / K	*p* range / MPa	Number of data points
Arjmandi *et al.* (2007)	0.05, 0.10, 0.20, 0.30	(287.15-298.15)	(1.421-41.369)	24
Oyama *et al*. (2008)	0.10	(282.15-287.95)	(0.510-3.650)	7
Li *et al.* (2010)	0.05, 0.099, 0.197, 0.385	(281.15-295.15)	(0.460-10.640)	40
Mohammadi and Richon (2010)	0.05	(283.6-290.1)	(1.310-11.080)	10
Sun and Sun (2010)	0.05, 0.10, 0.20, 0.2818, 0.45	(281.75-292.35)	(0.508-7.042)	40

Table 6.2. Experimental data available in the literature for (CO_2 + TBAB) semi-clathrates.

Reference	TBAB concentration (mass fraction)	*T* range / K	*p* range / MPa	Number of data points
Duc *et al.* (2007)	0.05, 0.10, 0.40, 0.65	(279.3-290.9)	(0.273-3.320)	8
Arjmandi *et al.* (2007)	0.10, 0.427	(285.6-291.2)	(1.250-4.090)	7
Oyama *et al.* (2008)	0.01, 0.02, 0.03, 0.045,0.10	(276.7-289.6)	(0.560-4.530)	44
Lin *et al.* (2008)	0.901, 0.702, 0.443	(279.4-288.1)	(0.344-2.274)	24
Deschamps and Dalmazzone (2009)	0.40	(286.5-288.6)	(0.830-2.250)	4
Li *et al.* (2010)	0.05, 0.10	(280.2-288.8)	(0.400-3.210)	11

Table 6.3. Experimental data available in the literature for (N_2 + TBAB) semi-clathrates.

Reference	TBAB concentration (mass fraction)	*T* range / K	*p* range / MPa	Number of data points
Arjmandi *et al.* (2007)	0.10	(285.15-292.95)	(4.688-33.503)	7
Duc *et al.* (2007)	0.05, 0.10	(279.3-284.0)	(2.900-10.850)	3
Deschamps and Dalmazzone (2009)	0.40	(286.0-291.6)	(6.27-20.5)	5
Lee *et al.* (2010)	0.50, 0.20, 0.40, 0.60	2(81.3-289.4)	(4.040-9.490)	19

This chapter is divided in two parts. In the first part, the thermodynamic stability of semi-clathrates of (CO_2, CH_4 or N_2 + TBAB) in non-stoichiometric aqueous solutions is examined. The second part deals with measurements of equilibrium and compositional properties for (CO_2 + N_2) gas mixtures in TBAB aqueous mixtures.

Table 6.4. Experimental data available in the literature for (CO_2 + N_2 + TBAB) semi-clathrates.

Reference	Feed Gas Composition	TBAB mass fraction	Range of experiments	Number of experimental points	Type of data*
Duc *et al.* (2007)	CO_2 (0.155 mole) + N_2 (0.845 mole)	0.05	287.15 - 289.75 K 5.00 - 5.32 MPa	4	GHLE (*p*,*T*) and GHLE (*p*,*y*,*z*) at 285.15 and 286.15 K
	CO_2 (0.192 mole) + N_2 0.808 mole)		286.25 - 295.25 K 3.63 - 4.43 MPa	6	
	CO_2 (0.215 mole) + N_2 (0.785 mole)		282.25 - 286.95 K 0.55 - 1.92 MPa	4	
	CO_2 (0.234 mole) + N_2 (0.766 mole)		285.75 - 286.75 K 3.12 - 3.23 MPa	3	
Fan *et al.* (2009)	CO_2 (0.166 mole) + N_2 (0.834 mole)	0.05	277.65 K 3.36 - 7.31 MPa	7	VHE (*p*,*T*,*y*,*z*)
Deschamps and Dalmazzone (2009)	CO_2 (0.249 mole) + N_2 (0.751 mole)	0.40	284.8 - 293.3 K up to 9.180 MPa	5	HDC (*p*,*T*)
Lu *et al.* (2009)	CO_2 (0.159 mole) + N_2 (0.841 mole)	0.05, 0.153, 0.348, 0.407, 0.457	278.05 - 287.85 K 1.17 - 5.84 MPa	12	HDC (*p*,*T*)
Meysel *et al.* (2011)	CO_2 (0.75 mole) + N_2 (0.25 mole)	0.05, 0.1, 0.2	284.1 - 290.0 MPa 1.964 - 3.822 MPa	14	HDC (*p*,*T*,*y*)
	CO_2 (0.50 mole) + N_2 (0.50 mole)		282.3 - 290.4 K 1.956 - 5.754 MPa	16	
	CO_2 (0.20 mole) + N_2 (0.80 mole)		281.8 - 288.3 K 2.976 - 5.901 MPa	12	

**HDC*: Hydrate Dissociation Conditions. *GHLE*: Gas-Hydrate-Liquid Equilibrium.

6.1 Phase Equilibria of Semi-Clathrate Hydrates of Carbon Dioxide, Methane and Nitrogen in Non-Stoichiometric TBAB Aqueous Solutions

In spite of the number of experimental studies dedicated to understanding the phase behavior of TBAB sc hydrates, the thermodynamic properties of TBAB semi-clathrates with carbon dioxide, methane or nitrogen have been scarcely studied above the TBAB stoichiometric composition, namely 0.4 and 0.32 mass fraction, for type *A* and *B* hydrates, respectively (Lin *et al.*, 2008). The equilibrium temperature for the pure TBAB hydrate of stoichiometric composition at atmospheric pressure is 285.15 K (Shimada *et al*., 2003). Therefore, it is expected that the use of TBAB with gases like CO_2, CH_4 or N_2 yields a reduction in the equilibrium pressure and thereby extend the hydrate stability region to higher temperatures. At the time of writing, the only experimental dissociation data available in the literature in a non-stoichiometric concentration of TBAB aqueous solution are those reported by Duc *et al*. (2007) for sc of (TBAB + CO_2) at 0.65 mass fraction TBAB in aqueous solution, and by Hashimoto and coworkers (2008) for (hydrogen + TBAB) semi-clathrates.

In the present work, dissociation pressures of (CO_2, CH_4 or N_2 + TBAB) sc hydrate systems are investigated at 0.25 and 0.50 mass fraction of TBAB in aqueous solution in the temperature ranges of (282.6 to 287.9), (285.6 to 292.8), and (286.1 to 289.1) K, respectively. Purities and suppliers of the chemicals used are given in Table 6.5. Solutions with mass fractions of 0.25 were prepared by gravimetric method using an accurate analytical balance (Mettler, AT200), with mass uncertainty of $\pm$ 0.0001 g. Consequently, uncertainties on the basis of mole fraction are estimated to be less than 0.01. Double-distilled and deionized water from Direct-Q5 Ultrapure Water Systems (Millipore^{TM}), with a resistivity of 18.2 MΩ cm at 298 K, was used in all experiments.

The dissociation measurements were carried out following the isochoric pressure search method described in Chapter 4. The measured data are given in Tables A.8 and A.9 (Appendix A) and are plotted in Figures 6.1 to 6.3. The uncertainties for the hydrate dissociation temperatures and pressures are expected to be within ± 0.2 K and ± 0.05 MPa, as indicated in Chapter 2. Literature data at lower concentrations of TBAB in aqueous solution and in the presence of pure water are

also shown in Figures 6.1 to 6.3 to study the hydrate promotion effect of TBAB above its stoichiometric concentration.

A semi-logarithmic scale is used to better study the hydrate promotion effects of TBAB aqueous solutions and also the consistency of the experimental data. It should be emphasized that hydrate promotion effect means shifting to low pressures / high temperatures the dissociation conditions of gas hydrates due to the presence of TBAB in the aqueous solution (Sloan & Koh, 2008). As observed in Figures 6.1 to 6.3, the data measured in this work are in consistent agreement with literature data in the whole region where a comparison could be made.

Many experimental dissociation data have been reported for (methane + TBAB) and (carbon dioxide + TBAB) semi-clathrates at concentrations below 0.40 (mass fraction TBAB). Figures 6.1 and 6.2 show as expected, that a concentration of 0.25 mass fraction TBAB shifts the three-phase equilibrium curves to the lower pressures / higher temperatures region when compared to the corresponding gas hydrates systems (without TBAB). A comprehensive phase equilibrium study at additional TBAB concentrations in its aqueous solutions can be found in the paper of Mohammadi *et al*. (2011*a*). Interestingly, the addition of 0.50 mass fraction TBAB in aqueous solution generally weakens its pressure-reducing effect in the temperature ranges studied in this work, in comparison to lower concentrations relative to water (*i.e*. 0.25 mass fraction TBAB) that significantly decrease the dissociation pressure at a given temperature. However, this effect depends on pressure and can vary for each semi-clathrate system. The promotion effect is indeed considerable for the nitrogen containing systems.

Table 6.5**.** Purities and suppliers of materials.

Chemical	**Supplier**	**Purity**
Carbon dioxide	Air Liquide	0.99 (mole fraction)
Nitrogen	Air Liquide	0.99 (mole fraction)
Methane	Air Liquide	0.99 (mole fraction)
TBAB aqueous solution, 50.00 ±0.01 (mass %)	Sigma-Aldrich	0.99 (mass fraction)

For (TBAB + nitrogen) semi-clathrates, the addition of 0.50 mass fraction TBAB aqueous solutions (*i.e.* non-stoichiometric aqueous solution) unexpectedly causes a continued decrease in the equilibrium pressure at a given temperature. Furthermore, an unusual behavior is particularly observed in Figure 6.3 at temperatures below 286.5 K with the addition of 0.25 and 0.50 mass fraction of TBAB in aqueous solutions. Oyama *et al.* (2005) demonstrated that two types of TBAB hydrates, namely type A and type B, are formed over the concentration range from 0 to 45 wt.%. Possible structural transitions from type A to type B and/or coexistence of both crystal structures could cause such an abrupt pressure decrease, compared to smaller concentrations (*i.e.* 0.05 and 0.10 mass fraction TBAB) which display rather parallel straight lines.

As the crystal structure of semi-clathrates typically depends on the hydration number, it is not possible to withdraw any conclusion regarding semi-clathrates structural transitions from phase equilibrium measurements by PVT studies alone (as performed in this work). The use of suitable physical techniques (*e.g.* NMR, Raman spectroscopy, *etc.*) is therefore recommended to further investigate such phenomena, especially for studying compositional changes in (TBAB + N_2) semi-clathrates. The dissociation data presented in this section are of scientific interest, since they are the first to show the thermodynamic stability of (CH_4 or N_2 + TBAB) semi-clathrates in non-stoichiometric aqueous solutions.

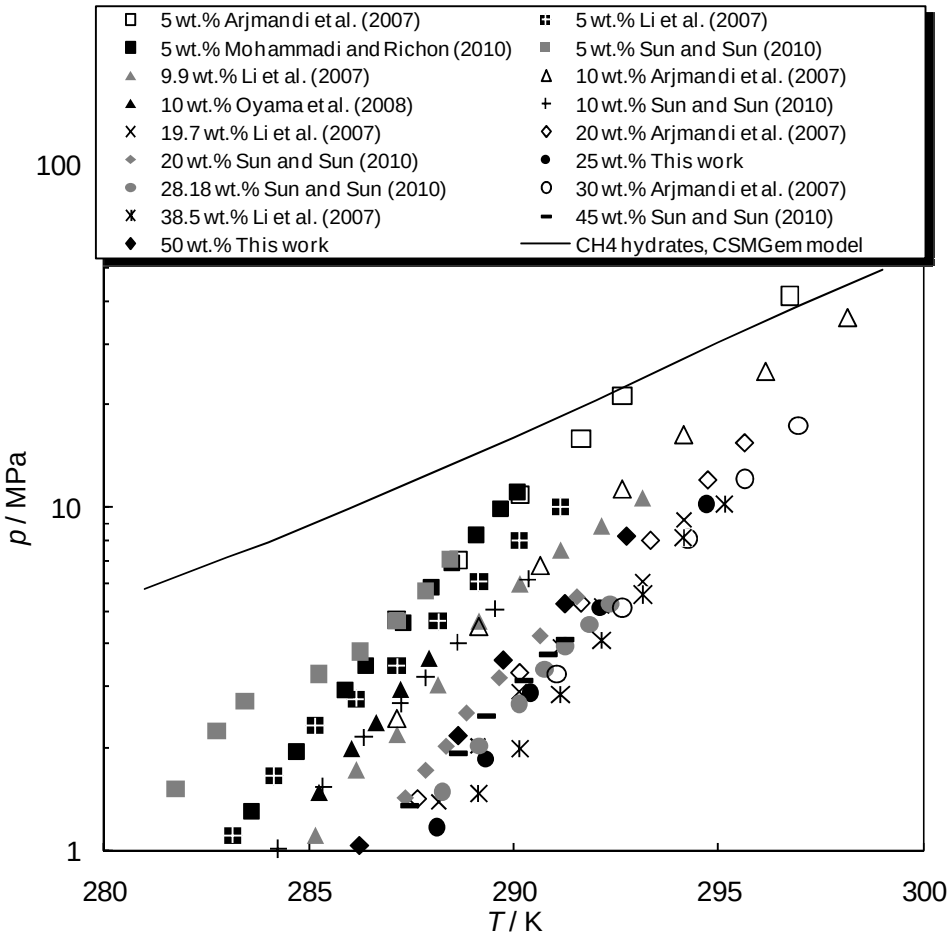


Figure 6.1. Experimental dissociation conditions (literature and this work) for (methane + TBAB) semi-clathrates.

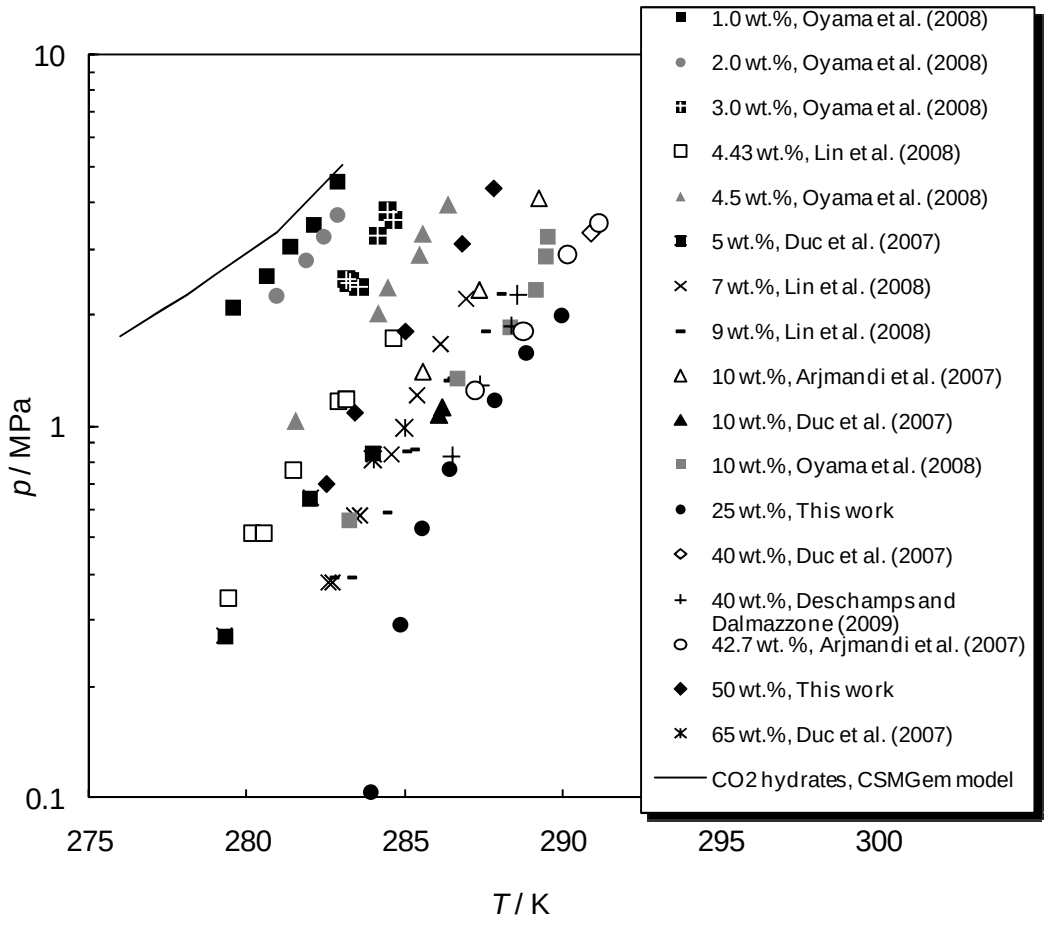


Figure 6.2. Experimental dissociation conditions (literature and this work) for (carbon dioxide + TBAB) semi-clathrates.

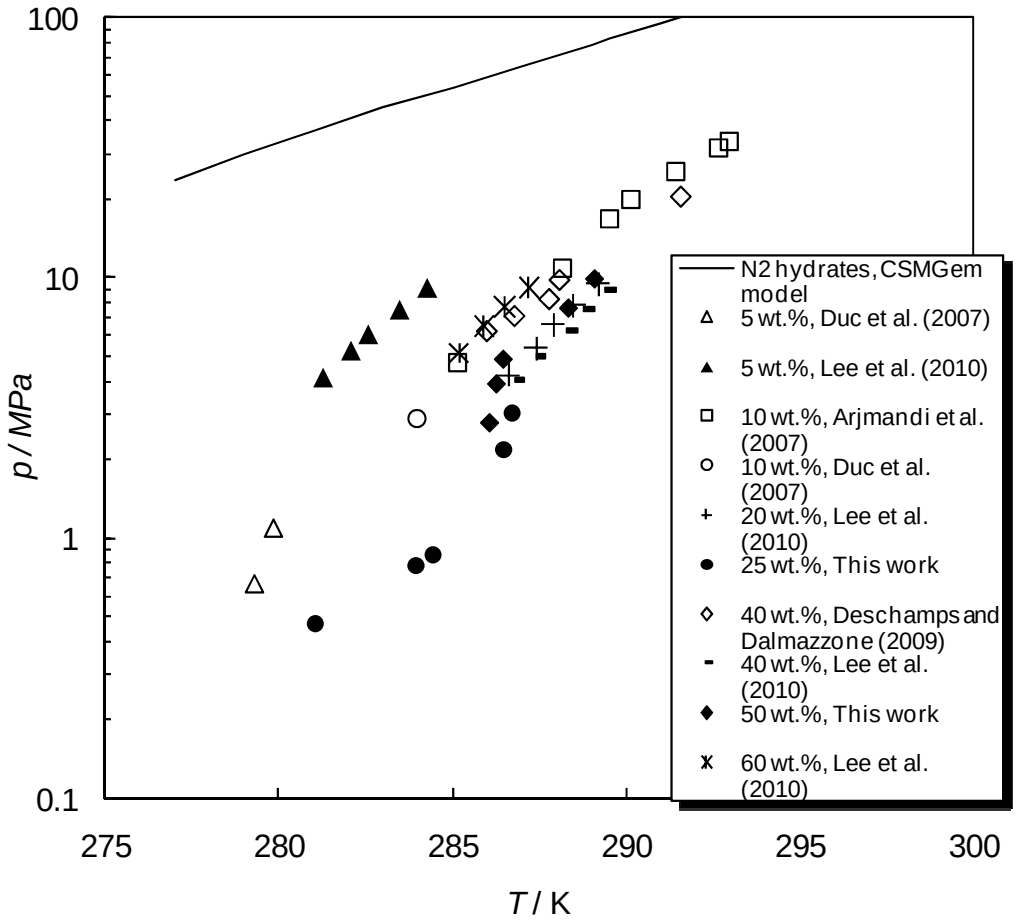


Figure 6.3. Experimental hydrate dissociation conditions (literature and this work) for (nitrogen + TBAB) semi-clathrates.

6.2 Thermodynamic Properties of Semi-Clathrate Hydrates of (Carbon Dioxide + Nitrogen) Gas Mixtures in TBAB Aqueous Mixtures

This section is devoted to further investigate the thermodynamic validity of a hydrate-based CO_2 separation process from industrial/flue gases by using TBAB as thermodynamic promoter. Dissociation and compositional data for the (CO_2 + N_2 + TBAB + water) systems with various CO_2 feed gas molar compositions were experimentally measured in the (275.2 to 291.0) K and (0.58 to 19.09) MPa ranges, using the methodologies described in Chapter 4. In addition, the refractive index of the liquid phase was measured under three-phase equilibrium to determine its composition at each temperature step (during dissociation). With respect to the accuracy of the experimental data, ± 0.2 K and ± 0.05 MPa are the maximum expected uncertainties, derived from the isochoric plots, in the dissociation measurements (section 6.2.1). For compositional data (section 6.2.2), maximum uncertainties in molar concentrations in the gas phase are estimated to be within ± 1-2%, from TCD calibrations, while measurement uncertainty in the equilibrium temperature and pressures is estimated to be better than ± 0.02 K and ± 0.002 MPa, respectively, from instrument calibrations (Chapter 2). The maximum deviations on refractive index measurement are expected to be about ± 0.1%. Uncertainties in the amount of TBAB aqueous solution supplied to the system are expected to be lower than ± 0.5%, in both studies presented in sections 6.2.1 and 6.2.2.

The three gas mixtures used in this work were supplied by Air Liquide and their compositions were chosen to cover a wide range of CO_2 and N_2 ratios. The relative molar fractions of CO_2 were (0.151, 0.399, and 0.749) with 2 % of relative uncertainty on the molar composition stated by the supplier. TBAB with 99 *wt.* % purity was purchased from Sigma-Aldrich. Double-distilled and deionized water from Direct-Q5 Ultrapure Water Systems (Millipore^{TM}), with a resistivity of 18.2 MΩ cm at 298 K, was used in all experiments. TBAB aqueous mixtures with mass fractions of (0.05 and 0.30) were prepared following the gravimetric method described in section 6.1. Thus, uncertainties on the basis of mole fraction are estimated to be less than 0.01.

Semi-clathrates were formed with the addition of TBAB aqueous solutions with mass fractions of (0.05 and 0.30). The measured dissociation data are discussed and compared with literature

data. The promotion effect of TBAB under different conditions (temperature, pressures and gas phase compositions) is studied to determine the stability region of the (CO_2 + N_2) semi-clathrates and the most favorable operating conditions for separating CO_2 from flue gases through sc hydrate formation.

6.2.1 Phase Equilibrium Measurements for Semi-Clathrate Hydrates of the CO_2 + N_2 + Tetra-n-Butylammonium Bromide Aqueous Solution Systems

Depending on the industrial application, the concentration of CO_2 in the gas mixture to be treated can significantly vary over the whole composition range. For instance, in large-scale power plants, flue gas typically contains mostly N_2 and usually low to medium CO_2 fractions. Three different molar concentrations of CO_2 (0.151, 0.399 and 0.749) in the feed gas are studied to cover a large range of industrial interest. The dissociation conditions for (CO_2 + N_2) semi-clathrates from TBAB aqueous solutions with mass fractions of (0.05 and 0.30) were experimentally measured to confirm the thermodynamic feasibility of the separation process.

The equilibrium dissociation measurements were carried out in the (281.0 to 291.0) K and (0.67 to 19.07) MPa ranges. A summary of the experimental conditions at which the equilibrium data were measured is provided in Table 6.6. The results are shown in the pressure-temperature phase diagrams of Figures 6.4 to 6.7. All equilibrium data along with the corresponding feed gas compositions and mass fractions of TBAB in aqueous solutions are given in Table A.10 *(*Appendix A).

The phase boundaries shown in Figures 6.4 (*a* and *b*) define the pressure and temperature region at which (CO_2 + N_2 + TBAB) semi-clathrates are thermodynamically stable. Typical flue gas mixtures (0.151 mole fraction CO_2) can form hydrates with water at 275.2 K and pressures above 10.103 MPa (Belandria *et al.*, 2011). However, such a high pressure requirement may be considered as a major drawback of the hydrate-based separation process because of the high energy costs implicated (Spencer, 1997). As mentioned earlier, most favorable operating conditions are expected to be achieved in the presence of TBAB (Shimada *et al*., 2003; Duc *et*

al., 2007; Fan *et al*., 2009). Therefore, the promotion effect of TBAB is investigated at two different salt concentrations in aqueous solutions.

As expected, by adding 0.05 mass fractions TBAB in aqueous solutions (Figure 6.4*a*), CO_2 can be separated from a typical flue gas mixture at 282.6 K and 3.157 MPa. The minimum equilibrium dissociation condition is shifted to 285.7 K and 1.568 when 0.30 mass fraction TBAB aqueous solutions are added (Figure 6.4*b*). A significant decrease in the equilibrium dissociation pressure is observed for all studied gas mixtures in the presence of TBAB. Although the experimental determination of the dissociation data for the (CO_2 + N_2 + TBAB + water) systems was restricted to three-phase (gas-hydrate-liquid) equilibrium, the upper phase boundaries (0.151 and 0.399 mole fraction CO_2) intersect at temperatures below 282.7 K (Figure 6.4*a*). Thus, the data measured below this temperature most likely represent dissociation conditions for TBAB semi-clathrates (without gas).

As can be expected from the equilibrium pressure-temperature diagrams of Figures 6.4 to 6.7, semi-clathrates of (CO_2 + N_2 + TBAB) form at lower pressures than gas hydrates of (CO_2 + N_2) at a given temperature. Similar findings on the thermodynamic promotion effect of TBAB semi-clathrate hydrates of (CO_2 + N_2) have been reported in the literature (Meysel *et al*., 2011; Mohammadi *et al*., 2011*b*). In sum, it can be observed that increasing the concentration of TBAB (at constant temperature) decreases the pressure required for semi-clathrate hydrate formation. In contrast, the required pressure for forming semi-clathrates is increased as the concentration of nitrogen in the feed gas increases under the same concentration of TBAB and temperature. Comparable results on the dependency of the required pressure for semi-clathrate formation with the feed gas composition and TBAB concentration are reported in the work of Meysel *et al*. (2011).

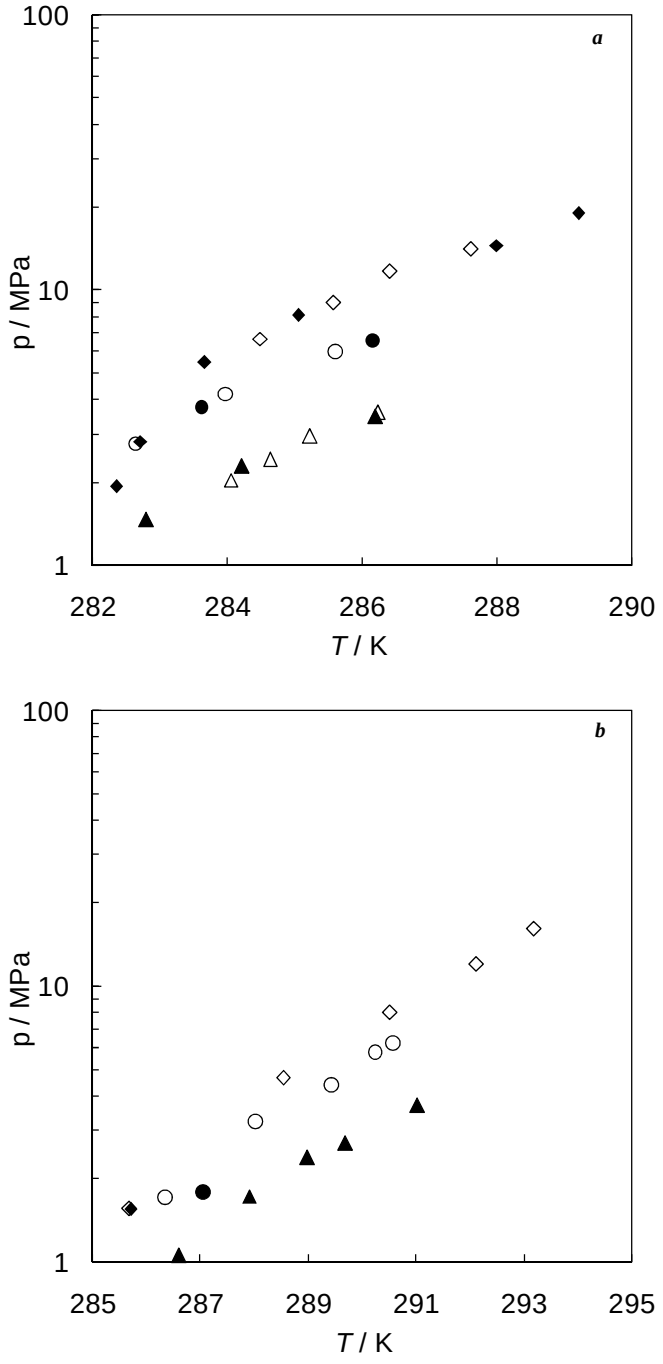


Figure 6.4. Dissociation conditions for semi-clathrates of (CO_2 + N_2) formed at various CO_2 feed gas compositions in the presence of TBAB aqueous solutions: *a*) 0.05 mass fraction TBAB; *b*) 0.30 mass fraction TBAB. This work: ♦, 0.151 mole fraction; ●, 0.399 mole fraction; ▲, 0.749 mole fraction. Literature: ◊, 0.151 mole fraction (Mohammadi *et al*., 2011*b*); ○, 0.399 mole fraction (Mohammadi *et al*., 2011*b*); Δ, 0.75 mole fraction (Meysel *et al*., 2011).

Table 6.6. Semi-clathrate hydrate phase equilibrium data (this work) for the (CO_2 + N_2 + TBAB + H_2O) systems.

Feed Composition	TBAB mass fraction	Type of data	*T* Range / K	*p* Range / MPa	Number of experimental points
CO_2 (0.151 mole) + N_2 (0.849 mole)	0.05, 0.15, 0.30	HDC (*p*,*T*)	282.4 - 285.7	1.55 - 19.07	7
	0.05	GHLE (*p*,*T*,*x*,*y*)	275.2 - 289.2	12.254 - 19.085	17
CO_2 (0.399 mole) + N_2 (0.601 mole)	0.05, 0.15, 0.30	HDC (*p*,*T*)	283.6 - 287.1	1.78 - 6.58	3
	0.05, 0.30	GHLE (*p*,*T*,*x*,*y*)	275.2 - 287.2	1.633 - 6.575	28
CO_2 (0.749 mole) + N_2 (0.251 mole)	0.05, 0.30	HDC (*p*,*T*)	281.0 - 291.0	0.67 - 3.70	10
	0.05, 0.30	GHLE (*p*,*T*,*x*,*y*)	275.2 - 285.7	0.581 - 0.942	17

Comparing phase equilibrium data from different sources on the same basis is generally not easy. Thus, a direct comparison of the experimental data obtained in this work with those reported in the literature was only possible under similar feed gas compositions and TBAB concentrations. The only other experimental study reporting three-phase equilibrium measurements for TBAB semi-clathrate hydrates of (CO_2 + N_2) with a composition of (0.75 mole fraction of CO_2) in 0.05 mass fraction aqueous solutions of TBAB is that of Meysel *et al*. (2011). As shown in Figures 6.4*a* and 6.5, their equilibrium data are in generally good agreement with the results of the present study within experimental error over (284.1 and 286.2) K. Likewise, the agreement between the dissociation temperature measured at 0.151 mole fraction of CO_2 and 0.30 mass fraction of TBAB aqueous solutions with the previously reported value by Mohammadi and coworkers (2011*b*) at 1.5 MPa is remarkably good (Figures 6.4*b* and 6.7). However, at 0.399 mole fraction of CO_2 (Figures 6.4*b* and 6.6) the dissociation temperature resulted about 0.7 K higher than the value reported by Mohammadi *et al*. (2011*b*) at 1.7 MPa. The observed deviation can be attributed to multiple causes. For instance, calibration of measuring devices, heating rate applied during hydrate dissociation and/or the interpretation of the measured data could be some of the sources of the above difference. Nevertheless, experimental uncertainties of up to 1 K in hydrate dissociation temperatures have already been reported in the literature (Beltran & Servio, 2008).

To the best knowledge of the author, this is the first study to report the effect of 0.30 mass fraction TBAB aqueous solutions on semi-clathrates of (CO_2 + N_2) at 0.749 mole fraction of CO_2 in the feed gas. In consequence, no comparison of the hydrate dissociation conditions at such CO_2 gaseous feed composition can be done.

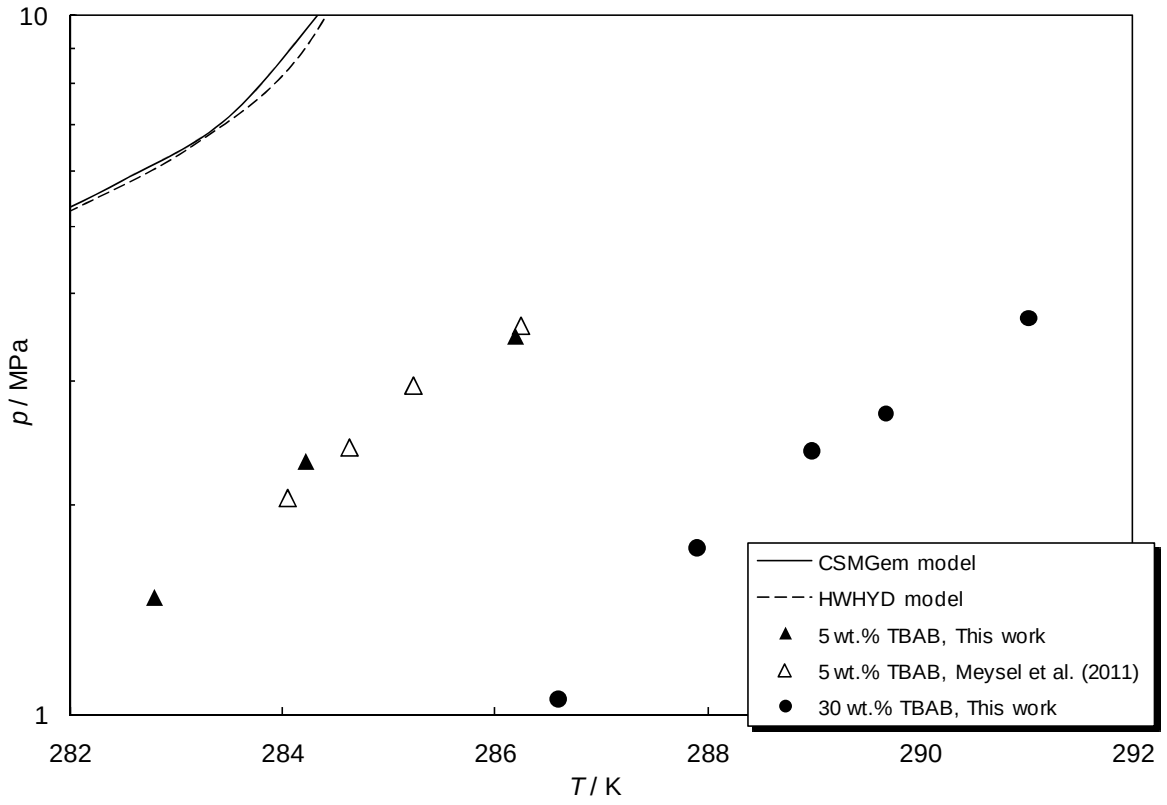


Figure 6.5**.** Experimental dissociation conditions for semi-clathrates of (0.749 mole fraction CO_2 + 0.251 mole fraction N_2) formed in the presence of TBAB aqueous solutions and predictions of CSMGem and HWHYD thermodynamic models in the absence of thermodynamic promoter

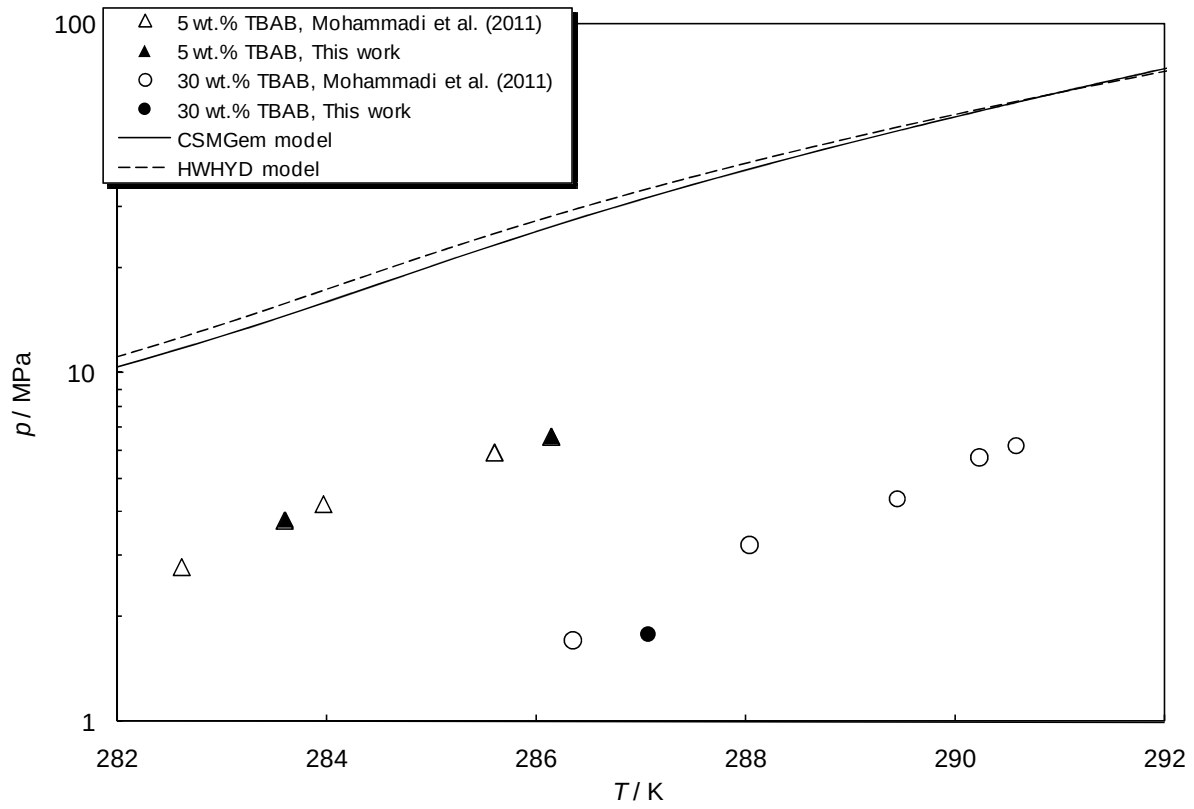


Figure 6.6. Experimental dissociation conditions for semi-clathrates of (0.399 mole fraction CO_2 + 0.601 mole fraction N_2) formed in the presence of TBAB aqueous solutions and predictions of CSMGem and HWHYD thermodynamic models in the absence of thermodynamic promoter.

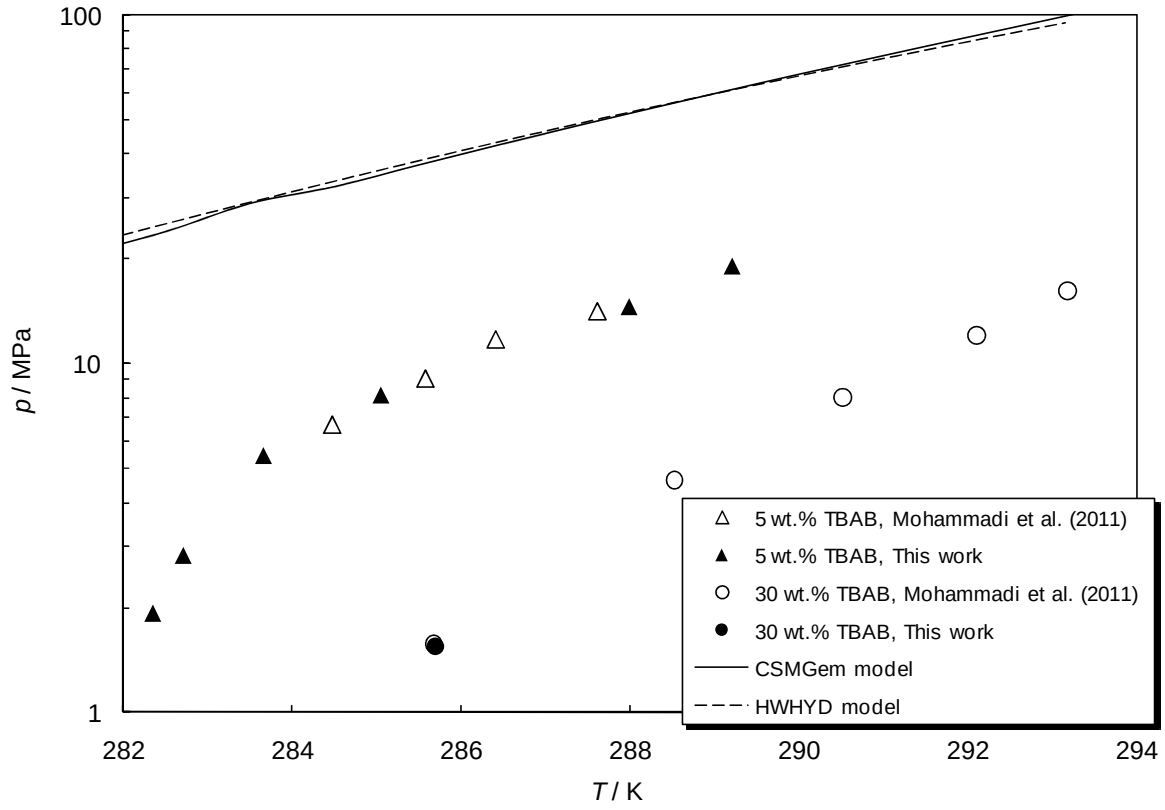


Figure 6.7. Experimental dissociation conditions for semi-clathrates of (0.151 mole fraction CO_2 + 0.849 mole fraction N_2) formed in the presence of TBAB aqueous solutions and predictions of CSMGem and HWHYD thermodynamic models in the absence of thermodynamic promoter.

The predicted *p-T* three-phase boundary for (CO_2 + N_2) hydrates is also plotted in Figures 6.5 to 6.7. Based on the composition of the feed gas, the hydrate dissociation pressures (in the absence of TBAB) were predicted over the region of temperature considered using two commercial thermodynamic models: CSMGem (2008) and HWHYD (2000). The predicted values were obtained at the corresponding equilibrium temperature, CO_2 mole fraction in the feed gas, and water mole fraction introduced to the system. Dissociation pressures were observed to be lower for forming semi-clathrates than gas hydrates at a given temperature, and they generally decreased as the TBAB concentration increased.

Additionally, a comparison of Figures 6.5 to 6.7 shows that (under the same TBAB concentration and temperature conditions) increasing the concentration of CO_2 in the feed

generally decreases the pressure required for semi-clathrate formation. However, a higher molar concentration of CO_2 may also increase the competition between CO_2 and N_2 for cage occupancy, thus compromising CO_2 selectivity in the hydrate phase.

6.2.2 Compositional Properties for Semi-Clathrate Hydrates of the CO_2 + N_2 + Tetra-n-Butylammonium Bromide Aqueous Solution Systems

With the hydrate dissociation conditions for (CO_2 + N_2 + TBAB) semi-clathrates experimentally established in the previous section, the next step is to evaluate the compositions of the gas, liquid and hydrate phases under three-phase (L-H-G) equilibrium. The greatest experimental difficulties are generally encountered in the analysis of the equilibrium phases. In this work, compositional analyses for the gas and liquid phases have been carried out and are discussed herein. Gas chromatography and refractive index were used for this purpose. Measuring the compositional change in the hydrate phase remains a challenging task and it is not addressed in this study, as it requires other experimental techniques that are far beyond the scope of this research, namely X-ray diffraction, Raman or Nuclear magnetic resonance spectroscopy.

Three different molar concentrations of CO_2 (0.151, 0.399 and 0.749) in the feed gas are studied to cover a large range of potential applications, as mentioned earlier. The effect of TBAB aqueous solutions with mass fractions of (0.05 and 0.30) was also investigated in this work. The purities and chemicals used are similar to those reported in section 6.2. The equilibrium data were measured in the (275 to 289) K and (0.58 to 19.09) MPa ranges. The density data and correlation reported in the Appendix B were used to determine the density of TBAB aqueous solutions loaded into the system and their number of moles.

A summary of the experimental conditions where compositional measurements were carried out is given in Table 6.6. All compositional equilibrium data are reported in Tables A.11 and A.12 (Appendix A). It should be noted that the compositions of the gas phase are reported in water and TBAB free basis. The molar concentration of CO_2 resulted lower at the final (gas-hydrate-liquid) equilibrium state when compared to the loading. Thus, CO_2 is preferentially trapped into the hydrate lattice and a high selectivity of CO_2 in the hydrate phase is expected.

The experimental determination of compositional data of the gas phase for the (CO_2 + N_2 + TBAB + water) systems carried out in this work was restricted to (L-H-G) equilibrium. However, by examining the *T-w* phase diagram for (TBAB + water) systems at atmospheric pressure (Figure 1.12), the equilibrium data measured below 277.15 K and 285.15 K for 0.05 and 0.30 TBAB mass fractions, respectively, most likely represent equilibrium conditions for (TBAB + H_2O) semi-clathrates (without gas).

To verify the effect of temperature on the molar concentration of CO_2 in the gas phase, the hydrate dissociation process was studied at selected isothermal conditions. A pressure-composition phase diagram for the (CO_2 + N_2 + TBAB + H_2O) systems measured at various temperatures and 0.05 mass fractions TBAB is shown in Figure 6.8. It is clear from this figure that under similar pressure conditions, the concentration of CO_2 in the gas phase increases as the equilibrium temperature increases. Therefore, most likely less amount of CO_2 is trapped in the hydrate phase at high temperatures. Also, a lower CO_2 gas phase composition is observed at higher pressures, for a given temperature. For example, by adding 0.05 mass fraction TBAB aqueous solutions, the molar concentration of CO_2 in the gas phase at 282.2 K changed from 0.114 to 0.623, while the equilibrium pressure decreases from 18.12 to 0.9 MPa, as indicated in Table A.11. Similar behavior is observed at all studied temperatures.

The effect of 0.30 mass fraction TBAB aqueous mixtures on the equilibrium pressures and gas phase compositions of (CO_2 + N_2 + TBAB + H_2O) semi-clathrates is shown in Figure 6.9. The tendencies in the molar concentrations of CO_2 in the gas phase with respect to pressure or temperature are comparable to those observed in Figure 6.8 for 0.05 mass fractions TBAB. However, larger pressure reductions are observed for a given temperature in the presence of 0.30 mass fraction TBAB aqueous solutions. This effect can be better distinguished at the two selected temperatures presented in Figure 6.10. For instance, at temperatures ~ 285.2 K a pressure reduction of at least four times is observed for systems with initial TBAB mass fractions of 0.30 compared to systems where initial TBAB mass fractions are 0.05. Such pressure reduction effect is intensified at temperatures ~ 287.2 K. On the other hand, similar equilibrium pressures (~ 0.90 MPa) are only observed at lower temperatures (~ 282.2 K) for systems in 0.05 mass fractions TBAB, while by adding 0.30 mass fractions TBAB such pressures are achieved at

higher temperatures (~ 285.7 K). Therefore, the initial concentration of TBAB in aqueous solutions has a substantial effect on the thermodynamic stability of studied semi-clathrates systems and most likely results in different crystalline structures. Furthermore, the equilibrium data suggest that (CO_2 + N_2) gas mixtures can be stabilized in the form of semi-clathrates at low pressures by adding TBAB.

In addition to the gas phase compositional measurements, the compositional change of TBAB in the liquid phase was measured through refractometry technique under three-phase equilibrium conditions. A needle valve (identified as V_3 in Figure 4.1) was used to withdraw ~ 0.05 ml liquid samples, which were then analyzed by refractive index technique, as suggested by Duc and coworkers (2007), to determine the concentration of TBAB in the liquid phase. It is assumed that TBAB does not have a significant effect on the solubility of CO_2 and N_2 in the liquid phase (Duc *et al*., 2007). Thus, gases possibly dissolved in the liquid do not affect the refractive index measurements (Assane, 2008). Again, the measured data are given in Tables A.11 and A.12. Only few points are reported in Table A.12 for the experiments with a loading concentration of 0.30 mass fractions TBAB. In fact, such a high concentration of TBAB increases the volumetric fraction of hydrate formed, which in turn blocks the sampling line and in most cases it makes impossible to sample the liquid phase. Similar technical difficulties have been previously reported in the doctoral dissertation of Assane (2008). A representative pressure - liquid composition phase diagram is shown in Figure 6.11 for initial TBAB mass fractions of 0.05. As expected, the reduction of the concentration of TBAB in the liquid phase with pressure (at a given temperature) suggests that more TBAB incorporates in the crystalline structure as pressure increases. It should also be noted that under similar pressure conditions (*e.g*. at ~ 6, ~14 and ~18 MPa), the concentration of TBAB in the liquid phase increases with temperature. This possibly suggests less occupancy of TBAB in the hydrate structure at higher temperatures. However, no conclusions can be drawn in this respect from the present study. Indeed, such hypothesis requires further investigation through suitable crystallographic techniques.

For practical purposes, an isothermal operation is considered during the hydrate formation process and mass fractions of TBAB in the liquid phase are shown at three selected temperatures. It can be noticed that the equilibrium pressure increases as the concentration of TBAB in the

liquid phase decreases at a given temperature. Such behavior is consistent with the fact that mixed (CO_2 + N_2) hydrates form at higher pressures without TBAB. On the other hand, at constant TBAB concentration, an increase in the equilibrium pressure is evidenced as temperature rises.

Based on the above results, a conceptual three-stage hydrate separation process for capturing CO_2 from industrial/flue gases is proposed. The most favorable operating conditions (feeds, temperatures and pressures for two different concentrations of TBAB aqueous solution) of the three stages are given in Table 6.7. The three (CO_2 + N_2) gas mixtures studied, with CO_2 mole fractions of (0.151, 0.399 and 0.749) were used as the feed gases in the first, second and third separation stages, respectively. Two sets of operating conditions are provided at constant temperature and two concentrations of TBAB in the aqueous solution. Thus, a highly concentrated (> 75 mole %) CO_2 stream can be obtained from a typical flue gas mixture of (15.1 mole % CO_2/N_2), under moderate temperature and pressures in the presence of TBAB.

The experimental results presented in this chapter provide a better understanding of the phase behavior of simple and mixed TBAB semi-clathrates of carbon dioxide, methane or nitrogen and (carbon dioxide + nitrogen). Therefore, a better assessment of CO_2 hydrate-based technologies with TBAB as thermodynamic promoter can be obtained from practical point of view. Finally, it should be pointed out that modeling the hydrate phase equilibria for the systems studied here is still a challenge. To the best of our knowledge no predictive (thermodynamic or mathematical) model has ever been developed for semi-clathrates formed from gas mixtures + TBAB aqueous solutions. Only two predictive approaches have been reported in the literature for (gas) semi-clathrate systems: 1) A modeling tool based on an artificial neural network (ANN) algorithm proposed by Mohammadi *et al*. (2010) for hydrogen + TBAB semiclathrate hydrates and 2) A thermodynamic model proposed by Paricaud (2011) which combines the van der Waals-Platteeuw theory and the SAFT-VRE equation of state to determine the dissociation conditions of carbon dioxide + TBAB + H_2O systems. Hence, further investigation in this subject is required. Substantial savings in experimental effort could be indeed achieved with the development of accurate thermodynamic models capable of predicting the phase behavior of semi-clathrate hydrates.

Table 6.7. Conceptual three-stage CO_2 hydrate-based separation process from (CO_2 + N_2) gas mixtures using two different concentrations of TBAB in aqueous solutions.

	TBAB / mass fraction	0.05	0.30
	Temperature / K	282.6	285.7
Feed gas molar composition / fraction	Stage	*p* / MPa	*p* / MPa
CO_2 (0.151) + N_2 (0.849 mole)	1	3.157	1.568
CO_2 (0.399) + N_2 (0.601 mole)	2	2.782	1.373
CO_2 (0.749) + N_2 (0.251 mole)	3	1.471	0.881

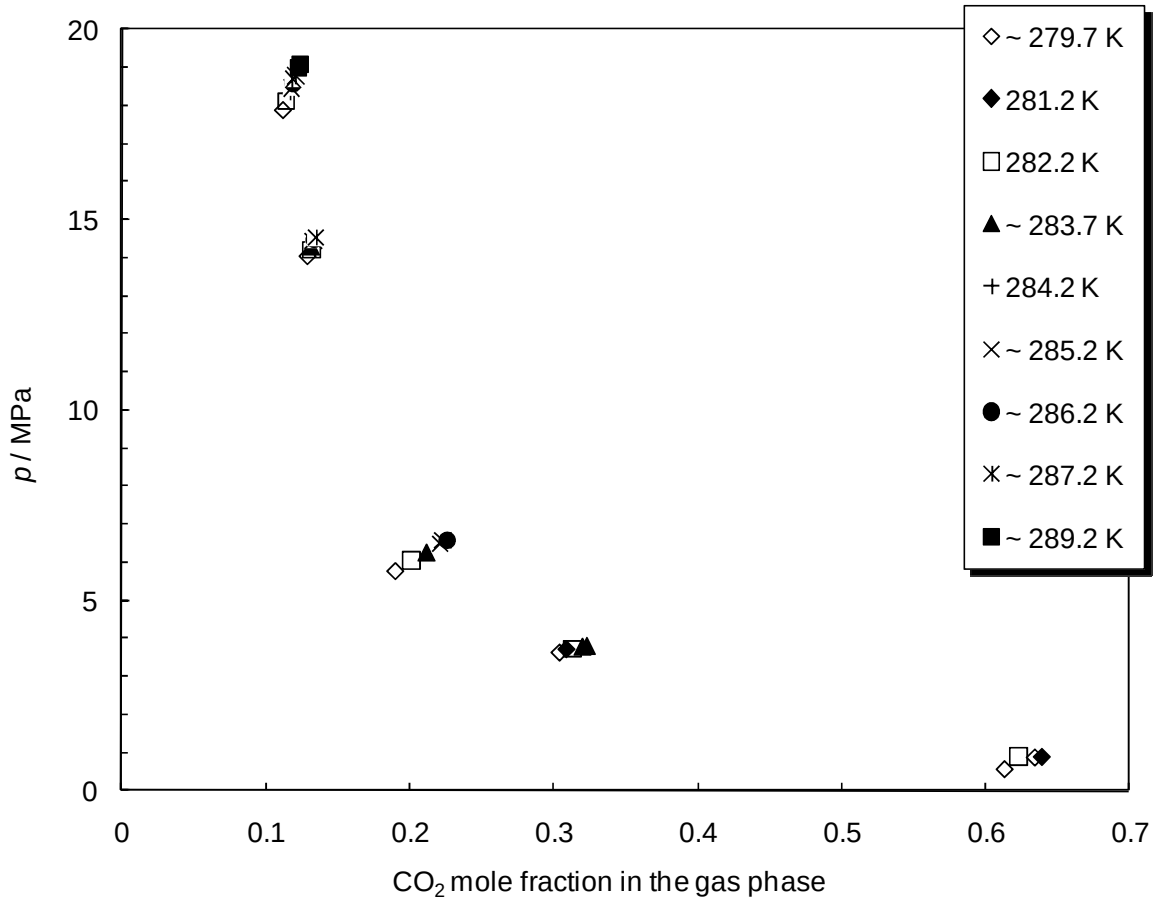


Figure 6.8. Pressure-composition (gas phase) diagram for semi-clathrates of the (CO_2 + N_2 + TBAB + H_2O) systems at various temperatures and 0.05 mass fraction TBAB.

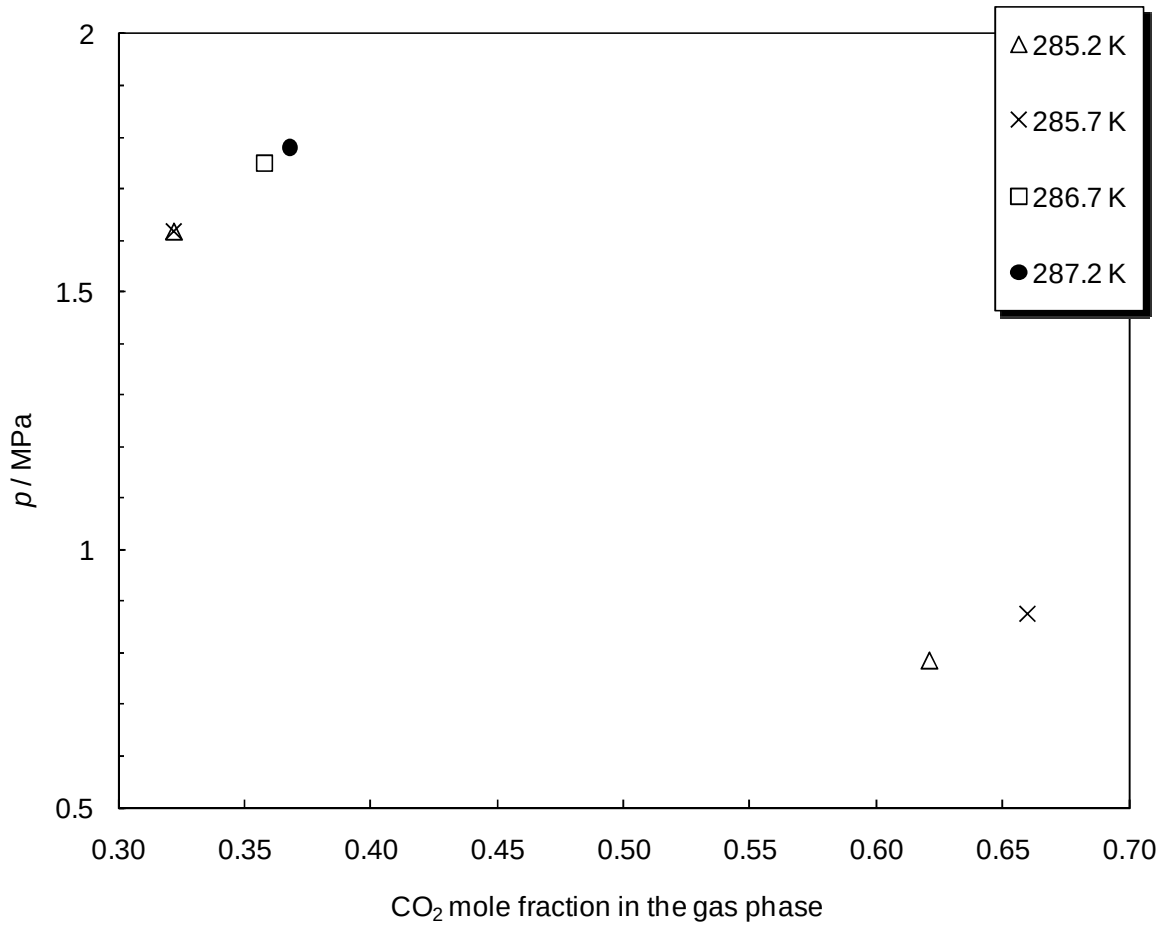


Figure 6.9. Pressure-composition (gas phase) diagram for semi-clathrates of the (CO_2 + N_2 + TBAB + H_2O) systems at various temperatures and 0.30 mass fraction TBAB.

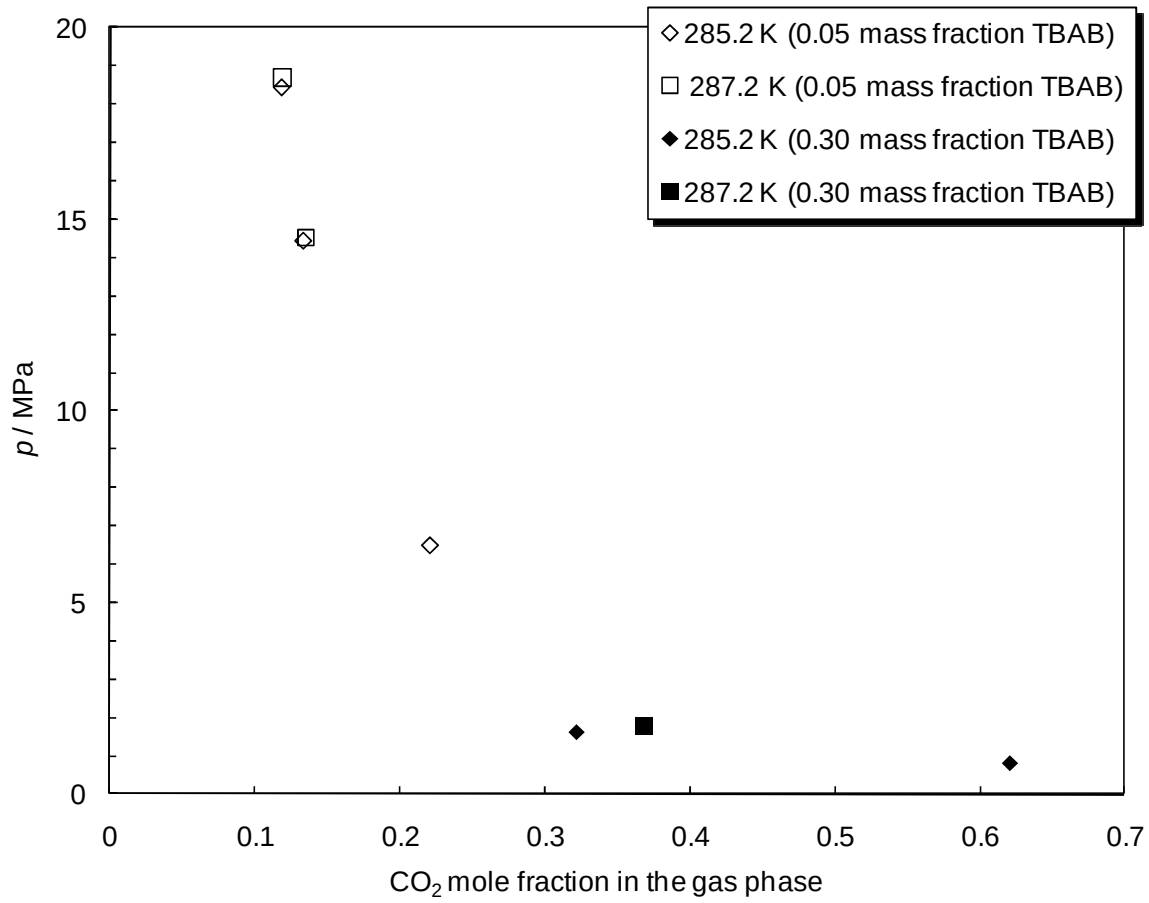


Figure 6.10. Pressure-composition (gas phase) diagram for semi-clathrates of the (CO_2 + N_2 + TBAB + H_2O) systems at selected temperatures and different initial TBAB concentrations.

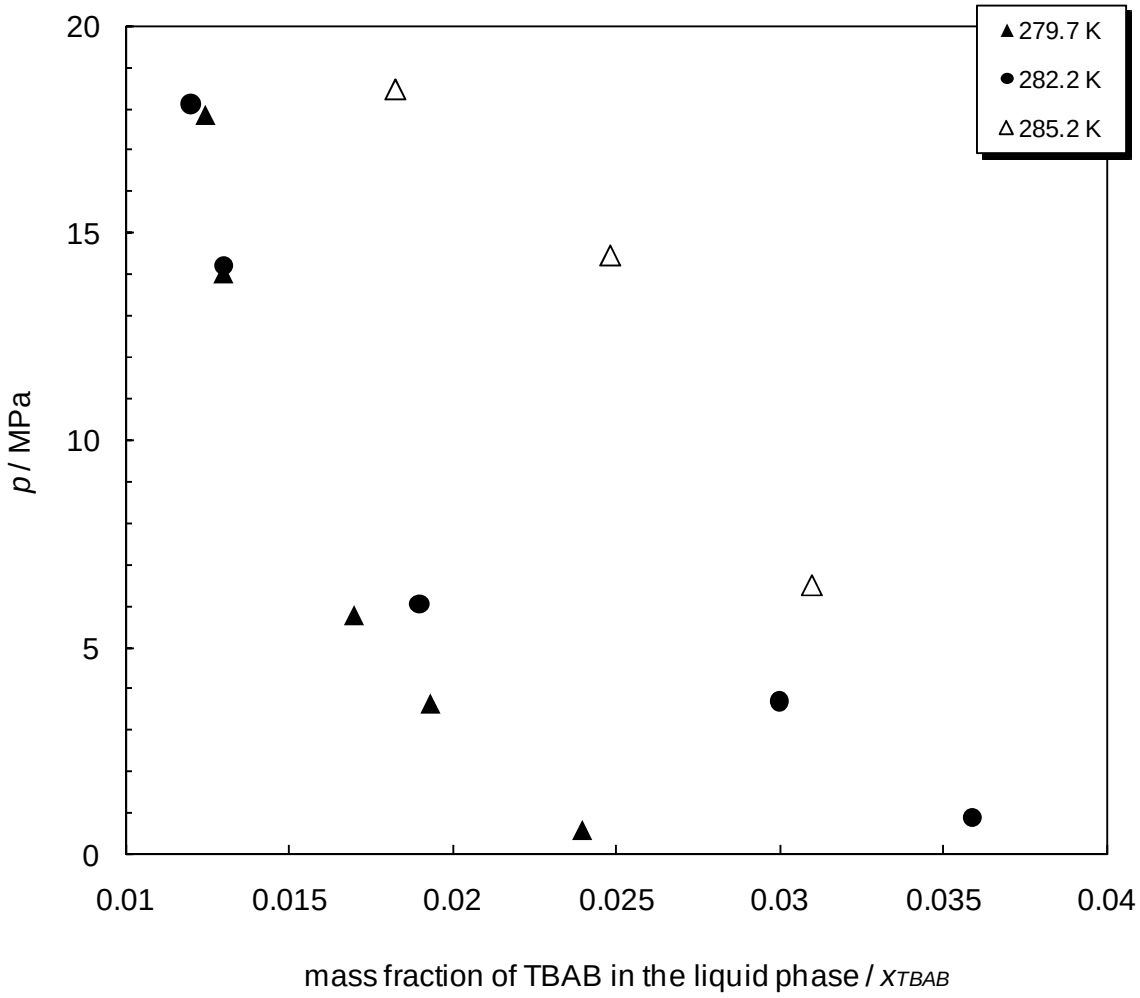


Figure 6.11. Pressure - composition (TBAB in the liquid phase) diagram for semi-clathrates of (CO_2 + N_2 + TBAB + H_2O) systems at various temperatures. TBAB mass fraction loaded = 0.05.

7

7 Conclusions et Perspectives

Le but de ce chapitre est de fournir les conclusions majeures concernant les travaux de recherche effectués dans cette thèse. La nécessité de données fiables d´équilibres de phases, sur des systèmes avec formation d'hydrate de CO_2, pertinentes dans le cadre des systèmes de technologies de captage-stockage géologique de CO_2 (CSC) a été le moteur principal de la thèse. Cette dernière a porté principalement sur des mesures expérimentales (équilibres à trois phases) sur des systèmes formateurs d´hydrates: CO_2, CH_4, N_2 et H_2 en présence d'eau pure et de solutions aqueuses de TBAB. Un nouvel appareil basé sur la technique 'statique-analytique' avec échantillonnage par capillaire (ROLSI™) de la phase gazeuse, a été développé avec le soutien de la chromatographie en phase gazeuse pour les analyses. Les résultats de l'interprétation thermodynamique des données expérimentales sont décrits. Les résultats des comparaisons avec les données de la littérature et avec les prédictions à partir de deux modèles thermodynamiques sont mis en évidence. L'effet de promotion thermodynamique dû au TBAB dans les équilibres de phases des gaz purs et des mélanges de gaz est souligné. Enfin, nous faisons des recommandations pour de futures recherches.

7 Conclusions and Outlook

The aim of this chapter is to provide the major conclusions from the research work carried out in this thesis. The need of reliable phase equilibrium data in CO_2 hydrate-forming systems relevant to CCS technologies was the main driver of the thesis. The thesis focused primarily on experimental measurements in the (CO_2, CH_4, N_2 and H_2) hydrate-forming systems in the presence of pure water and TBAB aqueous solutions under three-phase equilibrium. A new apparatus based on the 'static-analytic' technique and capillary gas phase sampling, with support from gas chromatography was developed for this purpose. Results from the thermodynamic interpretation of the experimental data are outlined. The outcome of comparisons with literature data and the predictions of two thermodynamic models are highlighted. The thermodynamic promotion effect of TBAB in the phase equilibria of pure gases and a gas mixture is emphasized. Directions for recommended future research are suggested.

7.1 Conclusions

La thermodynamique expérimentale joue un rôle important dans le cadre de la conception de technologies économiques, plus sûres, et durables. Dans cette thèse, une enquête approfondie concernant les travaux expérimentaux relatifs aux mélanges de gaz avec formation d'hydrate de CO_2 a été réalisée dans le cadre d'une approche alternative de capture du CO_2 par formation d'hydrates de gaz.

La compréhension des équilibres de phases avec hydrates requière d´une part un aperçu historique et d´autre part le contexte théorique tous deux présentés de façon concise au chapitre 1. Une description des structures les plus courantes des cristaux d'hydrates et de leurs implications microscopiques dans le comportement de phase des systèmes formateurs d´hydrates fournit la base pour l'étude des diagrammes de phases de ces systèmes. Le rôle des promoteurs thermodynamiques dans l'amélioration des conditions opératoires des procédés industriels potentiels de séparation à base d´hydrates est important en raison de la nécessité de réduire la pression requise pour la formation des hydrates par rapport aux systems aqueux en absence de promoteur. L'additif choisi pour cette étude, le TBAB, appartient à la famille des promoteurs thermodynamiques solubles dans l'eau et forme un clathrate particulier nommé «semi-clathrate».

Dans le deuxième chapitre, les techniques expérimentales disponibles pour les études à haute pression des équilibres de phases sont discutées en référence à des exemples actuels de la littérature. Le choix de la procédure expérimentale adoptée, à savoir: ‘isochoric-pressure search method’, se justifie en termes d'exactitude et de fiabilité de la méthode. Comme les données d'équilibres de phases en présence d'hydrates sont souhaitées avec la précision la plus élevée possible, et ce, à des fins de modélisation et d'ingénierie, les étalonnages de tous les outils de mesure ont été effectués soigneusement. En conséquence, les incertitudes expérimentales maximales estimées sont inférieures à ± 0.02 K et ± 0.002 MPa, pour la température et la pression, respectivement; ± 1-2 % pour les fractions molaires en phase gazeuse; ± 0.1 % pour les mesures des indices de réfraction; ± 0.5 cm^3 pour les volumes de liquide transferrés dans la cellule d'équilibre. En outre, l'incertitude globale maximale pour les mesures de dissociation d'hydrates devrait se situer à ± 0.05 MPa et ± 0.2 K, comme résultante des déterminations graphiques à partir des courbes isochores.

Le cœur du travail expérimental réalisé dans cette thèse est discuté dans les chapitres 3 à 6. La résolution des difficultés techniques et expérimentales doit être inévitablement prise en compte en vue de la mesure précise des équilibres de phases. Les mesures préliminaires des équilibres de phases réalisées en présence d´hydrates (pour le mélange gazeux "CO_2 + CH_4") ont été présentées au chapitre 3. Dans cette étude, les mélanges de gaz "CO_2 + CH_4" (différentes compositions) ont été étudiés entre 279 et 290 K pour des pressions jusqu'à 13 MPa, en utilisant un appareil existant basé sur la méthode ‘statique-analytique’. Les mélanges de gaz ont été préparés directement dans la cellule d'équilibre et la composition de la charge gazeuse a été déterminée par chromatographie en phase gazeuse. La procédure expérimentale liée à la méthode dite: “isochoric-pressure search method” a été suivie pour mesurer les conditions de dissociation des hydrates. Les données expérimentales ainsi que les données de la littérature ont été comparées aux prédictions du modèle thermodynamique HWHYD. De grandes déviations sur les pressions de dissociation (jusqu'à ~ 400%) ont été observées. Sur la base des données d'équilibre, il a été suggéré que la structure stable relative aux hydrates de gaz (dioxyde de carbone + méthane) est la structure I (AARD: 13.7%). En outre, les comparaisons de nos valeurs expérimentales de dissociation et des données de la littérature avec les prédictions d'une équation proposée par Adisasmito *et al*. (1991) montrent un accord plus cohérent (AARD: 7.9%).

Les expérimentations et les innovations continues pour améliorer à la fois l'appareil et les procédures expérimentales avec pour but d'accroître la précision des résultats, ont été la base du développement réussi d´un nouvel appareil. Ce dernier reposant sur la méthode ‘statique-analytique’ a ainsi été développé avec succès au cours de la thèse pour la mesure d'équilibres de phases avec hydrates. Le nouvel appareil et le contour des procédures d'exploitation sont le résultat de raffinements successifs tout au long de l'expérimentation conséquente. L´explication de la mesure simultanée, avec cet appareil, des conditions de dissociation des hydrates et des compositions de la phase gazeuse en équilibre avec les phases hydrate et liquide a été largement couverte dans les chapitres 4 et 5. La fiabilité de l´appareil et des procédures expérimentales est démontrée au travers de nouvelles mesures de dissociation d'hydrates effectuées sur le système: (CO_2 + CH_4 + H_2O) entre 278 et 286 K et entre 2.72 et 6.09 MPa. La comparaison entre les données expérimentales générées au cours de cette étude et les données de la littérature correspondantes montre une cohérence satisfaisante dans toutes les conditions étudiées. Les données d'équilibre *p*, *T*, *y* entre 274 et 284 K, jusqu'à environ 7 MPa, permettent de déterminer

les compositions en phase liquide et en phase hydrate en utilisant une approche par bilans de matière. La composition du CO_2 dans les phases gaz et hydrate diminue généralement alors que la pression augmente. Une concentration maximale de CO_2 égal à 0.88 en fraction molaire a été observée dans la phase hydrate à (~ 276 K et 1.99 MPa). L'augmentation de la température conduit généralement à une diminution de la quantité de CO_2 piégé en phase hydrate. Les données d'équilibre mesurées dans ce travail ont été comparées aux prédictions de deux modèles thermodynamiques, à savoir CSMGem (basé sur la minimisation de l'énergie Gibbs) et HWHYD (basé sur l'égalité de la fugacité de chaque composant dans toutes les phases). Les conditions de dissociation d'hydrates prédites présentent des écarts relatifs absolus moyens (AARD) d'environ 10 et 5 %, pour HWHYD et le modèle CSMGem, respectivement. Concernant les données d'équilibre *p*, *T*, *y*, *z*, le modèle HWHYD n'a pas du tout convergé aux conditions expérimentales étudiées. Les compositions de CO_2 prédites grâce au modèle CSMGem aboutissent à des accords moyens pour la phase hydrate. De meilleurs accords ont été obtenus pour la composition en CO_2 de la phase gazeuse en équilibre avec les phases hydrate et liquide.

Le chapitre 5 présente les équilibres de phases avec hydrate des systèmes: (CO_2 + N_2 + H_2O) et (CO_2 + H_2 + H_2O). Les mesures d'équilibre ont été effectuées à l´aide de l'appareil, et de procédures expérimentales similaires, comme décrit dans le chapitre 4. Des teneurs moyennes à hautes en CO_2 dans les mélanges ont été étudiées sur une large gamme de conditions expérimentales: *p* et *T*. Le comportement de phases de (CO_2 + N_2 + H_2O) a été d'abord étudié entre 274 et 282 K jusqu'à ~ 17.63 MPa. Les fractions molaires de CO_2 dans le gaz d'alimentation variant entre 0.271 et 0.812 ont été mesurées par chromatographie en phase gazeuse. Il a été conclu que la structure d'hydrate stable dans le cadre du mélange (CO_2 + N_2) aux conditions étudiées dans ce travail est la structure I. La pression de dissociation dépend de la composition de la charge (gaz d´alimentation) et est une function inverse de fraction molaire de CO_2 dans la charge. La fiabilité des modèles thermodynamiques CSMGem et HWHYD a été discutée pour les hydrates de gaz étudiés (CO_2 + N_2). Les valeurs des AARD sur les pressions de dissociation des hydrates prédites par les modèles thermodynamiques CSMGem et HWHYD sont respectivement de 3.4 et 10 %. Les données de composition mesurées dans les gammes: 279 à 285 K et 3.24 à 29.92 MPa, ont été comparées aux données de la littérature avec un accord acceptable. Les données de dissociation générées ici et les données expérimentales disponibles dans la littérature pour les mélanges de gaz (CO_2 + N_2) ont été comparées aux prédictions de

deux modèles thermodynamiques de la littérature. En général, les comparaisons entre pressions de dissociation expérimentales d'hydrates (ce travail) et celles prédites pour le mélange (CO_2 + N_2) et pour le mélange (CO_2 + CH_4) suggèrent la nécessité de reconsidérer les modèles thermodynamiques actuels lorsque l´on s´intéresse à des mélanges binaires contenant du CO_2. La révision des paramètres du modèle en utilisant à la fois des données de dissociation d'hydrates fiables et des données de composition des phases à l´équilibre avec l'hydrate de gaz est nécessaire pour les systèmes avec hydrate de CO_2. Cela est surtout nécessaire parce que ces modèles ont été historiquement développés pour les mélanges d'hydrocarbures.

La deuxième partie du chapitre 5, présente les mesures d'équilibres de phases des systèmes (CO_2 + H_2 + H_2O). Les compositions molaires de CO_2 (et H_2) dans la phase gazeuse en équilibre avec de l'hydrate de gaz et les phases aqueuses mesurées pour différents mélanges de gaz (CO_2 + H_2) + eau ont été étudiées entre 274 et 281 K jusqu´à environ 9 MPa. Les données expérimentales obtenues dans cette étude ont été comparées de manière satisfaisante aux données disponibles dans la littérature. A partir d´une étude bibliographique on a supposé que H_2 n´est pas piégé dans les cavités d'hydrates aux conditions étudiées.

Dans les chapitres 3 à 5, les conditions de dissociation d'hydrates relatives à des mélanges de gaz contenant du CO_2 en présence d'eau ont été établies expérimentalement à des températures basses et des pressions relativement élevées. Dans le but d'examiner l'effet promoteur d´hydrate par le TBAB, la stabilité thermodynamique de semi-clathrates formés à partir de CO_2, CH_4, N_2 et (CO_2 + N_2) dans mélanges aqueux de TBAB est étudiée au chapitre 6. Tout d´abord, la stabilité thermodynamique de semi-clathrates de (CO_2, CH_4 ou N_2 + TBAB) a été examinee pour des fractions massiques de TBAB en solution aqueuse allant de 0.25 à 0.50, dans des plages de températures de (283 à 288), (286 à 293), et (286 à 289) K, respectivement. L'effet promoteur le plus important est observé pour les systèmes avec azote, où l´on constate des réductions substantielles des pressions de dissociation d'hydrates de l´ordre de 90 %. Des accords satisfaisants avec les données de la littérature sont observés dans tous les domaines de comparaisons possibles. Dans la deuxième partie du chapitre 6, nous présentons les résultats des mesures de dissociation et de compositions pour les systèmes: (CO_2 + N_2 + TBAB + H_2O), avec des charges (gaz d´alimentation) de diverses compositions en CO_2, effectuées expérimentalement de 275 à 291 K et de 0.58 à 19.09 MPa, en utilisant les méthodes décrites dans le chapitre 4. Les

semi-clathrates sont formés avec l'addition de solutions aqueuses de TBAB (fractions massiques de TBAB: 0.05 et 0.30). Les fractions molaires de CO_2 dans le gaz d'alimentation sont: 0.151, 0.399, et 0.749). Les temperatures et pressions d'operation d'un procédé de separation du CO_2 par voie d'hydrates ont été établies sur la base des conditions expérimentales de dissociation et de compositions de mélanges de gaz. Un effet de promotion significatif est observé pour la formation des semi-clathrates, avec TBAB comme additif thermodynamique, et ce, par rapport à la formation des hydrates de gaz à la même température. Comme prévu, les pressions de dissociation diminuent généralement quand la concentration en TBAB de la solution aqueuse augmente. Dans les mêmes conditions de concentration en TBAB et de température, il a été mis en évidence que l´augmentation de la concentration en azote dans le gaz d'alimentation conduit à l´augmentation de la pression nécessaire à la formation des semi-clathrates. La comparaison avec les données de la littérature montre un accord cohérent sur tous les domaines de température et de pression. Le changement compositionnel dans les phases gazeuse et liquide, à différentes températures dans le cadre d'équilibres à trois phases, a été mesuré respectivement par chromatographie en phase gazeuse et par réfractométrie. L'effet de promotion thermodynamique dû au TBAB en solutions aqueuses a été établi en termes de pressions et de températures de dissociation. Les conditions d'exploitation les plus favorables pour un procédé de séparation du CO_2 par des hydrates ont été proposées. Le plus fort degré de promotion thermodynamique a été observé pour le mélange de gaz (CO_2 + N_2) à 0.749 molaire en CO_2, où une réduction de la pression de l´ordre de 60 % a été atteinte à 282.6 et 285.7 K, par rapport à des systèmes sans additif.

Les résultats expérimentaux permettent de montrer que le CO_2 peut être séparé des gaz industriels / de combustion qu'il soit à très faibles ou très hautes concentrations, et ce, à des conditions d'exploitation raisonnables, en présence de solutions aqueuses de TBAB. Les analyses thermodynamiques présentées dans les chapitres 3 à 6 fournissent des informations précieuses sur le comportement de phase des hydrates mixtes de dioxyde de carbone dans une gamme utile de températures et de pressions. Les données d'équilibre fournies dans la présente étude sont fondamentales pour le développement futur de modèles thermodynamiques et la conception de nouvelles technologies impliquant des hydrates de gaz de dioxyde de carbone. D'autres domaines d'amélioration et quelques indications pour des recherches futures sont suggérés dans la section suivante.

7.2 Perspectives

Bien que des résultats intéressants aient été exposés tout au long de ce travail, des recherches complémentaires sont encore nécessaires pour acquérir une meilleure compréhension de la complexité structurelle et thermodynamique des systèmes avec formation d'hydrates et semi-clathrates en présence de CO_2.

Il est clair, à l'examen de la littérature, que la quantité de données d'équilibres de phases disponibles pour les mélanges de gaz, contenant du CO_2, en solution dans des solutions aqueuses de TBAB est encore insuffisante. Les mesures des conditions de dissociation de l'hydrate de CO_2 pour d'autres mélanges de gaz, tels que (CO_2 + CH_4) et (CO_2 + H_2) en solutions aqueuses de TBAB seraient particulièrement utiles pour établir la zone de stabilité thermodynamique et estimer le degré de promotion du TBAB dans de tels systèmes, et également pertinentes pour les technologies de CSC ainsi que pour l'industrie du pétrole. De nouvelles études sur le comportement de phases sont nécessaires pour les mélanges binaires de gaz riches en hydrogène afin de mieux évaluer la forte dépendance des pressions de dissociation avec les concentrations molaires en H_2. D'autre part, l'effet des impuretés (par exemple: CO, O_2, NO, etc.), qui se trouvent généralement dans les gaz d'échappement industriels / de combustion au côté de CO_2, N_2, CH_4 et H_2, sur les équilibres de phase de systèmes avec formation d´hydrate de CO_2 a été peu étudié. Cela pourrait être, du point de vue pratique, un formidable champ d'intérêt de la recherche.

Comme il a été souligné à maintes reprises, la caractérisation directe de la phase hydrate est fortement encouragée et nécessaire afin de fournir des interprétations plus concluantes des observations thermodynamiques. Ceci peut être réalisé à l'aide de techniques physiques non intrusives appropriées (par exemple, RMN, rayons X, ou spectroscopie Raman). La connaissance des structures stables des hydrates, des occupations de cages et d'éventuelles transitions structurelles est nécessaire pour mieux comprendre le comportement de phases des hydrates mixtes et semi-clathrates de TBAB.

Dans cette thèse, il a été argumenté sur le fait que les paramètres du modèle thermodynamique doivent être réajustés sur des données d'équilibre fiables de systèmes formant des hydrates de CO_2, car les modèles existants ont généralement été développés uniquement pour des mélanges

d'hydrocarbures. Seulement deux approches thermodynamiques prédictives (Mohammadi *et al.*, 2010 et Paricaud, 2011) ont été proposées, à ce jour, pour les semi-clathrates de (H_2 + TBAB) et (CO_2 + TBAB), respectivement. En conséquence, le développement de nouvelles approches thermodynamiques prédictives spécialement adaptées aux semi-clathrates est fortement encouragé, d´autant plus qu´un comportement structurel complexe (possibles transitions de structure) a été évoqué, comme hypothèse, à partir des équilibres de phases mesurés dans ce travail. Des économies substantielles sur les efforts expérimentaux sont attendues avec le développement de modèles thermodynamiques précis capables de prédire le comportement de phases des semi-clathrates hydrates.

Li *et al.* (2010) ont mené une étude comparative sur l'effet promoteur de divers sels d'ammonium quaternaire (par exemple TBAF, TBAB et TBAC) sur les équilibres de phases impliquant le CO_2. La recherche de Chapoy *et al.* (2007) a montré une capacité de stockage accrue de l'hydrogène dans les semi-clathrates de TBAB d'un ordre de grandeur (à 1 MPa), par rapport aux clathrates (H_2 + THF). En outre, Deschamps et Dalmazzone (2010) ont écrit qu'environ deux fois plus d'hydrogène peut être stocké dans les systèmes (H_2 + TBAC) et (H_2 + bromure de tétrabutylphosphonium) par rapport aux semi-clathrates (H_2 + TBAB). Sur la base de ces études, des travaux complémentaires concernant l'effet des sels de tétra alkyl ammonium sur les équilibres de phases des mélanges gazeux: (H_2 + CO_2), seraient certainement très utiles pour les applications en séparation et stockage.

Une procédure expérimentale alternative aux mesures fastidieuses des équilibres de phase en présence d'hydrates par la méthode dite: ‘isochoric pressure-search method’ a été récemment étudiée à CEP-TEP. Une étude préliminaire a été effectuée pour les hydrates de CO_2 pur à l´aide d´une cellule à volume variable en titane (Fontalba *et al.*, 1984), et a montré des résultats prometteurs (D. Richon, communication personnelle, 9 Mars, 2012). En effet, l´équilibre thermodynamique est atteint en quelques minutes et la pression de dissociation des hydrates est identifiée par la présence d'un plateau sur la courbe représentant la pression en fonction du volume accessible au mélange étudié. La composition de la phase hydrate peut être déterminée à partir des données PVT et de la détermination de la quantité de gaz émis lors de la dissociation des hydrates (à partir de la largeur du plateau). Cette méthode mériterait d´être approfondie.

Bien que l'appareil développé dans cette thèse fonctionne de manière satisfaisante, certaines améliorations sont recommandées pour les futurs montages expérimentaux destinés aux mesures d'équilibre de phases avec hydrates de gaz: un mélangeage plus efficace, la suppression des volumes morts dans les accessoires et dispositifs de mélange et une bonne caractérisation des compositions des phases liquide et hydrate au travers d'échantillonnages in situ. Enfin, la réalisation de mesures d'équilibres de phases à haute pression et avec des composés toxiques est potentiellement dangereuse. Ainsi, le souci de la sécurité doit être la priorité de tous les instants que ce soit au niveau de la conception des appareillages, de la conduite des manipulations et lors des opérations de routine.

7.1 Conclusions

Experimental thermodynamics play an important role in the design of economical, safer and sustainable technologies. In this thesis a comprehensive experimental investigation for CO_2 hydrate-forming gas mixtures has been carried out in the context of an alternative CO_2 capture approach, through gas hydrate formation.

The understanding of hydrate phase equilibrium implies a historical overview and theoretical background concisely presented in Chapter 1. An insight of the most common hydrate crystal structures and their microscopic implications in the phase behavior of hydrate forming systems provided the basis for studying the phase diagrams in gas hydrates forming systems. The role of thermodynamic promoters in enhancing the operating conditions of potential industrial gas hydrates-based processes was supported with the need of reducing the required pressure for hydrate formation compared to systems in the absence of promoter. The additive chosen for this investigation, TBAB, belongs to the water-soluble family of thermodynamic promoters and forms a different clathrate compound labeled ‘semi-clathrate’.

In the second chapter, the experimental techniques available for high-pressure phase equilibrium studies are discussed with reference to current examples from the literature. The choice of the experimental procedure adopted, namely ‘isochoric-pressure search method’, is justified in terms of the accuracy and reliability of the method. As hydrate phase equilibrium data with the highest possible accuracy are needed for modeling and engineering purposes, calibrations of all

measuring devices were carefully performed. Accordingly, maximum expected experimental uncertainties are within ± 0.02 K and ± 0.002 MPa, for temperature and pressure equilibrium measurements, respectively; ± 0.5 cm^3 for liquids supplied to the equilibrium cell; ± 1-2% for molar gas phase compositions and ± 0.1% for refractive indices measurements. In addition, the maximum overall uncertainty for hydrate dissociation measurements is expected to be within ± 0.05 MPa and ± 0.2 K, derived from isochoric curves.

The core of the experimental work carried out in this thesis is discussed in Chapters 3 to 6. The resolution of technical and experimental difficulties must be unavoidably taken into account in the measurement of accurate hydrate phase equilibrium data. Preliminary phase equilibrium measurements carried out for clathrate hydrates of (CO_2 + CH_4) mixtures were presented in Chapter 3. In this study, gas mixtures with different CO_2 / CH_4 ratios were investigated in the temperature ranges from (279 to 290) K and pressures up to 13 MPa, using an existent 'static-analytic' apparatus. The gas mixtures were prepared directly in the equilibrium cell and the composition of the feed was determined through gas chromatography. An isochoric pressure-search method was followed to measure the hydrate dissociation conditions. The experimental data along with the literature data were compared with the predictions of HWHYD thermodynamic model. Large deviations on the dissociation pressures (up to ~ 400%) were observed. Based on the equilibrium data, it was suggested that the stable hydrate structure for the (carbon dioxide + methane) gas hydrates is likely structure I (AARD: 13.7%). In addition, comparisons between dissociation experimental and literature data with the predictions of an equation proposed by Adisasmito *et al.* (1991) resulted more consistent (AARD: 7.9%).

As a result of continuous experimentation and innovation to improve both the apparatus and experimental procedures and with the aim of increasing the accuracy of the results, a new 'static-analytic' apparatus for hydrate phase equilibrium measurements was successfully developed within this thesis. The new apparatus and the outline of operating procedures are the outcome of successive refinement throughout substantial experimentation. Simultaneous measurement of hydrate dissociation conditions and compositions of the gas phase in equilibrium with the hydrate and liquid phases using this new apparatus were extensively covered in Chapters 4 and 5. The reliability of the apparatus and experimental procedures is demonstrated through new hydrate dissociation measurements carried out for (CO_2 + CH_4 + H_2O) systems in the (278 to

286) K and (2.72 to 6.09) MPa ranges. Comparison between the experimental data generated in this study and the corresponding literature data show satisfactory consistency throughout the investigated conditions. The measured *p, T, y* equilibrium data in the (274 to 284) K and up to ~ 7 MPa, enabled the determination of liquid and hydrate phase compositions using a material balance approach. Composition of CO_2 in the gas and hydrate phases generally decreased as pressure increased. A maximum concentration of 0.88 mole fraction of CO_2 in the hydrate phase was observed at (~ 276 K and 1.99 MPa). Increasing the temperature generally leads to less CO_2 being trapped in the hydrate phase. The equilibrium data measured in this work were compared with the predictions of two thermodynamic models, namely CSMGem (based on the Gibbs energy minimization) and HWHYD (based on the equality of fugacity of each component throughout all phases). Predicted hydrate dissociation conditions showed average absolute relative deviations (AARD) of about 10 % and 5 %, for HWHYD and CSMGem models respectively. As for the *p, T, y, z* equilibrium data, the HWHYD model did not converge at all at the studied experimental conditions. The predicted CO_2 compositions through CSMGem model resulted in poor agreements for the hydrate phase. Better agreements were obtained for the composition of CO_2 in the gas phase in equilibrium with hydrate and liquid phases.

Chapter 5 presents the hydrate phase equilibria of (CO_2 + N_2 + H_2O) and (CO_2 + H_2 + H_2O) systems. The equilibrium measurements were carried out using the apparatus described in Chapter 4 and following similar experimental procedures. Medium to high content CO_2 gas mixtures were investigated over a wide range of experimental conditions. The phase behavior of (CO_2 + N_2 + H_2O) systems was first investigated in the (274 to 282) K temperature range and pressures up to ~ 17.63 MPa. The relative molar ratios of CO_2 and N_2 in the feed gas varying between from (0.271 to 0.812) were measured by gas chromatography. It was suggested that the stable hydrate structure for the (CO_2 + N_2) clathrate hydrates at the conditions studied in this work is likely structure I. The equilibrium dissociation pressures were found to be dependent of the composition of the feed and were shifted to lower values as the mole fraction of CO_2 increased in the feed. The reliability of CSMGem and HWHYD thermodynamic models was investigated for the studied (CO_2 + N_2) gas hydrates. AARD of the predicted hydrate dissociation pressures by HWHYD and CSMGem thermodynamic models are 3.4 % and 10 %, respectively. The measured compositional data, in the (279 to 285) K and (3.24 to 29.92) MPa ranges, were compared with the literature data and a generally consistent agreement is found. The dissociation

data generated along with the experimental data reported in the literature for (CO_2 + N_2) gas mixtures were compared with the predictions of two thermodynamic literature models. In general, comparisons between experimental and predicted hydrate dissociation pressures carried out in this work for the latter system and for (CO_2 + CH_4) gas mixtures suggest a need for reconsidering current thermodynamic models for binary mixtures containing CO_2. Readjustment of model parameters using reliable both hydrate dissociation and compositional data of the existing phases in equilibrium with gas hydrate is necessary for CO_2 hydrate-forming systems. Especially, since such models have traditionally been developed for hydrocarbon systems.

The second part of Chapter 5, presents the phase equilibrium measurements carried out for (CO_2 + H_2 + H_2O) systems. The molar compositions of CO_2 (and H_2) in the gas phase in equilibrium with gas hydrate and aqueous phases measured for various (CO_2 + H_2) gas mixtures + water systems were investigated in the temperature range of (274 to 281) K at pressures up to ~ 9 MPa. The experimental data generated in this study were compared with the data reported in the literature and acceptable agreement is generally observed. It was assumed that H_2 was not trapped in the hydrate cavities in the studied conditions, based on literature investigations.

In Chapters 3 through 5, hydrate dissociation conditions for gas mixtures containing CO_2 in the presence of water were experimentally established at low temperatures and relatively high pressures. With the aim of examining the hydrate promotion effect of TBAB, the thermodynamic stability of semi-clathrates formed from CO_2, CH_4, N_2 and (CO_2 + N_2) in TBAB aqueous mixtures is investigated in Chapter 6. First, the thermodynamic stability of semi-clathrates of (CO_2, CH_4 or N_2 + TBAB) in aqueous mixtures was examined, at 0.25 and 0.50 mass fraction of TBAB in aqueous solution, in the temperature ranges of (283 to 288), (286 to 293), and (286 to 289) K, respectively. The largest promotion effect is observed for nitrogen systems, where substantial reductions in the hydrate dissociation pressures of ~ > 90 % are evidenced. Consistent agreements with the literature data in the whole region where comparisons could be made are generally found. In the second part of Chapter 6, dissociation and compositional data for the (CO_2 + N_2 + TBAB + H_2O) systems with various CO_2 feed gas molar compositions were experimentally measured in the (275 to 291) K and (0.58 to 19.09) MPa ranges, using the methodologies described in Chapter 4. Semi-clathrates were formed with the addition of TBAB aqueous solutions with mass fractions of (0.05 and 0.30). The relative molar fractions of CO_2 in

the feed gas were (0.151, 0.399, and 0.749). Fundamental process variables were established based on the experimental dissociation conditions and phase compositional data. A significant promotion effect is observed for forming semi-clathrates, with TBAB as thermodynamic additive, compared to gas hydrates at the same temperature. As expected, the dissociation pressures generally decrease as the concentration of TBAB in the aqueous solution increases. Under the same TBAB concentration and temperature conditions, it was evidenced that increasing the concentration of nitrogen in the feed gas increases the pressure required to form semi-clathrates. Comparison with literature data shows consistent agreement over the entire temperature and pressure ranges investigated. The compositional change in the gas and liquid phases, at different temperatures under three-phase equilibrium, was measured by gas chromatography and refractometry technique, respectively. The thermodynamic promotion effect of TBAB in aqueous solutions was established in terms of dissociation pressures and temperatures and the most favorable operating conditions for a CO_2 hydrate-based separation process were proposed. The highest degree of thermodynamic promotion was observed for the (0.749 mole fraction CO_2 + 0.251 mole fraction N_2) gas mixture, where a pressure reduction of ~ 60% was achieved at both temperatures (282.6 and 285.7) K, compared to clathrate hydrates systems (without additive).

The experimental results suggest that CO_2 can be separated from highly to low concentrated industrial / flue gas mixtures at reasonable operating conditions in the presence of TBAB aqueous solutions. The thermodynamic analyses presented in Chapters 3 to 6 provide valuable information on the phase behavior of mixed carbon dioxide hydrates at a useful range of temperatures and pressures. The equilibrium data provided in this underlying study are fundamental for future development of thermodynamic models and design of novel technologies involving carbon dioxide gas hydrates. Further areas of improvement and some directions on future research are suggested in the following section.

7.2 Outlook

Although some interesting findings have been outlined throughout this investigation, further research is still required to gain a better understanding of the thermodynamic and structural

complexity of CO_2 hydrate-forming systems and semi-clathrates.

It is clear from literature examination that the phase equilibrium data available for CO_2 containing gas mixtures in TBAB aqueous mixtures are still limited. Measurements of the dissociation conditions of other CO_2 hydrate-forming systems, such as (CO_2 + CH_4) and (CO_2 + H_2) gas mixtures in TBAB aqueous solutions would be particularly useful for establishing the thermodynamic stability region and investigating the degree of promotion of TBAB in such systems, also relevant to CCS technologies and petroleum industry. Especially, further phase behavior studies are required in H_2-rich binary gas mixtures for better assessing the strong dependency of the dissociation pressures on H_2 molar concentrations. On the other hand, besides CO_2, N_2, CH_4 and H_2, the effect of impurities (*e.g.* CO, O_2, NO *etc.*), that are usually found in industrial / flue exhaust gases, on the phase equilibria of CO_2 hydrate-forming systems has been scarcely studied. This could be an interest field of research from practical point of view.

As it has been pointed out repeatedly, direct characterization of the hydrate phase is highly encouraged and necessary to provide further conclusive interpretations of thermodynamic observations. This can be achieved using suitable non-intrusive physical techniques (*e.g.*, NMR, X-ray, or Raman spectroscopy). Knowledge on the stable hydrate structures, cage occupancies and possible structural transitions is needed for better understanding the phase behavior of mixed hydrates and TBAB semi-clathrates.

In this thesis, it was argued that the parameters of thermodynamic model should be readjusted using reliable equilibrium data for CO_2 hydrate-forming systems, as the existent models have been generally developed for hydrocarbon systems. Provided that only two thermodynamic predictive approaches (Mohammadi *et al.*, 2010 and Paricaud, 2011) have been proposed for semi-clathrates of (H_2 + TBAB) and (CO_2 + TBAB), respectively, the development of thermodynamic predictive approaches for semi-clathrates requires further research. Especially, since a complex structural behavior (possible structure transitions) is suspected from the phase equilibrium data measured in this work. Substantial savings in experimental effort are expected with the development of accurate thermodynamic models capable of predicting the phase behavior of semi-clathrate hydrates.

Li *et al*. (2010) conducted a comparative investigation on the promotion effect of various quaternary ammonium salts (*e.g*. TBAF, TBAB and TBAC) on the phase equilbria of CO_2. Moreover, the research of Chapoy *et al*. (2007) has shown an increased storage capacity for hydrogen in TBAB semi-clathrates of one order of magnitude (at 1 MPa), compared to (H_2 + THF) clathrates. Moreover, Deschamps and Dalmazzone (2010) suggested that approximately two times more hydrogen can be stored in (H_2 + TBAC) and (H_2 + tetrabutylphosphonium bromide) systems compared to (H_2 + TBAB) semi-clathrates. Based on these studies, further investigations on the effect of such tetra alkyl ammonium salts on the phase equilibria of H_2 and CO_2 containing gas mixtures, could be attractive for gas separation and storage applications.

An alternative experimental procedure to the time-consuming hydrate phase equilibrium measurements through the 'isochoric pressure-search method' has been recently investigated at CEP-TEP. A preliminary study has been conducted for pure CO_2 hydrates in a titanium variable volume cell (Fontalba *et al*., 1984), with promising results (D. Richon, Personal Communication, March 9, 2012). Thermodynamic equilibrium is reached within few minutes and the hydrate dissociation pressure is identified by the presence of a plateau in a pressure versus piston displacement plot. The composition of the hydrate phase can be determined from the PVT data and the amount of gas released during hydrate dissociation (known from the with of the plateau). This method should be further investigated.

Although the apparatus developed in this thesis operated satisfactorily, certain improvements are recommended for future experimental set-ups destined to gas hydrates phase equilibrium measurements: an efficient mixing, the avoidance of dead volumes in accessories and mixing devices and accurate characterization of the liquid and hydrate phases composition through *in situ* sampling. Finally, performing phase equilibrium measurements at high pressures and with toxic compounds is likely hazardous. Safety considerations must be thus a priority at all times in the design of experimental set-ups, start-up of new equipment and routine operation.

References

Aaron, D., Tsouris, C., "Separation of CO_2 from Flue Gas: A Review", *Separ. Sci. Technol.,* 40, 321-348 (2005).

Adisasmito, S., Frank, R., Sloan, D., "Hydrates of Carbon Dioxide and Methane Mixtures", *J. Chem. Eng. Data*, 36 (1), 68-71 (1991).

Afzal, W., Mohammadi, A.H., Richon, D., "Experimental measurements and predictions of dissociation conditions for carbon dioxide and methane hydrates in the presence of triethylene glycol aqueous solutions", *J. Chem. Eng. Data*, 52, 2053-2055 (2007).

Afzal, W., Mohammadi, A.H., Richon, D. "Measuring Vapor-liquid Equilibria in Sour Gas + Glycol Aqueous Solutions Using Static Techniques", in Proc. of AIChE Annual Meeting, Philadelphia, USA (2008*a*).

Afzal, W., Mohammadi, A.H., Richon, D., "Impact of Sulfur Species on Glycol Dehydration (GPA 992-3): Solubility Study of Certain Sulfur Species in Glycol Aqueous Solutions. Experimental Vapor-Liquid Equilibrium Data for (COS/H_2S/ MEG/ H_2O) and (COS/ H_2S/ TEG/ H_2O) Systems", Research Report RR-204, January (2008*b*).

Afzal, W., "Phase equilibria of glycol-natural gas systems", PhD Dissertation, Ecole Nationale Supérieure des Mines de Paris, France (2009).

Anderson, G. K., "Enthalpy of Dissociation and Hydration Number of Carbon Dioxide Hydrate from the Clapeyron Equation", *J. Chem. Thermodyn.*, 35, 1171-1183 (2003).

Arjmandi, M., Chapoy, A., Tohidi, B., "Equilibrium Data of Hydrogen, Methane, Nitrogen, Carbon Dioxide, and Natural Gas in Semi-Clathrate Hydrates of Tetrabutyl Ammonium Bromide", *J. Chem. Eng. Data*, 52, 2153-2158 (2007).

Avlonitis, D., Danesh, A., Todd, A. C., "Prediction of VL and VLL Equilibria of Mixtures Containing Petroleum Reservoir Fluids and Methanol with a Cubic EOS", *Fluid Phase Equilib*. 94, 181-216 (1994).

Azmi, N., Mukhtar H., Sabil, K.M., "Removal of high CO_2 content in natural gas by formation of gas hydrates as a potential solution for CO_2 gas emission", in Proc. International Conference on Environment, Dec. 13-15, Penang, Malaysia (2010).

Belandria, V., Mohammadi, A.H., Richon, D., "Phase equilibria of clathrate hydrates of methane + carbon dioxide: New experimental data and predictions", *Fluid Phase Equilib*., 296, 60-65 (2010).

Belandria, V., Eslamimanesh, A., Mohammadi, A. H., Théveneau, P., Legendre, H., Richon, D., "Compositional analysis and hydrate dissociation conditions measurements for carbon dioxide + methane + water system", *Ind. Eng. Chem. Res.* 50 (9), 5783-5794 (2011).

Belandria,V., Mohammadi, A.H., Eslamimanesh, A., Richon, D., Sánchez, M. F., Galicia-Luna, L. A., "Phase Equilibrium Measurements for Semi-clathrate Hydrates of the (CO_2 + N_2 + Tetra-n-butylammonium Bromide) Aqueous Solution Systems", *Fluid Phase Equilib.* 322, 105-112 (2012).

Beltran, J., Servio P., "Equilibrium Studies for the System Methane + Carbon Dioxide + Neohexane + Water", *J. Chem. Eng. Data*, 53, 1745-1749 (2008).

Berecz, E., Balla-Achs, M., *Gas Hydrates (Studies in Inorganic Chemistry Vol. 4), Chapter 3*, Elsevier Science Publishers, Amsterdam, Oxford, New York (1983).

BP's Statistical Review of World Energy June 2011, Pureprint Group Limited, UK (2011).

Bruusgaard, H., Beltran, J. G., Servio, P., "Vapor-Liquid Water-Hydrate Equilibrium Data for the System N_2 + CO_2 + H_2O", *J. Chem. Eng. Data* 53, 2594-2597 (2008).

Bruusgaard, H., Beltran, J., Servio, P., "Solubility measurements for the CH_4 + CO_2 + H_2O system under hydrate–liquid–vapor equilibrium", *Fluid Phase Equilib.*, 296 (2), 106-109 (2010).

Burgass,R.W., Tohidi,B., Danesh,A., Todd,A.C., in Proc. Fourth InternationalConference on Gas Hydrates, Yokohama, Japan, May 19-23, 380 (2002) [cited in Sloan and Koh, 2008].

Cailletet, L., Bordet, R., *Compt. Rend*., 95, 58 (1882) [cited in Sloan & Koh, 2008].

Carroll J., *Natural Gas Hydrates: A Guide for Engineers*, second ed., Gulf Professional Publishing, Burlington, MA (2009).

Chapoy, A., Anderson, R., Tohidi. B., "Low-Pressure Molecular Hydrogen Storage in Semi-clathrate Hydrates of Quaternary Ammonium Compounds", *J. Am. Chem. Soc*., 129, 746-747 (2007).

Chatti, I., Delahaye, A., Fournaison, L., Petitet, J. P., "Benefits and Drawbacks of Clathrate Hydrates: A Review of Their Areas of Interest", *Energy Convers. Manage*., 46, 1333-1343 (2005).

Chazallon, B., "CO_2 Capture by Gas Hydrate Crystallization: Investigation of Equilibrium and Compositional Properties of CO_2-N_2 Hydrates by Micro-Raman Spectroscopy", in Proc. Twelfth International Conference on the Physics and Chemistry of Ice, September 5-10, Sapporo, Japan (2010).

Christov, M., Dohrn, R., "High-pressure Fluid Phase Equilibria: Experimental Methods and Systems Investigated (1994-1999)", *Fluid Phase Equilib*., 202, 153-218 (2002).

Collodi, G., Wheeler, F., "Hydrogen Production via Steam Reforming with CO_2 Capture," *Chemical Engineering Transactions,* 19, 37-42 (2010).

Constantinides, A., Moustofi, N., Numerical Methods for Chemical Engineers with Matlab Applications, Prentice Hall PTR (1999).

CSMGem, Phase-equilibrium Calculation Program Package Accompanying the Following Book: Sloan, E. D., Jr. Clathrate Hydrates of Natural Gases, 3rd ed.; Taylor & Francis Group: Boca Raton (2008).

Dalmazzone, D., Kharrat, M., Lachet, V., Fouconnier B., Clausse, D., "DSC and PVT Measurements: Methane and Trichlorofluoromethane Hydrate Dissociation Equilibria", *J. Therm. Anal. Cal.*, 70, 493-505 (2002).

Darbouret, M., Cournil, M., Herri, J.M., "Rheological Study of TBAB Hydrate Slurries as Secondary Two-phase Refrigerants", *Int. J. Refrig.*, 28, 663-671 (2005).

Davy, H., *Phil. Trans. Roy. Soc. Lond.*, 101, 1 (1811) [cited in Sloan & Koh, 2008].

Davidson, D.W., *Clathrate Hydrates, in Water: A Comprehensive Treatise*, Plenum Press, New York, Chap. 3, 115 (1973).

de Forcrand, R., *Compt. Rend.*, 135, 959- 961 (1902) [cited in Sloan & Koh, 2008].

Deaton,W.M., Frost, E.M., *Oil Gas J.*, 36, 75 (1937) [cited in Sloan & Koh, 2008].

Deaton, W.M., Frost, E.M., "Gas Hydrates and Their Relation to the Operation of Natural-Gas Pipe Lines", 101 pp, U.S. Bureau of Mines Monograph 8 (1946) [cited in Sloan and Koh, 2008].

Deiters, U.K., Schneider, G.M., "High pressure phase equilibria: experimental methods", *Fluid Phase Equilib.*, 29, 145-160 (1986).

Deiters, U. K., Kraska, T., *High-Pressure Fluid Phase Equilibria, Volume 2: Phenomenology and Computation*, Elsevier Science Ltd.: Amsterdam (2012), (D. Richon, Personal Communication, June 30, 2011).

Delahaye, A., Fournaison, L., Marinhas, S., Chatti, I., Petitet, J., Dalmazzone, D., Furst, W., "Effect of THF on Equilibrium Pressure and Dissociation Enthalpy of CO_2 Hydrates Applied to Secondary Refrigeration", *Ind. Eng. Chem. Res.*, 45, 391-397 (2006).

Deschamps, J., Dalmazzone, D., "Dissociation Enthalpies and Phase Equilibrium for TBAB semi-Clathrate Hydrates of N_2, CO_2, N_2 + CO_2 and CH_4 + CO_2", *J. Therm. Anal. Calorim.*, 98, 113-118 (2009).

Deschamps, J., Dalmazzone, D., "Hydrogen Storage in Semiclathrate Hydrates of Tetrabutyl Ammonium Chloride and Tetrabutyl Phosphonium Bromide", *J. Chem. Eng. Data*, 55, 3395-3399 (2010).

Dohrn, R., Brunner, G., "High-pressure fluid-phase equilibria: Experimental methods and systems investigated (1988-1993)", *Fluid Phase Equilib.*, 106, 213-282 (1995).

Dohrn, R., Peper, S., Fonseca, J.M.S., "High-pressure phase equilibria: experimental methods and systems investigated (2000-2004)", *Fluid Phase Equilib.*, 288, 1-54 (2010).

Duc, N.H., Chauvy, F., Herri, J.M., "CO_2 Capture by Hydrate Crystallization - A Potential Solution for Gas Emission of Steelmaking Industry", *Energy Convers. Manage*., 48(4), 1313-1322 (2007).

Dyadin, Y.A., Udachin, K.A., "Clathrate Formation in Water Peralkylonium Salts Systems", *J. Incl. Phenom.*, 2, 61-72 (1984).

Englezos, P., "Clathrate Hydrates", *Ind. Eng. Chem. Res*., 32, 1251-1274 (1993).

Eslamimanesh A., Mohammadi A. H., Richon D., Naidoo P., Ramjugernath D., "Application of Gas Hydrate Formation in Separation Processes: A Review of Experimental Studies", *J. Chem. Thermodyn*., 46, 62-71 (2012).

European Commission, 6^{th} EU framework on CO_2 Capture and Storage Projects, Projects Synopses EUR 22574, European Communities, Belgium (2007).

Fan, S. S., Guo, T. M., "Hydrate Formation of CO_2-Rich Binary and Quaternary Gas Mixtures in Aqueous Sodium Chloride Solutions", *J. Chem. Eng. Data*, 44, 829-832 (1999).

Fan, S., Li, S., Wang, J., Lang, X., Wang, Y., "Efficient Capture of CO_2 from Simulated Flue Gas by Formation of TBAB or TBAF Semiclathrate Hydrates", *Energy Fuels*, 23, 4202-4208 (2009).

Faraday, M., *Phil. Trans. Roy. Soc. Lond*., 113, 160 (1823) [cited in Sloan & Koh].

Figueroa, J., Currier, R., Anderson, G., Tam, S., Deppe, G., Spencer, D., "Developments in the SIMTECHE Process CO_2 Capture by Formation of Hydrates", in Proc. Third Annual Conference on Carbon Capture and Sequestration, May 3-6, Washington DC, USA (2004).

Figueroa, J., Fout, T., Plasynski, S., Mcllvried, H., Srivastava, R., "Advances in CO_2 Capture Technology - The U.S. Department of Energy's Carbon Sequestration Program", *Int. J. Greenhouse Gas Control*, 2, 9-20 (2008).

Folger, P., "Carbon Capture: A Technology Assessment", Congressional Research Service (CRS) Report for Congress (2010).

Fonseca, J.M.S., Dohrn, R., Peper. S., "High-pressure fluid-phase equilibria: Experimental methods and systems investigated (2005–2008)", *Fluid Phase Equilib.*, 300 1-69 (2011).

Fontalba, F., Richon, D., Renon, H., "Simulaneous determination of PVT and VLE datof binary mixtures up to 45 MPa and 433 K: a new apparatus without phase sampling and analysis", *Rev. Sci. Instrum.*, 55(6), 944-952 (1984).

Fowler, D.L., Loebenstein, W.V., Pall, D.B., Kraus, C.A., "Some Unusual Hydrates of Quaternary Ammonium Salts", *J. Am. Chem. Soc*., 62 (5), 1140-1142 (1940).

Fukushima, S., Takao, S., Ogoshi, H., Ida, H., Matsumoto, S., Akiyama, T., Otsuka, T. NKK Technical Report (*in Japanese*), JFE steel corporation, 166, 65-70 (1999).

Gas Hydrate Dynamics Center. Gas Hydrates Equilibrium. Ecole Nationale Supérieure des Mines de Saint-Etienne (ENSMSE), France. Retrieved June 6, 2009 from http://www.emse.fr/spin/depscientifiques/GENERIC/hydrates/introduction/thermo.htm.

Galloway, T. J., Ruska, W., Chappelear, P. S., Kobayashi, R., "Experimental measurement of hydrate number for methane and ethane and comparison with theoretical values" *Ind. Eng. Chem. Fundam.*, 9, 237-243 (1970) [cited in Sloan and Koh, 2008].

Giavarini, C., Hester K., *Gas Hydrates: Immense Energy Potential and Environmental Challenges*, Springer-Verlag: London Limited (2011).

Gjertsen, L. H., Fadnes, F. H., "Measurements and Predictions of Hydrate Equilibrium Conditions, Gas Hydrates: Challenges for the future", *Ann. N.Y. Acad. Sci.*, 912, 722-734 (2006).

Goel, N., "In Situ Methane Hydrate Dissociation with Carbon Dioxide Sequestration: Current Knowledge and Issues", *J. Pet. Sci. Eng.*, 51, 169-184 (2006).

Granite, E. J., O'Brien, T., "Review of Novel Methods for Carbon Dioxide Separation from Flue and Fuel Gases", *Fuel Process. Technol.*, 86, 1423-1434 (2005).

Gudmundsson, J.S., Hveding, F., Børrehaug, A., "Transport of Natural Gas as Frozen Hydrate", in Proc. Fifth International Offshore and Polar Engineering Conf., The Hague, June 11-16, I, 282-288 (1995).

Guilbot, P., Valtz, A., Legendre, H., Richon, D., "Rapid on line sampler-injector: A reliable tool for HT-HP sampling and on line GC analysis", *Analusis* 28, 426-431, 2000.

Hachikubo, A., Miyamoto, A., Hyakutake, K., Abe, K., Shoji, H., "Phase Equilibrium Studies on Gas Hydrates Formed from Various Guest Molecules and Powder Ice", in Proc. Fourth International Conference on Gas Hydrates, Yokohama, Japan, May 19-23 (2002).

Hammerschmidt, E.G., *Ind. Eng. Chem.*, 26, 851 (1934) [cited in Sloan & Koh, 2008].

Hashimoto, S., Murayama, S., Sugahara, T., Sato, H., Ohgaki, K., "Thermodynamic and Raman Spectroscopic Studies on H_2 + Tetrahydrofuran + Water and H_2 + Tetra-n-butyl Ammonium Bromide + Water Mixtures Containing Gas Hydrates", *Chem. Eng. Sci.*, 61, 7884-7888 (2006).

Hashimoto, S., Sugahara, T., Moritoki, M., Sato, H., Ohgaki, K., "Thermodynamic Stability of Hydrogen + Tetra-n-butyl Ammonium Bromide Mixed Gas Hydrate in Nonstoichiometric Aqueous Solutions", *Chem. Eng. Sci.*, 63, 1092-1097 (2008).

Herri, J. M., Bouchemoua, A., Kwaterski, M., Fezoua, A., Ouabbas, Y., Cameirao. A., "Gas Hydrate Equilibria for CO_2-N_2 and CO_2-CH_4 Gas Mixtures - Experimental Studies and Thermodynamic Modelling", *Fluid Phase Equilib.*, 301, 171-190 (2011).

Herzog, H., *Carbon Dioxide Capture and Storage, Chapter 13 in The Economics and Politics of Climate Change*, Dieter Helm and Cameron Hepburn, Oxford University Press (2009).

HWHYD, Phase-equilibrium Calculation program Developed at the Centre for Gas Hydrate Research, Heriot-Watt University, U.K., (2000).

IEA Greenhouse Gas R&D Programme, *Putting Carbon Back into the Ground*, Cheltenham, UK (2001).

International Energy Agency (IEA). *Energy technology perspectives 2008. Scenarios and Strategies to 2050*. Organisation for Economic Co-operation and Development (OECD)/IEA: Paris, France (2008).

International Panel on Climate Control (IPCC), 2005. "Carbon Dioxide Capture and Storage", Special Report. New York, Cambridge University Press, available at http://www.ipcc.ch/ipccreports/srccs.htm.

International Panel on Climate Control (IPCC), *Climate Change 2007: Synthesis Report* (2007).

James, A.T, Martin, A. J. P., "Gas Liquid Partition Chromatography. The Separation and Microestimation of Volatile Fatty Acids from Formic Acid to Dodecanoic Acid", *Biochem. J.*, 50, 679-690 (1952).

Jeffrey, G.A., "Hydrate Inclusion Compounds", *J. Inclusion Phenom*., 1(3), 211-222 (1984).

Jeffrey, G. A., McMullan, R. K., *Progress in Inorganic Chemistry*, John Wiley: New York, Vol. 8, pp 43-108 (1967) [cited in Arjmandi *et al*., 2007].

Kamata, Y., Oyama, H., Shimada, W., Ebinuma, T., Takeya. S., "Gas Separation Method Using Tetra-n-butyl Ammonium Bromide Semi-Clathrate Hydrate", *Jpn. J. Appl. Phys.*, 43, 362-365 (2004).

Kang, S.P., Lee, H., "Recovery of CO_2 from Flue Gas Using Gas Hydrate: Thermodynamic Verification through Phase Equilibrium Measurements", *Environ. Sci. Technol*., 34, 4397-4400 (2000).

Kang, S.P., Lee, H., Lee, C.S., Sung, W.M., "Hydrate Phase Equilibria of the Guest Mixtures Containing CO_2, N_2 and Tetrahydrofuran", *Fluid Phase Equilib.*, 185, 101-109 (2001).

Khalil, W., "Développement d'un appareil automatisé de mesure simultanée d'équilibres de phases et de propriétés volumétriques. Exploitation des données volumétriques pour le calcul prédictif de grandeurs thermodynamiques dérivées", PhD Dissertation, Ecole Nationale Supérieure des Mines de Paris, France (2006).

Kim, D.Y., Lee, H., "Spectroscopic Identification of the Mixed Hydrogen and Carbon Dioxide Clathrate Hydrate", *J. Am. Chem. Soc*.,127, 9996-9997, (2005).

Klara, S. M., Srivastava, R. D., "US DOE Integrated Collaborative Technology Development Program for CO_2 Separation and Capture." *EnViron. Prog*., 21, 247-253 (2002).

Koh, C.A., “Towards a Fundamental Understanding of Natural Gas Hydrate”, *Chem. Soc. Rev*. 31, 157-167 (2002).

Koh, C.A., Sloan, E. D., Sum, A. K., Wu, D. T., “Fundamentals and Applications of Gas Hydrates”, Annual Review of Chemical and Biomolecular Engineering, 2, 237 -257 (2011).

Kumar, R., Wu, H., Englezos, P., “Incipient Hydrate Phase Equilibrium for Gas Mixtures Containing Hydrogen, Carbon Dioxide and Propane”, *Fluid Phase Equilib*. 244, 167-171 (2006).

Kumar, R., Englezos, P., Moudrakovski, I., Ripmeester, J. A., “Structure and Composition of CO_2/H_2 and $CO_2/H_2/C_3H_8$ Hydrate in Relation to Simultaneous CO_2 Capture and H_2 Production”, *AIChE J*., 55, 1584-1594 (2009).

Larson, S.D., “Phase Studies of the Two-Component Carbon Dioxide-Water System, Involving the Carbon Dioxide Hydrate”, University of Illinois, Urbana, IL (1955) [cited in Sloan & Koh, 2008].

Laugier, S., Richon, D., “New apparatus to perform fast determinations of mixture vapor-liquid equilibria up to 10 MPa and 423 K”, *Rev. Sci. Instrum*., 57(3), 469-472 (1986).

Lee, B. R., Sa, J. H., Park, D. H., Cho, S., Lee, J., Kim, H. J., Oh, E., Jeon, S., Lee, J. D., Lee K. H., “Continuous Method for the Fast Screening of Thermodynamic Promoters of Gas Hydrates Using a Quartz Crystal Microbalance”, *Energy Fuels* 26, 767-772 (2012).

Lee, H., Lee, J., Kim, D. Y., Park, J., Seo, Y. T., Zeng, H., Moudrakovski, I. L., Ratcliffe, C. I., Ripmeester, J. A., “Tuning Clathrate Hydrates for Hydrogen Storage”, *Nature* 434, 743-746 (2005).

Lee, H. J., Lee, J. D., Linga, P., Englezos, P., Kim, Y. S., Lee, M. S., Kim, Y. D., “Gas Hydrate Formation Process for Pre-Combustion Capture of Carbon Dioxide”, *Energy*, 35, 2729-2733. (2010).

Le Parlouër, P., Dalmazzone, C., Herzhaft, B., Rousseau L., Mathonat, C., “Characterisation of Gas Hydrates Formation Using a New High Pressure Micro-DSC”, *J. Therm. Anal. Cal*., 78, 165-172 (2004).

Li, D. L., Du, J. W., Fan, S. S., Liang, D. Q., Li, X. S., Huang, N. S., “Clathrate Dissociation Conditions for Methane + Tetra-n-butyl Ammonium Bromide (TBAB) + Water”, *J. Chem. Eng. Data*, 52, 1916-1918 (2007).

Li, S., Fan, S., Wang, J., Lang, X., Wang, Y., “Semiclathrate Hydrate Phase Equilibria for CO_2 in the Presence of Tetra-n-butyl Ammonium Halide (Bromide, Chloride, or Fluoride)”, *J. Chem. Eng. Data*, 55 (9), 3212-3215 (2010).

Li, X. S., Xia, Z. M., Chen, Z. Y., Yan, K. F., Li, G., Wu, H. J., “Equilibrium Hydrate Formation Conditions for the Mixtures of CO_2 + H_2 + Tetrabutyl Ammonium Bromide”, *J. Chem. Eng. Data*, 55, 2180-2184 (2010).

Lide, D. R., *CRC Handbook of Physics and Chemistry, Section 6: Fluid Properties*, CRC Press, 85th edition (2004).

Lin, W., Delahaye, A., Fournaison, L., "Phase Equilibrium and Dissociation Enthalpy for Semi-Clathrate Hydrate of CO_2 + TBAB". *Fluid Phase Equilib.* 264, 220-227 (2008).

Linga, P., Kumar, R., Englezos, P., "Gas Hydrate Formation from Hydrogen/Carbon Dioxide and Nitrogen/Carbon dioxide Gas Mixtures", *Chem. Eng. Sci*., 62, 4268-4276 (2007*a*).

Linga, P., Kumar, R., Englezos. P., "The Clathrate Hydrate Process for Post and Pre-combustion Capture of Carbon Dioxide", *J. Hazard. Mater*. 149, 625-629 (2007*b*).

Lipowski, J., Komarov, V. Y., Rodionova, T. V., Dyadin Y. A., Aladko, L. S., "The Structure of Tetrabutylammonium Bromide Hydrate $(C_4H_9)_4NBr.2^{1/3}H_2O$", *J Supramol. Chem.*, 2, 435-439 (2002).

Lu, T., Zhang, Y., Li, X. S., Chen, Z. Y., Yan, K. F., "Equilibrium Conditions of Hydrate Formation in the Systems of CO_2-N_2-TBAB and CO_2-N_2-THF" (in Chinese), *The Chinese Journal of Process Engineering*, 9, 541-544 (2009).

Makogon, Y.F., *Gazov. Promst*., 5, 14 (1965) [cited in Sloan & Koh, 2008].

Makogon, Y.F., *Hydrates of Natural Gas*, PennWell Publishing Corp., Tulsa, OK (1997).

Makogon, Y.F, "Natural Gas Hydrates - A promising Source of Energy", *Journal of Natural Gas Science and Engineering*, 2 (1), 49-59 (2010).

Mandal, A., Laik, S., "Effect of the Promoter on Gas Hydrate Formation and Dissociation", *Energy Fuels*, 22, 2527-2532 (2008).

Mao, W.L., Mao, H.K. "Hydrogen Storage in Molecular Compounds", *Nat. Aca. Sci. USA*, 101(3), 708-710 (2004).

Marshall, D. R., Saito, S., Kobayashi, R., "Hydrates at high pressures: Part I. Methane-water, argon-water, and nitrogen-water systems", *AIChE J.*, 10 (2), 202-205 (1964).

McMullan, R.K., Jeffrey, G.A., "Hydrates of the Tetra n-butyl and Tetra i-amyl Quaternary Ammonium Salts", *J. Chem. Phys*., 31, 1231-1234 (1959).

Meysel, P., Oellrich, L., Bishnoi, P. R., Clarke, M. A., "Experimental Investigation of Incipient Equilibrium Conditions for the Formation of Semi-clathrate Hydrates from Quaternary Mixtures of (CO_2+N_2+TBAB+H_2O)", *J. Chem. Thermodynamics.*, 43, 1475-1479 (2011).

Mohammadi, A.H., Tohidi, B., Burgass, R.W., Equilibrium data and thermodynamic modeling of nitrogen, oxygen, and air clathrate hydrates, *J. Chem. Eng. Data*, 48, 612 (2003) [cited in Sloan & Koh, 2008].

Mohammadi, A.H., Chapoy, A., Richon, D., Tohidi, B., "Experimental measurement and thermodynamic modeling of water content in methane and ethane systems", *Ind. Eng. Chem. Res.*, 43, 7148-7162 (2004).

Mohammadi, A.H., Afzal, W., Richon, D., "Experimental data and predictions of dissociation conditions for ethane and propane simple hydrates in the presence of distilled water and methane, ethane, propane, and carbon dioxide simple hydrates in the presence of ethanol aqueous solutions", *J. Chem. Eng. Data*, 53, 683-686 (2008).

Mohammadi, A. H., Richon, D., "Equilibrium Data of Nitrous Oxide and Carbon Dioxide Clathrate Hydrates", *J. Chem. Eng. Data*, 54 (2), 279–281 (2009*a*).

Mohammadi, A. H., Richon, D., "Development of predictive techniques for estimating liquid water-hydrate equilibrium of water-hydrocarbon system", *J. Thermodynamics*. 1-12 (2009*b*).

Mohammadi, A. H., Belandria, V., Richon, D., "Can toluene or xylene form clathrate hydrates ?" *Ind. Eng. Chem. Res*., 48, 5916-5918 (2009).

Mohammadi, A. H., Richon, D., "Phase Equilibria of Semi-clathrate Hydrates of Tetra-n-butylammonium Bromide + Hydrogen Sulfide and Tetra-n-butylammonium Bromide + Methane", *J. Chem. Eng. Data*, 55, 982-984. (2010).

Mohammadi, A. H., Belandria, V., Richon. D., "Use of an Artificial Neural Network Algorithm for Predictions of Hydrate Dissociation Conditions for Hydrogen + Water and Hydrogen + Tetra-n-Butyl Ammonium Bromide + Water Systems", *Chem. Eng. Sci*., 65, 4302-4305 (2010).

Mohammadi, A. H., Eslamimanesh, A., Belandria, V., Richon, D., "Phase Equilibria of Semiclathrate Hydrates of CO_2, N_2, CH_4, or H_2 + Tetra-n-butylammonium Bromide Aqueous Solution", *J. Chem. Eng. Data*, 56, 3855-3865, (2011*a*).

Mohammadi, A. H., Eslamimanesh, A., Belandria, V., Richon, D., Naidoo, P., Ramjugernath, D., "Phase Equilibrium Measurements for Semi-clathrate Hydrates of the (CO_2 + N_2 + tetra-n-butylammonium bromide) Aqueous Solution System", *J. Chem. Thermodyn.*, doi:10.1016/j.jct.2011.10.004 (2011*b*).

Mohammadi, A. H., Eslamimanesh, A., Belandria, V., Richon, D., Naidoo, P., Ramjugernath, D., "Phase Equilibrium Measurements for Semi-clathrate Hydrates of the (CO_2 + N_2 + tetra-n-butylammonium bromide) Aqueous Solution System", *J. Chem. Thermodyn*., 46, 57-61 (2012).

Mokraoui, S., Valtz, A., Coquelet, C., Richon, D., "Volumetric Properties of the Isopropanolamine-Water Mixture at Atmospheric Pressure from 283.15 to 353.15 K", Thermochimica Acta, 440, 122-128 (2006).

National Mining Association (NMA), *CCS: Carbon Capture and Storage, Project Status*. Retrieved on March 12, 2012 from http://www.nma.org/ccs/ccsprojects.asp

National Oceanic and Atmospheric Administration (NOAA). Trends in Carbon Dioxide from Mauna Loa CO_2 annual mean data. Retrieved on March 15, 2012 from ftp://ftp.cmdl.noaa.gov/ccg/co2/trends/co2_mm_mlo.txt

Ng, H.J., Robinson, D.B, "Equilibrium Phase Composition and Hydrating Conditions in Systems Containing Methanol, Light Hydrocarbons, Carbon Dioxide, and Hydrogen Sulfide". Gas Processors Association Research Report 66, April 1983 [cited in Sloan & Koh, 2008].

NIST ChemistryWebBook, NIST Standard Reference Database Number 69, 2001, National Institute of Standards and Technology, Gaithersburg MD, 20899. Retrieved on March 9, 2012 from http://webbook.nist.gov/chemistry.

Obara, S., Yamada, T., Matsumura, K., Takahashi, S., Kawai, M., Rengarajan, B., "Operational Planning of an Engine Generator Using a High Pressure Working Fluid Composed of CO_2 Hydrate", *Applied Energy*, 88 (12), 4733-4741 (2011).

Obata, Y., Masuda, N., Joo, K., Katoh, A., *Advanced Technologies Towards the New Era of Energy Industries*, NKK Technical Review, 88, 103-115 (2003).

Oellrich, L.R., "Natural Gas Hydrates and their Potential for Future Energy Supply", in Proc. 17th National and 6th ISHMT/ASME Heat and Mass Transfer Conference (HMT), IGCAR, Kalpakkam, Jan. 5-7 (2004).

Ohgaki, K., Takano, K., Moritoki, M., "Exploitation of CH_4 Hydrates under the Nankai Trough in Combination with CO_2 Storage", Kagaku Kōgaku Kyōkai, 20(1), 121-123 (1994).

Ohgaki, K., Sangawa, H., Matsubara, T., Nakano, S., "Methane Exploitation by Carbon Dioxide from Gas Hydrates-Phase Equilibria for CO_2-CH_4 Mixed Hydrate System", *J. Chem. Eng. Jpn.*, 29, 478-483 (1996).

Ohmura, R., Takeya, S., Uchida, T., Ebinuma, T., "Clathrate Hydrate Formed with Methane and 2-Propanol:. Confirmation of Structure II Hydrate Formation", *Ind. Eng. Chem. Res.* 43, 4964-4966 (2004).

Olivier, J. G. J., Janssens-Maenhout, G., Peters, J. A. H. W., Wilson, J., "Long-term Trend in Global CO_2 Emissions", prepared by the European Commission's Joint Research Centre and PBL Netherlands Environmental Assessment Agency, (2011).

Organisation for Economic Co-operation and Development (OECD) / International Energy Agency (IEA). *Energy technology perspectives 2008. Scenarios and Strategies to 2050*, OECD / IEA: Paris, France (2008).

Oyama, H., Shimada, W., Ebinuma, T., Kamata, Y., Takeya, S., Uchida, T., Nagao, J., Narita, H., « Phase diagram, latent heat, and specific heat of TBAB semiclathrate hydrate crystals", *Fluid Phase Equilib.*, 234, 131-135 (2005).

Oyama, H., Ebinuma, T., Nagao, J., Narita, H., Shimada, W., "Phase Behavior of TBAB Semiclathrate Hydrate Crystal under Several Vapor Components", in Proc. 6th International Conference on Gas Hydrates (ICGH), Vancouver, British Columbia, Canada, July 6-10 (2008).

Paricaud, P., “Modeling the Dissociation Conditions of Salt Hydrates and Gas Semiclathrate Hydrates: Application to Lithium Bromide, Hydrogen Iodide, and Tetra-n-butylammonium Bromide + Carbon Dioxide Systems”, *J. Phys. Chem. B*, 115, 288-299 (2011).

Parrish, W.R., Prausnitz, J.M., “Dissociation Pressures of Gas Hydrates Formed by Gas Mixtures”, *Ind. Eng. Chem. Proc. Des. Dev*., 11, 26-34 (1972).

Peng, D. Y., Robinson, D. B., “A new two-constant equation of state”, *Ind. Eng. Chem. Fundam*. 15, 59-64 (1976).

Pennline, H. W., Leubke, D. R., Jones, K. L., Myers, C. R., Morsi, B. I., Heintz, Y. J., Ilconich, J. B., "Progress in Carbon Dioxide Capture and Separation Research for Gasification-Based Power Generation Point Sources", *Fuel Process. Technol*., 89 (9), 897-907 (2008).

Perkins, D., Brady, J., *Teaching Phase Equilibria* (2007). Retrieved on June 6, 2009 from http://serc.carleton.edu/research_education/equilibria/other_diagrams.html

Peters, G. P., Marland, G., Le Quéré, C., Boden, T., Canadell, J. G., Raupach, M. R., “Rapid Growth in CO_2 Emissions After the 2008–2009 Global Financial Crisis”, *Nature Clim. Change*, 2, 2-4 (2012).

Price, K., Storn, R., “Differential Evolution”, *Dr. Dobb’s J.* 22, 18-24 (1997).

Priestley, J., *Experiments and Observations on Different Kinds of Air and Other Branches of Natural Philosophy Connected with the Subject* (in Three Volumes), T. Pearson, Birmingham, 359 (1790) [cited in Sloan & Koh, 2008].

Raal, J. D., Mühlbauer, A. L. *Phase Equilibria: Measurement and Computation*, Taylor & Francis: Bristol, PA (1998).

Richon, D., “New experimental developments for phase equilibrium measurements,” *Fluid Phase Equilib*., 116, 421-428 (1996).

Richon, D., “Experimental techniques for the determination of thermophysical properties to enhance chemical processes”, *Pure Appl. Chem*., 81 (10), 1769-1782 (2009).

Richon D., de Loos, T.W., “Vapour-liquid equilibrium at high pressure,” Measurement of the Thermodynamic Properties of Multiple Phases (Experimental Thermodynamics, Vol VII), R.D. Weir and T.W. de Loos, eds., Elsevier, pp. 90-136 (2005).

Rivollet, F., “Etude des propriétés volumétriques (PVT) d’hydrocarbures légers (C1- C4), du dioxyde de carbone et d’hydrogène sulfure”, PhD Dissertation, Ecole Nationale Supérieure des Mines de Paris, France (2005).

Ripmeester, J.A., Tse, J.S., Ratcliffe, C.I., Powell, B.M., “A New Clathrate Hydrate Structure”, *Natur*e, 325, 135-136 (1987).

Robinson, D. B., Mehta, B. R., “Hydrates in the Propane-Carbon Dioxide-Water System”, *J. Can. Pet. Technol*., 48, 33-35 (1971).

ROLSI™. Rapid Online Micro Sampler Injector, http://www.rolsi.com/English.htm.

Rovetto, L.R., Strobel, T.A., Koh, C.A., Sloan, E.D., Is gas hydrate formation thermodynamically promoted by hydrotrope molecules?, *Fluid Phase Equilib*., 247, 84-89 (2006).

Rubin, E. S., Rao, A. B., "A Technical, Economic and Environmental Assessment of Amine-based CO_2 Capture Technology for Power Plant Greenhouse Gas Control", Carnegie Mellon University, Center for Energy and Environmental Studies Pittsburgh, PA (2002).

Ruffine, L., Donval J. P., Charlou J. L., Cremiere A., Zehnder B. H., "Experimental study of gas hydrate formation and destabilisation using a novel high-pressure apparatus", *Mar. Pet. Geol*., 27(6), 1157-1165 (2010).

Sabil K. M., "Phase Behaviour, Thermodynamics and Kinetics of Clathrate Hydrate Systems of Carbon Dioxide in Presence of Tetrahydrofuran and Electrolytes", Ph.D. Thesis, Delft Uni. of Technology, Delft, The Netherlands, 2010.

Schroeter, J. P., Kobayashi, R., Hildebrand, M. A., "Hydrate decomposition conditions in the system hydrogen sulfide-methane-propane", *Ind. Eng. Chem., Fundam*., 22 (4), 361-364 (1983).

SECOHYA, "Separation of CO_2 by Gas Hydrate Crystallization", Project Proposal (2007).

Seo, Y.T., Kang, S.P., Lee, H., Lee, C.S., Sung, W.M., "Hydrate Phase Equilibria for Gas Mixtures Containing Carbon Dioxide: A Proof-of-Concept to Carbon Dioxide Recovery from Multicomponent Gas Stream", *Korean J. Chem. Eng*., 17, 659-667 (2000).

Seo, Y. T., Lee, H., "A New Hydrate-Based Recovery Process for Removing Chlorinated Hydrocarbons from Aqueous Solutions", *Environ. Sci. Technol*., 35, 3386–3390 (2001).

Seo, Y.T., Kang, S.P., Lee, H., "Experimental Determination and Thermodynamic Modeling of Methane and Nitrogen Hydrates in the Presence of THF, Propylene oxide, 1,4- dioxane and Acetone", *Fluid Phase Equilib.*, 189, 99-110 (2001).

Seo, Y. T., Lee, H., "Structure and Guest Distribution of the Mixed Carbon Dioxide and Nitrogen Hydrates as Revealed by X-ray Diffraction and C NMR spectroscopy", *J. Phys. Chem. B*, 108, 530-534 (2004).

Seo, Y., Kang, S. P., "Enhancing CO_2 Separation for Pre-combustion Capture with Hydrate Formation in Silica Gel Pore Structure", *Chem. Eng. J.*, 161, 308-312 (2010).

Shimada, W., Ebinuma, T., Oyama, H., Kamata, Y., Takeya, A., Uchida, T., Nagao, J., Narita, H., "Separation of Gas Molecule Using Tetra-n-butyl Ammonium Bromide Semi-Clathrate Hydrate Crystals", *Jpn. J. Appl. Phys*., 42, L129-L131 (2003).

Shimada, W., Ebinuma, T., Oyama, H., Kamata, Y., Narita. H., "Tetra-n-butylammonium bromide-water (1/38)", *J. Cryst. Growth*, 274, 246-250 (2005).

Sloan E. D., *Clathrate Hydrates of Natural Gases*. Second edition, Marcel Dekker Inc.: New York (1998).

Sloan, E. D., “Fundamental Principles and Applications of Natural Gas Hydrates”, *Nature*, 426, 353-363 (2003).

Sloan, E.D., Koh, C.A., *Clathrate Hydrates of Natural Gases*, third ed., Taylor & Francis Group: Boca Raton (2008).

Smith, J.M., Van Ness, H.C., Abbott. M.M., *Introduction to Chemical Engineering Thermodynamics*, McGraw-Hill: New York (2001).

Soo, C. B., “Experimental Thermodynamic Measurements of Biofuel-related Associating Compounds and Modeling using the PC-SAFT Equation of State”, PhD Dissertation, Ecole Nationale Supérieure des Mines de Paris, France (2011).

Spencer, D.F., *Methods of selectively separating CO_2 from a multicomponent gaseous stream*, US Patent 5700311 (1997).

Strobel, T. A., Taylor, C. J., Hester, K. C., Dec, S. F., Koh, C. A., Miller, K. T., Sloan, E. D., “Molecular Hydrogen Storage in Binary THF−H_2 Clathrate Hydrates”, *J. Phys. Chem. B.*, 110 (34), 17121-17125 (2006).

Sugahara, T., Murayama, S., Hashimoto, S., Ohgaki, K., “Phase Equilibria for H_2 + CO_2 + H_2O System Containing Gas Hydrates”, *Fluid Phase Equilib*. 233, 190-193 (2005).

Sugahara, T., Mori, H., Sakamoto, J., Hashimoto, S., Ogata, K., Ohgaki, K., “Cage Occupancy of Hydrogen in Carbon Dioxide, Ethane, Cyclopropane, and Propane Hydrates”. *Open Thermodyn. J.* 2, 1-6, (2008).

Suginaka, T., Sakamoto, H., Iinoa, K., Takeya, S., Nakajima, M., Ohmura, R., “Thermodynamic Properties of Ionic Semiclathrate Hydrate Formed with Tetrabutylphosphonium Bromide”, *Fluid Phase Equilib.*, 317, 25-28 (2012).

Sun, Z. G., Sun, L., “Equilibrium Conditions of Semi-clathrate Hydrate Dissociation for Methane + Tetra-n-butyl ammonium Bromide”, *J. Chem. Eng. Data*, 55, 3538-3541 (2010).

Sum, A.K., Burruss, R.C., Sloan. E.D., “Measurement of clathrate hydrates via Raman spectroscopy”, *J. Phys. Chem. B*, 101 (38), 7371-7377 (1997).

Surovtseva, D., Amin, R., Barifcani, A., “Design and Operation of Pilot Plant for CO_2 Capture from IGCC Flue Gases by Combined Cryogenic and Hydrate Method”, *Chem. Eng. Res. Des.*, 89, 1752-1757 (2011).

Söhnel, O., Novotny, P., *Densities of Aqueous Solutions of Inorganic Substances*, Elsevier Science Pub. Co, Amsterdam (1985).

Tajima, H., Yamasaki, A., Kiyono, F., “Energy Consumption Estimation for Greenhouse Gas Separation Processes by Clathrate Hydrate Formation”, *Energy*, 29, 1713-1729 (2004).

Takeya, S., Uchida, T., Kamata, Y., Nagao, J., Kida, M., Minami, H., Sakagami, H., Hachikubo, A., Takahashi, N., Shoji, H., Khlystov, O., Grachev, M., Soloviev, V., “Lattice expansion of

clathrate hydrates of methane mixtures and natural gas", *Angewandte Chemie International Edition*, 44, 6928-6931 (2005).

Tam, S. S., Santon, M. E., Ghose, S., Deppe G., Spencer, D. F., Currier, R. P., Young, J. S., Anderson, G. K., Le, L. A., Devlin, D. J., "A High Pressure Carbon Dioxide Separation Process for IGCC Plants", in Proc. First National Conference on Carbon Sequestration, Washington DC, May 14-17 (2001).

Tanasawa, I., Takao, S., "Low-temperature Storage Using Clathrate Hydrate Slurries of Tetra-n butylammonium Bromide: Thermophysical Properties and Morphology of Clathrate Hydrate Crystals", in Proc. Fourth International Conference on Gas Hydrates, Yokohama, Japan, May 19-23 (2002).

Thakore, J. L., Holder, G. D., "Solid-Vapor Azeotropes in Hydrate-Forming Systems", *Ind. Eng. Chem. Res*., 26, 462-469 (1987).

Thiam, A., *Etude des Conditions Thermodynamiques et Cinétiques du Procédé de Captage de CO_2 par Formation d'hydrates de Gaz : Application au Mélange CO_2-CH_4*, Dissertation, Ecole Nationale Supérieure des Mines de Saint Etienne, France (2008).

Tohidi, B., Burgass, R. W., Danesh, A., Todd, A.C., "Hydrate Inhibition Effect of Produced Water, Part-1. Ethane and Propane Simple Gas Hydrates" in Proc. of the SPE Offshore Europe 93 Conference, SPE 26701, 255-265 (1993).

Tohidi, B., Burgass, R.W., Danesh, A., Østergaard, K.K., Todd, A.C., Improving the Accuracy of Gas Hydrate Dissociation Point Measurements, in *Proc. Gas Hydrates: Challenges for the Future*, (Holder, G.D., Bishnoi, P.R., eds), *Ann. N.Y. Acad. Sci*., 912, 924-931 (2000).

TOTAL S.A. (2007), Lacq Project Information Dossier. Retrieved on March 9, 2012 from http://www.total.com/en/special-reports/capture-and-geological-storage-of-co2-200959.html

Tranchant, J., *Manuel pratique de chromatographie en phase gazeuse*, Masson, fourth ed. : Paris (1995).

Tzimas, E., Peteves, S., *Controlling Carbon Emissions: The Option of Carbon Sequestration*, European Communities: Luxembourg (2003).

Uchida, T., Ikeda, I.Y., Takeya, S., Kamata, Y., Ohmura, R., Nagao, J., Zatsepina, O.Y., Buffett, B.A., "Kinetics and Stability of CH_4–CO_2 Mixed Gas Hydrates during Formation and Long-Term Storage", *Phys. Chem.*, 6, 646-654 (2005).

Udachin, K.A., Ratcliffe, C.I., Ripmeester, J.A., "Structure, Composition, and Thermal Expansion of CO_2 Hydrate from Single Crystal X-ray Diffraction Measurements", *J. Phys. Chem. B*, 105, 4200-4204 (2001).

Unruh, C.H., Katz, D.L., "Gas Hydrates of CO_2-CH_4 Mixtures", *Trans AIME*, 186, 83-86 (1949).

Valderrama, J. O., “A generalized Patel-Teja Equation of State for Polar and Non-Polar Fluids and Their Mixtures”, *J. Chem. Eng. Jpn*., 23, 87-91 (1990).

Valtz, A., Teodorescu, M., Wichterle, I., Richon, D., “Liquid Densities and Excess Molar Volumes for Water + Diethylene Glycolamine, and Water, Methanol, Ethanol, 1-Propanol + Triethylene Glycol Binary Systems at Atmospheric Pressure and Temperatures in the Range of 283.15-363.15 K”, *Fluid Phase Equilib*. 215, 129-142 (2004).

van der Waals, J.H., Platteeuw, J.C., “Clathrate Solutions”, *Adv. Chem. Phys*., 2, 1-57 (1959).

Villard, M., P., “On the Carbonic Hydrate and the Composition of Gas Hydrates”, *Acad. Sci. Paris, Comptes Rendus*, 119, 368-371 (1894) [cited in Sloan & Koh, 2008].

Villard, M., P., “Experimental Study of Gas Hydrates”, *Ann. Chim. Phys*. 7 (11), 353-360 (1897) [cited in Sloan & Koh, 2008].

von Stackelberg, M., Müller, H. R., “Feste Gashydrate II. Structur und Raumchemie”, *Z. Electrochem*., 58, 25-39 (1954) [cited in Sloan & Koh, 2008].

Wagner, W., Cooper, J. R., Dittmann, A., Kijima, J., Kretzschmar, H.J., Kruse, A., Mareš, R., Oguchi, K., Sato, H., Stöcker, I., Šifner, O., Takaishi, Y., Tanisjita, I., Trübenbach J., Willkommen, T., “Release on the IAPWS Industrial Formulation for the Thermodynamic Properties of Water and Steam”, *J. Eng. Gas Turbines & Power*, 122 (1), 150-184 (2000).

Weir, R.D., de Loos, T.W., eds., *Measurement of the Thermodynamic Properties of Multiple Phases (Experimental Thermodynamics, Vol VII)*, IUPAC Commission on Thermodynamics, Elsevier Science: Amsterdam (2005).

World Energy Council, *World Energy Issues Monitor*, London, UK (2012).

Wróblewski, S.V., “On the Combination of Carbonic Acid and Water”, *Acad. Sci. Paris Compt. Rend*., 94, 212-213 (1882) [cited in Sloan & Koh, 2008].

Yang, S.O., Yang, I.M., Kim, YS, Lee, C.S., “Measurement and Prediction of Phase Equilibria for Water + CO_2 in Hydrate Forming Conditions”, *Fluid Phase Equilib.*, 175 (1-2), 75-89 (2000).

Yang, H., Xu, Z., Fan, M., Gupta, R., Slimane, R. B., Bland, A. E., Wright. I., “Progress in Carbon Dioxide Separation and Capture: A Review”, *J. Environ Sci. (China)*. 20 (1), 14-27 (2008).

Zachary, J., Titus. S., “CO_2 Capture and Sequestration Options: Impact on Turbomachinery Design”. Bechtel Corporation (2008).

Acknowledgements

This thesis has been carried out in the Laboratory of Thermodynamics and Phase Equilibria (TEP) of MINES ParisTech from 2008 to 2012. Thus, it is a pleasure to acknowledge all those who have contributed to its successful achievement. Firstly, I would like to sincerely thank Professor Dominique Richon, for giving me the opportunity to join his prestigious research group at École des Mines de Paris. I am indebted to him for his trust, his continuous support and encouragement. His passion for experimental thermodynamics and enthusiasm are exceptionally motivating.

I gratefully acknowledge Dr. Amir Mohammadi for introducing me to such fascinating subject to study and for closely supervising and guiding me. His constructive advice was helpful to perform a high-quality research. I appreciate his precious time for revising all my written communications and his well-intended pressure that turned out in an important number of scientific contributions. I also thank him for involving himself in the project to allow me finishing my thesis manuscript.

I am greatly obliged to the members of the examining and reading committee for kindly accepting to judge my work and for meaningful discussions.

Success in experiments would have not been possible without the support of the exceptionally experienced technical staff from CEP-TEP laboratory. Pascal Théveneau, Hervé Legendre and David Marques deserve special credit for the construction of the new apparatus and for their continuous technical support. I would also like to thank Alain Valtz for his useful advice and the great deal of technical assistance provided, and above all for making such a pleasant working environment in the lab.

My warmest gratitude goes to the whole staff of the CEP-TEP laboratory for their support, collaboration, and assistance throughout all the years I have been working in the laboratory. Many thanks go in particular to the management and administration staff: Didier Mayer, Christophe Coquelet, Marie-Claude Watroba, Jocellyne Keller and Dominique Blondeau. Further, Jeffy deserves my warm thanks for always helping me out in the lab in the early stages of my thesis and for enjoyable times. Ali Eslamimanesh and Albert Chareton are deeply thanked for continuing the experiments while I was on maternity leave. To the trainees who I had the pleasure to work with: Kévin Reigner, Tarik Jaakou, Nico Janssen and Maria Fernanda Sanchez, I appreciate all your enthusiasm and commitment.

I would also like to extend this acknowledgement to all people and institutions that contributed through a collaborative effort to the outcome of SECOHYA project and this thesis. My gratitude goes to Jean-Michel Herri (MINES Saint-Étienne), Bertrand Chazallon (Université de Lille), Didier Dalmazzone (ENSTA ParisTech), Daniel Broseta (Université UPPA), Chakib Bouallou (MINES ParisTech), Rafael Lugo (IFP Energies Nouvelles), Luis A. Galicia-Luna (Instituto Politecnico Nacional), Deresh Ramjugernath (University of KwaZulu-Natal), José F. Martínez (Universidad de Zaragosa) and their research groups.

I specially would like to acknowledge Professor Cor Peters for giving me the opportunity to join the Process and Energy Laboratories of TU Delft in The Netherlands for a period of study. The knowledge that I gained during my research stay at TU Delft was of great benefit for the completion of this thesis. I thank Maaike Kroon, Geert-Jan Witkamp and his group for stimulating discussions and for their kind hospitality. Special thanks to Michel van der Brink for his technical assistance and to Somayeh Kazemi for fruitful collaboration.

All these would have not been possible without funding from the Agence Nationale de la Recherche (ANR) as part of the SECOHYA project, the Orientation Strategique des Ecoles des Mines (OSEM) and the Fondation FI3M.

De mi pais: Venezuela, agradezco a la Fundacion Gran Mariscal de Ayacucho por el financiamiento otorgado. A PDVSA Intevep por el espacio y tiempo concedido para llevar a cabo este proyecto y concluirlo y en especial al Ing. Hector Perozo por sus oportunos consejos y apoyo para emprender esta tesis doctoral.

Finalmente, un profundo y sincero agradecimiento va para toda mi familia, en especial a mis amados padres y hermanos, y a la familia Marfisi-Gonzalez, por todo el animo, apoyo y oraciones a Dios Todopoderoso. Y, por supuesto, a mi esposo y a mis hijas mi gratitud por su infinito amor, su tolerancia, y sobre todo por haber vivido conmigo esta experiencia que pasó de ser una meta profesional a un emprendimiento mas de nuestra familia.

Paris, June 2012.

Veronica BELANDRIA

Curriculum Vitae

Veronica Belandria

Education

2008 - 2012	Ph.D in process engineering (with European label). Thermodynamics and Phase Equilibria Laboratory (CEP-TEP). Mines ParisTech, Fontainebleau. France.
1995 - 2001	B.Sc in chemical engineering. Universidad de Los Andes. Merida. Venezuela
1994 - 1995	Foreign exchange student program. Concord High School, Elkhart, IN. USA.
1989 - 1994	High school education. Colegio La Salle, Merida. Venezuela.

Employment

2003 - 2008	Research engineer in oil & gas exploration and production. PDVSA Intevep. Los Teques, Venezuela.
2002 - 2003	Junior field engineer in well completion and productivity operations Schlumberger Oilfield Services, Venezuela, Trinidad and Tobago.
2001 - 2002	English language instructor. VEN-USA Institute of International Studies and Modern languages. Merida, Venezuela.
2000 - 2002	Assistant researcher. Laboratory of Formulation, Interfaces, Rheology and Processes (FIRP). Universidad de Los Andes. Merida, Venezuela.
1996 - 1999	English language instructor. Anglo-American Institute. Merida, Venezuela.
2000	Research internship in heavy oil dehydration processes. Intevep. Petróleos de Venezuela S.A (PDVSA).

Awards and Achievements

2009	Finalist (France) for the Best Young Researcher Award. 24th European Symposium on Applied Thermodynamics. Santiago de Compostela, Spain.
2008 - 2011	Scholarship for overseas graduate studies. FUNDAYACUCHO. Venezuela.
2001	*B.Sc. Eng*. outstanding thesis research. Chemical Engineering. Universidad de Los Andes, Merida. Venezuela.
1995 - 2001	Scholarship for undergraduate studies. FUNDAYACUCHO. Venezuela.
1994	Finalist of the 11th and 12th Venezuelan Olympiads for Chemistry. CENAMEC. Venezuela.
1994 - 1996	Distinguished student award. FUNDACITE. Merida, Venezuela.
1995	Academic-athlete award for outstanding academic achievement. Concord Community High School. Elkhart. IN, USA.
1990-1994	Honor rolls student. Colegio La Salle. Merida, Venezuela.

Publications

Journal Papers

Belandria V.; Mohammadi A. H.; Richon D. Compositional Analysis of the Gas Phase for the CO_2 + N_2 + Tetra-n-Butylammonium Bromide Aqueous Solution Systems under Hydrate Stability Conditions, **2012** (*submitted*).

Belandria V.; Pimentel A.; Mohammadi A. H.; Galicia-Luna, L. A.; Richon D. Clarification of the Volumetric Properties of the (Tetrahydrofuran + water) Systems [J. Chem. Thermodyn. 41 (2009) 1382-1386]: Author's Statement, **2012** (*submitted*).

Ben Attouche Sfaxi, I.; **Belandria V**.; Mohammadi A. H.; Lugo, R.; Richon D. Phase Equilibria of CO_2 + N_2 and CO_2 + CH_4 Clathrate Hydrates: Experimental Measurements and Thermodynamic Modelling. **2012** (*submitted*).

Belandria V.; Mohammadi A. H.; Eslamimanesh, A.; Richon D. ; Sánchez-Mora, M. F. ; Galicia-Luna, L. A. Phase equilibrium measurements for semi-clathrate hydrates of the (CO_2 + N_2 + tetra-n-butylammonium bromide) aqueous solution systems : Part II. *Fluid Phase Equilib.* **2012**, 322, 105-112.

Mohammadi A. H.; Eslamimanesh A.; **Belandria V**.; Richon D.; Naidoo P.; Ramjugernath D. Phase equilibrium measurements for semi-clathrate hydrates of the (CO_2 + N_2 + tetra-n-butylammonium bromide) aqueous solution system. *J. Chem. Thermodyn*. **2012**, 46, 57-61.

Mohammadi A.H.; Eslamimanesh, A.; **Belandria V**.; Richon D. Phase Equilibria of Semiclathrate Hydrates of CO_2, N_2, CH_4, or H_2 + Tetra-n-butylammonium Bromide Aqueous Solution. *J. Chem. Eng. Data* **2011**, 56 (10), 3855-3865.

Belandria V.; Eslamimanesh A.; Mohammadi A. H.; Richon D. Study of Gas Hydrate Formation in Carbon dioxide + Hydrogen + Water System: Compositional Analysis of Gas Phase. *Ind. Eng. Chem. Res.* **2011**, 50 (10), 6455-6459.

Belandria V.; Eslamimanesh A.; Mohammadi A. H.; Théveneau P.; Legendre H.; Richon D. Compositional analysis and hydrate dissociation conditions measurements for carbon dioxide + methane + water system. *Ind. Eng. Chem. Res.* **2011**, 50 (9), 5783-5794.

Belandria V.; Eslamimanesh A.; Mohammadi A. H.; Richon D. Gas hydrate formation in carbon dioxide + nitrogen + water system: Compositional analysis of equilibrium phases. *Ind. Eng. Chem. Res.* **2011**, 50 (8), 4722-4730.

Mohammadi A. H.; **Belandria V**.; Richon D. Use of an Artificial Neural Network Algorithm for Predictions of Hydrate Dissociation Conditions for Hydrogen + Water and Hydrogen + Tetra-n-Butyl Ammonium Bromide + Water Systems **.***Chem. Eng. Sci*. **2010**, 65, 4302-4305.

Belandria V.; Mohammadi A. H.; Richon D. Phase Equilibria of Clathrate Hydrates of Methane + Carbon dioxide: New Experimental Data and Predictions. *Fluid Phase Equilib.* **2010**, 296, 60-65. Appears on the "Top 25 Hottest Articles on ScienceDirect.com".

Belandria V.; Mohammadi A. H.; Richon D. Volumetric properties of the (tetrahydrofuran + water) and (tetra-n-butyl ammonium bromide + water) systems: Experimental measurements and correlations. *J. Chem. Thermodyn*. **2009**, 41 (12), 1382-1386.

Mohammadi A. H.; **Belandria V**.; Richon D. Can Toluene or Xylene Form Clathrate Hydrates? *Ind. Eng. Chem. Res.* **2009**, 48 (12), 5916-5918.

Conference Papers

V. Belandria, A. Eslamimanesh, A. H. Mohammadi, D. Richon. Hydrate Phase Equilibria of Gas Mixtures conatining CO_2. To be presented in the 7th International Conference on Gas Hydrates (ICGH 2011), Edinburgh, Scotland, United Kingdom, July 17-21, **2011**. Poster.

A. H. Mohammadi, A. Eslamimanesh, **V. Belandria**, D. Richon. Phase Equilibria of Semi-Clathrate Hydrates of Tetra-n butyl Ammonium Bromide + Mixtures of Carbon Dioxide with Methane, Nitrogen and Hydrogen. To be presented in the 25th European Symposium on Applied Thermodynamics, June 24 - 27, **2011**. Poster.

V. Belandria, P. Théveneau, H. Legendre, A. H. Mohammadi, D. Richon. Compositional analysis + hydrate dissociation conditions measurements for carbon dioxide + methane + water system. AIChE annual meeting, Salt Lake City, UT, USA, November 7-12, **2010**.

V. Belandria, A. H. Mohammadi, D. Richon. Etude expérimentale des équilibres d'hydrates de mélanges de gaz contenant du CO_2 en présence de solutions aqueuses de TBAB. Journées des doctorants de seconde année de l'Ecole doctorale Sciences des Métiers de l'Ingénieur. Paris, France. June 8-9, **2010**. Poster.

V. Belandria, P. Théveneau, H. Legendre, A. H. Mohammadi, D. Richon. Design and Construction of a New High-pressure, Low-temperature Apparatus for Hydrate Phase Equilibrium Measurements of Gases Containing Carbon Dioxide. 12th International Conference on Properties and Phase Equilibria for Product and Process Design. Suzhou, Jiangsu, China. May 16-21, **2010**. Poster.

V. Belandria, P. Théveneau, H. Legendre, A. H. Mohammadi, D. Richon. New apparatus for simultaneous measurements of gas hydrate phase equilibrium + compositional analysis. Atelier "Clathrates dans les environnements naturels : études thermodynamiques et méthodes d'analyses". Besançon, France. January 7-8, **2010**. Poster.

V. Belandria, A. H. Mohammadi, D. Richon. Gas Hydrate Phase Equilibria in the Methane + Carbon Dioxide + Water System: Experimental Measurements and Predictions of Dissociation Conditions. Proceedings of the AIChE 2009 Annual Meeting, Nashville, TN, USA, November 8-13, **2009**, p 695e.

V. Belandria, A. H. Mohammadi, D. Richon. A Static-Analytic Apparatus with a Mobile Sampler for Simultaneous Compositional and Gas Hydrate Phase Equilibrium Measurements. Proceedings of the 24th European Symposium on Applied Thermodynamics, Santiago de Compostela, Spain, June 27- July 1, **2009**, p 149.

V. Belandria, A. H. Mohammadi, D. Richon. Volumetric Properties of Tetrahydrofuran + Water System: Experimental Measurement and Correlation. Proceedings of the 24th European Symposium on Applied Thermodynamics, Santiago de Compostela, Spain, June 27- July 1, **2009**, p 719.

APPENDIX A

Measured Hydrate Phase Equilibrium Data for CO_2 Containing Gases

Table A.1. Experimental (p_{exp}) and predicted (p_{pred}) dissociation conditions using thermodynamic model (HWHYD, 2000) and the equation proposed by Adisasmito and coworkers (1991) for (carbon dioxide + methane) clathrate hydrates in the presence of pure water.

$CO_{2\,(load)}$ / mole fraction	T / K	p_{exp} / MPa	p_{pred} / MPa using thermodynamic model (HWHYD, 2000) assuming structure I	RD / %	p_{pred} / MPa using thermodynamic model (HWHYD, 2000) assuming structure II	RD / %	p_{pred} / MPa the equation proposed by Adisasmito and coworkers (1991)	RD / %
0.264	284.2	5.29	6.80	-2.9E+01	12.23	-1.3E+02	6.64	-2.6E+01
	287.2	9.83	9.94	-1.1E+00	18.86	-9.2E+01	9.76	7.1E-01
	289.2	11.62	13.16	-1.3E+01	25.51	-1.2E+02	12.76	-9.8E+00
0.272	279.1	3.60	3.79	-5.3E+00	6.40	-7.8E+01	3.62	-5.6E-01
0.490	284.8	5.82	6.47	-1.1E+01	17.32	-2.0E+02	6.36	-9.3E+00
	289.9	12.41	15.10	-2.2E+01	40.36	-2.3E+02	12.90	-3.9E+00
0.500	284.9	5.88	6.65	-1.3E+01	17.86	-2.0E+02	6.42	-9.2E+00
0.504	279.1	2.96	3.18	-7.4E+00	7.53	-1.5E+02	3.09	-4.4E+00
	280.6	3.16	3.42	-8.2E+00	11.55	-2.7E+02	3.34	-5.7E+00
0.730	281.9	4.02	4.03	-2.5E-01	15.47	-2.8E+02	3.95	1.7E+00
	289.1	13.06	15.21	-1.6E+01	63.88	-3.9E+02	10.92	1.6E+01
AARD [c] %				13.7E+00		16.1E+01		7.9E+00

Maximum uncertainties in mole fractions and dissociation temperatures and pressures are expected to be within $\pm$ 1- 2%, ± 0.2 K and ± 0.05 MPa, respectively.

Table A.2. Experimental (p^{exp}) and predicted (p^{pred}) dissociation conditions using two thermodynamic models: HWHYD (2000) and CSMGem (2008), for (carbon dioxide + methane) clathrate hydrates in the presence of pure water.

Mole fraction of CO_2 in the gas feed	Mole fraction of H_2O supplied to the system	T / K	p^{exp} / MPa	p^{pred} / MPa using HWHYD model [a]	ARD [b] / %	p^{pred} / MPa using CSMGem model	ARD / %
0.206	0.871	279.3	4.03	4.18	3.7	3.98	1.2
0.206	0.961	282.0	5.48	5.86	6.9	5.67	3.5
0.206	0.975	285.5	8.27	8.84	6.9	8.71	5.3
0.476	0.877	277.9	2.72	2.97	9.2	2.78	2.2
0.476	0.959	279.8	3.61	3.94	9.1	3.68	1.9
0.476	0.973	285.0	6.09	7.62	25	7.34	21
0.744	0.877	279.0	2.72	2.85	4.8	2.73	0.4
0.744	0.956	280.1	3.21	3.42	6.5	3.26	1.6
0.744	0.972	283.2	4.70	5.39	15	5.12	8.9
AARD [c] %					9.7		5.1

Maximum uncertainties in CO_2 mole fractions and dissociation temperatures and pressures are expected to be within $\pm$ 1-2%, $\pm$ 0.2 K and $\pm$ 0.05 MPa, respectively. Uncertainties in mole fractions of H_2O supplied to the system are expected to be within 0.5%.

[a] (Assuming *sI*).

[b] $ARD = 100 \times \frac{\left| p^{\exp} - p^{pred} \right|}{p^{\exp}}$

[c] $AARD = \frac{1}{n} \sum \left| ARD \right|$

Table A.3. Three-phase equilibrium data for (CO_2 + CH_4 + H_2O) systems at different temperatures and pressures.

Feed			Experimental data (Compositional analysis)							CSMGem model predictions (Compositional analysis)					Absolute relative deviations (*ARD* %)				
					Gas phase	***Hydrate phase***	***Aqueous phase***			***Gas phase***	***Hydrate phase***	***Aqueous phase***			***Gas phase***	***Hydrate phase***	***Aqueous phase***		
CO_2 / mole	CH_4 / mole	H_2O / mole	*T* / K	*p* / MPa	y_{CO2} / mole fraction	z_{CO2} / mole fraction (water free base)	CO_2 / mole fraction	CH_4 / mole fraction	H_20 / mole fraction	y_{CO2} / mole fraction	z_{CO2} / mole fraction (water free base)	x_{CO2} / mole fraction	x_{CH4} / mole fraction	x_{H2O} / mole fraction	y_{CO2} / mole fraction	z_{CO2} / mole fraction (water free base)	x_{CO2} / mole fraction	x_{CH4} / mole fraction	x_{H2O} / mole fraction
0.048	0.165	1.43	273.6	2.234	0.141	-[b]	-[b]	-[b]	-[b]	0.151	0.296	0.0036	0.0008	0.9956	7.1	-	-	-	-
0.048	0.165	5.236	273.6	2.416	0.125	-[b]	-[b]	-[b]	-[b]	-[c]	-[c]	-[c]	-[c]	-[c]	-	-	-	-	-
0.048	0.165	8.185	273.6	2.440	0.081	0.096	0.0055	0.0006	0.9940	-[c]	-[c]	-[c]	-[c]	-[c]	-	-	-	-	-
0.116	0.115	1.65	273.6	1.844	0.345	0.549	0.0099	0.0003	0.9898	0.376	0.538	0.0075	0.0005	0.9920	9.0	2.0	24.2	66.7	0.2
0.116	0.115	5.355	273.6	1.941	0.288	0.392	0.0062	0.0006	0.9932	0.291	0.478	0.0062	0.0006	0.9932	1.0	21.9	0.0	0.0	0.0
0.116	0.115	8.48	273.6	2.048	0.220	0.294	0.0095	0.0003	0.9902	-[c]	-[c]	-[c]	-[c]	-[c]	-	-	-	-	-
0.181	0.057	1.696	273.6	1.510	0.630	0.884	0.0127	0.0001	0.9872	0.626	0.765	0.0107	0.0002	0.9891	0.6	13.5	15.7	100.0	0.2
0.181	0.057	5.182	273.6	1.607	0.545	0.801	0.0128	0.0001	0.9871	-[c]	-[c]	-[c]	-[c]	-[c]	-	-	-	-	-
0.048	0.165	1.43	275.2	2.583	0.166	0.338	0.0071	0.0008	0.9921	0.171	0.320	0.0044	0.0008	0.9948	3.0	5.3	38.0	0.0	0.3
0.048	0.165	5.236	275.2	2.712	0.129	-[b]	-[b]	-[b]	-[b]	-[c]	-[c]	-[c]	-[c]	-[c]	-	-	-	-	-
0.048	0.165	8.185	275.2	2.766	0.086	0.179	0.0030	0.0009	0.9961	0.109	0.225	0.003	0.0009	0.9961	26.7	25.7	0.0	0.0	0.0
0.116	0.115	1.65	275.2	2.123	0.384	0.650	0.0108	0.0003	0.9889	0.392	0.574	0.0085	0.0005	0.9910	2.1	11.7	21.3	66.7	0.2
0.116	0.115	5.355	275.2	2.220	0.302	0.586	0.0075	0.0006	0.9919	0.295	0.520	0.0075	0.0006	0.9919	2.3	11.3	0.0	0.0	0.0
0.116	0.115	8.48	275.2	2.400	0.228	0.366	0.0108	0.0003	0.9889	0.245	0.419	0.0059	0.0007	0.9934	7.5	14.5	45.4	133.3	0.5
0.181	0.057	1.696	275.2	1.792	0.657	0.831	0.0123	0.0002	0.9875	0.634	0.786	0.0123	0.0002	0.9875	3.5	5.4	0.0	0.0	0.0
0.181	0.057	5.182	275.2	1.865	0.565	0.752	0.0113	0.0003	0.9884	0.589	0.732	0.0113	0.0003	0.9884	4.2	2.7	0.0	0.0	0.0
0.048	0.165	1.43	276.1	2.813	0.179	0.264	0.0062	0.0007	0.9931	0.183	0.397	0.0049	0.0008	0.9943	2.2	50.4	21.0	14.3	0.1
0.048	0.165	5.236	276.1	3.025	0.134	0.239	0.0034	0.0009	0.9957	0.128	0.335	0.0034	0.0009	0.9957	4.5	40.2	0.0	0.0	0.0
0.048	0.165	8.185	276.1	3.027	0.096	0.238	0.0062	0.0007	0.9931	-[c]	-[c]	-[c]	-[c]	-[c]	-	-	-	-	-
0.116	0.115	1.65	276.1	2.318	0.405	0.644	0.0113	0.0004	0.9883	0.664	0.397	0.0092	0.0005	0.9903	64.0	38.4	18.6	25.0	0.2
0.116	0.115	5.355	276.1	2.503	0.315	0.400	0.0113	0.0004	0.9883	0.408	0.584	0.0074	0.0006	0.9920	29.5	46.0	34.5	50.0	0.4
0.116	0.115	8.48	276.1	2.690	0.232	0.312	0.0113	0.0004	0.9883	-[c]	-[c]	-[c]	-[c]	-[c]	-	-	-	-	-
0.181	0.057	1.696	276.1	1.985	0.669	0.877	0.0158	0.0002	0.984	-[c]	-[c]	-[c]	-[c]	-[c]	-	-	-	-	-

0.181	0.057	5.182	276.1	2.174	0.579	0.784	0.0114	0.0004	0.9882	-[c]	-[c]	-[c]	-[c]	-[c]	-	-	-	-	-
0.048	0.165	1.43	278.1	3.416	0.202	0.233	0.0088	0.0021	0.9890	-[c]	-[c]	-[c]	-[c]	-[c]	-	-	-	-	-
0.048	0.165	5.236	278.1	3.631	0.139	0.225	0.0074	0.0009	0.9917	-[c]	-[c]	-[c]	-[c]	-[c]	-	-	-	-	-
0.048	0.165	8.185	278.1	3.802	0.103	0.148	0.0068	0.0008	0.9924	0.095	0.193	0.0030	0.0011	0.9959	7.8	30.4	55.9	37.5	0.4
0.116	0.115	5.355	278.1	3.037	0.323	0.457	0.0124	0.0004	0.9871	-[c]	-[c]	-[c]	-[c]	-[c]	-	-	-	-	-
0.116	0.115	8.48	278.1	3.319	0.233	0.273	0.0126	0.0004	0.987	0.232	0.392	0.0066	0.0009	0.9926	0.4	43.6	47.6	125.0	0.6
0.181	0.057	1.696	278.1	2.450	0.694	-[b]	-[b]	-[b]	-[b]	-[c]	-[c]	-[c]	-[c]	-[c]	-	-	-	-	-
0.181	0.057	5.182	278.1	2.580	0.609	0.786	0.0137	0.0004	0.9859	0.604	0.786	0.0137	0.0004	0.9859	0.8	0.0	0.0	0.0	0.0
0.048	0.165	1.43	279.2	3.565	0.202	0.266	0.0071	0.0009	0.992	-[c]	-[c]	-[c]	-[c]	-[c]	-	-	-	-	-
0.048	0.165	5.236	280.2	4.486	0.147	0.307	0.0023	0.0079	0.9898	-[c]	-[c]	-[c]	-[c]	-[c]	-	-	-	-	-
0.048	0.165	8.185	280.2	4.655	0.108	0.245	0.0013	0.0070	0.9917	-[c]	-[c]	-[c]	-[c]	-[c]	-	-	-	-	-
0.116	0.115	5.355	280.2	3.541	0.344	0.727	0.0146	0.0005	0.9849	-[c]	-[c]	-[c]	-[c]	-[c]	-	-	-	-	-
0.116	0.115	8.48	280.2	4.109	0.235	0.420	0.0114	0.0005	0.9881	0.255	0.409	0.0078	0.0009	0.9912	8.5	2.6	31.6	80.0	0.3
0.181	0.057	5.182	280.2	3.139	0.620	0.860	0.0167	0.0004	0.983	-[c]	-[c]	-[c]	-[c]	-[c]	-	-	-	-	-
0.181	0.057	8.395	280.2	3.481	0.490	0.788	0.0150	0.0002	0.9848	-[c]	-[c]	-[c]	-[c]	-[c]	-	-	-	-	-
0.048	0.165	8.185	282.2	5.767	0.114	0.276	0.0065	0.0016	0.9919	-[c]	-[c]	-[c]	-[c]	-[c]	-	-	-	-	-
0.048	0.165	8.185	284.2	7.190	0.115	0.107	0.0067	0.0012	0.9921	-[c]	-[c]	-[c]	-[c]	-[c]	-	-	-	-	-
AAD %															9.7	20.3	27.1	38.8	0.2

*: HWHYD model does not converge for the studied conditions.

[a] Some/all of constraints are not satisfied.

[b] No three phase flash convergence using CSMGem model.

Table A.4. Hydrate dissociation conditions of (CO_2 + N_2) binary gas mixtures in the presence of water.

Mole fraction of CO_2 in the gas feed	Mole fraction of H_2O supplied to the system	T^a / K	p^{exp} / MPa	p^{pred} / MPa using HWHYD model [b]	*ARD* / %	p^{pred} / MPa using CSMGem model	*ARD* / %
0.812	0.779	284.1	7.07	7.44	5.2	8.05	14
0.773	0.847	279.2	3.24	3.37	4.0	3.49	7.7
0.773	0.965	280.0	5.00	4.72	5.6	5.60	12
0.748	0.889	280.5	4.16	4.17	0.2	4.50	8.2
0.476	0.803	278.1	4.76	4.87	2.3	4.95	4.0
0.476	0.943	280.7	10.67	10.59	0.8	10.60	0.7
0.271	0.666	279.6	9.76	10.63	8.9	10.92	12
0.271	0.895	282.4	19.17	19.38	1.1	20.06	4.6
0.271	0.956	285.3	29.92	29.13	2.6	38.77	30
AAD %					3.4		10.3

[a] Maximum uncertainties in dissociation temperatures and pressures are expected to be within ± 0.2 K and ± 0.05 MPa, as indicated in Chapter 2.

[b] Assuming sI for N_2 simple hydrates.

$$ARD = 100 \times \frac{\left| p^{\exp} - p^{pred} \right|}{p^{\exp}}$$

Table A.5. Three-phase equilibrium data for gas mixtures of (CO_2 + N_2) in the presence of water at different temperatures (T) and pressures (p): Experimental and predicted values.

feed			experimental data							CSMGem model predictions [a]										absolute relative deviation (ARD %)[b]					
					gas phase	***hydrate phase***	***aqueous phase***			***gas phase***	***hydrate phase***						***aqueous phase***			***gas phase***	***hydrate phase***	***aqueous phase***		
CO_2 / mole	N_2 / mole	H_2O / mole	T / K	p / MPa	yCO_2 / mole fraction (water content free base)	zCO_2 / mole fraction (water free base)	CO_2 / mole fraction	N_2 / mole fraction	H_20 / mole fraction	y_{CO2} / mole fraction (water content free base)	z_{CO2} / mole fraction (water free base)	S [e]	$\theta\ CO_{2\ -\ S}$	$\theta\ CO_{2\ -\ L}$	$\theta\ N_{2\ -\ S}$	$\theta\ N_{2\ -\ L}$	CO_2 / mole fraction	N_2 / mole fraction	H_20 / mole fraction	y_{CO2} / mole fraction (water content free base)	z_{CO2} / mole fraction (water free base)	CO_2 / mole fraction	N_2 / mole fraction	H_20 / mole fraction
0.2086	0.0695	1.543	273.6	2.032	0.617	0.97	0.0136	0.0001	0.9862	0.618	0.938	I	0.4416	0.9277	0.1407	0.033	0.0140	0.0001	0.9857	0.2	3.3	2.9	0.0	0.1
0.1947	0.5842	1.5516	273.6	8.149	0.171	0.657	0.0123	0.0009	0.9868	0.109	0.537	I	0.1312	0.6096	0.6557	0.3451	0.0069	0.0012	0.9919	36.4	18.3	43.8	32.8	0.5
0.1947	0.5842	6.6615	273.6	11.943	0.179	0.373	0.0037	0.0018	0.9945	0.045	0.261	I	0.0396	0.307	0.7986	0.6417	0.0036	0.0018	0.9946	74.8	30.0	3.2	0.8	0.0
0.2086	0.0695	7.649	273.6	2.962	0.429	0.897	0.0123	0.0003	0.9874	0.405	0.855	I	0.3625	0.8814	0.2768	0.0775	0.0123	0.0003	0.9874	5.6	4.7	0.0	0.0	0.0
0.1845	0.196	1.553	273.6	3.761	0.32	*c*	*c*	*c*	*c*	0.306	0.797	I	0.3066	0.8402	0.3685	0.1175	0.0112	0.0005	0.9883	4.4				
0.2547	0.0898	2.7525	274.6	2.543	0.728	0.739	0.0141	0.0002	0.9857	0.552	0.909	I	0.433	0.9177	0.1844	0.0448	0.0141	0.0002	0.9857	24.2	23.0	0.0	0.0	0.0
0.4371	0.1472	2.0555	274.9	5.204	0.717	0.788	0.0277	0.0002	0.972	*d*	*d*	*d*	*d*	*d*	*d*	*d*	*d*	*d*	*d*					
0.2086	0.0695	1.543	275.2	2.29	0.656	0.897	0.0154	0.0001	0.9845	0.682	0.941	I	0.478	0.9369	0.1244	0.0277	0.0202	0.0001	0.9797	4.0	4.9	31.2	0.0	0.5
0.2547	0.0898	2.7525	275.2	2.643	0.729	0.888	0.0148	0.0002	0.985	0.574	0.914	I	0.4476	0.922	0.1762	0.0419	0.0148	0.0002	0.9850	21.3	2.9	0.0	0.0	0.0
0.2086	0.0695	7.649	275.2	3.256	0.449	0.879	0.014	0.0003	0.9857	0.443	0.866	I	0.3994	0.8959	0.2549	0.0671	0.0140	0.0003	0.9860	1.3	1.5	0.0	0.0	0.0
0.1845	0.196	1.553	275.2	4.045	0.357	*c*	*c*	*c*	*c*	0.356	0.820	I	0.3457	0.8614	0.34	0.1006	0.0130	0.0004	0.9866	0.3				
0.1845	0.196	6.273	275.2	7.45	0.174	0.817	0.0139	0.0062	0.9799	0.166	0.622	I	0.1889	0.7034	0.5822	0.2556	0.0091	0.0010	0.9899	4.6	23.9	34.5	83.9	1.0
0.1947	0.5842	1.5516	275.2	8.246	0.176	0.799	0.0086	0.0011	0.9903	0.144	0.590	I	0.1641	0.6646	0.6204	0.2939	0.0120	0.0010	0.9871	18.2	26.2	39.5	9.1	0.3
0.1947	0.5842	6.6615	275.2	12.745	0.16	0.382	0.011	0.0014	0.9876	0.066	0.370	I	0.0697	0.4338	0.7685	0.5227	0.0050	0.0020	0.9930	59.0	3.2	54.5	42.9	0.5
0.2547	0.0898	2.7525	275.6	2.714	0.73	0.764	0.0153	0.0002	0.9845	0.590	0.917	I	0.4573	0.9248	0.1708	0.04	0.0153	0.0001	0.9844	19.2	20.0	0.1	50.0	0.0
0.4371	0.1472	2.0555	275.8	5.381	0.719	0.802	0.0359	0.0003	0.9638	*d*	*d*	*d*	*d*	*d*	*d*	*d*	*d*	*d*	*d*					
0.2086	0.0695	1.543	276.1	2.5	0.682	0.984	0.0164	0.0001	0.9835	0.690	0.943	I	0.4952	0.94	0.1211	0.0264	0.0164	0.0001	0.9835	1.2	4.2	0.0	0.0	0.0
0.2547	0.0898	2.7525	276.1	2.865	0.731	0.79	0.0177	0.0002	0.9821	0.595	0.917	I	0.465	0.926	0.1715	0.0398	0.0158	0.0002	0.9840	18.6	16.1	10.7	0.0	0.2
0.2086	0.0695	7.649	276.1	3.703	0.488	0.703	0.0156	0.0003	0.9841	0.449	0.864	I	0.4027	0.8933	0.2707	0.0715	0.0147	0.0003	0.9850	8.0	22.9	5.8	0.0	0.1
0.1845	0.196	1.553	276.1	4.401	0.396	0.688	0.015	0.0004	0.9817	0.370	0.823	I	0.3579	0.8653	0.3398	0.0987	0.0137	0.0005	0.9859	6.6	19.6	8.7	25.0	0.4
0.1947	0.5842	1.552	276.1	8.58	0.196	0.574	0.0095	0.0011	0.9894	0.162	0.611	I	0.181	0.6872	0.6071	0.2739	0.0095	0.0011	0.9894	17.3	6.4	0.0	0.0	0.0
0.2086	0.0695	7.6487	276.7	3.703	0.488	0.703	0.0156	0.0003	0.9841	0.489	0.878	I	0.4269	0.9038	0.2469	0.0625	0.0156	0.0003	0.9841	0.2	24.9	0.0	0.0	0.0

0.2086	0.0695	1.543	277.1	2.706	0.705	0.838	0.0177	0.0001	0.9822	*d*	*d*	*d*	*d*	*d*	*d*	*d*	*d*	*d*	*d*				
0.2547	0.0898	2.7525	277.3	3.13	0.732	0.83	0.0185	0.0002	0.9814	0.639	0.927	I	0.4938	0.9336	0.1564	0.0349	0.0174	0.0002	0.9824	12.7	11.7	5.9	0.0	0.1
0.4371	0.1472	2.0555	277.8	6.159	0.747	0.864	0.0336	0.0057	0.9607	*d*	*d*	*d*	*d*	*d*	*d*	*d*	*d*	*d*	*d*					
0.2086	0.0695	1.543	278.1	2.974	0.729	0.89	0.0213	0.0068	0.9719	*d*	*d*	*d*	*d*	*d*	*d*	*d*	*d*	*d*	*d*					
0.2547	0.0898	2.7525	278.1	3.411	0.734	0.752	0.0185	0.0002	0.9814	0.692	0.937	I	0.5075	0.9358	0.1554	0.0342	0.0184	0.0002	0.9814	5.7	24.6	0.5	0.0	0.0
0.2086	0.0695	7.649	278.1	4.194	0.521	0.655	0.0173	0.0003	0.9824	*d*	*d*	*d*	*d*	*d*	*d*	*d*	*d*	*d*	*d*					
0.1947	0.5842	1.552	278.1	9.146	0.229	0.541	0.0121	0.0011	0.9869	0.212	0.662	I	0.2303	0.743	0.5627	0.2234	0.0118	0.0011	0.9870	7.4	22.4	2.5	0.0	0.0
0.1947	0.5842	6.6615	278.1	14.26	0.127	0.513	0.008	0.0017	0.9903	0.110	0.474	I	0.1145	0.5529	0.7303	0.412	0.0080	0.0017	0.9904	13.4	7.6	0.0	0.0	0.0
0.2086	0.0695	7.649	279.7	4.817	0.557	0.698	0.0167	0.0003	0.983	*d*	*d*	*d*	*d*	*d*	*d*	*d*	*d*	*d*	*d*					
0.1845	0.196	6.273	279.7	10.021	0.263	0.607	0.0137	0.0083	0.9781	0.261	0.695	I	0.2644	0.7723	0.5373	0.1977	0.0141	0.0011	0.9848	0.8	14.5	2.9	86.7	0.7
0.1947	0.5842	6.6615	279.7	15.816	0.148	0.551	0.0095	0.0018	0.9887	0.140	0.508	I	0.135	0.5915	0.7178	0.3773	0.0095	0.0018	0.9887	5.4	7.8	0.0	0.0	0.0
0.1947	0.5842	6.6615	281.2	17.628	0.176	0.584	0.0112	0.0018	0.987	0.170	0.536	I	0.1547	0.6229	0.7065	0.3494	0.0112	0.0018	0.9870	3.4	8.2	0.0	0.0	0.0
0.4371	0.1472	2.0555	281.7	6.329	0.746	0.806	0.0207	0.0006	0.9788	*d*	*d*	*d*	*d*	*d*	*d*	*d*	*d*	*d*	*d*					
Total																				13.8	14.1	9.9	13.2	0.2

[a] Predictions of HWHYD model are not shown as N_2 hydrate is modeled considering structure I.

[b] $$ARD = 100 \times \frac{\left| p^{\exp} - p^{pred} \right|}{p^{\exp}}$$

[c] Some/all of constraints are not satisfied.

[d] No three phase flash convergence using CSMGem model.

[e] Gas hydrate structure.

Table A.6. Hydrate dissociation conditions of (CO_2 + H_2) binary gas mixtures in the presence of water.

Mole fraction of CO_2 in the gas feed	T / K	p / MPa
0.829	277.2	2.44
0.829	277.7	2.58
0.829	278.1	2.66
0.709	279.6	3.84
0.709	280.1	4.46
0.508	279.8	7.21
0.508	280.4	8.53
0.508	283.0	24.76

Table A.7. Compositional data for the gas phase in equilibrium with the hydrate and aqueous phases at different temperatures (T) and pressures (p) for various (CO_2 + H_2) gas mixtures in the presence of water.

Gaseous feed	(L_w-H-G) equilibrium		
CO_2 / mole fraction	T / K	p / MPa	y_{CO2} / mole fraction of CO_2 in the gas phase
0.780	273.6	1.888	0.686
0.829	273.6	1.753	0.737
0.829	273.6	1.992	0.667
0.508	273.6	4.669	0.317
0.508	273.6	7.156	0.202
0.709	273.6	3.005	0.427
0.829	275.2	1.984	0.764
0.829	275.2	2.234	0.706
0.508	275.2	4.922	0.377
0.508	275.2	7.442	0.225
0.709	275.2	2.754	0.568
0.709	275.2	3.272	0.474
0.709	275.2	8.282	0.188
0.829	276.2	2.184	0.783
0.829	276.2	2.430	0.734
0.508	276.2	5.131	0.388
0.508	276.2	7.655	0.238
0.709	276.2	2.936	0.602
0.709	276.2	3.442	0.502
0.829	277.1	2.586	0.745
0.508	277.1	5.343	0.436
0.709	277.1	3.162	0.620
0.508	278.1	5.611	0.410
0.508	278.1	7.909	0.274
0.709	278.1	3.417	0.640
0.709	278.1	3.945	0.553
0.709	279.1	5.911	0.437
0.709	279.1	8.278	0.316
0.709	279.1	4.249	0.590
0.709	280.1	6.050	0.453
0.709	280.1	8.521	0.354
0.709	281.2	8.570	0.365

Table A.8. Experimental dissociation conditions of (TBAB + methane), (TBAB + carbon dioxide) and (TBAB + nitrogen) semi-clathrate hydrates (w = 0.25).

***T*/ K**	***p* / MPa**
(TBAB + methane) semi-clathrate hydrates	
285.2	0.235
286.7	0.444
287.1	0.678
287.6	0.954
288.1	1.171
289.3	1.848
290.4	2.888
292.1	5.124
294.7	10.217
(TBAB + carbon dioxide) semi-clathrate hydrates	
284.0	0.104
284.9	0.293
285.6	0.530
286.5	0.769
287.9	1.178
288.9	1.575
290.0	1.989
(TBAB + nitrogen) semi-clathrate hydrates	
281.1	0.470
284.0	0.780
284.5	0.870
286.5	2.190
286.8	3.000

Table A.9. Experimental dissociation conditions of (TBAB + methane), (TBAB + carbon dioxide) and (TBAB + nitrogen) semi-clathrate hydrates (w = 0.50).

***T*/ K**	***p* / MPa**
(TBAB + methane) semi-clathrate hydrates	
285.6	0.317
285.8	0.522
286.0	0.868
286.3	1.036
288.7	2.166
289.8	3.596
291.3	5.247
292.8	8.260
(TBAB + carbon dioxide) semi-clathrate hydrates	
282.6	0.698
283.5	1.086
285.1	1.800
286.9	3.104
287.9	4.380
(TBAB + nitrogen) semi-clathrate hydrates	
286.1	2.790
286.3	3.930
286.5	4.885
288.4	7.670
289.1	9.920

Table A.10. Semi-clathrate hydrate phase equilibrium data for the (CO_2 + N_2 + TBAB + H_2O) mixtures.

Feed gas composition / CO_2 mole fraction	TBAB / mass fraction	T / K	p / MPa
0.749	0.05	281.0	0.67
		281.5	0.91
		282.8	1.47
		284.2	2.31
		286.2	3.48
	0.30	286.6	1.06
		287.9	1.73
		289.0	2.39
		289.7	2.70
		291.0	3.70
0.399	0.05	283.6	3.78
		286.2	6.58
	0.30	287.1	1.78
0.151	0.05	282.4	1.93
		282.7	2.83
		283.7	5.46
		285.1	8.14
		288.0	14.59
		289.2	19.07
	0.30	285.7	1.55

Table A.11. Compositional phase equilibrium data for (CO_2 + N_2) gas mixtures in (0.05 mass fraction) TBAB aqueous solutions.

Feed						Compositional Equilibrium Data			
CO_2 / molar fraction	p / MPa	$n_{\text{gas mixture}}$ / mole	CO_2 / mole	N_2 / mole	TBAB aqueous sol. (0.05 mass fraction)	T / K	p / MPa	y_{CO2} / molar composition of CO_2 in the gas phase	x_{TBAB} / mass fraction of TBAB in the liq. phase
0.749	0.960	0.076	0.057	0.019	0.241	275.15*	0.786	0.640	0.024
0.749	1.415	0.113	0.085	0.028	0.213	275.20*	0.942	0.586	0.024
0.399	3.236	0.256	0.102	0.154	0.195	275.18*	3.519	0.289	0.018
0.399	3.236	0.256	0.102	0.154	0.423	275.18*	5.492	0.172	0.017
0.151	12.606	0.980	0.147	0.833	0.149	275.17*	12.254	0.080	0.013
0.151	12.606	0.980	0.147	0.833	0.268	275.23*	14.525	0.058	0.012
0.749	0.960	0.076	0.057	0.019	0.241	276.20*	0.803	0.596	0.039
0.749	0.960	0.076	0.057	0.019	0.241	277.20*	0.821	0.606	0.026
0.399	3.236	0.256	0.102	0.154	0.195	277.17*	3.559	0.295	0.017
0.749	0.960	0.076	0.057	0.019	0.241	279.65	0.581	0.613	0.024
0.399	3.236	0.256	0.102	0.154	0.195	279.66	3.639	0.304	0.019
0.399	3.236	0.256	0.102	0.154	0.423	279.65	5.774	0.190	0.017
0.151	12.606	0.980	0.147	0.833	0.149	279.69	14.032	0.129	0.013
0.151	12.606	0.980	0.147	0.833	0.268	279.69	17.860	0.112	0.012
0.749	0.960	0.076	0.057	0.019	0.241	280.20	0.889	0.634	0.026
0.749	0.960	0.076	0.057	0.019	0.241	281.15	0.893	0.639	0.036
0.399	3.236	0.256	0.102	0.154	0.195	281.15	3.694	0.309	0.017
0.399	3.236	0.256	0.102	0.154	0.195	282.15	0.897	0.623	0.036
0.399	3.236	0.256	0.102	0.154	0.195	282.18	3.712	0.313	0.030
0.399	3.236	0.256	0.102	0.154	0.423	282.16	6.045	0.201	0.019
0.151	12.606	0.980	0.147	0.833	0.149	282.15	14.209	0.132	0.013
0.151	12.606	0.980	0.147	0.833	0.268	282.21	18.117	0.114	0.012

Cont. Table A.11. Compositional phase equilibrium data for (CO_2 + N_2) gas mixtures in (0.05 mass fraction) TBAB aqueous solutions.

Feed						Compositional Equilibrium Data			
CO_2 / molar fraction	p / MPa	$n_{\text{gas mixture}}$ / mole	CO_2 / mole	N_2 / mole	TBAB aqueous sol. (0.05 mass fraction)	T / K	p / MPa	y_{CO2} / molar composition of CO_2 in the gas phase	x_{TBAB} / mass fraction of TBAB in the liq. phase
0.399	3.236	0.256	0.102	0.154	0.195	283.23	3.768	0.320	0.035
0.151	12.606	0.980	0.147	0.833	0.149	283.20	14.284	0.132	0.013
0.399	3.236	0.256	0.102	0.154	0.195	283.69	3.791	0.323	0.035
0.399	3.236	0.256	0.102	0.154	0.423	283.73	6.244	0.212	0.025
0.151	12.606	0.980	0.147	0.833	0.268	284.20	18.333	0.117	0.018
0.399	3.236	0.256	0.102	0.154	0.423	285.20	6.489	0.221	0.031
0.151	12.606	0.980	0.147	0.833	0.149	285.15	14.450	0.133	0.025
0.151	12.606	0.980	0.147	0.833	0.268	285.16	18.460	0.118	0.018
0.399	3.236	0.256	0.102	0.154	0.423	285.70	6.563	0.223	0.036
0.399	3.236	0.256	0.102	0.154	0.423	286.20	6.575	0.226	0.048
0.151	12.606	0.980	0.147	0.833	0.149	286.73	14.481	0.134	0.031
0.151	12.606	0.980	0.147	0.833	0.268	286.22	18.584	0.119	0.018
0.151	12.606	0.980	0.147	0.833	0.149	287.20	14.525	0.135	0.031
0.151	12.606	0.980	0.147	0.833	0.268	287.21	18.694	0.119	0.024
0.151	12.606	0.980	0.147	0.833	0.268	287.70	18.780	0.121	0.030
0.151	12.606	0.980	0.147	0.833	0.268	288.71	18.996	0.123	0.036
0.151	12.606	0.980	0.147	0.833	0.268	289.21	19.085	0.124	0.036

*: Likely represents semi-clathrates of (TBAB + water).

Table A.12. Compositional phase equilibrium data for (CO_2 + N_2) gas mixtures in (0.30 mass fraction) TBAB aqueous solutions.

Feed						Compositional Equilibrium Data			
CO_2 / molar fraction	p / MPa	$n_{\text{gas mixture}}$ / mole	CO_2 / mole	N_2 / mole	TBAB aqueous sol. (0.30 mass fraction)	T / K	p / MPa	y_{CO2} / molar composition of CO_2 in the gas phase	x_{TBAB} / mass fraction of TBAB in the liq. phase
0.749	1.061	0.084	0.063	0.021	0.239	275.15*	0.841	0.604	-[a]
0.399	1.664	0.132	0.053	0.079	0.127	275.20*	1.633	0.332	-[a]
0.399	1.664	0.132	0.053	0.079	0.422	275.20*	2.945	0.217	-[a]
0.399	1.664	0.132	0.053	0.079	0.127	277.23*	1.644	0.335	-[a]
0.399	1.664	0.132	0.053	0.079	0.127	277.20*	2.915	0.215	-[a]
0.749	1.061	0.084	0.063	0.021	0.239	279.65*	0.822	0.605	-[a]
0.399	1.664	0.132	0.053	0.079	0.127	279.68*	1.659	0.335	-[a]
0.399	1.664	0.132	0.053	0.079	0.422	279.68*	2.924	0.216	-[a]
0.749	1.061	0.084	0.063	0.021	0.239	280.65*	0.821	0.605	-[a]
0.749	1.061	0.084	0.063	0.021	0.239	281.15*	0.818	0.606	-[a]
0.399	1.664	0.132	0.053	0.079	0.127	281.21*	1.668	0.335	-[a]
0.749	1.061	0.084	0.063	0.021	0.239	282.20*	0.774	0.604	-[a]
0.749	1.061	0.084	0.063	0.021	0.239	283.16*	0.777	0.604	-[a]
0.399	1.664	0.132	0.053	0.079	0.127	283.19*	1.679	0.335	-[a]
0.749	1.061	0.084	0.063	0.021	0.239	284.16*	0.782	0.607	-[a]
0.749	1.061	0.084	0.063	0.021	0.239	284.65*	0.794	0.613	-[a]
0.749	1.061	0.084	0.063	0.021	0.239	285.21	0.786	0.621	0.301
0.399	1.664	0.132	0.053	0.079	0.127	285.19	1.616	0.322	0.296
0.399	1.664	0.132	0.053	0.079	0.127	285.69	1.617	0.322	0.296
0.749	1.061	0.084	0.063	0.021	0.239	285.71	0.875	0.660	0.299
0.399	1.664	0.132	0.053	0.079	0.127	286.68	1.749	0.358	0.301
0.399	1.664	0.132	0.053	0.079	0.127	287.17	1.780	0.368	0.301

*: Likely represents semi-clathrates of (TBAB + water); [a]: no liquid phase sample due to valve obstruction by hydrates.

APPENDIX B

Tetra-n-Butyl Ammonium Bromide + Water Systems: Density Measurements and Correlation[†]

[†] Content published in *J. Chem. Thermodyn. 2009, 41 (12), 1382-1386.*

Appendix B: Tetra-n-Butyl Ammonium Bromide + Water Systems: Density Measurements and Correlation

In this study, density data for the binary mixtures of (water + tetra-n-butyl ammonium bromide) at atmospheric pressure and various temperatures are given and correlated. Research grade TBAB aqueous solution with a concentration of (50 mass% TBAB) was purchased from Aldrich. Double-distilled and deionized water obtained from a Direct-Q5 Ultrapure Water System (Millipore^{TM}) was degassed and used to prepare the aqueous solutions. Samples were prepared following the gravimetric procedure described below. An Anton Paar vibrating-tube digital densimeter (model DMA 5000) with a certified precision of 10^{-5} g.cm^{-3} for density and ±0.01 K for temperature was used to carry out the density measurements. The density determination is based on measuring the period of oscillation of a vibrating U-shaped hollow tube that is filled with the sample. The densimeter was calibrated with double-distilled, degassed water, and dry air at 293.15 K and atmospheric pressure before measuring each sample. Samples were carefully loaded using a syringe avoiding the introduction of any air bubbles and achieving satisfactory purging. Densities were measured at thermal equilibrium after successive increases of temperature. After each series of measurements, the densimeter was washed and dried. All measurements were repeated at least three times and average density values are reported.

The gravimetric procedure used to prepare the TBAB aqueous solutions is essentially similar to that of previous studies performed in our laboratory (Valtz *et al*. 2004). Briefly, 20 cm^3 glass bottles were air-tight closed with a septum and then evacuated using a vacuum pump through a syringe needle introduced across the septum. Empty bottles were weighed, and then water (freshly degassed through vacuum distillation) was introduced by means of a syringe. After weighing the bottle loaded with water, TBAB was added and the bottle was weighed again. All weighing were carried out using an analytical balance (Mettler AT200) with an accuracy of 0.0001 g. As no chemical reaction is expected to occur between the two components in the mixture, the average uncertainty in molar compositions is assumed to be better than 0.0003, as demonstrated by Mokraoui and coworkers (2006). The above preparation and loading procedures were followed not only to obtain accurate compositions, but also to avoid the formation of gas bubbles inside the vibrating tube. This may occur at high temperatures, especially if the liquid is not well degassed (Mokraoui *et al*., 2006).

As TBAB aqueous solutions may crystallize under atmospheric pressure and temperatures between 0 and 12 °C (Darbouret *et al*., 2005), density measurements were carried out from (293.15 to 333.15) K. The measured density data are reported in Table B.1 and are correlated using the equation proposed by Söhnel and Novotny (1985), as follows:

$$\rho_3 = \rho_2 + B_1 100w + B_2(100w)^2 + B_3(100w)^3 \quad \text{(B.1)}$$

where w is the mass fraction of salt, which is used instead of mole fraction for this system, and ρ_2 is the density of water. B_i are assumed temperature dependent as follows:

$$B_i = e_i + f_i(T/K) + g_i(T/K)^2 \quad \text{(B.2)}$$

where e_i, f_i and g_i are empirical constants. Results of density calculations using equation (B.1) are given in Table B.1. The derived coefficients are used section 6.2.2 to estimate the density of the liquid phase (at the given equilibrium temperature) and the corresponding number of moles loaded to the system, reported in Tables A.11 and A.12.

Experimental and calculated values from equation (B.1) for densities of (TBAB + water) systems show a consistent agreement. The average absolute deviation (*AAD*) between measured and calculated values from this polynomial equation for density was 0.06 %. The concentration dependence of the present density measurements and the TBAB mass fraction is shown in Figure B.1. It is evident from the values given in Table B.2 and shown Figure 6.1 that density increases as the mass fraction of TBAB increases at a given the temperature. Also, density decreases as temperature increases at a given concentration of TBAB.

The *AAD* [%] was determined using the following relationship:

$$AAD(\rho) = \frac{1}{N}\sum_{s=1}^{N}\left|\frac{\rho_{exp} - \rho_{cal}}{\rho_{exp}}\right| \quad \text{(B.3)}$$

Table B.1. Determined parameters of density equation (eq. B.1) for (TBAB + H_2O) binary system.

Parameters	TBAB/H_2O
g_1	$-1.707 \cdot 10^{-8}$
f_1	$5.963 \cdot 10^{-6}$
e_1	$4.549 \cdot 10^{-4}$
g_2	$4.570 \cdot 10^{-9}$
f_2	$-3.099 \cdot 10^{-6}$
e_2	$5.304 \cdot 10^{-4}$
g_3	$-5.951 \cdot 10^{-11}$
f_3	$4.088 \cdot 10^{-8}$
e_3	$-7.091 \cdot 10^{-6}$
AAD %	0.06
No. of data points	90

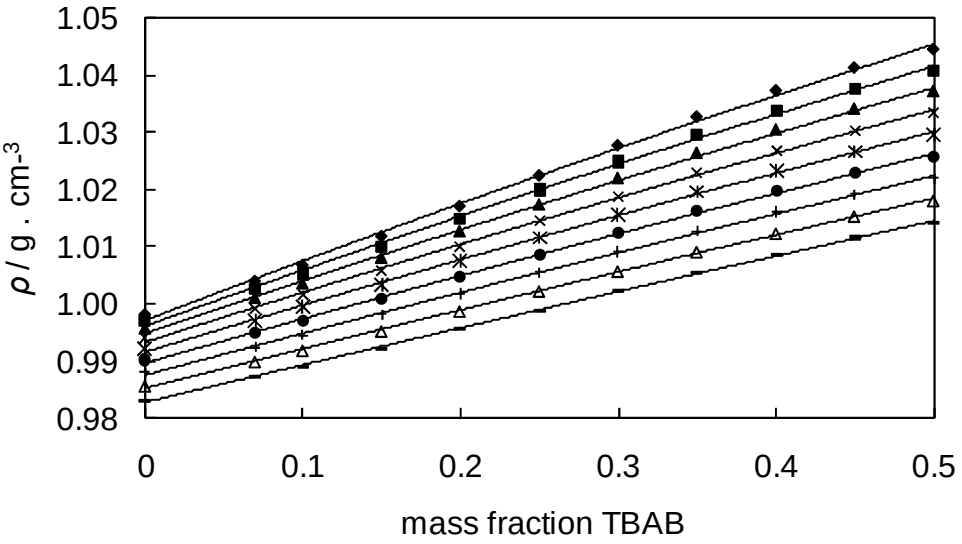


Figure B.1. Density (ρ) against mass fraction (w) for binary mixtures of (TBAB + H_2O) calculated with equation (6.1), at T = 333.15 K (-); 328.15 K (△); 323.15 K (+); 318.15 K (●); 313.15 K (∗); 308.15 K (×); 303.15 K (▲); 298.15 K (■), and 293.15 K (◆). Density values at w = 0 are experimental data. Solid lines are tendency curves.

Table B.2. Mass fraction of TBAB and density (ρ (g.cm^{-3})) of (TBAB + H_2O) mixtures from (293.15 to 333.15) K.

T / K	*mass fraction, TBAB*				
	0.0697	0.0999	0.1500	0.1996	0.2500
293.15	1.00385	1.00663	1.01135	293.15	1.02173
298.15	1.00243	1.00508	1.00955	298.15	1.01926
303.15	1.00080	1.00331	1.00754	303.15	1.01666
308.15	0.99895	1.00134	1.00534	308.15	1.01392
313.15	0.99691	0.99919	1.00297	313.15	1.01106
318.15	0,99470	0.99686	1.00045	318.15	1.00808
323.15	0.99232	0.99438	0.99778	323.15	1.00500
328.15	0.98978	0.99174	0.99496	328.15	1.00181
333.15	0.98709	0.98896	0.99200	333.15	0.99850

T / K	*mass fraction, TBAB*				
	0.2998	0.3499	0.4002	0.4498	0.5000
293.15	1.03049	1.03098	1.03625	1.04141	1.04473
298.15	1.02744	1.02791	1.03290	1.03783	1.04106
303.15	1.02431	1.02477	1.02949	1.03423	1.03736
308.15	1.02110	1.02155	1.02604	1.03059	1.03362
313.15	1.01782	1.01826	1.02253	1.02692	1.02985
318.15	1.01447	1.01490	1.01898	1.02321	1.02605
323.15	1.01105	1.01147	1.01538	1.01946	1.02222
328.15	1.00756	1.00797	1.01171	1.01567	1.01835
333.15	1.00400	1.00440	1.00800	1.01183	1.01445

Etude expérimentale des équilibres d'hydrates de mélanges de gaz contenant du CO_2 en solutions aqueuses de promoteur thermodynamique

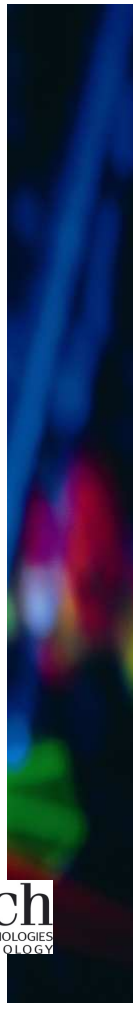
RESUME : Cette thèse présente les mesures et l'analyse thermodynamique d'équilibres de phases de systèmes d'hydrates contenant du dioxyde de carbone (CO_2), dans le contexte de procédés alternatifs de captage du CO_2. Le développement de nouveaux procédés de séparation par voie de cristallisation par hydrates est un point crucial de cette thématique. Les conditions de température et de pression requises et l'utilisation de promoteurs thermodynamiques sont au-delà des opérations habituelles et des bases de données existantes. La connaissance précise des conditions de formation et dissociation d'hydrates de gaz en présence d'additifs chimiques constitue une contrainte importante d'un point de vue thermodynamique et est nécessaire pour la modélisation et l'établissement de la faisabilité de nouveaux procédés industriels impliquant des hydrates de gaz. Dans cette thèse, nous présentons un nouveau dispositif expérimental qui combine techniques statiques et techniques analytiques, ce dernier a été spécialement développé pour mesurer des données d'équilibres des phases hydrate-liquide-gaz à des températures variant entre 233 et 373 K et à des pressions jusqu' à 60 MPa. De nouvelles données d'équilibre de phases des systèmes (CO_2 + méthane), (CO_2 + azote) et (CO_2 + hydrogène) ont été mesurées dans des conditions de formation d'hydrates en suivant la méthode isochorique avec variation de la pression en fonction de la température, et en analysant la composition en phase gazeuse. Les données d'équilibre et les conditions de dissociation d'hydrates générées dans ce travail sont comparées avec les données de la littérature. La fiabilité des modèles thermodynamiques les plus couramment utilisés est aussi étudiée. Les comparaisons entre les données expérimentales et prédites de dissociation d'hydrates suggèrent la nécessité de réajuster les paramètres des modèles thermodynamiques pour les systèmes contenant des hydrates de CO_2. En outre, l'effet promoteur du bromure de tetrabutylammonium (TBAB) sur les équilibres des phases des gaz purs et de mélanges contenant du CO_2 a été étudié. L'effet le plus important de promotion (réduction de la pression de formation des hydrates > 90%) est observé pour le système (TBAB + azote). Les résultats expérimentaux suggèrent que le CO_2 peut être séparé de mélanges de gaz industriels ou de combustion à des températures douces et à de basses pressions à l'aide de TBAB en tant que promoteur thermodynamique. La pression requise pour la formation d'hydrates à partir de mélanges de (CO_2 + azote) est réduite de 60 % en présence de TBAB.

Mots clés : Hydrates de gaz, semi-clathrate, dioxyde de carbone, TBAB, mesure expérimentale, équilibre des phases.

Hydrate Phase Equilibria Study of CO_2 Containing Gases in Thermodynamic Promoter Aqueous Mixtures

ABSTRACT : This thesis addresses the measurement and thermodynamic analysis of the phase equilibrium behavior of carbon dioxide (CO_2) hydrate-forming systems in the context of alternative capture engineering approaches. The development of new technologies based on gas hydrates requires specific temperature and pressure conditions and the utilization of thermodynamic promoters that are beyond usual operations and existing databases. Accurate knowledge of gas hydrates formation and dissociation from thermodynamics point of view in the presence of chemical additives is necessary for modeling purposes and to establish the feasibility of emerging industrial processes involving gas hydrates. In this thesis, a new experimental set-up and method for measuring pressure, temperature and compositional phase equilibrium data of high accuracy are presented. The equipment is based on the 'static-analytic' technique with gas phase capillary sampling and it is suitable for measurements in a wide temperature range (*i.e.* 233 to 373 K) and pressures up to 60 MPa. New phase equilibrium data in the (CO_2 + methane), (CO_2 + nitrogen) and (CO_2 + hydrogen) systems under hydrate formation conditions were measured following an isochoric pressure-search method in combination with gas phase compositional analysis. The equilibrium data generated in this work are compared with literature data and also with the predictions of two thermodynamic literature models. Comparisons between experimental and predicted hydrate dissociation data suggest a need of readjusting model parameters for CO_2 hydrate-forming systems. In addition, the thermodynamic stability of Tetra-n-Butyl Ammonium Bromide (TBAB) semi-clathrates (sc) with pure and mixed gases was investigated. The largest promotion effect (> 90% reduction in hydrate formation pressure) is observed for (TBAB + nitrogen) sc. The experimental results suggest that CO_2 can be separated from highly to low concentrated industrial/flue gas mixtures at mild temperatures and low pressures by using TBAB as thermodynamic promoter. The pressure required for hydrate formation from (CO_2 + nitrogen) gas mixtures is reduced by 60% in the presence of TBAB.

Keywords : Gas hydrate, semi-clathrate, carbon dioxide, TBAB, experimental measurement, phase equilibria



MINES ParisTech

ParisTech
INSTITUT DES SCIENCES ET TECHNOLOGIES
PARIS INSTITUTE OF TECHNOLOGY